Advances in Cell-based Therapeutic Process Development

_____

zur Erlangung des akademischen Grades eines
DOKTORS DER INGENIEURWISSENSCHAFTEN (Dr.-Ing.)

von der KIT-Fakultät für Chemieingenieurwesen und Verfahrenstechnik des
Karlsruher Instituts für Technologie (KIT)
genehmigte

DISSERTATION

von
M.Sc. Sarah Gretzinger
geboren in Laupheim

Referent: Prof. Dr. Jürgen Hubbuch
Korreferent: Prof. Dr. Cornelia Lee-Thedieck
Tag der mündlichen Prüfung: 15.03.2019

Danksagung

Die Anfertigung dieser Arbeit wäre ohne die Unterstützung von zahlreichen Menschen in diesem Rahmen so nicht möglich gewesen. Für diese Unterstützung in den letzten Jahren bin ich sehr dankbar und möchte meinen besonderen Dank folgenden Personen ausdrücken.

Prof. Dr. Jürgen Hubbuch danke ich für die Möglichkeit, meine Promotion in seiner Arbeitsgruppe durchführen zu können. Vielen Dank für das entgegen gebrachte Vertrauen, die zahlreichen fachlichen Diskussionen, die Begeisterung für neue Technologien und die Möglichkeit, diese in meine Arbeit integrieren zu können. Prof. Dr. rer. nat. Cornelia Lee-Thedieck danke ich für das Interesse an meiner Arbeit und die Übernahme des Korreferats. Prof. Dr. Andrea Hartwig und Prof. Dr.-Ing. Matthias Franzreb sowie Ihren Arbeitsgruppen danke ich für die Möglichkeit, Labore und Equipment zu nutzen.

Bei der gesamten Arbeitsgruppe des MABs bedanke ich mich für die Zusammenarbeit, die sehr gute Arbeitsatmosphäre und die gemeinsam verbrachte Zeit bei zahlreichen Feierabendveranstaltungen. Danke für die Unterstützung auch wenn ich meine Zeit zwischen Süden und Norden splitten musste. Besonderen Dank gilt allen Kooperationspartnern und Leuten, die mich in der Zellkultur unterstützt haben: Stefanie Sazinger, Pascal Baumann, Nicole Beckert, Andrew Gleadall, Saskia Kraus und Sarah Zimmermann. Sarah, ich danke Dir für die Unterstützung und das Mentoring vor allem am Anfang meiner Promotion. Stefanie, ich bedanke mich besonders für Deine Bereitschaft, dich in die Zellkulturarbeiten einzulernen und die gemeinsamen Projekte sowie Deine Ehrlichkeit und Offenheit bei all unseren fachlichen Diskussionen und den emotionalen Beistand in der Zellkultur. Ich bedanke mich bei allen Bürokollegen im Süden und Norden. Danke für die sehr gute Büroatmosphäre auch wenn ich zahlreich das Büro wechseln musste. Vielen Dank Josefine Morgenstern für die Unterstützung und die 15 Uhr Spezies, wenn dies mal wieder nötig war. Auch möchte ich mich herzlich bei Barbara Schmieg für Ihre Unterstützung und der Hilfe bei der Navigation durch die Campus Nord Administration bedanken. Margret Meixner, Dr. Angela Weiss, Marion Krenz, Iris Perner-Nochta und Michael Wörner danke ich für die administrative Unterstützung. Dem gesamten Ingenieursteam (ehemalig und aktuell) danke ich für die hervorragende Laborорganisation: Marc Hoffmann, Marie-Luise Schwab, Cathrin Dürr, Stefanie Sazinger, Nicolai Bluthardt, Kristina Schleining, Birgit Roser und Susanna Suhm. Susanna, mein besonderer Dank gilt Deiner unermüdlichen Unterstützung beim Bestellen von Materialien. Danke, dass du nie aufgegeben hast, auch wenn die Bestellung mal wieder etwas schwieriger zu tätigen war. Danke auch an das gesamte IT-Team (aktuell und ehemalig): Ralph Lange, Simon Woll, Jonas Haas und Jan C. Müller.

Zuletzt möchte ich mich bei meinen Eltern und meiner Schwester bedanken. Mum, Dad und Kiwi, vielen Dank für Eure unermüdliche Unterstützung und den Rückhalt.

CHAPTER 1

Abstract

The prospect of substituting damaged or diseased tissue by cell-based therapeutics has created much excitement in the last decades, since cell-based therapeutics open up new possibilities in patient treatment towards regenerative medicine. However, the first generation of cell-based therapeutics could not live up to market expectations and some were even withdrawn due to low reimbursement levels. While these products might be considered as market failures, identifying the obstacles early cell-based products were facing represents a major opportunity to improve the market performance of future products. In general, the inherent complexity of cell-based products in combination with limited experience represents a major obstacle translating a possible candidate from bench to bedside. A deeper insight was gained by the retrospective evaluation of the translational challenges where they could be further classified in three categories: (1) pre-market challenges, (2) manufacturing challenges and (3) post-market challenges.

A fundamental step towards commercialization is the process development (industrial scale and grade) which affects all three translational challenge categories. Thus, looking at the process development associated translational challenges is important. Currently, process development for cell-based therapeutics is often done using a heuristic approach, however, a more directed and systematic approach would be highly beneficial in order to overcome the process development associated challenges. Such an approach would allow for gaining process knowledge and improve process performance and, thus, improve market performance.

Effective process development for cell-based therapeutics is extremely important for product commercialization and could be achieved by implementing general bioprocess development tools and strategies. Hence, this doctoral thesis addresses the question if bioprocess development tools and strategies from the pharmaceutical industry can also be used for cell-based products. While process development requirements differ between unit operations and development stages, a general obstacle is to deal with limited material and time resources. As a consequence, most of the applied tools follow the principles of miniaturization, parallelization and automation. In order to demonstrate the power and versatility of bioprocess development tools, the objective of this thesis is the development and implementation of tools for different cell-based therapeutic manufacturing unit operations.

The first part of the thesis focuses on the unit operation cell separation, more specific, the usage of cell partitioning in aqueous two-phase systems (ATPS) as cell separation method. Here, the usage of a high-throughput screening (HTS) platform is used to investigate the influence of the critical parameters polymer molecular weight and tie-line length on

the cell partitioning behavior of five model cell lines, followed by a technology transfer project. Here, batch data (cell partitioning in ATPS) is transferred into a microfluidic flow-through mode. The main scope of this project is the evaluation of 3D printing as a process development tool, since it allows for a fast and cheap realization of tailored process equipment. Whereas the second part of the thesis is focusing on cell formulation unit operations, namely, cell cryoperservation and bioprinting. A major clinical cell cryopreservation topic is the cryomedia formulation, since it needs to be toxin- and xenogen-free. Thus, the focus of the second part of this thesis is the development of a tool box to predict cryomedia performance to shorten development time. Additionally, an analytical strategy, allowing for evaluation of bioprinting process parameter on critical cell parameter, is developed.

The evaluation of cell partitioning in ATPS as separation method in industrial scale cell downstream processing is the first central topic of this thesis. Cell partitioning in ATPS represents a promising alternative cell separation method to tackle the bottleneck condemned by limited availability of industrial scale methods, since it is scalable and facilitates a label-free separation. Up to now, the usage of cell partitioning in ATPS is limited due to its complex nature and not fully described partitioning theory. Thus, a time intensive and empirical screening is necessary in order to find optimal process parameter for each cell separation problem. First, a previously developed HTS platform (batch mode) is used for the investigation of critical ATPS parameter on cell partitioning behavior of five model cell lines aiming for a systematic and automated screening. The previously developed HTS platform was extended by a cell barcoding strategy allowing for a multiplexed high-throughput cell analysis in order to speed up the analytical strategy. Followed by a case study investigating the influence of the molecular weight and tie-line length on the resolution of the five model cell-lines in PEG-dextran ATPS. Both factors have an influence on cell partitioning behavior. The highest resolution of the five model cell lines could be achieved using low molecular weight PEG in combination with high molecular weight dextran. Additionally, a countercurrent distribution model was applied to calculate the theoretical purity and yield for the described separation issue. By applying the screening conditions to the countercurrent distribution model, an isolation of four of the five model cell lines is theoretically possible with high purity (> 99.9 %) and yield.
A technology transfer of batch HTS cell partitioning data into a microfluidic flow-through mode is described in a subsequent project. Such a technology transfer is normally associated with high investment costs. Aiming for a flexible process development approach with low financial risk, the usage of 3D printing technologies as process development tool is proposed in this study. In general, 3D printing technologies allow for the layer-by-layer manufacturing of 3D objects. The advantage of those technologies is the relatively cheap and fast realization of complex geometries. Thus, they represent a promising and versatile tool for process development, since they enable a rapid manufacturing and implementation of tailored equipment. In this project, 3D printing was used to manufacture tailored devices complementing standard laboratory equipment for the realization of a cheap and flexible microfluidic experimental set up. The following tailored equipment was designed and 3D printed for the realization of the experimental set up:

- replication master for microfluidic device manufacturing
- camera mount, using the existing camera shaft, allowing for implementation of a small high performance camera
- manual tailor-made fractionator with optimal installation space enabling the integration on the microscope table
- frame for the microfluidic device: the frame consists of three parts, the bottom plate, an outlet- and inlet bridge. The in- and outlet tubing were connected with the microfluidic device and stabilized via the bridges using fittings.

Implementing these tailored equipment parts, analysis of cell partitioning in ATPS in a microfluidic flow-through set up was possible. Cell suspension, top and bottom phase are pumped individually into the microfluidic device using three pumps. The cell suspension is focused at the interphase of the top and bottom phase allowing for cell partitioning. Simultaneously, a video of the microfluidic channel near the outlet is recorded. Using the developed snap shot analytic of the video material, an automatic estimation of cells in top and bottom phase is performed. Additionally, live cell rate was determined via flow cytometry by analyzing pooled samples. In order to provide a systematic process development and performance evaluation, the technology transfer case study was performed using the DMAIC (Define, Measure, Analyse, Improve and Control) framework. Using this DMAIC framework a successful implementation of the developed microfluidic process set up was performed. Additionally, two main factors influencing cell partitioning in the flow-through mode were identified, namely, cell load and fluid velocity.

Process development of different cell formulation unit operations is the focus of the second part of this thesis. Depending on the manufacturing strategy of cell-based therapeutics, long-time storage of the cell product needs to be performed. Usually, the unit operation cryopreservation is performed for this purpose, since it allows for stocking of living material while maintaining critical cell characteristics (no genetic or metabolic alterations). While cell cryopreservation is a well described topic in literature, cell cryopreservation process development of cell-based therapeutics is currently rather time consuming and follows an empirical approach. Aiming for a streamlined and more systematic cell cryopreservation process development, a video-based tool for the characterization of the freezing and thawing behavior was developed in the first formulation project. Freezing and thawing profiles are critical process parameter influenced by many factors including e.g. cryomedia formulation and scale up (working volume and container geometry). In order to enable rapid process development for cryopreservation despite the high number of process variable, fast and directed analytical tools are required. To evaluate the performance and flexibility of the video-based tool, a cryopreservation case study was performed with the β-model cell line INS-1E. Here, the freezing and thawing behavior of two working volumes (1 mL and 2 mL) were analyzed. Additionally, cell recovery and proliferation were evaluated. As expected, a delay in freezing and thawing behavior due to scale up was detected, resulting in a decrease of process performance determined by live cell recovery. While a high live cell recovery

(0.94 (±0.14) %) was achieved with 1 mL working volume, a decrease to 0.61 (±0.05) % could be observed for the 2 mL working volume. These findings are in good agreement with expectations, confirming the tool performance.
The objective of the consecutive second cryopreservation project is the development of a tool box allowing for the prediction of cryomedia process performance by characterization of media properties, freeze/thaw behavior (using the previously developed video-based tool) and media toxicity. Using good manufacturing practice (GMP) compliant cryomedia is an essential requirement for the cryopreservation of cell-based therapeutics, meaning it needs to be chemically defined without the addition of animal-derived or toxic compounds. For this reason, using the well described and often used cryoprotectants dimethyl sulfoxide (DMSO) and fetal bovine serum (FBS) is not an option. Supplementing a cryomedia with cryoprotectant agents is, however, crucial for cryopreservation process performance since they protect cells from severe stress, e.g. non-physiological osmotic pressure conditions, during freezing and thawing. Hence, development of an effective and GMP compliant cryomedia formulation is necessary for cell-based therapeutics when long-term storage is part of the manufacturing strategy. In this project, the usage of the developed predictive tool box for cryomedia formulation screening is proposed. The project comprised a case study evaluating the developed predictive cryomedia screening tool box including two commercial, DMSO-free cryomedia, one negative (without any cryoprotectant) and one positive (supplemented with DMSO and FBS as cryoprotectants) cryomedia example. The case study was performed with the β-model cell line INS-1E. Additionally, a conventional cryomedia performance assessment was done in order to evaluate the predictive tool box. Using the tool box the commercial Biofreeze® media was classified as unsuitable for the β-model cell line INS-1E due to media toxicity, while the second commercial cryomedia CryoSOfree™ was classified as possible candidate. These findings were confirmed by the conventional screening proving the power and usefulness of the tool box. Thus, implementing the predictive tool box will facilitates a fast pre-selection of possible candidates with low sample volume and cell number, shortening the overall process development time for the development of cryomedia formulations.
The focus of the third cell formulation project within this thesis is bioprinting. More precisely the development of an analytical strategy for cell-based bioprinting applications. Bioprinting is a relatively new field, however, it is believed to have a huge impact on regenerative medicine and tissue engineering, since it enables the manufacturing of artificial 3D tissue. Great efforts are being made in this field to move from academic research towards pharmaceutical industry or clinical applications. A critical hurdle to overcome this transition process is the development of a robust and well-known process, while maintaining critical cell characteristics (CCC). In order to gain process knowledge, a systematic and more directed process development approach for 3D bioprinting applications is required which includes the monitoring of CCC. Depending on the application, the critical cell characteristics may vary. However, universal CCCs are cell viability and proliferation. Flow cytometry represents a highly flexible, powerful and often used cell analysis method capable of analyzing multiplex CCC issues in parallel and might also be useful in the field of 3D bioprinting. However, flow cytometry analysis can only be performed with cell suspensions and needs, therefore, a destruction of the cell-laden 3D-structure prior analysis.

Hence, the objective of this project is the development of a flow cytometry-based analytical strategy as a tool for 3D bioprinting research. The development of this anayltical strategy was conducted using a model process with the β-model cell line INS-1E, a commercially available alginate-based bioink and a direct dispensing system as 3D bioprinting method. The destructive strategy enables the evaluation of cell viability and proliferation. By using a flow cytometer set up including an autosampler, the strategy enables an automated high-throughput screening. Following the development of the strategy, an evaluation of the process steps was performed including: suspension of cells in bioink, 3D printing and cross-linking of the alginate scaffold after printing. The evaluation showed that each individual process step (using the selected process parameters) had a negative influence on cell viability and must therefore be carefully monitored. This highlights the importance of process optimization in 3D bioprinting and the usefulness of the flow cytometry-based analytical strategy. The presented strategy has a great potential as a cell characterization tool for 3D bioprinting and can even be extended to a multiplex CCC analysis. Thus, the developed tool may contribute to a more directed process development in the field of 3D bioprinting.

In summary, several process development tools and strategies for different process units were developed within this doctoral thesis, demonstrating the applicability of general bioprocess development tools for cell-based products. The presented methods facilitating a more directed and systematic process development approach for cell-based therapeutics. These powerful tools represent an opportunity to streamline process development time, tackle translational hurdles and, ultimately, improve process understanding aiming for a QbD approach in the cell therapy industry.

CHAPTER 2

Zusammenfassung - German Abstract

Die Aussicht geschädigtes oder krankes Gewebe durch zellbasierte Therapeutika zu ersetzen, hat in den letzten Jahrzehnten viel Aufsehen erregt. Der Grund hierfür ist, dass zellbasierte Therapeutika neue Möglichkeiten in der Patientenbehandlung in Richtung der regenerativen Medizin eröffnen. Die erste Generation zellbasierter Therapeutika konnte den Markterwartungen jedoch nicht gerecht werden und wurde teilweise aufgund der geringen Kostenrückerstattung wieder vom Markt genommen. Während diese Produkte als Marktversagen betrachtet werden könnten, stellt die Identifizierung der Hindernisse, mit denen die frühen zellbasierten Produkte konfrontiert waren, eine große Chance dar, die Marktleistung zukünftiger Produkte zu verbessern. Im Allgemeinen stellt die inhärente Komplexität zellbasierter Produkte in Kombination mit begrenzter Erfahrung ein großes Hindernis dar, einen möglichen Kandidaten aus der Froschung in eine klinische Applikation zu überführen. Ein tieferer Einblick wurde durch die retrospektive Bewertung der translatorischen Herausforderungen gewonnen, wobei diese in drei Kategorien eingeteilt werden können: (1) Herausforderungen vor dem Markt, (2) Herausforderungen während der Herstellung und (3) Herausforderungen nach dem Markt.
Ein grundlegender Schritt in Richtung Kommerzialisierung von Produkten ist die Prozessentwicklung (industrieller Maßstab und Qualität), welche eine Auswirkung auf alle drei Kategorien hat. Daher ist es wichtig Herausforderungen, die mit der Prozessentwicklung assoziiert sind, zu betrachten. Derzeit wird häufig ein heuristischer Ansatz für die Prozessentwicklung von zellbasierten Therapeutika angewandt. Ein gezielter und systematischer Ansatz wäre jedoch sehr vorteilhaft für die Bewältigung der Herausforderungen, die mit der Prozessentwicklung assoziiert sind. Mit Hilfe solch eines Ansatzes könnte Prozesswissen generiert und die Prozessleistung verbessert werden, was auch eine Marktleistungssteigerung zur Folge hätte.
Eine effektive Prozessentwicklung für zellbasierte Therapeutika ist daher für die Produktkommerzialisierung äußerst wichtig und könnte durch die Implementierung allgemeiner Werkzeuge und Strategien der Bioprozessentwicklung erzielt werden. Aus diesem Grund befasst sich diese Arbeit mit der Frage, ob Bioprozessentwicklungs-Werkzeuge und Strategien aus der Pharmazeutischen Industrie auch für zellbasierte Produkte angewandt werden können. Während sich die Anforderungen an die Prozessentwicklung zwischen den einzelnen Grundoperationen und Entwicklungsstufen unterscheiden, stellt der Zeitdruck und das limitierte Probenmaterial eine generelle Hürde dar. Daher folgen die meisten der eingesetzten Werkzeuge den Prinzipien der Miniaturisierung, Parallelisierung und Automatisierung. Zur Demonstration der Leistungsfähigkeit und Vielseitigkeit von Bioprozessentwicklungs-

Werkzeugen ist das Ziel dieser Arbeit die Entwicklung und Implementierung solcher Werkzeuge für verschiedene Grundoperationen des Herstellungsprozesses von zellbasierten Therapeutica.
Der erste Teil der Arbeit konzentriert sich auf die Grundoperation der Zelltrennung, konkreter, die Verwendung der Zellverteilung in wässrigen Zwei-Phasen-Systemen (*engl.* aqueous two-phase systems = ATPS) als Zelltrennungs-Methode. Hierbei wird mit Hilfe einer Hochdurchsatz Screening Plattform (*engl.* high-throughput screening = HTS) der Einfluss der kritischen Parameter Polymermolekulargewicht und Konodenlänge auf die Zellverteilung von fünf Modellzelllinien untersucht, gefolgt von einem Technologietransferprojekt. Hierbei werden die Batch-Daten (Zellverteilung in ATPS) in einen mikrofluidischen Durchflussmodus überführt. Das Hauptziel dieses Projektes ist die Evaluierung des 3D-Drucks als Prozessentwicklungswerkzeug, da er eine schnelle und kostengünstige Realisierung von maßgeschneidertem Prozessanlagenequipment ermöglicht. Wohingegen sich der zweite Teil der Arbeit auf Grundoperationen der Zellformulierung konzentriert, im Speziellen auf die Zellkryokonservierung und den Bio-3D-Druck. Ein wichtiges Thema der klinischen Zellkryokonservierung ist die Kryomedienformulierung, da sie toxin- und xenogenfrei sein muss. Dementsprechend ist der Schwerpunkt des zweiten Teils dieser Arbeit die Entwicklung einer Toolbox zur Vorhersage der Kryomedien-Leistung zur Verkürzung der Entwicklungszeit. Zusätzlich wird eine analytische Strategie entwickelt, die eine Bewertung der Prozessparameter des Bio-3D-Drucks hinsichtlich kritischer Zellparameter ermöglicht.

Die Evaluierung der Zellverteilung in ATPS als Trennmethode für die Zellaufarbeitung im industriellen Maßstab ist das erste zentrale Thema dieser Arbeit. Zellverteilung in ATPS stellt eine vielversprechende alternative Zelltrennungsmethode dar, da sie skalierbar ist und eine Marker-freie Trennung ermöglicht. Daher könnte diese alternative Trennmethode helfen den Engpass zu beseitigen, der durch die begrenzte Verfügbarkeit von Methoden im industriellen Maßstab bedingt ist. Bisher ist die Verwendung der Zellverteilung in ATPS als Trennmethode aufgrund ihrer komplexen Natur und der nicht vollständig beschriebenen Verteilungstheorie eingeschränkt. Daher ist ein zeitintensives und empirisches Screening für jedes einzelne Zelltrennungsproblem notwendig, um optimale Prozessparameter zu finden. Zuerst wird eine zuvor entwickelte HTS-Plattform (Batch-Modus) eingesetzt, um den Einfluss von kritischen ATPS-Parameter auf das Zellverteilungsverhalten von fünf Modellzelllinien systematisch und automatisiert zu untersuchen. Die zuvor entwickelte HTS-Plattform wurde um eine Zell-Barcodierungsstrategie erweitert, welche eine multiplexe Hochdurchsatz-Zellanalyse ermöglicht, um die Analysestrategie zu beschleunigen. Danach wurde in einer Fallstudie der Einfluss des Molekulargewichts und der Konoden-Länge auf die Auflösung der fünf Modellzelllinien in PEG-Dextran-ATPS untersucht. Beide Faktoren haben einen Einfluss auf das Zellverteilungsverhalten. Die höchste Auflösung der fünf Modellzelllinien konnte mit niedermolekularem PEG in Kombination mit hochmolekularem Dextran erzielt werden. Zusätzlich wurde ein Gegenstromverteilungs-Modell eingesetzt, um die theoretische Reinheit und Ausbeute für das beschriebene Trennproblem zu berechnen. Die Trennung von vier der fünf Modellzelllinien ist theoretisch mit hoher Reinheit ($>$ 99,9 %) und Ausbeute, unter der Anwendung der Screening Bedingungen auf das Gegenstromverteilungs-Modell, möglich.

Im Folgeprojekt wird ein Technologietransfer von Batch-HTS-Zellverteilungsdaten in einen mikrofluidischen Durchflussmodus beschrieben. Ein solcher Technologietransfer ist in der Regel mit hohen Investitionskosten verbunden. Mit dem Ziel einer flexiblen Prozessentwicklung mit geringem finanziellen Risiko wird in dieser Studie der Einsatz von 3D-Drucktechnologien als Werkzeug für die Prozessentwicklung vorgeschlagen. Generell ermöglichen 3D-Drucktechnologien die schichtweise Herstellung von 3D-Objekten. Der Vorteil dieser Technologien ist die relativ kostengünstige und schnelle Realisierung komplexer Geometrien. Damit stellen sie ein vielversprechendes und vielseitiges Werkzeug für die Prozessentwicklung dar und ermöglichen eine schnelle Herstellung und Implementierung von maßgeschneidertem Equipment. In diesem Projekt wurde der 3D-Druck zur Herstellung von maßgeschneiderten Teile zur Ergänzung von Standardlaborgeräten eingesetzt, um einen kostengünstigen und flexiblen mikrofluidischen Versuchsaufbau zu realisieren. Folgendes maßgeschneiderte Equipment wurde für die Realisierung des Versuchsaufbaus entworfen und 3D-gedruckt:

- Replikationsmaster zur Herstellung von Mikrofluidiksystemen
- Kamera-Halterung zur Implementierung einer kleinen Hochleistungskamera über den bereits vorhandenen Kameraschacht
- manueller, maßgeschneiderter Fraktionierer mit optimiertem Bauraum, wodurch die Integration auf dem Mikroskoptisch möglich ist
- Halterung für das Mikrofluidiksystem: die Halterung besteht aus drei Teilen, der Bodenplatte, sowie aus einem Einlauf- und Auslauf-Steg. Die Ein- und Auslaufschläuche werden mit dem Mikrofluidiksystem verbunden und über den Steg mit Hilfe von Fittings stabilisiert.

Die Implementierung dieser maßgeschneiderten Equipmentteile ermöglicht die Analyse der Zellverteilung in ATPS im mikrofluidischen Durchflussmodus. Die Zellsuspension, die Ober- und Unterphase werden individuell mit Hilfe von drei Pumpen in das Mikrofluidiksystem gepumpt. Die Fluidgeschwindigkeiten müssen so eingestellt werden, dass die Zellsuspension an der Interphase der Ober- und Unterphase fokussiert wird, um eine Zellverteilung zu ermöglichen. Gleichzeitig wird ein Video des mikrofluidischen Kanals in der Nähe des Auslasses aufgenommen. Das aufgenommene Videomaterial wird dann mittles der entwickelten Schnappschussanalytik (*engl.* snap shot analytic) automatisch ausgewertet. Hierbei erfolgt die automatische Bestimmung der Zellzahl in jeweils der Ober- und Unterphase. Zusätzlich werden gepoolte Proben mittels Durchflusszytometrie analysiert, um die Lebendzellzahl zu bestimmen. Die Technologietransfer-Fallstudie wurde mit Hilfe des DMAIC-Frameworks (*engl.* Define, Measure, Analyse, Improve and Control) durchgeführt, um eine systematische Prozessentwicklung und Leistungsbewertung zu gewährleisten. Unter Verwendung dieses DMAIC-Frameworks wurde eine erfolgreiche Implementierung des entwickelten mikrofluidischen Prozesses durchgeführt. Zusätzlich wurden zwei Hauptfaktoren identifiziert, die einen Einfluss auf die Zellverteilung im Durchflussmodus haben: die Beladung an Zellen am Eingang und die Fluidgeschwindigkeit.

Die Prozessentwicklung verschiedener Zellformulierungs-Grundoperationen steht im Mittelpunkt des zweiten Teils dieser Arbeit. Je nach der Herstellungsstrategie von zellbasierten Therapeutika muss eventuell eine Langzeitlagerung des Zellproduktes erfolgen. Hierfür erfolgt in der Regel eine Kryokonservierung des Produktes, da diese die Lagerung von lebendem Material ermöglicht ohne das kritische Zellcharakteristika verändert werden (keine genetischen oder metabolischen Veränderungen). Während die Zellkryokonservierung ein ausführlich diskutiertes Thema in der Literatur ist, erfolgt die Prozessentwicklung von Zellkryokonservierungsprozessen für zellbasierte Therapeutika derzeit meist empirisch und ist demnach eher zeitaufwändig. Mit dem Ziel eines rationalisierten und systematischeren Prozessentwicklungsansatzes für die Zellkryokonservierung wurde im ersten Formulierungsprojekt ein videobasiertes Werkzeug zur Charakterisierung des Einfrier- und Auftauverhaltens entwickelt. Einfrier- und Auftauprofile sind kritische Prozessparameter, die von vielen Faktoren wie z.B. der Kryomedia-Formulierung und dem Scale-up (Arbeitsvolumen und Behältergeometrie) beeinflusst werden. Eine generelle Voraussetzung für die Prozessentwicklung ist eine schnelle Umsetzung, trotz der Vielzahl an Prozessparameter. Somit werden schnelle und gerichtete Analysewerkzeuge benötigt. Um die Leistungsfähigkeit und Flexibilität des videobasierten Tools zu bewerten, wurde eine Kryokonservierungs-Fallstudie mit der β-Modellzelllinie INS-1E durchgeführt. Hierfür wurde das Einfrier- und Auftauverhalten von zwei Arbeitsvolumina (1 mL und 2 mL) analysiert. Zusätzlich wurde die Zellregeneration und -proliferation evaluiert. Wie erwartet, wurde eine Verzögerung im Einfrier- und Auftauverhalten aufgrund vom Scale-up detektiert, was eine Verringerung der Prozessleistung zur Folge hatte, welche anhand der Ausbeute an lebenden Zellen bestimmt wurde. Während beim 1 mL Arbeitsvolumen eine hohe Ausbeute an lebenden Zellen (0,94 ($\pm$0,14) %) erzielt wurde, sank diese beim 2 mL Arbeitsvolumen auf 0,61 ($\pm$0,05) %. Diese Ergebnisse stimmen mit den Erwartungen überein und bestätigen die Leistungsfähigkeit des Werkzeugs.
Ziel des zweiten Kryokonservierungsprojektes ist die Entwicklung einer Toolbox zur Vorhersage der Kryomedia-Prozessleistung durch die Charakterisierung von Medieneigenschaften, Einfrier-/Auftauverhalten (unter Verwendung des zuvor entwickelten videobasierten Tools) und der Medientoxizität. Der Einsatz von good manufacturing practice (GMP)-konformen Kryomedien ist eine wesentliche Voraussetzung für die Kryokonservierung von zellbasierten Therapeutika, d.h. sie müssen chemisch definiert sein und dürfen keine tierischen oder toxischen Substanzen beinhalten. Aus diesem Grund ist die Verwendung der häufig eingesetzten und gut beschriebenen Kryoprotektiva Dimethylsulfoxid (DMSO) und fetales Rinderserum (FBS) nicht möglich. Die Ergänzung des Kryomediums um ein Kryoprotektivum ist jedoch entscheidend für die Leistungsfähigkeit des Kryokonservierungsprozesses, da dieses die Zellen vor erheblichem Stress während dem Einfrieren und Auftauen schützt, z.B. vor nicht-physiologischem osmotischen Druck. Daher ist die Entwicklung einer effektiven und GMP-konformen Kryomedia-Formulierung für zellbasierte Therapeutika notwendig, wenn eine Langzeitlagerung für den Herstellungsprozess notwendig ist. In diesem Projekt wird für das Screening von Kryomedia-Formulierungen die Nutzung der entwickelten prädiktiven Toolbox vorgeschlagen. Das Projekt umfasste eine Fallstudie zur Evaluierung der entwickelten prädiktiven Kryomedia-Screening-Toolbox mit zwei kommerziellen, DMSO-freien

Kryomedien, einer negativen (ohne Kryoprotektivum) und einer positiven (ergänzt durch DMSO und FBS als Kryoprotektivum) Kryomedia-Kontrolle. Die Fallstudie wurde mit der β-Modellzelllinie INS-1E durchgeführt. Zusätzlich wurde eine konventionelle Leistungsbewertung der Kryomedien durchgeführt, um die prädiktive Toolbox zu evaluieren. Mit Hilfe der Toolbox wurde das kommerzielle Biofreeze®-Medium aufgrund der Medientoxizität als ungeeignet für die β-Modellzelllinie INS-1E eingestuft, während das zweite kommerzielle Cryomedia CryoSOfree™ als möglicher Kandidat eingestuft wurde. Diese Ergebnisse wurden durch das konventionelle Screening bestätigt, was die Leistungsfähigkeit und Nützlichkeit der Toolbox belegt. Die Implementierung der prädiktiven Toolbox ermöglicht somit eine schnelle Vorauswahl möglicher Kryomedium-Kandidaten mit geringem Probenvolumen und Zellzahl und verkürzt somit die gesamte Prozessentwicklungszeit für die Entwicklung von Cryomedia-Formulierungen.
Der Fokus des dritten Zellformulierungsprojektes innerhalb dieser Arbeit liegt im Bereich des Bio-3D-Druck. Genauer gesagt auf der Entwicklung einer analytischen Strategie für zellbasierte Bio-3D-Druck-Anwendungen. Bio-3D-Druck ist ein relativ neuer Forschungsbereich, der jedoch voraussichtlich einen großen Einfluss auf die regenerative Medizin und das Tissue Engineering haben wird, da diese Technologie die Herstellung von künstlichem 3D-Gewebe ermöglicht. Innerhalb dieses Forschungsbereiches werden große Anstrengungen unternommen, um von der akademischen Forschung in Richtung der pharmazeutischen Industrie oder zu klinischen Anwendungen überzugehen. Eine entscheidende Hürde zur Überwindung dieses Übergangsprozesses ist die Entwicklung eines robusten und gut beschriebenen Prozesses, während gleichzeitig kritische Zellcharakteristika (*engl.* critical cell characteristics = CCC) nicht beeinträchtigt werden. Um Prozesswissen zu gewinnen ist ein systematischer und zielgerichteter Prozessentwicklungsansatz für Bio-3D-Druck-Anwendungen erforderlich, der auch die Überwachung von CCC beinhaltet. Je nach Anwendung können die kritischen Zelleigenschaften variieren. Universelle CCCs sind jedoch Zellviabilität und Proliferation. Die Durchflusszytometrie stellt eine hochflexible, leistungsfähige und häufig verwendete Zellanalysemethode dar, die in der Lage ist, Multiplex-CCC-Probleme parallel zu analysieren und eventuell auch im Bereich des Bio-3D-Drucks nützlich sein könnte. Allerdings kann die Durchflusszytometrie nur mit Zellsuspensionen durchgeführt werden und erfordert daher vorab eine Zerstörung der zellbeladenen 3D-Struktur. Ziel dieses Projektes ist daher die Entwicklung einer Durchflusszytometrie-basierten Analysestrategie als Werkzeug für die Bio-3D-Druck-Forschung. Die Entwicklung dieser Analysestrategie erfolgte mittels eines Modellverfahrens mit der β-Modellzelllinie INS-1E, einer kommerziell erhältlichen Alginat-basierten Biotinte und einem Extrusion-basierten Bio-3D-Druck-Verfahren. Die destruktive Strategie ermöglicht die Bewertung der Zellviabilität und Proliferation. Durch die Verwendung eines Durchflusszytometers mit integriertem Autosampler ermöglicht die Strategie zusätzlich ein automatisiertes Hochdurchsatz-Screening. Im Anschluss an die Strategieentwicklung erfolgte eine Evaluierung der Prozessschritte: Mischen der Zellen in die Biotinte, 3D-Druck und Vernetzung des Alginat-Scaffolds nach dem Druck. Die Auswertung ergab, dass jeder einzelne Prozessschritt (unter Verwendung der ausgewählten Prozessparameter) einen negativen Einfluss auf die Zellviabilität hat und daher sorgfältig überwacht werden muss. Dies unterstreicht die Wichtigkeit der Prozessoptimierung im Bereich des Bio-3D-Drucks und den Nutzen der Durchflusszytometrie-basierten Analyses-

trategie. Die entwickelte Strategie hat großes Potenzial als Zellcharakterisierungstool für den Bio-3D-Druck und kann zusätzlich erweitert werden, wodurch eine Multiplex-CCC-Analyse möglich wäre. Folglich könnte das entwickelte Analysetool zu einer gezielteren Prozessentwicklung im Bereich des Bio-3D-Drucks beitragen.
Zusammenfassend wurden im Rahmen dieser Dissertation mehrere Prozessentwicklungs-Werkzeuge und Strategien für verschiedene Grundoperationen entwickelt, die die Anwendbarkeit allgemeiner Bioprozessentwicklungs-Werkzeuge für zellbasierte Produkte demonstrieren. Die vorgestellten Methoden ermöglichen eine gezieltere und systematischere Prozessentwicklung für zellbasierte Therapeutika. Diese leistungsstarken Werkzeuge bieten die Möglichkeit, die Prozessentwicklungszeit zu verkürzen, translatorische Hürden zu überwinden und letztendlich das Prozessverständnis für einen QbD-Ansatz (*engl.* Quality by Design = QbD) in der Zelltherapieindustrie zu verbessern.

Contents

CHAPTER 3

Introduction

The pharmaceutical industry was historically dominated by small molecule therapeutics. However, changes in society and scientific achievements have always triggered commercially relevant innovations and the pharmaceutical industry is no exception. One example is the usage of biological therapeutics (recombinant peptides and proteins), such as monoclonal antibodies (mAbs) or insulin, for about two decades. The invention of biological therapeutics represents a milestone in the healthcare sector and they have already proven their commercial success. Nowadays, they are an integral part in e.g. cancer treatment. [1, 2] Currently, the healthcare sector is undergoing another exciting revolution towards regenerative medicine which is an umbrella term for advanced therapeutic approaches enabling the curing or replacement of damaged or diseased tissue rather than treating the resulting symptoms. [1–3] Different strategies like cell and gene therapy can be used for this purpose. Especially, cell-based therapies are much discussed in literature as promising approach in the field of regenerative medicine. [1, 2, 4, 5] Thus, cell therapies are considered to be the third pillar of therapeutics in the pharmaceutical industry, besides small molecule therapeutics and biopharmaceuticals. [1, 2, 4, 5] An increasing scientific interest in regenerative medicine and cell therapy was also observed and manifests in a growing number of publications, as displayed in **fig. 3.1**. Shown is the general use of the buzzwords "cell therapy" and "regenerative medicine" over time (1980 - 2017), searching the scientific database PubMed (https://www.ncbi.nlm.nih.gov/pubmed/).

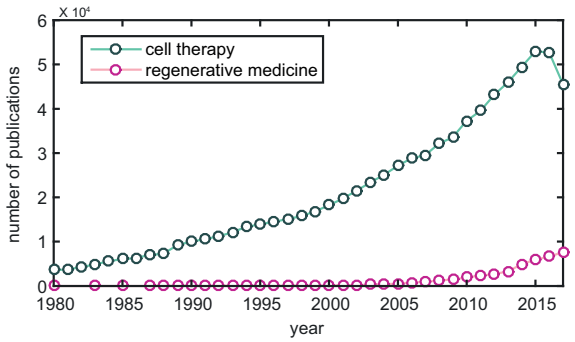

Figure 3.1: Number of publications in the field of "cell therapy" and "regenerative medicine" over time (1980 - 2017). Data was generated by a PubMed search (https://www.ncbi.nlm.nih.gov/pubmed/). The buzzwords "cell therapy" and "regenerative medicine" were entered in order to generate the above graph (accessed: April 26, 2018). The general observation is that usage of both buzzwords have increased over time, though, the term "cell therapy" was used more often.

In addition, an increasing number of clinical cell therapy trials are registered, comprising multiple applications e.g. in oncology, immunology or neurology. [6, 7]
The idea of using cells in patient treatment is quite old and was manifested in the 80s by the introduction of blood transfusion and bone marrow transplantation. [8–10] However, the commercialization of cell-based therapies is still in its infancy, resulting in a low number of authority approved cell-based therapeutics and penetration of the pharmaceutical market. [1, 11] Keeping in mind, that launching a new conventional therapeutic on the pharmaceutical market is time consuming, the novelty and complexity of cell therapies will naturally expand the research and development (R&D) time-line. [1, 2] In retrospective, a variety of crucial translational challenges are identified. In literature, much attention was paid to the fact that most of the translational work was located in academia and small biotechnology companies. They are limited in funding and often lack of experience in e.g. commercialization and business strategies. [1, 12–14]
Despite these challenges, some cell therapeutics are already approved by authorities like the Food and Drug Administration (FDA) and European Medicines Agency (EMA) and, thus, commercially available. [14, 15] However, their commercial success is still behind the expectations. [1]

3.1 Cell Therapeutics

The cell therapy industry is a promising and fast evolving sector within the healthcare environment. Thus, the following paragraph is briefly discussing the penetration of the market, concerning cell-based products, until Mai 2018 within the jurisdiction of the European Union (EU).
While the sector is still in its infancy, some cell-based therapy manufacturing companies were able to face the translational challenges and have already launched their products on the market. [14, 16, 17] These products are extremely diverse in their nature and can be categorized whether by their therapeutic indication (e.g. oncology, hematology, neurology, etc.) or cell source (autologous / allogeneic). However, the EU regulatory discriminates between products where cells are minimally manipulated and Advanced Therapy Medicinal Products (ATMPs). The ATMPs are further divided into somatic cell therapy, gene therapy and tissue engineered products. One difference between minimally manipulated cell-based products and ATMPs is that ATMPs need a market approval by the EMA before becoming commercially available. In order to obtain such an approval the company must demonstrate the products safety and efficacy. [16]
Up to now, ten ATMPs were approved by the EMA. They are summarized in **table 3.1** comprising three gene therapies, four tissue engineered products and three somatic cell therapies. However, four ATMPs are already withdrawn from the market, mainly because of poor commercial success. One example, often discussed in literature, is Provenge. [14–16, 18] Provenge is the trade name for an autologues dentric cell immunotherapy developed by Dentron for the treatment of metastatic prostate cancer. It was approved by the EMA in 2013 and withdrawn from the market only two years later in 2015 due to the manufacturer bankruptcy. In retrospective, some major obstacles were discussed, including high product pricing and unprofitable market access strategy. Ultimately, Provenge could not conquer the post-market challenges resulting in market failure. [14–18]

Table 3.1: Summary of European Medicines Agency (EMA) approved Advanced Therapy Medicinal Products (ATMPs) (until Mai 2018). Adapted form [14, 17] and http://www.ema.europa.eu/ema/

Trade Name	Developer	Indication	Product Category	Year of Approval	Status	EMA Info*
Alofisel	TiGenix	Perianal fistulas in Crohns disease	somatic cell therapy	2018	approved	http://www.ema.europa.eu/docs/en_GB/document_library/EPAR_-_Summary_for_the_public/human/004258/WC500246477.pdf
Spherox	CO.DON	Cartilage defects in the knee	tissue engineered	2017	approved	http://www.ema.europa.eu/docs/en_GB/document_library/EPAR_-_Summary_for_the_public/human/002736/WC500231921.pdf
Zalmoxis	MolMed	Stem cell transplantation in high-risk blood cancer	somatic cell therapy (genetically modified)	2016	approved	http://www.ema.europa.eu/docs/en_GB/document_library/EPAR_-_Summary_for_the_public/human/002801/WC500212516.pdf
Strimvelis	GSK	Adenosin-desaminase severe combined immunodeficiency (ADA-SCID)	gene therapy	2016	approved	http://www.ema.europa.eu/docs/en_GB/document_library/EPAR_-_Summary_for_the_public/human/003854/WC500208202.pdf
Imlygic	Amgen	Melanoma	gene therapy	2015	approved	http://www.ema.europa.eu/docs/en_GB/document_library/EPAR_-_Summary_for_the_public/human/002771/WC500201080.pdf
Holoclar	Chiesi	Severe limbal stem cell deficiency in the eye	tissue engineered	2015	approved	http://www.ema.europa.eu/docs/en_GB/document_library/EPAR_-_Summary_for_the_public/human/002450/WC500183406.pdf
Provenge	Dentron	Metastatic prostate cancer	somatic cell therapy (manipulated cells)	2013	withdrawn in 2015	http://www.ema.europa.eu/docs/en_GB/document_library/EPAR_-_Summary_for_the_public/human/002513/WC500151157.pdf
MACI	Vericel	Cartilage defects in the knee	tissue engineered	2013	withdrawn in 2014	http://www.ema.europa.eu/docs/en_GB/document_library/EPAR_-_Summary_for_the_public/human/002522/WC500145889.pdf
Glybera	uniQure	Lipoprotein lipase deficiency (LPLD)	gene therapy	2012	withdrawn in 2017	http://www.ema.europa.eu/docs/en_GB/document_library/EPAR_-_Summary_for_the_public/human/002145/WC500135474.pdf
ChondroCelect	TiGenix	Cartilage defects	tissue engineered	2009	withdrawn in 2016	http://www.ema.europa.eu/docs/en_GB/document_library/EPAR_-_Summary_for_the_public/human/000878/WC500026033.pdf

* accessed Mai 05, 2018

Nevertheless, such a failure can provide important lessons for future products to push the cell therapy industry towards their expected market volume.

3.2 Cell Therapy - Translational Challenges

Commonly, a new scientific approach is accompanied by a hype and high expectations. At the same time, the translation of such a new scientific finding into a commercially successful product is often difficult and prone to failure. Lack of knowledge often prolongs the translational time-line, and even though first generation products are launched on the market, the commercial success can fall short of expectations. Cell-based therapeutics are no exception and have faced major translational challenges in the past. [1, 15, 16]
Analyzing and tackling those translational challenges is essential in order to avoid them in future. In general, they can be divided into three categories: (1) pre-market challenges, (2) manufacturing challenges and (3) post-market challenges. [15]
The first category of pre-market challenges are closely related with proper funding. In general, developing a new therapeutic product usually starts with the pre-market phase which comprises basic research up to clinical trials. During this time, a vast amount of money is spend. While the pioneers in cell therapy industry were predominantly locate in academic and small biotechnology companies with limited access to funding, big pharma was mostly absent. Thus, some translational projects were struggling with inadequate funding. [1, 7, 11, 13–16, 18–21] The novelty and complexity of cell-based therapeutics, in combination with lack of experience on both sides, regulatory agencies and developer additionally reinforced these funding associated challenges. [12, 13, 15]
Lack of knowledge and experience in process development was identified as a major obstacle for the second category challenges, namely, manufacturing challenges. Yet, they are closely connected with pre-market challenges since the foundation for a successful commercial production must be established early in the R&D phase. [16] For example, in order to produce cell therapeutics, a technology transfer from research grade methods into a commercial scale process, which is in good manufacturing practice (GMP) compliance, must be performed. [15, 16] However, not every research grade method can be successfully transferred and implemented into a manufacturing process. Important requirements for a technology transfer are e.g scalability or the possibility for automation. [16] Automation is important since it has an impact on process robustness and reproducibility. Additionally, automation minimizes laboratory costs and the risk of human failure, which is crucial for a commercial GMP production. [1, 15, 16, 22–24] Raw material supply is another important criteria which must be considered early on. Otherwise, agents might be in conflict with GMP production e.g. when using xenogenic agents or the cost of goods (CoGs) might be extremely high. [12, 15, 16, 25, 26] Distribution logistics also need to be addressed early on in R&D since living cell material is highly sensitive with relatively short product shelf-life. Depending on the product specifications, the cells can be shipped in culture or frozen. In both cases, the shipping methods are part of the manufacturing process and must be validated concerning GMP compliance and risk management. [15] These considerations are often absent within the scientific mindset and cause trouble later on, thus, scientist must think ahead during R&D. Similar observations were made concerning the analytical strategy. [12, 15, 16, 20, 24, 27] Effective process development within a GMP environment

is mainly knowledge based. Meaning, a full product characterization needs to be performed in order to provide information about identity, potency, safety, sterility and purity. This information is summarized as critical quality attributes (CQAs), which have to be closely monitored and confirmed during process development. Thus, CQAs must be identified and defined early on. In combination, analytical tools, covering all these aspects, needs to be developed in parallel with the product itself. If this groundwork is not done during R&D, it will cause problems during the development of a commercial relevant process. [12, 15, 16, 20, 24, 27]

After market introduction, cell therapeutic products might face the third category post-market challenges. The adaption of cell therapeutics on the market is no major concern during development. However, it does affect the commercial success. In retrospective, different aspects hindering the widespread adaption of cell therapeutics could be identified: high product prices and timid acceptance by physicians. [15, 28] A hindered adaption of cell therapeutics by physicians could be observed due to the fact that they also had no experience with it and the administration procedure can be quite complex. [15] Thus, poor market adaption will result in low sales numbers and will, ultimately, lead to an insufficient reimbursement level. [4, 15, 16, 28] Such reimbursement challenges occurred in the past and even caused bankruptcies. A prominent example, often named in literature, is the company Dentron. Short after launching their product Provenge on the market, the company became insolvent due to high costs and low reimbursement level. This was not an isolated case. Up to now, in total four advanced therapeutics were withdrawn after approval from the European market due to commercial failure. [14, 15, 17, 18]

These cases highlight the need of a sufficient commercialization strategy, including an efficient business model from the very beginning. Thus, analyzing the challenges, faced by the cell therapeutic industry so far, is important to avoid them in future. Discussing those challenges in separate categories has the advantage that they can be assigned to individual project stages. Such an approach facilitates subsequent implementation of gained knowledge. However, it is important to note that a lot of the obstacles could be attributed to the location of first generation projects in academia and small to medium sized biotechnology companies. Additionally, they are often closely related. For example, not dealing with CoGs during R&D can lead to high manufacturing costs which later on need to be reimbursed. [15, 16, 19]

Lately, a slight increased interest of the pharmaceutical industry in cell-based therapeutics could be noted. The involvement of the big pharma is expected to be a booster for the cell therapy industry, since they are capable of providing sufficient funding, have a great expertise in business strategies and commercial scale process development, as well as, in bioprocessing techniques. Especially, the cooperation between academic researcher and the pharmaceutical industry seems to be a promising construct. [5, 14, 15, 19] An example is the cooperation between the University of Pennsylvania and Novartis. Their partnership was formed in 2012 and their chimeric antigen receptor T cell (CAR-T cell) therapy Kymrhia (formerly CTL019) was successfully approved by the FDA in 2017. [5, 14, 19] Subsequently, Novartis has already filed a marketing authorization application (MAA) to the EMA. [29, 30] Given that the FDA approval was in 2017, the commercial success on the US market still needs to be proven. [31]

However, it is not only the manufacturers who are decisive for the establishment of a successful therapy industry. Other parties like the authorities are equally important since e.g. the regulation of cell therapy products need to be adapted to their unique attributes. Also, harmonization of the different national authority regulations would be highly beneficial. [12, 13, 15] Ideally, the manufacturers and authorities work collectively towards a more systematic and directed process development approach for cell-based therapeutics, in order to minimize the manufacturing costs and patient risk. This could be achieved by implementing process development tools and strategies, already used by the biopharmaceutical industry. These tools should be adapted and evolve towards the requirements of the cell-based therapy manufacturing process.[1, 15] Thus, a comprehensive overview of the cell therapy manufacturing strategies is necessary.

3.3 Cell Therapy Manufacturing Strategies

The manufacturing strategy for cell therapeutics is highly dependent on whether it is an autologous or allogenic product. The main difference between these two product categories is the origin of the therapeutic cells. An autologous product is patient specific; meaning, the patient is likewise cell donor and recipient. In contrast to the cell origin of allogenic products, where the cell donor is universal and patients get the same cell therapeutic product. [1, 20, 23, 24]

In general, a manufacturing process is a sequence of unit operations. Depending on the manufacturing strategy and product specifications, the number and sequence of unit operations can differ. Typical manufacturing strategies for both product categories are shown in **fig. 3.2**. The processing steps for an autologous cell therapeutic product **(left)** and an allogenic product **(right)** are shown as flow charts. Both strategies are generalized. [1, 23, 24]

For the production of autologous product, patient tissue acquisition is typically performed de-centralized in a healthcare environment (e.g. clinic) and, subsequently, shipped to a central manufacturing facility. Since both process steps can influence the cell quality, both patient biopsy for cell acquisition and shipping needs to be performed by specialized personal. After the introduction of the starting material in the manufacturing facility, cell release from tissue matrix is performed if needed. Typically, cell therapy comprises a specific or well defined heterogeneous cell population. Thus, cell isolation is performed to purify the cell suspension obtained by a biopsy, followed by the cell cultivation in order to expand the purified cell population. Depending on the product, cell manipulation might need to be performed prior to cell harvest e.g. cell differentiation in case of stem cells. Subsequently, cell downstream processing is done, typically comprising a reduction of volume, washing step and the isolation of a specific cell population or well defined heterogeneous cell suspension. Additionally, cell formulation and release testing is performed before the patient-specific cell therapeutic product is returned to the healthcare site for administration of the product to the patient. [1, 23, 24]

The manufacturing process for allogenic cell therapeutic products is more similar to biopharmaceutical processes. Here, a master cell bank (MCB) and working cell bank (WCB) is generated from the tissue of a single donor during R&D. This procedure of donor biopsy, material shipping to R&D site, cell release for tissue and cell isolation as well as

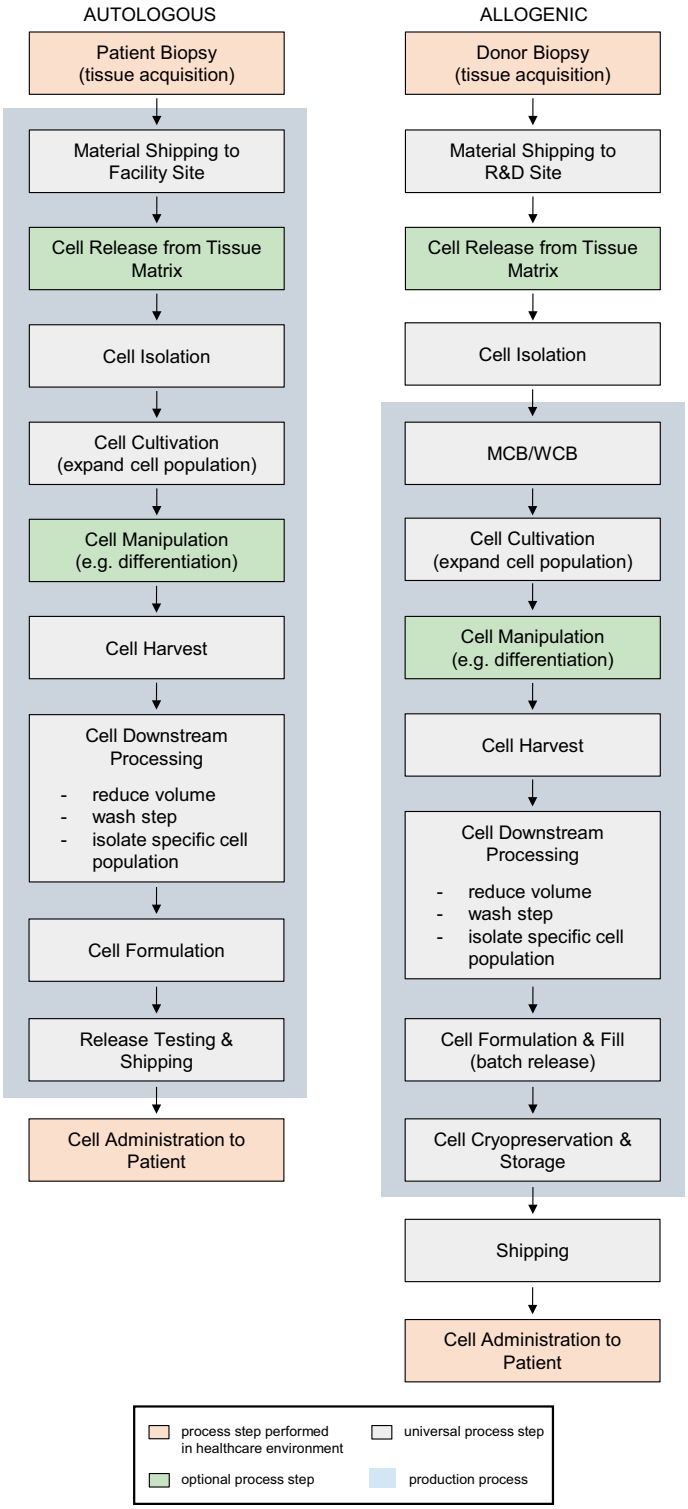

Figure 3.2: General manufacturing strategies for an autologous cell therapeutic product **(left)** and an allogenic product **(right)**. The typical processing steps are shown as flow charts. Adapted form: [1, 23, 24]

the generation of the MCB/WCB is done once during development. The generation of MCB/WCB is a concept for long-term storage of the starting material for production with a defined cell quality. The actual process starts with thawing cell material from the WCB for the cell cultivation process in order to expand the cell population. If needed an optional cell manipulation step can be introduced before harvesting the cells. Subsequently, cell downstream processing is performed. This typically involves a reduction of volume, washing step and isolation of a specific cell population if cell manipulation was performed. Then cell formulation and product filling is executed. Cell cryopreservation is performed in order to store the product. Thus, the product shipping is independent from production and can be done when requested. The cell therapeutic administration is done by specially trained physicians in a healthcare environment. [1]

Obviously, the two manufacturing strategies do not only differ in product processing, but also in infrastructure requirements. For allogenic products the infrastructure is similar to the biopharmaceutical infrastructure concerning quality assurance, storage and delivery. In case of autologous products the quality assurance infrastructure needs to be more elaborate. Tracking of sample probe and cell quality is extremely important since the patient cell samples differ in quality and there is a higher risk of cross contamination. Additionally, product identity must be assured during the whole process. Process scheduling is another important factor for autologous products. Coordination of patient biopsy, manufacturing and cell therapeutic administration needs to be closely coordinated involving the e.g. clinic and manufacturing site. [1, 23, 24] Batch-size and up-scale strategies also differ between autologous and allogenic cell therapeutic products. Again, allogenic products are similar to biopharmaceuticals. Up scaling in order to meet the market demand is normally done by increasing batch volume. This approach is not an option for autologous products, since each batch represents a patient-specific dose. Thus, scaling out rather than scaling up is performed. Scaling out is a parallelization approach, meaning multiple smaller batches are produced at the same time. [1, 24, 27]

Besides the differences, both product manufacturing strategies must be in compliance with current good manufacturing practice (cGMP) in order to get a market approval by the authorities. For cell therapeutics it is especially important to avoid the usage of xenogeneic agent in production e.g. fetal bovine serum (FBS) as media supplement or xenogeneic monoclonal antibodies (mAbs) for separation. Such agents pose a safety issue for patients since they can transmit diseases or cause an immune reaction. [12, 26]. Additionally, extractables and leachables should be avoided during production. [16, 22] Automation is another GMP relevant topic since it minimizes the process risk profile due to the avoidance of human intervention. [1, 16, 22–24] Using closed systems for e.g. cell cultivation is equally important concerning minimizing the risk of process contamination and product tracking. [1, 24] An aseptic work flow is especially recommended since living cell products cannot be sterilized. [32] A widespread tool in the biopharmaceutical production for the unit operation cell culture is the usage of closed bioreactors. The implementation of that knowledge would be highly beneficial for the cultivation of cell therapeutics. However, several aspects need to be considered for the cultivation of cell therapeutic products. In general, cell can grow in suspension, adherent as monolayers or as 3D tissue, resulting in different cultivation strategies. The majority of cell therapeutics are suspension cell lines

or grow adherent as monolayers, thus, 3D tissue cultivation is not discussed in this section. The cultivation of suspension cell lines is typically performed in closed, stirred tanks. The biopharmaceutical industry has gained a comprehensive knowledge using this type of bioreactors including upscaling, in-line monitoring, automated control and mass transfer which can be applied processing suspension cell therapeutics. Cultivation of adherent cell populations require a suitable substrate for cell attachment. For this purpose, hollow fiber and fixed or packed bed bioreactors can be used, as well as stirred tank bioreactors in combination with microcarrier as attachment substrate. Challenging aspects of this unit operation are the uniformly cell seeding and de-attachment of cells from substrate before harvesting. While these process steps are routinely performed in research scale, expertise must be gained for manufacturing scale. [1, 24, 33]

3.3.1 Cell Separation

Cell therapeutic downstream processing (DSP) is located after the cell harvest and comprises several unit operations including volume reduction, cell washing and isolation of the target cell population. [1, 34] Decreasing the process volume reduces processing times for the subsequent steps and also results in an appropriate sample volume for patient administration. The elimination of media components is achieved by washing the cells. This is especially important if serum was supplemented to the media for cell culturing. [35] Subsequently, cell seperation is performed in order to isolate the target cell population. This crucial unit operation is directly linked to patient safety e.g. for stem cell applications. Here, the risk of teratoma formation is extremely high if the cell separation does not achieve an entire depletion of undifferentiated cells. [36]

Currently, the availability of commercial scale cell DSP methods is limited and represents a bottleneck in cell therapy production. Yet, the cell therapy industry is mainly focusing on upstream processing (USP) development. To close the crucial juncture between research and commercialization, major efforts must be made in the field of cell DSP. [1, 34]

While multiple cell separation methods are available for research purpose, scalable methods for clinical applications are still lacking. [1, 34, 37] In general, cell separation methods are categorized into two main groups: the (1) physically-based and (2) affinity-based methods. [38] In the first category of physically-based separation methods, cells are separated according to their physical properties e.g. cell size and density. A common method within this group is the density-gradient centrifugation e.g. using percoll or ficoll as density media. [38–40] The cell separation within the second group is based on the recognition of characteristic cell surface antigens by specific antibodies. Prominent methods are the fluorescence activated cell sorting (FACS) which is a derivate of flow cytometry and the magnet activated cell sorting (MACS). In general, both methods are dependent on the existence of specific cell marker unique for the target cell population and the availability of respective antibodies. The main difference between these two methods is the antibody labeling determining the separation mode. For FACS the labeling is done with fluorochromes. Cells are separated according to the fluorescence signal emitted by the fluorochrome. In case of MACS, the antibodies are linked to magnetic particles. By using a magnetic field, cells binding an antibody with magnetic tag can be restrained and, thus, separated by non-binding cells. Both methods can be performed as negative or positive

selection. Negative selection is performed in a flow through mode. Here, the target cell population can be found in the flow through, while the contaminant cell populations are depleted. [1, 38, 41]
Up to now, few clinical scale DSP methods are available including a MACS set up [1, 42–44] and different centrifugation-based systems [1, 34, 36, 37, 45]. One example is the Elutra Cell Separation System (Terumo BCT). This counter-flow centrifugal elutriation system separates cells in five fractions due to size and density. It is a closed system for small-scale applications mainly suitable for autologous cell therapy products. [1, 42, 43, 46–48] Another centrifugation-based system for small-scale cell production is the Cell Saver (Haemonetics Corporation) [1, 40, 44], while the kSep (Sartorius) is a larg-scale system for allogenic cell therapy manufacturing. [1, 35, 48]
However, the integration of only one cell separation step in the manufacturing process is likely insufficient to achieve the needed cell purity. [42, 46] The DSP approach for biopharmaceuticals commonly includes three subsequent and orthogonal separation methods to significantly improve product purity. [49–51] Implementation of this approach in cell therapy DSP is restricted, since the availability of clinical scale cell separation methods differing in separation mode is still limited. Addressing this critical shortcoming is important and will contribute to master the obstacles faced in cell therapy process development. Re-engineering existing cell separation methods by optimizing key process parameter could be done, as well as developing alternative strategies. [1, 48] Though, both scenarios must follow the general requirements: scalability, closed systems, possibility of automation, minimal processing time and the physiological properties of cells must not be altered. Thus label-free cell separation methods are favorable since knowledge about the relationship between cell surface marker and their cellular function is often missing. Additionally, the use of antibodies in DSP can pose a safety issue. [1, 39, 41, 52]

Cell Partitioning in Aqueous Two-Phase Systems (ATPS)

Cell partitioning in aqueous two-phase systems (ATPS) represents such an alternative label-free cell separation method. [53, 54] The phenomenon of phase separation in an aqueous system was first described by *Beijerinck* in 1896. [55] He recognized that by mixing of two aqueous polymer solutions above a certain concentration, formation of a biphasic system will occur. The usage of ATPS for partitioning of bio-material, e.g. proteins or cells, was made decades later by *Albertsson*. [53] Major advantages of using this partitioning phenomenon as alternative separation method are the scale up possibility and that ATPS provide relative mild process conditions. However, the widespread adaption is limited since the partitioning of bio-material in ATPS is quite complex and not yet fully described. Extensive empirical screening for adequate separation conditions is necessary and need to be adapted for each separation issue individually. [41, 56, 57] Nowadays, time-consuming work can be compensated by using modern automated high-throughput screening (HTS) platforms to expand the commercial use of ATPS-based bio-material separation techniques. [58–60]
Fundamental as well as application-oriented work was done on protein and cell partitioning in ATPS from the 50s to the 80s by *Albertsson* and *Walter*, among *others*. [53, 54] Up to now, the theory is not fully understood since bio-material partitioning in ATPS is quite

complex. However, *Albertsson* assumed that the bio-material partitioning in ATPS is driven by physiochemical characteristics including size, hydrophobicity, electrochemical and bio-specific affinity. ATPS properties need to be adapted and optimized for each separation application individually. [53] While the ATPS characteristics are unique for each separation problem, some general requirements must be met in case of cell applications. Water content and osmotic pressure of both phases are important to maintain cell viability and physiological functions, while surface tension is associated with unspecific cell adsorption at the interphase. Thus, ATPS with low surface tension are favorable to facilitate high cell recovery. [53, 54, 61] Buffered polymer-polymer systems are most commonly used for cell applications. Especially, the usage of Dextran-polyethylene glycol (PEG) systems supplemented with salt additives (e.g. sodium chloride, sodium phosphate) to adjust osmotic pressure is extensively described in literature. [56, 62, 63]
Depending on process requirements regarding purity and recovery of the target cell population, a multi-stage rather than a single-stage setup needs to be performed. Countercurrent distribution (CCD) is a promising multi-stage liquid-liquid extraction method for cell applications and was first described by *Craig and Post*. [64] Using a CCD apparatus, the bottom phase is retained while the top phase is transferred. In each extraction stage, cell partitioning is achieved by mixing the ATPS with subsequent phase separation by gravity. Depending on the partitioning behavior of the target cell population, the interphase is retained or transferred. In the case of a predominantly partitioning of the target cell population between the top and interphase, the interphase is retained. While the interphase is transferred if the target cell population can mainly be found in the bottom and interphase. [65] Phase settling by gravity is the main advantage of this method since it allows a cell partitioning according to the physiochemical properties. In contrast, using centrifuge-based methods density-based partitioning will predominantly occur. Additionally, CCD facilitates low pressures and shear forces resulting in relatively low process related decrease in cell viability loss. [54, 63, 66]

3.3.2 Formulation

The formulation of cells is another unit operation which is rarely discussed within the cell therapy community. [67] It is located between cell DSP and fill/finish with the main purpose to stabilize the cell-based product and to provide physiological conditions e.g. osmotic pressure. The list of commonly used excipients includes buffers, salts, polymers, proteins and preservatives. [1, 67–69] Ideally, product formulation is suitable for storage and shipping, as well as for patient administration since it streamlines the administration procedure done by physicians. Using products without the need of an additional washing step right before administration is favorable since it minimizes the risk of product contamination. Additionally, there is no need for specialized clinic personal to perform this task which might lead to a higher adaption of cell therapy products by physicians. [67]
Considering the cell type, type of cell therapy product (autologous / allogeneic), patient administration strategy (injection, sheet of cells, intravenously or more complex ways) and storage conditions is important to meet manufacturing and end product requirements. Thus, an integrated product and process development (IPPD) approach is necessary for the development of a cell therapy formulation. [67] This applies in particular if long-time

storage of the cell-based product is required which can only be achieved by performing a cryopreservation. [1, 68–70] Here, the addition of cryoprotectant agents is necessary in order to achieve high post-thaw cell survival. However, the type and concentration of cryoprotectant agent do have an effect on optimal freezing and thawing parameter. [71] Another aspect which should be considered is the compatibility of cryoprotectant agents and packaging material e.g. when using dimethyl sulfoxide (DMSO) as cryoprotectant agent. DMSO is a widely used cryoprotectant agent. [1, 68, 71] However, DMSO can interact with polymeric packaging materials highlighting the need of an IPPD approach. [68]

Cryopreservation

Maintaining critical cell characteristics during long-term storage of cells is a challenging issue within the allogenic cell therapy manufacturing process. Here, bulk production is performed rather than on-demand production, resulting in the need of a cell storage strategy for the starting material as well as the final product. [1] Commonly, cryopreservation is performed when long-term storage of cells is needed to facilitate continuous access to cell material with unchanged characteristics [1, 72, 73] e.g for cell culture maintenance [72], biopharmaceutical production [74, 75] or reproduction medicine [71, 76]. In the production of allogenic cell therapy products cryopreservation is performed twice. Establishing a MCB/WCB with the production cell material involves cryopreservation. Additionally, cryopreservation of the end product is performed in order to prolong the product shelf-life. Effective cell cryopreservation usually comprises slow freezing, storage at ultra-low temperatures and fast thawing of cells. [1, 72, 74, 75, 77, 78] The advantage of this approach is the complete shut down of cell metabolism at ultra low temperatures, hindering any changes in cell characteristics e.g. genetic or metabolic. However, freezing and thawing induces severe cell stress. During sample phase transition osmotic effects as well as intra- and extracellular ice formation can occur, leading to cell membrane damages or cell death. [72, 79] In order to ensure high post-thaw cell survival, the cryopreservation process must be optimized with regards to minimize severe cell stress.

Critical cryopreservation process parameter are well described in literature and include cell loading [80], cell suspension condition (e.g. suspension, monolayer or colony) [71, 78, 81], process volume [73, 75, 77, 82, 83], freezing/thawing profile [73, 74, 77, 84–86] and cryomedia formulation (e.g. typ of cryoprotectant agents and concentration) [71, 87]. Thus, systematic screening of process parameter is necessary in order to optimize a cryopreservation process. Moreover, the critical process parameter can influence each other. [71, 72, 74, 75, 78] In addition, a systematic process development approach is highly beneficial for clinical applications like cell therapy products, since they must be manufactured in a GMP environment. [1] In order to meet the GMP requirements, a storage infrastructure must be available. This includes freezing of cells in a controlled manner, subsequent storage in a highly monitored environment and additional monitoring of critical cell characteristics during the whole process. [1, 72–75, 77, 78, 81, 84, 88, 89]

The cryomedia formulation represents a bottleneck for clinical applications since chemically defined formulations without animal-derived or toxic components should be used. Thus, commonly used cryoprotectant agents like DMSO and FBS should be excluded. [1, 90–93] In general, cryoprotectant agents can be categorized in to groups: (1) extracellular and

(2) intracellular cryoprotectant agents. [91, 93–98] Sugars and high molecular polymers e.g. PEG are extracellular cryoprotectant agents since they are not able to penetrate the cell membrane. Intracellular cryoprotectant agents like DMSO, glycerol or 1,2-propanediol facilitate this ability. [91, 93, 98] Effective DMSO- and FBS-free cryomedia formulations have already been described in literature. [99–102] However, optimal cryopreservation conditions differ between cell lines and need to be optimized individually. [75, 86, 95] For this purpose, type and concentration of cryoprotectant agents need to be screened within a systematic IPPD approach. Using this approach would be highly beneficial since critical process parameter can influence each other. [71, 72, 74, 75, 78] For example, the type and concentration of cryoprotectant agents influences the optimal freezing/thawing profiles. [71] Additionally, they might have an influence on media viscosity, causing complications in subsequent process steps. For example, fill/finish and administration of the product to the patient will be affected if high molecular polymers are used in a concentration which causes an increase in media viscosity.

Bioprinting

Fueled by further developments of three dimensional (3D) printing technologies towards biological applications, bioprinting is considered to be a key technology in the field of tissue engineering and regenerative medicine. The possibility to deposit biological material in a layer-by-layer manner allows for the production of biological 3D structures and nourishes the idea of producing artificial human tissue, which is of great interest to the pharmaindustry and the regenerative medicine sector. [103–105] Potential applications of such artificial tissue are very diverse and include the usage of them as tool for pre-clinical pharmacology and toxicological screenings, as customized patient-specific disease models, as therapeutic graft for tissue repair/replacement or as advanced cell-containing drug delivery systems. [1, 16, 106–108]

Traditionally, design of a desired 3D object is done using a computer-aided design (CAD) approach. Additionally, medical imaging technologies like computed tomography (CT) and magnetic resonance imaging (MRI) enable the creation of patient-specific designs in the field of regenerative medicine. [109, 110] Incorporating living material into such a 3D object represents a sophisticated and highly complex task due to the fragile nature of cells. Addressing these new challenges requires comprehensive knowledge in cell biology, material sciences and engineering. Multiple aspects including e.g. choice of material and 3D printing technology need to be considered, in order to print a "functional" artificial tissue. [106]

A cornerstone in the field of bioprinting is the availability of 3D printing technologies suitable for biological applications. Currently, several 3D printing technologies are applied in the field of bioprinting including robotic dispensing, inkjet printing, and stereolithography. [106, 109, 111] While these technologies differ in their modality, they share the frequent use of hydrogels as bioinks. Hydrogels have traditionally been used in the field of tissue engineer since they provide a cell-friendly environment if proper formulated. However, the hydrogel printability needs to be considered when used as bioink for bioprinting applications as well as compatibility with cell material. Each 3D printing technology differs in terms of bioink properties e.g. rheology, shape fidelity or cross-linking options. Additionally, cell type specific requirement need to be met concerning e.g. mechanical stiffness of the

hydrogel. [106, 109, 112, 113] Thus, a systematic process development approach considering material, printing process and post-printing behavior would be highly beneficial as depicted in **fig. 3.3**. [114–116]

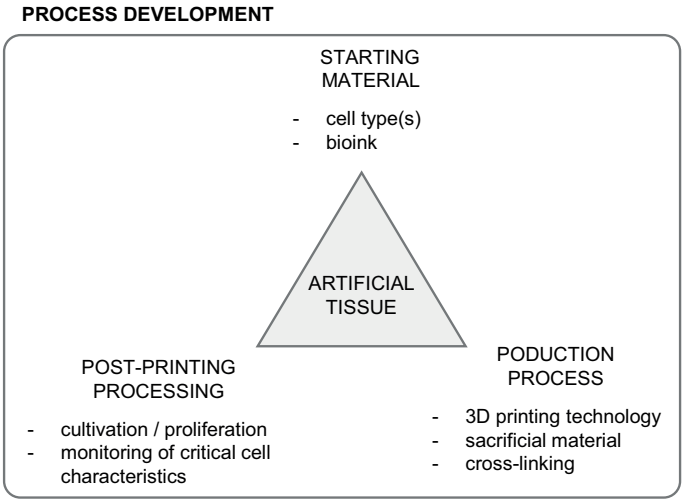

Figure 3.3: Essential consideration in bioprinting process development for the production of an artificial tissue.

For example, bioink compositions providing an optimal cell-friendly environment do often not meet printability requirements. One approach overcoming this hurdle would be to introduce hydrogel components allowing for cross-linking in combination with the use of a sacrificial material. Here, the sacrificial material is optimized towards printability and holds the bioink in shape during the process. During an additional step the bioink becomes cross-linked. [109, 117, 118] Additional considerations may need to be taken into account when bioprinting is used as a platform for commercial production e.g. CoG and material origin of hydrogel components.

3.4 Process Development

Developing an efficient and regulatory compliant manufacturing process is crucial for the commercial success of pharmaceutical products. Thus, a comprehensive and knowledge-based process development approach plays an integral part translating a therapeutic agent from bench to bedside. Currently, the cell therapy industry is lacking process development experience which is associated with translational challenges. However, experiences can be drawn from the protein bioprocessing field. Additionally, using general concepts and tools will facilitate a more directed and sophisticated process development approach for cell therapy products. [1, 69]

Cell therapeutics are inherently expensive products and represent an unique manufacturing challenge due to the highly sensitive nature of the living material. Thus, streamlining the production process and reducing manufacturing costs while maintaining critical quality attributes (CQAs) of the cells is an extremely sophisticated task. [69] Using a knowledge-based approach to link critical process parameters (CPPs) with CQAs would, therefore, be highly beneficial. [1, 119] Such an integrative approach has already been described by the

international council for harmonization of technical requirements for pharmaceuticals for human use (ICH) in the guideline ICH Q8 [120] and is referred to as Quality by Design (QbD). The QbD paradigm combines a scientific knowledge-based product and process development approach with risk assessment, in order to investigate relationships between CPPs and CQAs. The identification and description of these relationships allows for better process understanding and, ultimately, process control to minimize product variations. Thus, QbD will secure the quality, safety and efficacy of a therapeutic product in order to minimize the patient risk. Briefly, the Quality Target Product Profile (QTPP) is the starting point of the QbD framework. It is a summary of essential product characteristics e.g. dosage strength or route of administration and basis for the identification of CQAs which is done subsequently. Additionally, CPPs are analyzed and evaluated during risk assessment in order to develop a control strategy. Thus, a robust and reproducible manufacturing process is achieved by monitoring and controlling CPPs in combination with QCAs. [1, 7, 13, 16, 20, 21, 37, 119–122]
Describing CQAs for cell-based products, however, represents an unique cell characterization challenge due to the complex nature of living cells. [69, 121] Therefore it is important to address the development of a cell characterization strategy in combination with assay optimization/adaption in early process development. [1, 26, 27] The strategy should include simple QCAs like e.g. pH or cell density as well as more complex QCAs like e.g. cell population purity and identity. Additionally, applicability of the developed analytical methods during process development and process monitoring would be highly beneficial. Following these requirements automation of the analytical methods is necessary to eliminate human failure and reduce processing time. [119]

3.4.1 Cell Analytic

The development of an analytical strategy representing all QCAs of a cell-based product is essential within the QbD framework. Thus, the availability of cell analytic methods as tool for process development represents a bottleneck in the field of cell-based products. [27] A pool of different cell analytic methods is currently available and used in e.g. research and drug discovery screening platforms. [123–126] However, method applicability must be validated and optimized for each application individually.
One important cell-based product QCA is cell viability or to be precise, the live cell content. A lot of cell quantification methods are currently available allowing for live cell enumeration. In general, they are classified in indirect and direct methods. [127]
The indirect cell quantification methods are based on the measurement of a signal having linear dependence with the cell number. Depending on their underlying principle, they are further sub-classified in (1) DNA-based, (2) protein-based and (3) metabolite-based methods. The first sub-categorie methods (DNA-based) use fluorescent agents intercalating into the cellular DNA. The intercalation of such agents into the DNA results in an emission of a fluorescence signal showing a linear dependence with the cell number. [127] In general, these kind of methods do not allow for distinguishing between live and dead cells. However, several commercial DNA-based cell quantification assays are commercially available e.g. CyQuant® Direct Cell Proliferation. This assay combines a DNA-binding fluorescent dye with a quenching agent only penetrating dead cell membranes. Suppressing

the dead cell signal facilitates live cell quantification. [128, 129] Total protein concentration (protein-based) can also be used for cell quantification. However, using these method does not facilitate live cell number. [127] In contrast, metabolite-based methods exclusively enable estimation of live cell number since dead cells lack of metabolic activity. Several metabolic assays are commercially available, including the colorimetric assays such as e.g. MTT (3-(4,5-dimethylthiazole-2-yl)-2,5-diphenyl- tetrazoliumbromide) and AlamarBlue (resazurin-based) and ATP-based (adenosine triphosphate) methods. While the colorimetric assays rely on the metabolic transformation of a substrate (e.g. AlamarBlue: resazurin (blue) transformed into resorufin (pink)), ATP-based assays need a luminescence measurement. ATP is present as energy reservoir in living cells and can be used as co-factor for the enzyme luciferase in the presence of Mg^{2+}. Briefly, luciferin is catalyzed by the enzyme luciferase to oxyluciferin in the presence of Mg^{2+} and ATP, resulting in a luminescence signal. The signal can be measured and correlates with the ATP content and, subsequently, with live cell content. [123, 124, 130] Knowing the underlying mechanism is important for the selection of a cell quantification assay for cell-based products, since the mechanism directly correlates with the assay applicability and potential drawbacks. [125, 126, 131] For example, metabolic assays are prone to deviate from correct cell number since the metabolic activity varies e.g. during cell cycle and age. Additionally, metabolic assays tend to be not suitable for 3D applications. [123, 130, 131] DNA-based assays tend to be more reliable for non-synchronized cell cultures. [132]
The direct methods include several techniques. The most commonly used is the microscopic cell counting. Manual microscopic cell counting is routinely performed in cell culture laboratories using a hemocytometer in combination with dye exclusion, in order to distinguishing between live and dead cells. Trypan blue is such a dye which cannot penetrate the membrane of live cells, thus, only dead cells become stained blue. Additionally, impedance-based cell quantification setups and light scattering-based cell quantification using flow cytometry methods are available. [127, 128, 133]
Especially, flow cytometry is considered to be a highly beneficial analytical tool for cell-based products, since it allows for analyzing multiple cell characteristics and parallel cell quantification. [27, 128, 133] It is basically a flow-through fluorescence microscope. Briefly, cell samples are hydrodynamically focused, thus, single cells pass the laser beam. The emitted light is then collected via an array of photo-detectors and optical filters and visualized as histograms or dot-plots. Depending on the equipment set up (multiple laser and filter) and staining strategy, cell morphology, cellular physiology, surface and intracellular protein expression can be analyzed. For example, surface protein expression is analyzed using fluorophore-labeled antibodies. [134] A simultaneous cell quantification is, however, not routinely performed using a flow cytometer. Different strategies are available to facilitate parallel cell quantification. Spiking samples with a counting standard facilitate the enumeration of the cell number and represents a low investment solution. [133] Equipping the flow cytometer with an autosampler is associated with a higher investment. However, using an autosampler allows for cell quantification if a defined sample volume is measured and calibrated. [128] Another major advantage of a flow cytometer equipped with an autosampler is the HTS applicability and automation. [134, 135] The usefulness of HTS flow cytometry has already been demonstrated by different HTS applications e.g. stem cell

research [136, 137], drug screening [135] and cell downstream process development [60]. Establishing an analytical strategy for process development of cell-based products is extremely important. In general, the strategy should represent all QCAs and, therefore, comprise several analytical methods. The applicability of each method must be evaluated and, if necessary, optimized for each application. Several requirements need to be considered early on. For example, the underlying mechanisms of a method should be known. Automation and HTS compatibility is also a general requirement for the applicability of a cell characterization method in process development for cell-based products. [125, 126, 131] By using e.g. autosampler, multiwell plates and protocols without wash steps a lot of methods can be optimized towards HTS applicability. [124, 132] Additionally, method validation must be performed before an analytical method can be implemented in the process development. The validation should be performed according to the guideline ICH Q2 which comprises the evaluation of method accuracy, precision, specificity, detection limit, quantification limit, linearity, range and robustness. [138] Especially, the evaluation of robustness towards process related components is important. For example, cell quantification assays may interfere with media components or media characteristics (e.g. density, viscosity) may cause alterations when liquid handling is required. [123, 128]

3.4.2 High-Throughput Screening (HTS)

The usage of high-throughput screenings (HTSs) as a scientific tool is state-of-the-art for over two decades in various disciplines including e.g. stem cell research [136, 139], compound library screenings in pharmaceutical drug discovery campaigns [125, 126, 140–146] and toxicology screening of biomaterial for e.g. tissue engineering applications [147]. Additionally, the pharmaceutical industry is tackling cost and time pressure using HTS in process development for biopharmaceuticals. [148–155] This approach is referred to as high-throughput process development (HTPD). [148] Typically, a HTS platform is developed implementing the approaches of automation, miniaturization, parallelization as well as standardization. The core-piece of such a platform is most of the time a robotic liquid handling station with an integrated analytical strategy. Usually, multiwell plates (e.g. 96 Well or 384 Wells) are used as standardized consumables. An integral part of the platform development is establishing and validating a suitable scale-down model. For biopharmaceutical HTPD there are scale-down models for up and downstream process units already available e.g. scale-down bioreactor models for optimization of optimal cultivation process parameter [154, 155] and column scale-down models for chromatography optimization [152, 153]. Additionally, a data handling and storage strategy needs to be implemented in order to interpret the results correctly. [141, 147, 148, 150, 151]
The development of a HTS platform is a highly sophisticated task, since it is quite complex and requires expensive equipment. Thus, expertise is necessary in order to prevent failure and/or misinterpretation of experimental data. [142, 144] Another bottleneck during HTS platform development is the availability of inexpensive analytical methods. An analytical strategy addressing all scientific questions need to be developed and implemented. Such a strategy is typically tailored for each HTS campaign and comprises several analytical methods which all need to be suitable and validated in advance. [125, 141, 144, 147, 148, 156]

However, once a HTS platform is developed, systematic screenings with low sample volume can be performed in a short period of time. Due to automation, human failure is minimized resulting in higher reproducibility and accuracy. Additionally, using a HTS platform means standardization of screening protocols resulting in a better comparability between different HTS campaigns. [140, 141, 147] Thus, HTS represents a highly beneficial tool in process development especially in early process development in a QbD environment, where process knowledge needs to be established with only little material. [148–150]
A HTPD approach would be highly valuable for cell-based therapeutics. Streamlining process development while generating process knowledge would help to overcome translational challenges. Yet, the automated handling of living material will naturally increase the complexity of a HTS platform. However, experiences were already made with cell-based HTS assays for toxicity screenings and upstream process development for biopharmaceuticals. [147, 151, 154, 155] This expertise should be applied during process development for cell-based therapeutics.

3.4.3 3D Printing

The possibility to build 3D objects in a layer-by-layer manner has created much excitement in the last decades and is summarized in the umbrella term 3D printing. It is even believed that 3D printing is a disruptive technology and might revolutionize the way of manufacturing, contributing to another industrial revolution. [157–159]
The first 3D printing method, namely stereolithography, was described and patented by *Hull* in the 1980s. [160, 161] Stereolithography uses the principle of photopolymerization. Here, a liquid photosensitive monomer resin is placed in tank while thin layers of resin are cured via ultraviolet (UV) radiation on a building platform. By moving the building platform step-wise in z-direction, a 3D object is manufactured. [105, 162–164] Due to the fast evolving and highly innovative nature of the 3D printing field, nowadays various methods besides stereolithography are available including the prominent methods e.g. inkjet printing and fused deposition modeling (FDM). The inkjet technology originally derived form 2D applications. In the field of 3D printing, liquid polymer resin is deposited by a printhead in x- and y-direction (2D), which is repeated for each layer. Usually, liquid photosensitive monomer resins are used and also cured by UV radiation. [163, 164] While stereolithography and inkjet technologies are using liquid polymer resin, FDM printers are equipped with solid polymer filament. The filament is fed to a moving printhead (x- and y-direction) and simultaneously liquified due to the printhead temperature which is usually set about 1 °C higher than the melting point of the filament material. Thus, a thin layer of material is deposited on the built-table which is moved in z-direction in order to create the 3D object. [105, 162–164] Fueled by adaptation of 3D printing methods to all kind of economy/society branches, nowadays, commercial 3D printers are available in different price ranges. Additionally, 3D contract manufacturer services can be used. [157] The application of 3D printing ranges from e.g. aerospace, automotive, prosthetic, dental implants, art, education to life science/biotechnology. [158, 165, 166]
3D printing enhances an inexpensive and creative problem solving in a short time, which is highly contributing to innovations in academic biotechnology/life science applications. [167] For example, 3D printed replication master for microfluidic devices [168, 169] or direct 3D

printing of microfluidic devices [170, 171] speed up design optimization. Additionally, a surface treatment of 3D printed devices can be performed if necessary e.g. immobilization of enzymes on 3D printed bioreactor surfaces for enzyme cascade testing [172] or incorporating an active substance in the raw material prior to printing [173]. A huge advantage of the 3D printing approach is the possibility to tailor tools or labware for the specific applications e.g. designing and printing a tailored multiwell plate to enhance oxygen transfer [174, 175] or designing a simple orientation tool for automated zebra fish screening [176]. While for the orientation tool for automated zebra fish screening a rapid prototyping approach was used, 3D printed end-use devices for integration of automated screening platforms have already been described e.g. a Tip2Worl interface for integration of a commercial density sensor in a robotic liquid handling station platform [177] or designing and 3D printing of a stalagmometer for automated protein hydrophobicity determination using a HTS platform [178]. Those examples highlight the power and usefulness of 3D printing as a tool in HTPD.

The main advantages of using 3D printing as a tool in HTPD are the design freedom, the inexpensive and rapid production of tailored equipment. Additionally, the 3D printing approach also digitises 3D objects which is another advantage. In general, 3D printing starts with designing a 3D object using the computer-aided design (CAD) approach or medical 3D information of e.g. computed tomography (CT) scans. This information is than transferred into the stl-format which is further sliced to generate a g-code which is used by 3D printers. The digital nature is highly beneficial to share the designed objects within collaborations and for storage. Thus, the file can be printed on-demand which revolutionizes the supply chain management. Another advantage is that theoretically one 3D printer can manufacture a wide range of different designs. [157–159, 161, 162, 164, 167, 174, 175]

However, these advantages are only beneficial if the 3D printing approach is implemented in the work flow of a company or academic institute e.g. scientists need to be trained in CAD if they want to use the whole benefit of 3D printing. [167] Once the 3D approach is implemented the limitation of printable material represents a major challenge. In the beginning, mainly plastic materials were used for 3D printing. However, the field is constantly evolving and new materials and corresponding 3D printing methods are described. For example, metal printing is nowadays an option e.g. for orthopedic implant applications. [165, 179, 180] In general, the material needs to be compatible with the experimental set up which can differ for each biotechnological application. For example, martial which comes in contact with cells needs to be biocompatible [175, 179] while other applications need solvent resistant materials [171]. Thus, an integrative approach is necessary for a 3D printing campaign considering the experimental requirements, suitable material and 3D printing method. Currently, another challenging aspect of 3D printing is the need for post-processing of the printed objects which can be difficult and cause time delay. [158, 165] Other aspects like cyber security, intellectual property, real-time monitoring of the 3D printing process and validation of 3D printed object quality are rarely discussed at the moment, but will probably become more prominent in future. [158, 181] While those challenges are constantly tackled by new inventions, the 3D printing field is considered to become even more important. An exciting trend is expected towards printing

of functional devices due to hybrid material printing e.g. sensors which would be highly beneficial for biotechnological applications and the HTPD approach. [162, 180]

CHAPTER 4

Research Proposal

Cell-based therapeutics have gained increasing interest over the last decades since they enable the replacement of damaged or ill-functioning tissue. They are even believed to have a huge impact on the healthcare sector and are considered to be the fourth pillar in patient treatment besides small molecules, medical devices and biopharmaceuticals. While first generation cell-based therapeutics are already on the market, the inherent complexity of living cells and lack of experience are still representing major obstacles translating a promising cell-based therapeutic from academia to a commercially available product. In order to tackle these translational challenges, problems that have arisen during product development so far, were analyzed and underlying causes could be identified by the cell therapy community. In general, three categories of translational challenges could be identified: (1) pre-market challenges, (2) manufacturing challenges and (3) post-market challenges. However, the general lack of experience in combination with an heuristic process development approach could be identified as a major root-cause in all three categories.
Therefore, one key question is whether process development tools and strategies from the pharmaceutical industry can be applied for cell-based products. By using these tools and strategies the process development will be streamlined and optimized by enabling a systematic and more directed process development approach which is highly beneficial for the cell therapy industry and will contribute to a more widespread use of cell-based therapeutics. Thus, the main focus of this thesis is to validate whether the application of general process development tools from the pharmaceutical industry is possible for cell-based products.
The first part of this thesis is focusing on the unit operation cell separation. Here, the availability of scalable and label-free separation methods represents a bottleneck in process development. Evaluating alternative cell separation methods will open up new possibilities in downstream processing. Cell partitioning in ATPS represents an alternative method. However, the partitioning mechanism is yet not completely understood, resulting in a high screening effort for optimal key process parameter. Consequently, the question arises if HTS-platforms can be used to overcome the screening bottleneck. For this purpose, a previously developed HTS-platform is to be used to systematically investigate the influence of key parameter e.g., polymer molecular weight and tie-line length on cell partitioning behavior. While process development is normally associated with high investment costs, the usage of 3D printing methods might decrease the financial risk during process development. Thus, the question arises if 3D printing methods can be used as manufacturing tool in an early process development stage since they enable a fast and relative cost-effective

production of prototypes and equipment parts. For this purpose, 3D printing is to be used for the development of a microfluidic set up, to investigate the possibility for a technology transfer from batch ATPS cell partitioning into a microfluidic flow-through-mode. Using 3D printing technologies enables a faster and cheaper implementation of process equipment contributing to "Time To Market" demands.
The second part of this thesis is focusing on different unit operations in the field of cell formulation, namely, cell cryopreservation and bioprinting. Currently, cryopreservation is already used whenever cells need to be accessed with unaltered characteristics over a long period of time, e.g. for cell culture maintenance and biopharmaceutical, since it allows for long-time storage of living material. However, there is an urgent need for cryopreservation process optimization for clinical applications, especially, the formulation of cryomedia. This thesis is tackling the question if a predictive tool box for cryomedia evaluation towards process performance can be used for this purpose. Such an approach will enable a fast screening of cryomedia candidates with an decreased sample volume. Additionally, the possibility of implementing an automated image processing tool for the characterization of freezing/thawing profiles is to be investigated. Such a tool would be highly beneficial in order to gain process knowledge and might be used for optimization purpose. While cryopreservation is a storage approach, bioprinting methods can be used for manufacturing of artificial 3D tissue. The relatively young field of bioprinting is considered to have a huge impact in life sciences. However, huge effort in bioprinting process development need to be done for clinical applications. One important key factor is the integration of an analytical strategy in order to evaluate/monitor critical cell parameter (e.g. cell viability) during bioprinting process development. Flow cytometry is a versatile and powerful cell characterization tool, since it allows for analyzing multiple critical cell parameter in parallel and is capable of automation. Thus, the question arises whether it can also be used as analytical tool in the field of bioprinting. To answer this question, an analytical strategy to evaluate critical cell parameter (e.g. cell viability) in bioprinting process development by means of flow cytometry shall be developed.
In summary, the presented thesis aims at a systematic and more directed process development approach for cell-based therapeutics. This is accomplished by means of using the following process development tools and strategies: a HTS approach enabling an automated and systematic process optimization using low sample volume, applying 3D printing to speed up process set up development, miniaturization and developing of an analytical strategy to investigate critical bioprinting process parameter.

CHAPTER 5

Comprehensive Overview of Publications & Manuscripts

6 | Cell Separation in Aqueous Two-Phase Systems Influence of Polymer Molecular Weight and Tie-Line Length on the Resolution of Five Model Cell Lines

Sarah Zimmermann*, Sarah Gretzinger*, Philipp K. Zimmermann, Are Bogsnes, Mattias Hansson, Jürgen Hubbuch

* *Authors contributed equally*

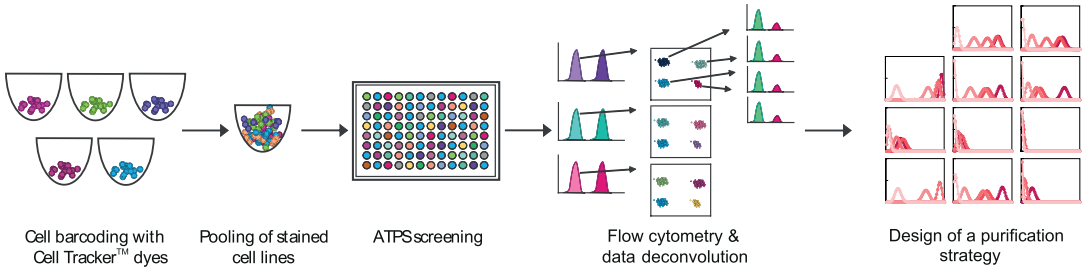

Aqueous two-phase systems (ATPS) have been a useful tool in downstream processing for cellbased products, since they facilitate labelfree, scalable, and costeffective separation of cells. Here, the authors report the extension of the previously developed high-throughput screening (HTS) platform by a cell barcoding procedure, to enable multiplexed cell partitioning analysis. Further, a case study demonstrated the influence of polymer molecular weight and tie-line length on the resolution of five model cell lines using a countercurrent distribution model.

Biotechnol J. 2018 Feb;13(2). doi: 10.1002/biot.201700250. Epub 2017 Nov 22.

7 | Application of Additive Manufacturing as Tool for Process Development in Biotechnology: A Case Study

Sarah Gretzinger, Stefanie Limbrunner, Pascal Baumann, Jürgen Hubbuch

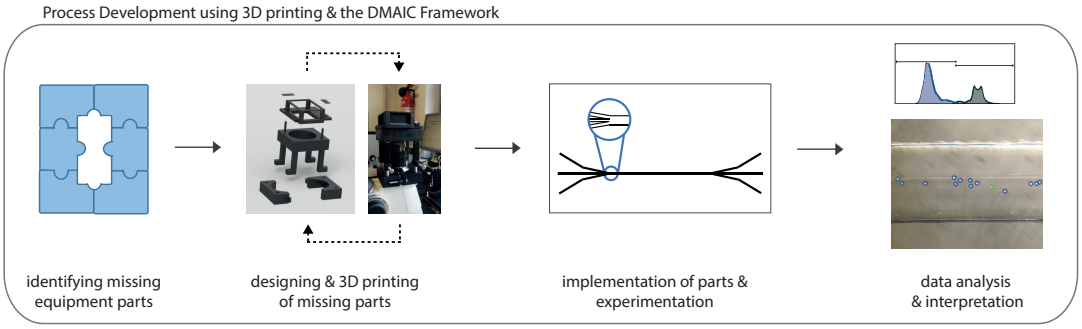

Additive manufacturing technologies represent a promising tool in biotechnology process development since they allow for the fast acquisition of tailored equipment. In this study, a successful technology transfer from batch cell partitioning in ATPS data was performed towards a microfluidic flow-through mode using the additive manufacturing approach. First, missing equipment parts were identified, designed and manufactured using different 3D printer. Subsequently, the tailored equipment was implemented in the process setup consisting of conventional laboratory equipment and experiments were conducted. The technology transfer study was performed using the DMAIC (Define, Measure, Analyze, Improve, Control) framework. Thus, critical process parameter, namely, cell load and fluid velocity were identified influencing cell partitioning in ATPS flow-through mode in comparison to the batch data.

in preparation

8 | Automated Image Processing as an Analytical Tool in Cell Cryopreservation for Bioprocess Development

Sarah Gretzinger, Stefanie Limbrunner, Jürgen Hubbuch

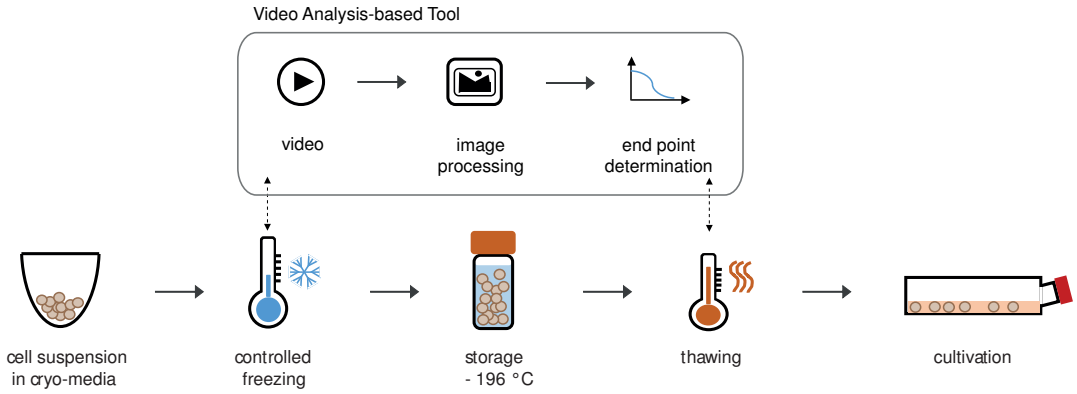

In this study, a video-based analytical tool was developed for the characterization of freezing and thawing behavior in cryopreservation process development. Evaluation of the usefulness and flexibility of the developed tool was done based on a scale up case study with the cell line INS-1E. Here, the influence of sample working volume on process performance was investigated. Increasing the volume from 1 mL to 2 mL led to a delay in freezing and thawing behavior resulting in a cell recovery loss. We believe that the developed tool is powerful and will facilitate more directed and systematic cryopreservation process development.

Bioprocess and Biosystems Engineering Feb 2019; 42, doi:10.1007/s00449-019-02071-3

9 | A Tool Box for the Prediction of Media Process Performance for Cell Cryopreservation

Sarah Gretzinger, Stefanie Limbrunner, Jürgen Hubbuch

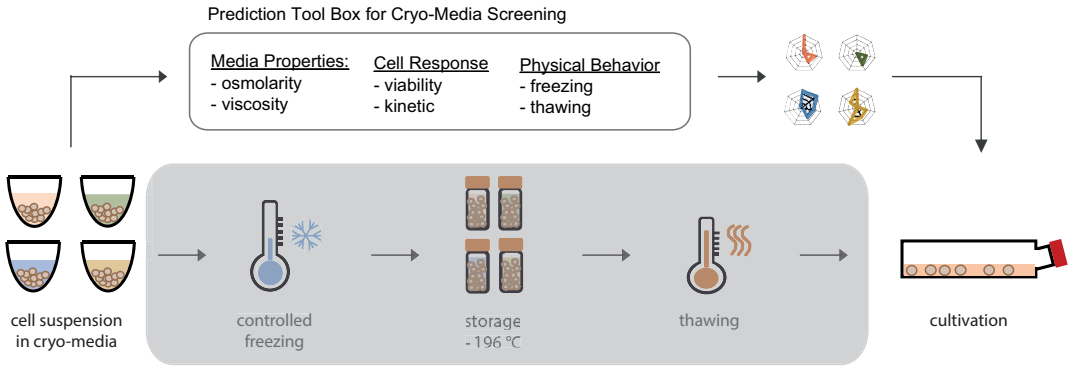

Cell Cryopreservation is an important unit operation whenever cell long-time storage is required. While the cryopreservation process and its critical parameter is well described in literature, performing cell cryopreservation for clinical applications are facing higher requirements. One of these is the cryomedia formulation without the use of toxic or animal-derived components. Thus, the commonly used cryoprotectans dimethyl sulfoxide (DMSO) and fetal bovine serum (FBS) are excluded from use. Cryoprotectant, however, are crucial for cell survival. For this reason, screening for optimal, alternative cryomediaformulations are necessary. In this study, a tool box for the prediction of cryomedia process performance was developed in order to speed up development time. The tool box enables the characterization of media properties, cell response and physical behavior. A case study, using the developed tool box, was performed with four cryomedia including a positive control (DMSO & FBS as cryoprotectant), negative control (culture media) and two commercially available DMSO-free cryomedia. The tool box data indicated that the commercial Biofreeze® media shows inferior performance for INS-1E, while the second commercial cryomedia CryoSOfree™ is clearly a possible candidate.

in preparation

10 | 3D Bioprinting - Flow Cytometry as Analytical Strategy for 3D Cell Structures

Sarah Gretzinger, Nicole Beckert, Andrew Gleadall, Cornelia Lee-Thedieck, Jürgen Hubbuch

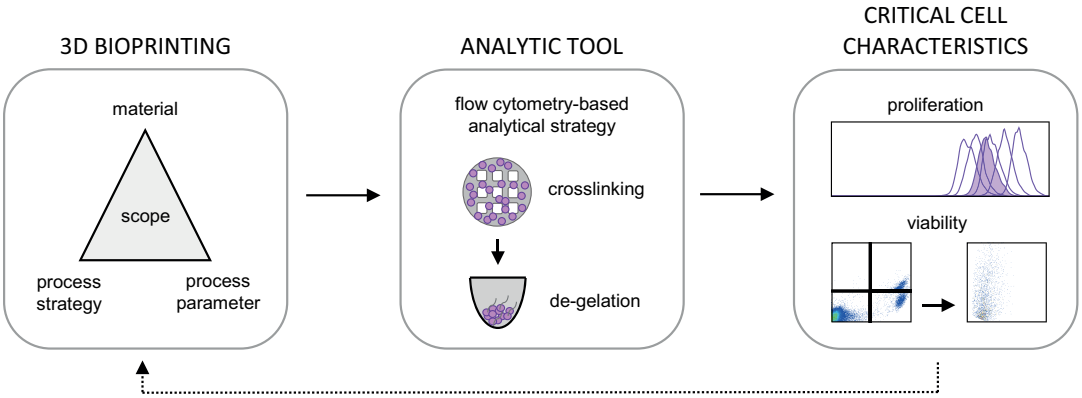

Bioprinting is considered to be a key technology in the field of tissue engineering and regenerative medicine since it allows for the manufacturing of 3D cell-laden objects. However, extensive process development in terms of material, process strategy and process parameter is likely to be necessary before 3D printed, artificial tissue becomes clinically relevant. In this study, a flow cytometry-based analytical strategy (destructive method) was developed regarding critical cell characteristics including cell viability and proliferation. The developed strategy can be used as analytical tool for bioprinting process development and might even be integrated in an automated screening platform since it is HTS-applicable.

Bioprinting 2018 Sep; 11, e00023. https://doi.org/10.1016/j.BPRINT.2018.e00023

CHAPTER 6

Cell Separation in Aqueous Two-Phase Systems Influence of Polymer Molecular Weight and Tie-Line Length on the Resolution of Five Model Cell Lines

Sarah Zimmermann[*,1], Sarah Gretzinger[*,1,2], Philipp K. Zimmermann[1], Are Bogsnes[3], Mattias Hansson[4], Jürgen Hubbuch[1,**]

[1] Institute of Engineering in Life Sciences, Section IV: Biomolecular Separation Engineering, Karlsruhe Institute of Technology (KIT), Karlsruhe, Germany

[2] Institute of Functional Interfaces (IFG), Karlsruhe Institute of Technology (KIT), Eggenstein-Leopoldshafen, Germany

[3] Biopharm Purification Development & Virology, Novo Nordisk A/S Gentofte, Denmark

[4] Diabetes Research, Novo Nordisk A/S, Måløv, Denmark

[*] Authors contributed equally
[**] Corresponding author. Email: juergen.hubbuch@kit.edu

Biotechnol J. 2018 Feb;13(2). doi: 10.1002/biot.201700250. Epub 2017 Nov 22.

Abstract

The availability of clinical-scale downstream processing strategies for cell-based products presents a critical juncture between basic research and clinical development. Aqueous two-phase systems (ATPS) facilitate the label-free, scalable, and cost-effective separation of cells, and are a versatile tool for downstream processing of cell-based therapeutics. Here, we report the application of a previously developed robotic screening platform, here extended to enable a multiplexed high-throughput cell partitioning analysis in ATPS. We investigated the influence of polymer molecular weight and tie-line length on the resolution of five model cell lines in charge-sensitive polyethylene-glycol (PEG)-dextran ATPS. We show, how these factors influence cell partitioning, and that the combination of low molecular weight PEGs and high molecular weight dextrans enable the highest resolution of the five cell lines. Furthermore, we demonstrate that the separability of each cell line from the mixture is highly dependent on the polymer molecular weight composition and tie-line length. Using a countercurrent distribution model we demonstrate that our screenings yielded conditions that theoretically enable the isolation of four of the five cell lines with high purity (>99.9%) and yield.

Keywords: aqueous two-phase systems (ATPS), cell separation, high-throughput flow cytometry, high-throughput screening, polymer molecular weight, tie- line length

6.1 Introduction

Cell-based therapeutics for a variety of diseases and from a variety of cell sources have made their way to clinical trials. The availability of clinical-scale downstream processing strategies for cell-based products represents a crucial juncture between basic research and clinical development. For clinical applications, cell-based products often need to be enriched to high purities, since certain contaminants can cause severe side effects, such as teratoma formation or graft-versus-host-disease (GvHD). [2, 182–186] The most widely applied cell purification methods are based on affinity-purification. These methods, however, require large amounts of clinical-grade antibodies, presenting a significant cost-factor. [185, 187, 188] Likewise, antibody-labels remaining on the cell surface, pose considerable regulatory obstacles for the treatment of patients, as they may cause adverse reactions. [184, 185] Aqueous two-phase systems (ATPS) present a gentle, cost-effective, scalable, and label-free method for cell purification. ATPS are aqueous solutions consisting of one or more compounds, e.g. different polymers, which form two immiscible phases above a certain threshold (e.g. concentration, temperature). The two phases have distinct physicochemical properties, consequently, biomolecules partition between them according to their respective physicochemical properties. By now, they are well established in downstream processing of biopharmaceuticals, such as protein- and DNA-based pharmaceuticals. [54, 189, 190] Polyethylene-glycol (PEG)-dextran ATPS have been successfully used to separate cells according to their surface properties, and it is well established that ATPS facilitate the separation of different cell types with high selectivity and resolution. [53, 54] In multi-stage experiments, e.g. countercurrent distribution (CCD), even complex cell mixtures were effectively separated. [54, 66] While the mechanisms underlying cell partitioning in ATPS are not fully understood, there is strong evidence that surface charge and lipid composition play a major role in cell separation. [53, 54] Several independent publications indicate that surface charge-dependent cell separation is possible in ATPS containing isotonic concentrations of phosphate (so called charge-sensitive ATPS), and partitioning coefficients could be correlated to the cells electrophoretic mobility. Charge-independent cell separation, on the other hand, can be achieved in ATPS containing isotonic concentrations of NaCl (charge-insensitive ATPS), and partitioning coefficients have been correlated with the cells membrane lipid composition, i.e., membrane hydrophobicity. [53, 54, 191, 192] One of the current theories states that these phenomena are based on different partitioning properties of the respective salts. While sodium chloride partitions almost equally between the phases, sodium phosphate has a stronger affinity to the dextran-rich bottom phase, resulting in an interfacial electrostatic potential difference (Donnan potential). [193, 194] The Donnan potential is highly dependent on salt-composition, tie-line length (TLL), polymer type, and molecular weight. [53, 54, 195] At the same time, TLL and polymer molecular weight significantly influence cell partitioning when using salts that partitioning equally between the phases. [53, 54] A key factor in cell partitioning is the interfacial tension [196], which is directly correlated with TLL and polymer molecular weight [197]. The interaction of all these parameters in respect to cell partitioning and the resolution of different cell populations is, however, unclear. In previous work, we developed an integrated high-throughput screening (HTS)-platform for the analysis of cell partitioning in ATPS.

We investigated the influence of TLL, salt composition, and pH on the resolution of several model cell lines and described strategies for fast and directed HT-downstream process development [60]. In this work, we used this HTS-platform to investigate the influence of the PEG and dextran molecular weights in dependence of the TLL on cell partitioning in ATPS. Using different CellTracker dyes in a combinatorial fashion for cell barcoding, enables multiplexing of several cell lines in a single experiment, and results in a substantial decrease in time and material consumption. Moreover, batch variability can be eliminated by analyzing numerous cell lines in the same experiment. The present work describes how TLL in dependence of the polymer molecular weight influence the resolution of five barcoded model cell lines in charge-sensitive ATPS, characterizes suitable screening ranges and shows how these data can be used to design purification strategies for the various cell populations.

6.2 Experimental Section

6.2.1 Disposables

For ATPS preparation, 1.3 mL deep well plates (Nalgene Nunc, Rochester, NY, cat. 260252) and for flow cytometry, 96-well U-bottom plates (BD Falcon, Franklin Lakes, NJ, cat. 353910) were used. Polypropylene flat-bottom microplates (Greiner Bio-One, Kremsmünster, Austria, cat. 655261) were used for all other purposes.

6.2.2 Software and Data Processing

Evoware 2.5 SP2 standard (Tecan, Crailsheim, Germany) was used to control the Tecan Freedom Evo 200 liquid handling station. Advanced applications such as sampling and cell resuspension were realized via visual basic scripts that were directly fed into Evoware. For data storage Excel 2013 (Microsoft, Redmond, WA, USA) was used. Matlab R2014a (The MathWorks, Natick, ME, USA) and Excel 2013 were used for data evaluation and visualization. Statistical data analysis was performed with Matlab R2014a. The BD LSR Fortessa Cell Analyzer was controlled using BD FACSDiva 8.0 (BD Biosciences, San Jose, CA, USA). In addition, BD FACSDiva 8.0 was used to calculate the compensation of spectral overlap and for raw data analysis. Flow cytometry data visualization was performed with Flow Jo V10 (Tree Star, Ashland, OR, USA).

6.2.3 Preparation of Buffers and Stock Solutions

For the preparation of buffers and stock solutions, ultra-pure water (0.55 μS/cm) obtained from an Arium®proUV water system (Sartorius Stedim Biotech, Goettingen, Germany) was used. Stock solutions of 2 and 20 % dextran 70,000 (Carl Roth Kalrsruhe, Germany, cat. 9228.2, Batch No.: 215229323), 2 and 20 % dextran 500,000 (Pharmacosmos A/S, Holbaeck, Denmark, cat. 5510 0500 9007, Batch No.: HT3229), 40 % PEG 4,000 (Merck Millipore, Billerica, MA, USA, Cat. 8.17066.5000, Batch No.: K46660006524), 30 % PEG 8,000 (Sigma Aldrich, St. Louis, MO, USA, cat. P2139, Batch No.: 059Ko121), and 20 % PEG 20,000 (Sigma Aldrich, cat. 95172-250G-F, Batch No.: BCBP5677V) were prepared in ultra-pure water and dissolved on a magnetic stirrer overnight. 500 mM sodium phosphate (NaPi) buffer stock solutions with pH 6.6, and 7.4 were prepared as described before [60]. Sodium chloride (NaCl) (Merck Millipore) was prepared as a 500 mM stock

solution. Sterile filtration (Ø 0.22 μm) was performed for all buffers and stock solutions. Polymer solutions were stored at 4°C whereas buffers were stored at room temperature. The flow cytometry staining buffer was prepared directly before use and consisted of phosphate buffered saline (PBS) (Life Technologies, Carlsbad, CA, USA) supplemented with 2 mM EDTA (Life Technologies) and 0.5 % bovine serum albumin (BSA) (Miltenyi Biotech, Bergisch Gladbach, Germany).

6.2.4 Cell Culture

Unless otherwise stated cell culture reagents were purchased from Life Technologies. The murine fibroblast cell line L929 was purchased from CLS (Cell lines Service Eppelheim, Germany, cat. 400260), and the rat ileum cell line IEC-18 was purchased from ATCC (cat. CRL-1589). The human lung carcinoma cell line A549 (ATCC, cat. CCL-185) and the human colorectal carcinoma cell line HCT 116 (ATCC, cat. CCL-247) were a gift from Prof. Hartwigs lab. The rat beta-cell line INS-1E [198] was kindly provided by Prof. Maechler from the Department of Cell Physiology and Metabolism at the University of Geneva Medical Centre, Switzerland. All cell lines were propagated at 37°C in a humidified 5 % CO_2 incubator. L929, A549 and HCT 116 cells were grown in DMEM with GlutaMAX supplemented with 10 % FBS and 1 % Penicillin/ Streptomycin. IEC-18 cells were cultivated in DMEM with GlutaMAX supplemented with 5 % FBS, 1 % NEAA, 1 % Penicillin/ Streptomycin, and 0.1 U per mL bovine insulin (Sigma-Aldrich, cat. I1882). INS-1E cells were cultivated in RPMI 1640 with GlutaMAX supplemented with 10 % FBS, 1 % sodium pyruvate, 1 % Penicillin/ Streptomycin, 10 mM HEPES, and 50 μM beta mercaptoethanol (Sigma Aldrich). All cell lines were split every 3-4 days to a concentration of 2 x 10^4 cells per cm^2 for a maximum of 20 passages, with the exception of INS-1E which were seeded at a concentration of 7 x 10^4 cells per cm^2. In order to obtain maximal reproducibility between different screenings, all cell lines were seeded at a density of 2.7 x 10^5, 48 hours prior to the screening.

6.2.5 Cell Barcoding and Viability Staining

In order to enable multiplexing of several cell lines and eliminate inter-experimental variability, the five cell lines were stained with different CellTracker (CT) dyes (LifeTechnologies) in a combinatorial fashion. For staining, cells were trypsinized and resuspended in serum-free medium to a final concentration of 2 x 10^6 cells per mL. The CellTracker dyes were added to a final concentration of 3 μM for CellTracker Violet BMQC, 0.2 μM for CellTracker Green CMFDA, and 0.05 μM for CellTracker Deep Red, respectively. The cell lines were stained in a combinatorial fashion as follows: L929: CellTracker Violet BMQC and CellTracker Green CMFDA, INS-1E: CellTracker Deep Red, IEC-18: CellTracker Deep Red and CellTracker Violet BMQC, HCT 116: CellTracker Violet BMQC, A549: CellTracker Deep Red and CellTracker Green CMFDA. The cells were stained at 37 °C for 30 min and subsequently resuspended in culture medium and incubated at 37 °C for 20 min to remove excess dye molecules and inactivate unbound, amine-reactive CellTracker Deep Red dye molecules. Prior to flow cytometric analysis, cells were stained with the viability dye 7-AAD (Biolegend, San Diego, CA, USA), according to the manufacturers instructions. Dead cells were gated using heat inactivated controls (70 °C, 10 min).

6.2.6 Cell Quantification using High-Throughput Flow Cytometry

Flow cytometric cell quantification was performed as previously described [60].

6.2.7 Liquid-Handling Calibration

Liquid handling calibration was performed for all buffers and stock solutions as described previously [60]. Calibration was performed in the range of 50-1,000 μL. Variation coefficients were below 1.6 % for all aqueous solutions and below 3 % for the more viscous polymer solutions.

6.2.8 HT-Binodal and Tie-Line Determination

A HTS-method for binodal determination based on could-point titration has previously been established in our group and was performed as described [60].

6.2.9 Automated High-Throughput Screening of Cell Partitioning in Aqueous Two-Phase Systems

The automated HTS-method was used as described in a previous publication [60]. The entire HTS was performed on a Tecan Freedom Evo® 200 liquid-handling station (LHS). Subsequently, the sample plates were transferred to the high-throughput sampler of the BD LSR Fortessa for cell quantification and analysis. ATPS were prepared in a 1.3 mL 96-well plate with a final volume of 637 μL. After mixing and addition of cells (1 x 10^6 cells per well), phases were allowed to settle by gravity (20 min, RT) and sampling was performed as previously described. During the sampling procedure samples were fivefold diluted in staining buffer. After adding an equal volume of staining buffer containing 7-AAD for viability staining and incubation for 10 minutes at RT in the dark, flow cytometric analysis was performed.

6.2.10 Statistical Data Analysis

Pre-processing of screening data was performed as described in previous work [60]. A two-sided students t-test was performed to determine differences in means, provided that equal variances were asserted by an F-test. Error propagation was considered throughout our analyses [199].

6.3 Results

We previously developed a fully automated screening set-up that integrates cell partitioning in ATPS on a Tecan liquid-handling station and cell quantification and analysis at the single cell level using high-throughput flow cytometry. [60] In the present study, we investigated the influence of PEG and dextran molecular weight at a defined TLL on the resolution of five cell lines in charge-sensitive ATPS. The following cell lines were chosen for this study: the murine fibroblast cell line L929, the rat ileum cell line IEC-18, the human lung carcinoma cell line A549, the human colorectal carcinoma cell line HCT 116, and the rat beta-cell line INS-1E. Due to their different origins, we expected these cell lines to differ significantly in their cell surface properties. We used a barcoding strategy that enabled multiplexing of several cell lines in a single experiment **(fig. 6.1 A)**. By using three different CellTracker dyes in a combinatorial fashion, the cell lines were successfully barcoded **(fig. 6.1 B)**. Spill-over between barcoded cell lines can result in inaccurate

analysis of cell partitioning, however, this was not observed here. We determined that spill-over was < 0.1 % in all experiments. The gating-strategy used for data deconvolution is shown in **fig. 6.2**. Partitioning factors were calculated based on the live cell counts of each cell line. Cell viability was high throughout the screening (> 98 % viable cells), and comparable between the cell lines.

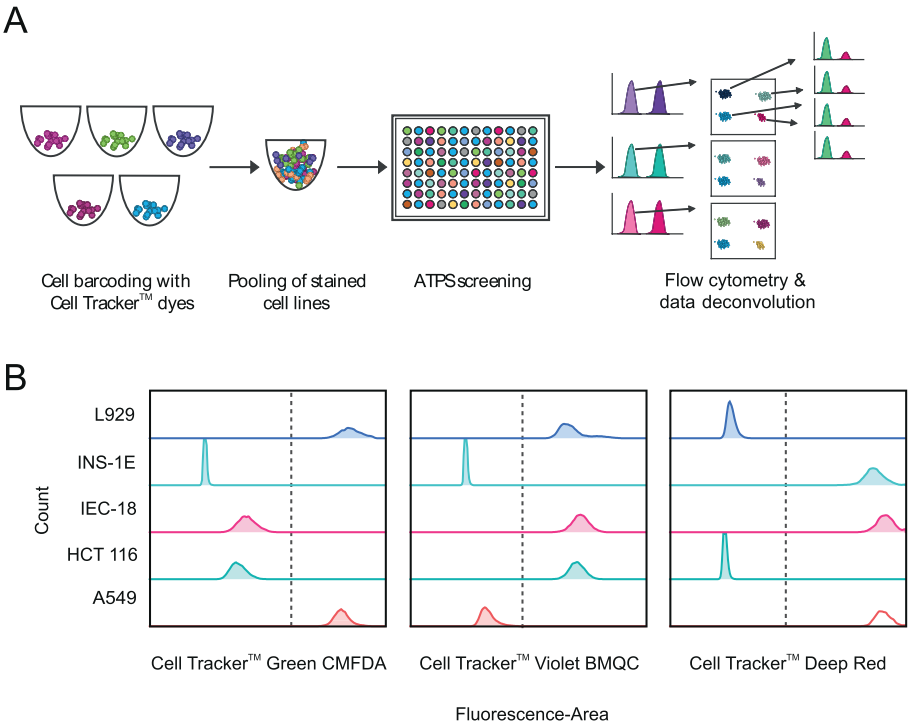

Figure 6.1: Cell barcoding for multiplexing of partitioning analysis in ATPS. **(A)** Scheme of the barcoding strategy. Several cell lines are stained with CellTracker dyes in a combinatorial fashion and pooled, before HT-partitioning analysis in ATPS. Cell quantification and analysis is performed by HT-flow cytometry. After data deconvolution, the partitioning factors of each cell type can be determined. **(B)** Efficient labelling of five cell lines with three CellTracker dyes. A549 cells were stained with CellTracker Green CMFDA and CellTracker Deep Red, INS-1E cell were stained with CellTracker Deep Red, IEC-18 cells were stained with CellTracker Deep Red and CellTracker Violet BMQC, HCT 116 cells were stained with CellTracker Violet BMQC, and L929 cells were stained with CellTracker Green CMFDA and CellTracker Violet BMQC.

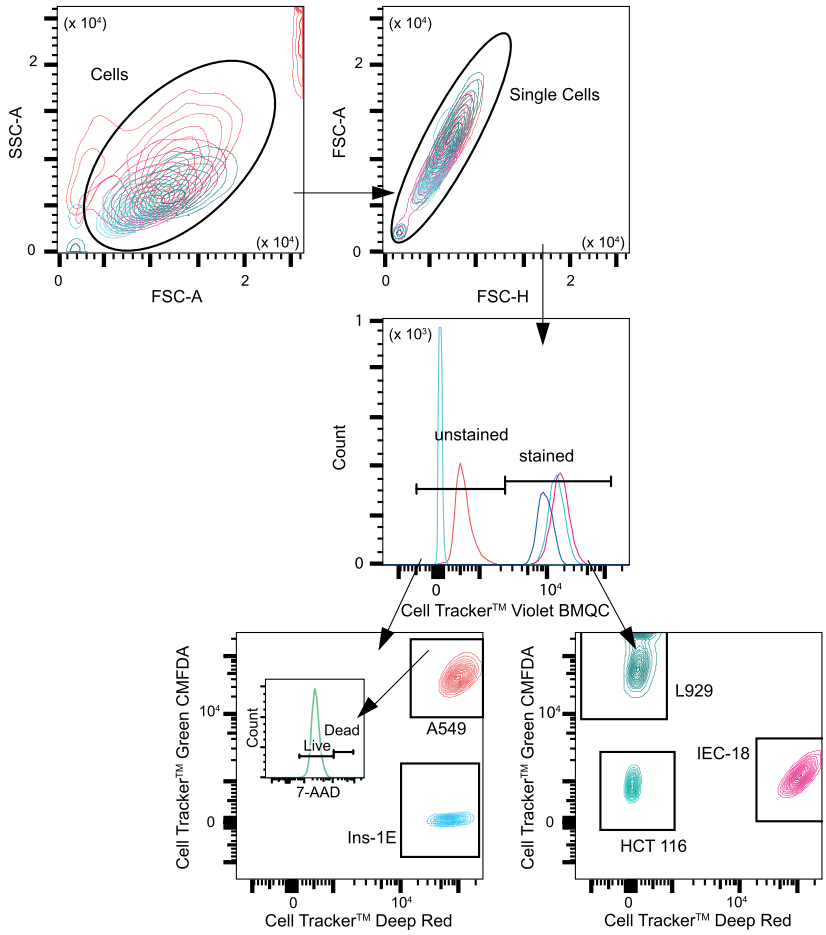

Figure 6.2: Deconvolution method for barcoded cell lines. Single cells are gated for CellTracker Violet BMQC staining and then further gated into single cell lines based on CellTracker Green CMFDA and CellTracker Deep Red staining. The live cell population of each cell line was the gated based on 7-AAD staining. FSC-A: Forward scatter peak area, SSC-A: side scatter peak area, FSC-H: Forward scatter peak height.

6.3.1 Characterization of PEG-Dextran ATPS

Phase diagrams are essential to determine suitable screening ranges in ATPS research, since they enable the selection of suitable volume ratios and TLL. The ATPS used in this work consisted of different combinations of PEG 4,000, 8,000, and 20,000, and dextran 70,000 and 500,000, buffered with isotonic concentrations of sodium phosphate. Phase diagrams were determined using a HTS-method described in previous studies [128] **(fig. 6.3 & table 6.1)**. Binodal curves were fitted to **eq. (6.1)** using least square regression.

$$y = a \times exp(b \times x^{0.5} + c \times x^3). \tag{6.1}$$

All binodal curves could be fitted with a Pearson's r^2 of at least 0.99. A change in shape and location of the binodal in dependence of the polymer molecular weight was observed.

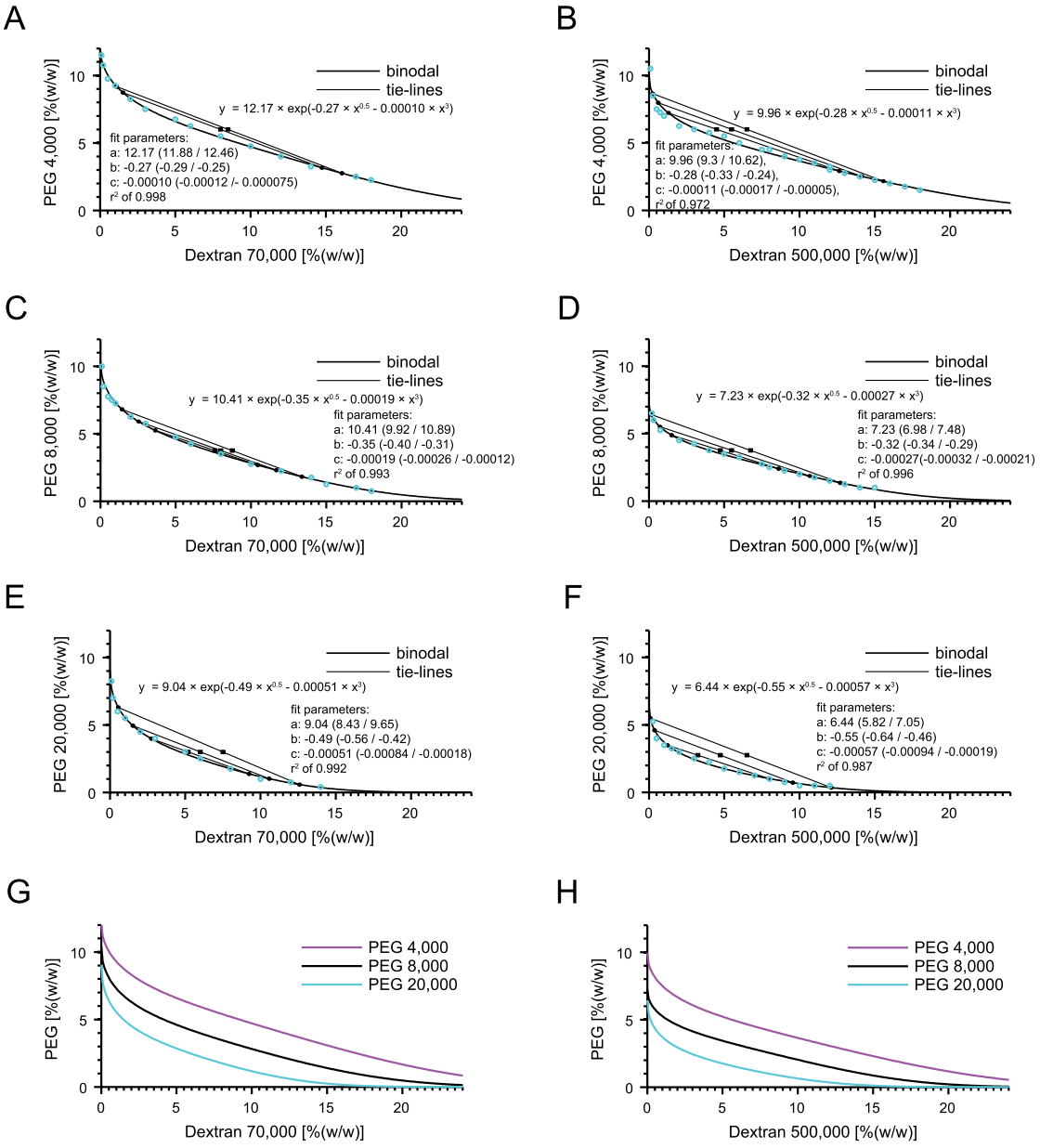

Figure 6.3: Phase diagrams of different PEG and dextran molecular weights. Blue circles represent binodal data points determined by HTS cloud point titration. Fit parameters of equation 1 with 95 % prediction bounds and Pearsonts r^2 are shown in parentheses. (A) PEG 4,000 and dextran 70,000 (fit parameters: a: 12.17 (11.88 / 12.46), b: -0.27 (-0.29 / -0.25), c: -0.00010 (-0.00012 /- 0.000075), r^2 of 0.998), (B) PEG 4,000 and dextran 500,000 (fit parameters: a: 9.96 (9.3 / 10.62), b: -0.28 (-0.33 / -0.24), c: -0.00011 (-0.00017 / -0.00005), r^2 of 0.972), (C) PEG 8,000 and dextran 70,000 (fit parameters: a: 10.41 (9.92 / 10.89), b: -0.35 (-0.40 / -0.31), c: -0.00019 (-0.00026 / -0.00012), r^2 of 0.993), (D) PEG 8,000 and dextran 500,000 (fit parameters: a: 7.23 (6.98 / 7.48), b: -0.32 (-0.34 / -0.29), c: -0.00027(-0.00032 / -0.00021), r^2 of 0.996), (E) PEG 20,000 and dextran 70,000 (fit parameters: a: 9.04 (8.43 / 9.65), b: -0.49 (-0.56 / -0.42), c: -0.00051 (-0.00084 / -0.00018), r^2 of 0.992), (F) PEG 20,000 and dextran 500,000 (fit parameters: a: 6.44 (5.82 / 7.05), b: -0.55 (-0.64 / -0.46), c: -0.00057 (-0.00094 / -0.00019), r^2 of 0.987). 95 % prediction bounds of the fit parameters are shown in parentheses. (G-H) Overlay of binodal fits.

Table 6.1: Summary of ATPS compositions used to investigate the influence of polymer molecular weight and TLL.[a)]

	Molecular weight		Total system composition		Bottom phase composition		Top phase composition		TLL
	PEG	dextran	PEG	dextran	PEG	dextran	PEG	dextran	
#	[Da]	[Da]	[% (w/w)]	[% (w/w)]	[% (w/w)]	[% (w/w)]	[% (w/w)]	[% (w/w)]	[% (w/w)]
1	4,000	70,000	6.00	8.00	3.16	14.74	8.72	1.53	14.30
2	4,000	70,000	6.00	8.50	2.76	16.06	9.17	1.10	16.30
3	4,000	500,000	6.00	4.50	2.92	12.64	7.21	1.30	12.13
4	4,000	500,000	6.00	5.50	2.52	14.13	7.97	0.62	14.57
5	4,000	500,000	6.00	6.50	2.15	15.57	8.65	0.25	16.64
6	8,000	70,000	3.75	7.60	2.67	10.45	5.24	3.65	7.27
7	8,000	70,000	3.75	8.00	2.30	11.69	5.90	2.54	9.84
8	8,000	70,000	3.75	8.75	1.82	13.38	6.80	1.44	12.94
9	8,000	500,000	3.75	4.75	2.40	8.61	4.88	1.52	7.52
10	8,000	500,000	3.75	5.50	1.85	10.68	5.49	0.74	10.59
11	8,000	500,000	3.75	6.75	1.35	12.70	6.41	0.14	13.55
12	20,000	70,000	3.00	5.20	1.38	9.24	3.98	2.76	6.99
13	20,000	70,000	3.00	6.00	1.02	10.57	4.94	1.53	9.86
14	20,000	70,000	3.00	7.50	0.58	12.60	6.30	0.55	13.34
15	20,000	500,000	2.75	3.25	1.02	7.96	3.49	1.23	7.17
16	20,000	500,000	2.75	4.75	0.72	9.55	4.60	0.37	9.97
17	20,000	500,000	2.75	6.50	0.35	12.11	5.50	0.08	13.08

[a)] All ATPS were buffered with 0.11 M sodium phosphate, pH 7.4. TLL: tie-line length.

With increasing PEG molecular weight, the binodal shifts towards lower PEG and dextran concentrations. This trend was observed for both dextran molecular weights. These findings are in good agreement with literature [53] **(fig. 6.3 G & H)**. We chose three screening points from each phase diagram, with TLL of 7, 10 and 13 % (w/w), with the exception of the phase diagrams of PEG 4,000. Due to the flatness of the binodals, even systems close to the critical point had TLL of $\geq$ 12 % (w/w). Thus, we chose TLL of 12, 14 and 16 % (w/w) for PEG 4,000 - dextran 500,000 and 14 & 16 % (w/w) for PEG 4,000 dextran 70,000.

6.3.2 Influence of Cell Barcoding on Their Partitioning in PEG-Dextran ATPS

Cell barcoding enables the evaluation of numerous cell lines in a single experiment. As cell partitioning in ATPS is primarily dependent on cell surface properties, we chose a barcoding reagent that does not bind to the cell surface, as for example described by [135]. Instead, we chose the CellTracker dyes, which are cell permeant fluorescent probes that are retained inside living cells after a glutathione S-transferase-mediated reaction, with the exception of CellTracker Deep Red, which is an amine-reactive dye. Even though amine reactive dye do not exclusively bind to proteins inside the cell, CellTracker Deep Red was used at relatively low concentrations (50 nM) compared to manufacturers recommendations (250 nM - 1 μM). Thus, we expected that the CellTracker dyes can be used for cell barcoding without significantly altering their partitioning behavior. To confirm this assumption, we mixed CellTracker Violet BMQC stained and unstained HCT 116 cells and CellTracker Deep Red stained and unstained INS-1E cells, and studied their partitioning in a number of ATPS. We chose ATPS composed of 4 % PEG 8,000, 5 % dextran 500,000, 0.11 M

NaPi, pH 7.4, with a TLL of 10.4 and of 4 % PEG 8,000, 4 % dextran 500,000, 0.11 M NaPi, pH 7.4, with a TLL of 6.9, which were previously shown to enable cell separation based on surface charge [54]. In addition, we chose a ATPS consisting of 4 % PEG 8,000, 4 % dextran 500,000, 0.01 M NaPi, 0.138 M NaCl, pH 6.6, with a TLL of 6.9 which was previously shown to enable cell separation based on their membrane lipid composition [54]. In **fig. 6.4**, the fold change of the percentage of stained HCT 116 and INS-1E cells after partitioning is shown. No significant enrichment or depletion of the CellTracker stained cell populations was observed ($p > 0.05$).

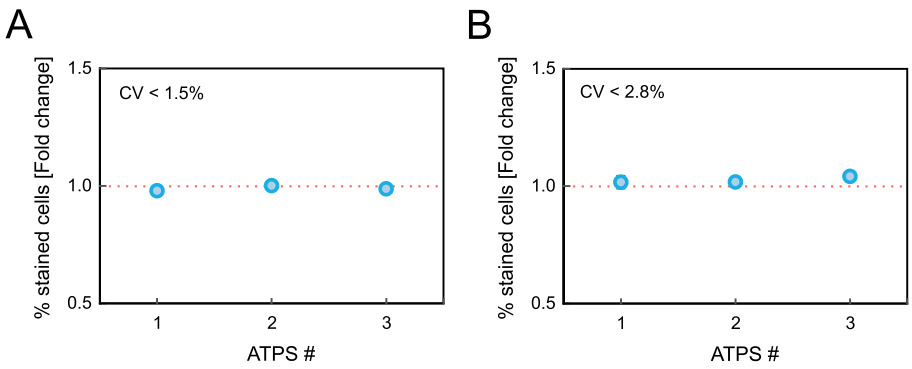

Figure 6.4: Influence of cell barcoding on partitioning in charge-sensitive and charge-insensitive ATPS at different TLL (#1: 4 % PEG 8,000, 4 % dextran 500,000, 0.01 M NaPi, 0.138 M NaCl, pH 6.6, TLL: 6.9; #2: 4 % PEG 8,000, 4 % dextran 500,000, 0.11 M NaPi, pH 7.4, TLL: 6.9; #3: 4 % PEG 8,000, 5 % dextran 500,000, 0.11 M NaPi, pH 7.4, TLL: 10.4). Two of the cell lines were barcoded with different CellTracker dyes and mixed with an equal number of unstained cells of the same cell line. HCT 116 (A) was stained with Cell Tracker Violet BMQC and INS-1E (B) was stained with CellTracker Deep Red. Partitioning analysis was performed in HTS and the fold change of the percentage of stained cells was calculated compared to a PBS control. Error bars represent 1 s.d. of 4 technical replicates. Pairwise t-test showed no significant changes of partitioning due to CellTracker staining ($p > 0.05$). Error bars are within symbol size.

6.3.3 Resolution of Five Model Cell Lines in Charge-Sensitive ATPS in Dependence of TLL and Polymer Molecular Weight

The aim of this case study was to investigate the influence of TLL and polymer molecular weight on the resolution of different cell lines. To do so, the partitioning of five cell lines that differ in species and tissue type was investigated in charge-sensitive ATPS at different TLL and different combinations of PEG and dextran molecular weights. The partitioning factor P of each cell line towards the top or bottom phase was defined as the fraction of cells in that phase compared to the total cell number added. For the top phase, P can be calculated using **eq. (6.2)**.

$$P = \frac{Count_{TP} \times V_{TP}}{Count_C \times V_C} \tag{6.2}$$

TP: top phase, C: PBS control, V: volume

In **fig. 6.5** the partitioning factors of each cell line in dependence of TLL and polymer molecular weight in charge-sensitive ATPS is summarized. The screenings revealed a number of trends. Firstly, in the presence of NaPi, cells generally partitioned between top phase and interface, which is well described for charge-dependent cell partitioning. Furthermore, partitioning factors decrease with increasing PEG molecular weight, while an increase in dextran molecular weight results in an increase of cell recovery in the top phase. Even though ATPS consisting of PEG 4,000 and either dextran 70,000 or 500,000 had considerably higher TLL very high partitioning factors were observed. Secondly, when comparing the partitioning factors for a given molecular weight combination, partitioning factors decrease with increasing TLL. This trend is more pronounced for ATPS consisting of PEG 8,000 than PEG 4,000 and either dextran 70,000 or 500,000. In ATPS consisting of PEG 20,000 and either dextran 70,000 or 500,000, less than 7 % of either cell line was recovered in the top phase. In ATPS consisting of dextran 500,000, cells were almost completely adsorbed at the interface, while in ATPS consisting of PEG 4,000 and dextran 70,000 approximately 25 % of the cells partitioned to the bottom phase, which is not consistent with charge-dependent cell partitioning and might be a consequence of strong exclusion effects due to high PEG molecular weight. These ATPS were thus not included in further analyses. Thirdly, the same overall trends were observed when comparing the partitioning factors of the five cell lines in a given ATPS. The cell line A549 has the strongest affinity for the top phase, followed by HCT 116, L929, IEC-18, and INS-1E. However, absolute partitioning factors as well as differences between partitioning factors change in dependence of TLL and molecular weight of the polymers. This means that the resolution, i.e., separability, between the cell lines changes. Next, we determined enrichment / depletion factors for each cell line.

In **fig. 6.6**, the fold change of the percentage of each cell line in dependence of TLL and polymer molecular weight is summarized. The fold change of each cell line was determined using **eq. (6.3)**.

$$fold\ change = \frac{\%cell\ line X_{TP}}{\%cell\ line X_C} \tag{6.3}$$

%cell line X: ratio of each cell line, TP: top phase, C: PBS control

We observed up to threefold enrichment of A549 cells in the top phase and > 30-fold depletion of INS-1E cells from the top phase. Moreover, the resolution of the five cell lines changes in dependence of TLL and polymer molecular weight. For example, in ATPS consisting of PEG 4,000 dextran 70,000 large differences exist between the fold change-values of IEC-18 and INS-1E, while those values are close to identical in ATPS consisting of PEG 8,000 and dextran 70,000. This indicates that by changing the polymer molecular weight and TLL of charge-sensitive ATPS, the separation of two cell types might be possible even if initial screenings indicate that they are not. In order to evaluate the separability of the five cell lines in more detail, CCD-curves were calculated. CCD is a well-established technique in liquid-liquid extraction, and has successfully been applied in cell separation [54, 66]. In CCD, the top phase is sequentially transferred, while the

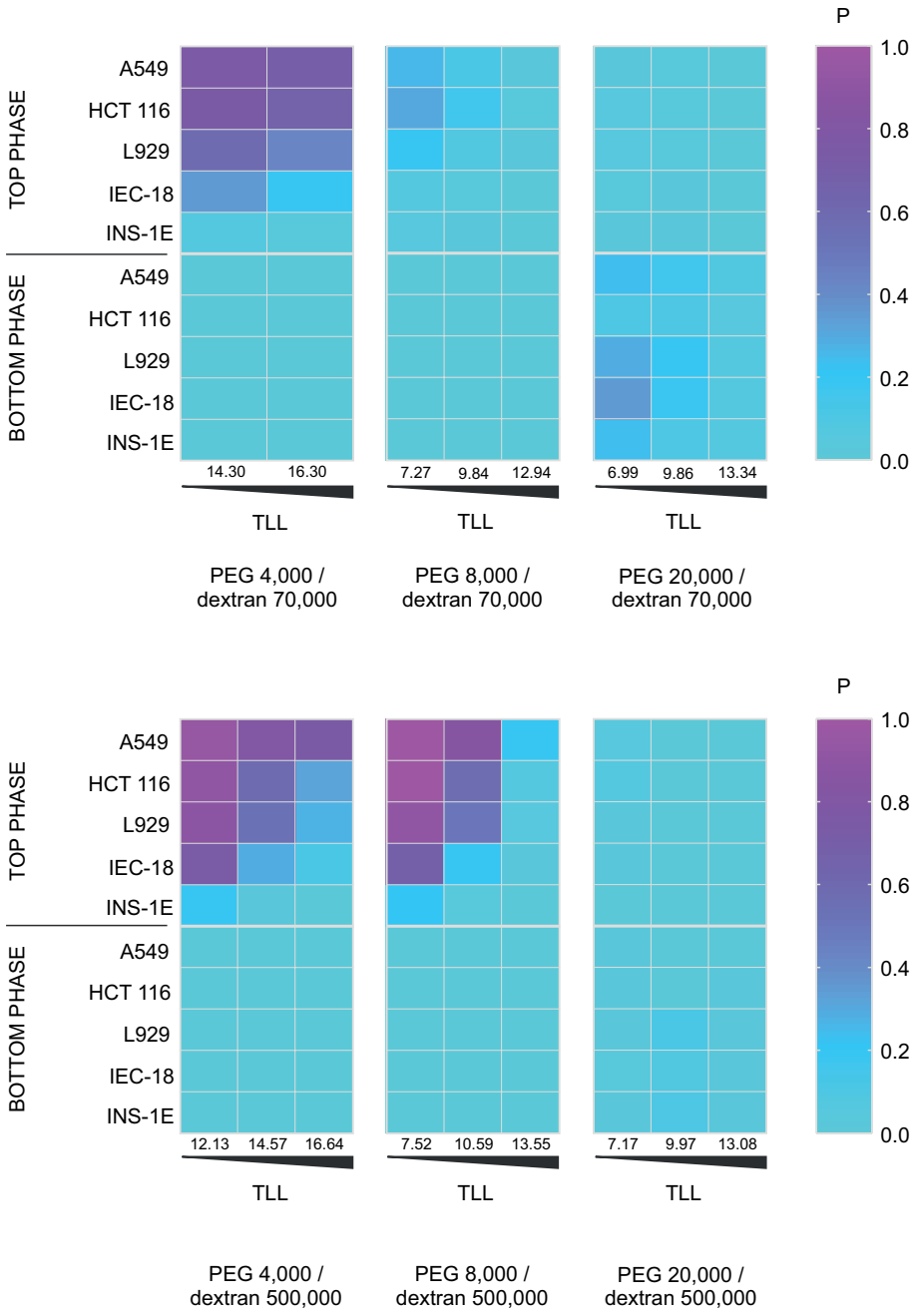

Figure 6.5: Partitioning factors of five model cell lines in ATPS containing 0.11 M NaPi, pH 7.4, in dependence of PEG and dextran molecular weight and TLL. ATPS compositions are summarized in **table 6.1**. Heat maps represent the mean percentage of live cells in each phase (3 technical replicates). TLL: tie-line length.

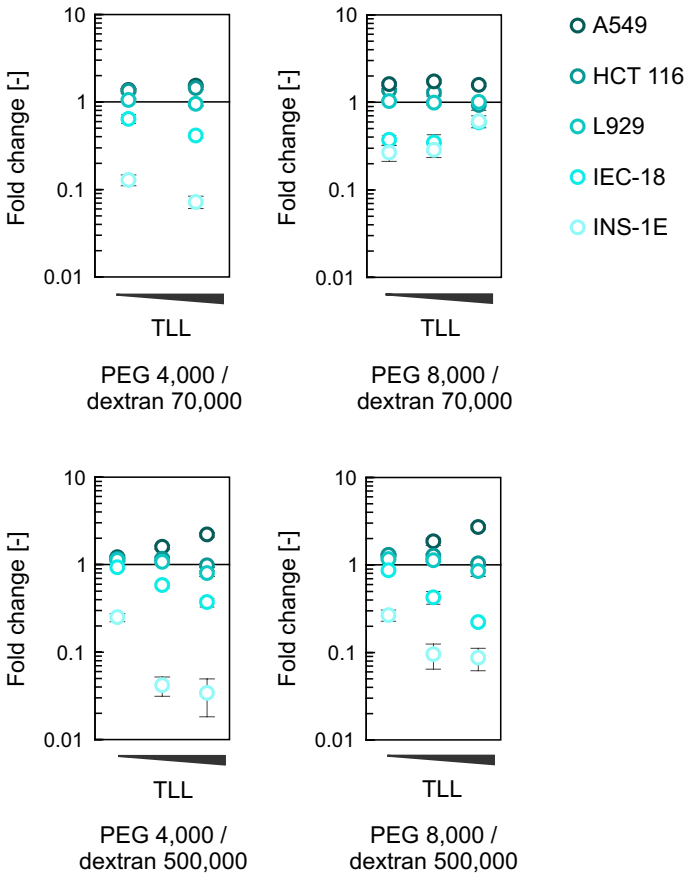

Figure 6.6: Fold change of the percentage of five model cell lines compared to a PBS control in the top phase of charge-sensitive ATPS in dependence of polymer molecular weight and TLL. ATPS compositions are summarized in **table 6.1**. Error bars represent 1 s.d. of 3 technical replicates. TLL: tie-line length.

bottom phase is retained. Between transfers, the ATPS are mixed and allowed to settle, to achieve phase separation. Dependent on the application, the interface is either transferred or retained. Since cells partition between one of the bulk phases and the interface, the interface is retained when cells partition between top phase and interface, and transferred when the cells partition between interface and bottom phase. As a consequence, cells that partition mainly into the top phase move faster through the CCD-apparatus than cells that partition mostly to the interface. As a result, the two cell types are separated.
Based on the data shown in **fig. 6.5**, CCD-curves were calculated by applying **eq. (6.4)** [54]:

$$F(r) = \frac{n!}{r!(n-r)!} P^r (1-P)^{n-r} \tag{6.4}$$

where F represents the fraction of the total cell population appearing in each theoretical cavity (r) of the CCD-apparatus, and n the total number of transfers. The experimental validation of the model was reported in previously work [200]. We calculated CCD-curves with 60 transfers for each cell line. The results are shown in **fig. 6.7**. The distribution between the 60 theoretical cavities is strongly dependent on the partitioning factors, and thus directly influences the resolution of the five cell lines [53, 54]. In ATPS in which high partitioning factors were obtained, e.g., ATPS #3 and #9 the calculated CCD-curves are skewed towards the right, and only cell lines with the lowest partitioning factors, i.e., IEC-18 and INS-1E can be separated from the mixture. In ATPS #9 A549 and HCT 116 have partitioning factors of 1 and thus do not distribute in CCD. In ATPS in which very low partitioning factors were obtained, e.g., ATPS #7 and #8 the calculated CCD-curves are skewed towards the left and very little resolution can be obtained, whereas in ATPS in which intermediate partitioning (~ 0.5) factors were obtained, e.g., ATPS #1 and #4 the calculated CCD-curves are symmetrical and distribute evenly. Moreover, we observed that the resolution varies with TLL and polymer molecular weight at comparable partitioning factors. In ATPS #1 and #4 for example, intermediate partitioning factors were obtained, however, in ATPS #4 A549 and HCT 116 cell can be separated but not in ATPS #1. This demonstrates that the combination of PEG and dextran molecular weights can influence the separability of different cell types. Finally, the calculated CCD-curves indicate that we identified conditions that enable peak separation of four of the five cell lines from the mixture, indicating that very high purities and yields can be obtain with 60 transfers. ATPS #5 enables the isolation of A549 with > 99.9 % purity and yield, and ATPS #2 enables the separation of L929 cells with > 99.9 % purity and > 45 % yield. Moreover, ATPS #9 enables the isolation of IEC-18 with > 99.9 % purity and > 95 % yield and ATPS #3 enables the isolation of INS-1E with > 99.9 % purity and yield.

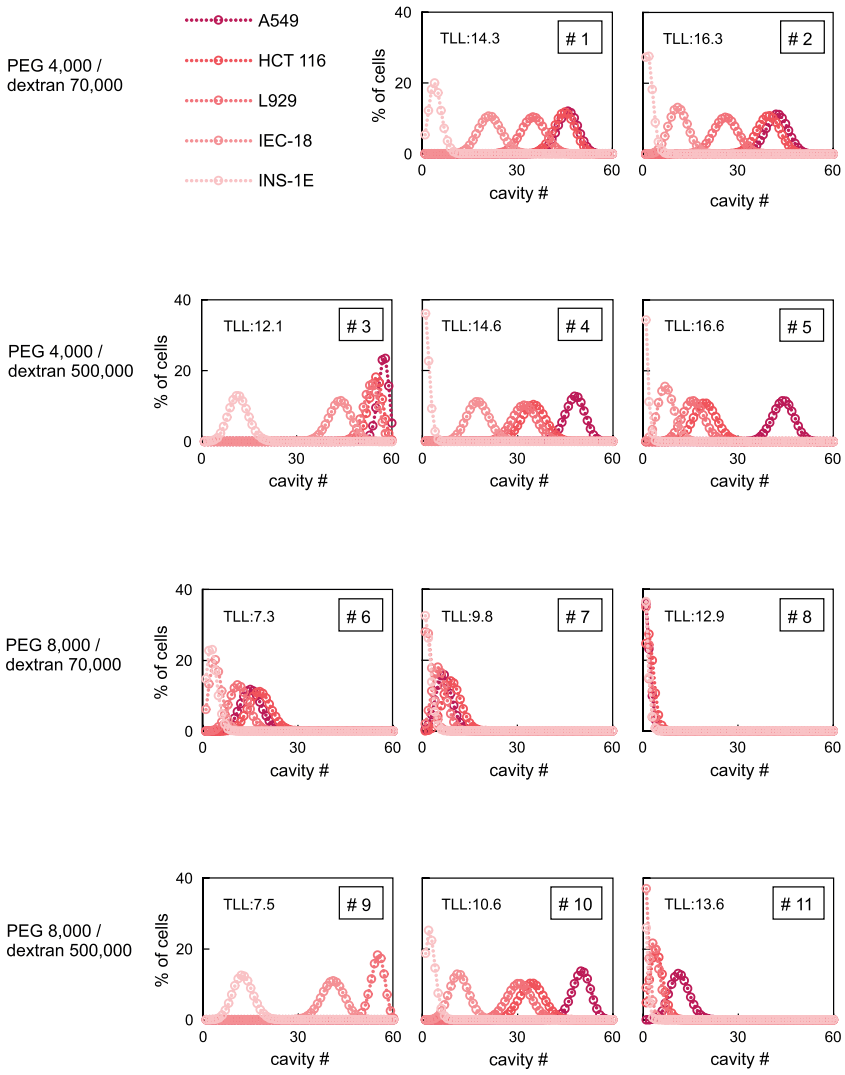

Figure 6.7: CCD-curves. CCD-curves were calculated for each cell line based on the partitioning factors determined by HTS, with 60 theoretical transfers for ATPS #1-11. The corresponding ATPS composition and TLL are summarized in **table 6.1**. TLL: tie-line length in % (w/w).

6.4 Discussion

The aim of the present work was to investigate the influence of polymer molecular weight at a defined TLL on the resolution of five model cell lines in charge-sensitive ATPS. Prior to the screenings, phase diagrams for all PEG and dextran molecular weight combinations were determined. We chose charge-sensitive ATPS consisting of different combinations of PEG 4,000, 8,000, and 20,000, and dextran 70,000 and 500,000, with three TLL per combination. Trends in location and shape on the binodals are in good agreement with literature [53]. Higher polymer molecular weights result in a shift of the binodal towards

lower concentrations of PEG and dextran, and the larger the difference in the molecular weights of PEG and dextran, the more asymmetric is the binodal curve [53]. Furthermore, the influence of the barcoding strategy on the cell partitioning was evaluated prior to the screenings. We expected that staining with CellTracker dyes has no significant effect on the partitioning behavior, since CellTracker Green CMFDA und CellTracker Violet BMQC are cell permeant fluorescent probes that are retained inside living cells after a glutathione S-transferase mediated reaction, thus, the cell surface remains unaltered. As cell partitioning is largely dependent on cell surface properties, these dyes should not influence cell partitioning. CellTracker Deep Red, however, is an amine reactive dye and, thus, binds to cell surface proteins, which might influence cell partitioning by altering cell surface properties. It was thus evaluated whether significant effects are observed at the concentration used in this study. Partitioning studies showed no significant changes in partitioning factors due to CellTracker staining. Consequently, CellTracker dyes are an excellent tool for multiplexing in screenings investigating cell surface properties and enable a substantial decrease in time and material consumption. Moreover, batch variability can be eliminated by analyzing numerous cell lines in the same experiment, and the longevity (>72 h) and nontoxicity of the dyes enables prolonged screening times. Since our data indicate that relatively low concentrations of amine-reactive dyes do not significantly alter cell partitioning in here investigated ATPS, it might be feasible to apply more complex barcoding strategies, as for example described by *Krutzik et al.* [135], which enables a further increase in throughput. Subsequently, we investigated the influence of polymer molecular weight and TLL on the resolution of five model cell lines in ATPS containing sodium phosphate, i.e., charge-sensitive ATPS. In contrast to smaller biomolecules, such as proteins and nucleic acids, cells partition between either top or bottom phase and the interface, depending on the ATPS composition [54]. The interfacial tension is one of the major driving forces in the partitioning of molecules and particles in ATPS, as it acts to minimize the interfacial area. Accordingly, TLL and polymer molecular weight, which determine the interfacial tension in a given ATPS, play a major role cell partitioning in ATPS [197]. The adsorption of cells and other particles at the interface reduces the interfacial area, and consequently the total free energy of the system. Thus, partitioning into either phase can only take place if the interaction with the cell surface is strong enough to pull the cells out of the interface. The higher the interfacial tension, the stronger the required interactions to enable partitioning to either bulk phase [53, 54, 197]. These interactions can be influenced by the type and concentration of salts is added. An extensive amount of work have been done investigating the influence of phosphate salts and NaCl on cell partitioning [53, 54]. One observation was the correlation between the cells electrophoretic mobility, due to charge-associated surface properties, and cell partitioning [53]. It has been shown that salts with polyvalent anions, e.g., phosphate have a higher affinity for the dextran-rich bottom phase that the PEG-rich top phase, while salts of halides, for example, NaCl, partition almost equally between the phases [201]. It was further proposed that unequal partitioning of a salt results in the generation of an interfacial electrostatic potential difference (Donnan potential), and molecules and particles partition in such ATPS according to their surface charge [54, 191, 194, 202]. In PEG-dextran ATPS containing phosphate with moderate interfacial tensions cells can, therefore, be separated based on

surface charge differences (charge-dependent partitioning). Cells have a negative net surface charge and consequently partition into the top phase in ATPS containing phosphate [189, 194]. This phenomenon was observed throughout the screenings. Both interfacial tension and Donnan potential have been shown to increase with increasing TLL, but have opposite effects on cell partitioning [195, 197, 203]. While the Donnan potential pulls the cells into the top phase, the interfacial tension promotes cell adsorption at the interface. However, the increase of interfacial tension with TLL is stronger than the increase of the potential difference between the phases. Thus, at some distance from the critical point, the increase in interfacial tension offsets the increase in electrostatic potential difference [54]. *Forciniti* and several others [53, 197, 203] described a logarithmic increase of the interfacial tension with increasing TLL, and an increase in interfacial tension with polymer molecular weight at a given TLL, while a linear correlation between Donnan potential and TLL has been described in several publications [195, 204, 205]. These finding correlate well with the data presented in this work. With increasing TLL and polymer molecular weight, cell adsorption at the interface increased. Although this theory of a charge-dependent partitioning is supported by the findings of different groups [54, 191, 194, 202], doubts have been expressed about the existence of an electrochemical potential in ATPS [206]. Despite the debate about the existence of Donnan potentials and their significance in cell partitioning, the data presented here show a clear influence of sodium phosphate on cell partitioning and the resolution of different cell types.

At a PEG molecular weight of 20,000 Da no partitioning into the top phase was observed, even at low TLL. This indicates that the interfacial tension was too high for specific cell partitioning. Interestingly, the change of dextran molecular weight from 500,000 to 70,000 Da, at a given PEG molecular weight, did not result in an increase of partitioning factors, as assumed due to a decrease in interfacial tension, but a decrease. Our data showed that combinations of low PEG molecular weights, i.e., $\leq$ 8,000 Da, and high dextran molecular weights, i.e., 500,000 Da, at TLL between 10 and 15 % (w/w) enable high resolution of the five model cell lines. This is in good agreement with the findings of *Albertsson* [53], who described increased partitioning to the top phase when decreasing the PEG molecular weight. We assume that a further decrease in PEG molecular or an increase in dextran molecular weight might result in higher partitioning factors and in changes in resolutions. This, however, needs to be validated in future work. Furthermore, our data indicate that sodium phosphate-dependent, i.e., charge-dependent, cell separation is the major driving force, independent of TLL and polymer molecular weight, since the order of the affinity the five model cell lines exhibited to the top phase is independent of TLL and polymer molecular weight. However, the resolution between the five cell lines, which was evaluated by the calculation of CCD-curves, changes with TLL and polymer molecular weight. Thus, comprehensive screenings are necessary to investigate the separability of two cell populations. As hypothesized by *Walter et al.* [54], factors other than surface charge may play a minor role in charge-sensitive ATPS, and we assume that their contribution is dependent on TLL and polymer molecular weight. In addition, a number of other factors, such as phase densities and viscosities, and cell size and density may play a role [53]. However, the exact role and interaction of all of these factors need to be further investigated. In addition, the calculated CCD-curves indicate that the differences in partitioning factors

can be used for cell separation. Our data show that we identified conditions that enable peak separation of each of the five cell lines from the mixture in a single CCD-run, with the exception of HCT 116 where two consecutive CCD-runs are necessary. Likewise, it should be noted that partitioning ratios of cells are highly dependent on vessel geometry, fill volume, mixing efficiency, and phase separation time. Thus, these conditions need to be identical in batch- and CCD- experiments, otherwise predicted CCD-curves will not be accurate [54]. While the calculation of fold-change values are an excellent means to evaluate separability of certain cell populations, CCD-models enable the estimation of obtainable purities, yields and overall processing time, and are thus an excellent tool for downstream process development of cell-based products. Finally, it should be noted that *Walter et al.* [207] showed that cell age, cell cycle stage, and the use of enzymes for cell dissociation can influence cell partitioning [207–209]. Therefore, the effect of these parameters on cell partitioning needs to be considered when designing a purification process.

6.5 Conclusions

We investigated the influence of TLL and polymer molecular weight on cell partitioning in charge-sensitive ATPS. We showed that the interfacial tension, which is directly dependent on TLL and polymer molecular weight, is a main factor in cell partitioning. The present study showed that combinations of low PEG molecular weights and high dextran molecular weights enable high resolution of different cell lines. Moreover, we showed that the order of the affinity the five model cell lines exhibited to the top phase is independent of TLL and polymer molecular weight, indicating that the major driving forces remain the same in ATPS containing phosphate. However, the separability of the cell lines strongly depends on TLL and polymer molecular weight. Thus, comprehensive screenings are necessary to investigate the separability of specific cell populations. Finally, we demonstrated that the combination of a HTS-platform for the investigation of cell partitioning in ATPS with the here described barcoding strategy and the application of CCD-modelling, is a powerful tool to study factors in cell separation and enables fast and directed downstream process development for cell-based products.

Acknowledgements

S.Z. and S.G. contributed equally to this work. We thank Prof. A. Hartwig and co-workers from the Institute of Food Chemistry and Toxicology at the Karlsruhe Institute of Technology (KIT) for sharing their labs, equipment, and cell lines with us. We would also like to thank Prof. Maechler, from the Department of Cell Physiology and Metabolism at the University of Geneva Medical Centre, Switzerland for providing the rat beta-cell line INS-1E. Finally, we would like to thank Stefanie Limbrunner for assisting with the cell culture work. This work was supported by Novo Nordisk A/S; the German Federal Ministry for Education and Research (BMBF) (grant number 0315520); and the Helmholtz Program BioInterfaces in Technology and Medicine (BIFTM).

Competing financial interests

The authors declare no financial or commercial conflict of interests.

6.6 References

2. M. A. Fischbach, J. A. Bluestone, and W. A. Lim: 'Cell-based therapeutics: the next pillar of medicine'. *Science translational medicine* (2013), vol. 5(179): 179ps7.

53. P.Å. Albertsson: 'Partitioning of cell particles and macromolecules: Separation and purification of biomolecules, cell organelles, membranes and cells in aqueous polymer two phase systems and their use in biochemical analysis and biotechnology'. 3rd ed. John Wiley & Sons, New York, 1986.

54. H. Walter, D. E. Brooks, and D. Fisher: 'Partitioning in Aqueous Two-Phase Systems: Theory, Methods, Uses, and Applications to Biotechnology'. Academic Press, Inc., Orlando, USA, 1985.

55. M. W. Beijerinck: 'Ueber eine Eigentümlichkeit der löslichen Stärke'. *Centralblatt für Bakteriologie und Parasitenkunde und Infektionskrankheiten* (1896), vol. 2: pp. 697–699.

56. R. Hatti-Kaul: *Aqueous Two-Phase Systems: Methods and Protocols: Methods and Protocols*. Totowa, NJ: Humana Press, 2000.

57. M. Rito-Palomares and J. Benavides: *Aqueous Two-Phase Systems for Bioprocess Development for the Recovery of Biological Products*. Food Engineering Series. Springer International Publishing, 2017.

58. M. Bensch, B. Selbach, and J. Hubbuch: 'High throughput screening techniques in downstream processing: Preparation, characterization and optimization of aqueous two-phase systems'. *Chemical Engineering Science* (2007), vol. 62(7): pp. 2011–2021.

59. S. A. Oelmeier, F. Dismer, and J. Hubbuch: 'Application of an aqueous twophase systems highthroughput screening method to evaluate mAb HCP separation'. *Biotechnology and Bioengineering* (2010), vol. 108(1): pp. 69–81.

60. S. Zimmermann, S. Gretzinger, M.-L. Schwab, C. Scheeder, P. K. Zimmermann, S. A. Oelmeier, E. Gottwald, A. Bogsnes, M. Hansson, A. Staby, and J. Hubbuch: 'High-throughput downstream process development for cell-based products using aqueous two-phase systems'. *Journal of Chromatography A* (2016), vol. 1464: pp. 1–11.

61. P. A. Albertsson: 'Particle fractionation in liquid two-phase systems The composition of some phase systems and the behaviour of some model particles in them application to the isolation of cell walls from microorganisms'. *Biochimica et Biophysica Acta* (1958), vol. 27: pp. 378–395.

62. H. Walter, F. D. Raymond, and D. Fisher: 'Erythrocyte partitioning in dextranpoly(ethylene glycol) aqueous phase systems: Events in phase and cell separation'. *Journal of Chromatography A* (1992), vol. 609(1): pp. 219–227.

63. H. Walter, E. J. Krob, R. Garza, and G .S. Ascher: 'Partition and countercurrent distribution of erythrocytes and leukocytes from different species'. *Experimental Cell Research* (1969), vol. 55(1): pp. 57–64.

64. L. C. Craig and O. Post: 'Apparatus for Countercurrent Distribution'. *Analytical Chemistry* (1949), vol. 21(4): pp. 500–504.

65. G. Johansson: 'EXTRACTION | Multistage Countercurrent Distribution'. *Encyclopedia of Separation Science*. Ed. by I. D.Wilson. Oxford: Academic Press, 2000: pp. 1398–1405.

66. P. Å. Albertsson and G. D. Baird: 'Counter-current distribution of cells'. *Experimental Cell Research* (1962), vol. 28(2): pp. 296–322.

128. S. Zimmermann, S. Gretzinger, C. Scheeder, M.L. Schwab, S. A. Oelmeier, A. Osberghaus, E. Gottwald, and J. Hubbuch: 'Highthroughput cell quantification assays for use in cell purification development enabling technologies for cell production'. *Biotechnology Journal* (2016), vol. 11(5): pp. 676–686.

135. P. O. Krutzik and G. P. Nolan: 'Fluorescent cell barcoding in flow cytometry allows high-throughput drug screening and signaling profiling'. *Nature methods* (2006), vol. 3: pp. 361–368.

182. M. Al-Rubeai, M. Naciri: *Stem Cells and Cell Therapy*. Springer, Netherlands, 2014.

183. A. Trounson and C. McDonald: 'Stem Cell Therapies in Clinical Trials: Progress and Challenges'. *Cell Stem Cell* (2015), vol. 17(1): pp. 11–22.

184. P. J. Amos, E. Cagavi Bozkulak, and Y. Qyang: 'Methods of Cell Purification: A Critical Juncture for Laboratory Research and Translational Science'. *Cells Tissues Organs* (2012), vol. 195: pp. 26–40.

185. G. M. C. Rodrigues, C. A. V. Rodrigues, T. G. Fernandes, M. M. Diogo, and J. M. S. Cabral: 'Clinical-scale purification of pluripotent stem cell derivatives for cell-based therapies'. *Biotechnology journal* (2015), vol. 10: pp. 1103–1114.

186. C. Stemberger et al.: 'Novel Serial Positive Enrichment Technology Enables Clinical Multiparameter Cell Sorting'. *PLOS ONE* (2012), vol. 7(4): e35798.

187. T. G. Fernandes, C. A.V. Rodrigues, M. M. Diogo, and J. M. S. Cabral: 'Stem cell bioprocessing for regenerative medicine'. *Journal of Chemical Technology & Biotechnology* (2014), vol. 89(1): pp. 34–47.

188. A. Chen, S. Ting, J. Seow, S. Reuveny, and S. Oh: 'Considerations in designing systems for large scale production of human cardiomyocytes from pluripotent stem cells'. *Stem Cell Research & Therapy* (2014), vol. 5(1): p. 12.

189. J. M. S. Cabral: 'Cell Partitioning in Aqueous Two-Phase Polymer Systems'. *Adv. Biochem. Eng. Biotechnol* (2007), vol. 106: pp. 151–171.

190. R. R. G. Soares, A. M. Azevedo, J. M. Van Alstine, and M. R. Aires-Barros: 'Partitioning in aqueous twophase systems: Analysis of strengths, weaknesses, opportunities and threats'. *Biotechnology Journal* (2015), vol. 10(8): pp. 1158–1169.

191. P. S. Gascoine, D. Fisher: 'The dependence of cell partition in two-polymer aqueous phase systems on the electrostatic potential between the phases'. *Biochemical Society Transactions* (1984), vol. 12(6): pp. 1085–1086.

192. H. Walter: 'Cell partitioning in two-polymer aqueous phase systems'. *Trends in Biochemical Sciences* (1978), vol. 3(2): pp. 97–100.

193. G. Johansson: 'Partition of salts and their effects on partition of proteins in a dextran-poly(ethylene glycol)-water two-phase system'. *Biochimica et Biophysica Acta (BBA) - Protein Structure* (1970), vol. 221(2): pp. 387–390.

194. R. Reitherman, S. D. Flanagan, and S. H. Barondes: 'Electromotive phenomena in partition of erythrocytes in aqueous polymer two phase systems'. *Biochimica et Biophysica Acta (BBA) - General Subjects* (1973), vol. 297(2): pp. 193–202.

195. W. Fan, U. Bakir, and C. E. Glatz: 'Contribution of protein charge to partitioning in aqueous twophase systems'. *Biotechnology and Bioengineering* (1998), vol. 59(4): pp. 461–470.

196. H. Walter, E. J. Krob, and A. Pedram: 'Subfractionation of cell populations by partitioning in dextran-poly (ethylene glycol) aqueous phases. Discriminating and Nondiscriminating systems'. *Cell Biophysics* (1982), vol. 4(4): pp. 273–284.

197. D. Forciniti, C. K. Hall, and M .R. Kula: 'Interfacial tension of polyethyleneglycol-dextran-water systems: influence of temperature and polymer molecular weight'. *Journal of Biotechnology* (1990), vol. 16(3): pp. 279–296.

198. A .Merglen, S. Theander, B. Rubi, G. Chaffard, C. B. Wollheim, and P. Maechler: 'Glucose Sensitivity and Metabolism-Secretion Coupling Studied during Two-Year Continuous Culture in INS-1E Insulinoma Cells'. *Endocrinology* (2004), vol. 145(2): pp. 667–678.

199. P. R. Bevington and D. K. Robinson: 'Data Reduction and Error Analysis for the Physical Sciences'. 3rd ed. McGraw Hill, New York, USA, 2003.

200. S. Zimmermann, C. Scheeder, P. K. Zimmermann, A. Bogsnes, M. Hansson, A. Staby, and J. Hubbuch: 'Highthroughput downstream process development for cellbased products using aqueous twophase systems (ATPS) A case study'. *Biotechnology Journal* (2017), vol. 12(2): p. 1600587.

201. G. Johansson: 'Effects of salts on the partition of proteins in aqueous polymeric biphasic systems.' *Acta chemica Scandinavica. Series B: Organic chemistry and biochemistry* (1974), vol. 28: pp. 873–82.

202. M. Vis, V. F. D. Peters, R. H. Tromp, and B. H. Erné: 'Donnan Potentials in Aqueous Phase-Separated Polymer Mixtures'. *Langmuir* (2014), vol. 30(20): pp. 5755–5762.

203. Y. Liu, R. Lipowsky, and R. Dimova: 'Concentration Dependence of the Interfacial Tension for Aqueous Two-Phase Polymer Solutions of Dextran and Polyethylene Glycol'. *Langmuir* (2012), vol. 28(8): pp. 3831–3839.

204. R. S. King, H. W. Blanch, and J. M. Prausnitz: 'Molecular thermodynamics of aqueous twophase systems for bioseparations'. *AIChE Journal* (1988), vol. 34(10): pp. 1585–1594.

205. J. R. Luther and C. E. Glatz: 'Genetically engineered charge modifications to enhance protein separation in aqueous twophase systems: Charge directed partitioning'. *Biotechnology and Bioengineering* (1995), vol. 46(1): pp. 62–68.

206. J. M. Van Alstine: 'Eukaryotic cell partitioning: experimental considerations'. *Aqueous Two-Phase Systems: Methods and Protocols*. Ed. by R. Hatti-Kaul. Totowa, New Jersey: Humana Press, 2000: pp. 119–142.

207. H. Walter, F. A. Al-Romaihi, E. J. Krob, and G. V. Seaman.: 'Fractionation of K-562 cells on the basis of their surface properties by partitioning in two-polymer aqueous-phase systems'. *Cell Biophysics* (1987), vol. 10(3): pp. 217–232.

208. H. Walter and K. E. Widen: 'Cell partitioning in two-polymer aqueous phase systems and cell electrophoresis in aqueous polymer solutions. Human and rat young and old red blood cells'. *Biochimica et Biophysica Acta (BBA) - Biomembranes* (1994), vol. 1194(1): pp. 131–137.

209. H. Walter and R. P. Coyle: 'Effect of membrane modification of human erythrocytes by enzyme treatment on their partition in aqueous dextran-polyethylene glycol two-phase systems'. *Biochimica et Biophysica Acta (BBA) - General Subjects* (1968), vol. 165(3): pp. 540–543.

CHAPTER 7

Application of Additive Manufacturing as Tool for Process Development in Biotechnology: A Case Study

Sarah Gretzinger[1,2], Stefanie Limbrunner[2], Pascal Baumann[2], Jürgen Hubbuch[1,2,**]

[1] Institute of Functional Interfaces (IFG), Karlsruhe Institute of Technology (KIT), Eggenstein-Leopoldshafen, Germany

[2] Institute of Engineering in Life Sciences, Section IV: Biomolecular Separation Engineering, Karlsruhe Institute of Technology (KIT), Karlsruhe, Germany

[**] Corresponding author. Email: juergen.hubbuch@kit.edu

in preparation

Abstract

Early process development in biotechnology research and pharmaceutical industry is always related with high investment costs. Especially, the lack of experience and process knowledge in emerging fields, such as cell therapy, pose a financial risk. However, using the aspiring additive manufacturing (AM) technologies could be a shortcut during research and development. AM technology is an umbrella term for manufacturing methods building an object in a layer-by-layer manner. They represent a promising and versatile tool for process development in the field of biotechnology. Since they are relative cheap and facilitate a fast manufacturing of tailor-made equipment within a short cycle time.
Here, we demonstrate the power of AM as a tool in process development based on a technology transfer case study. The transfer of high-throughput (HTS) batch data for cell partitioning in aqueous two-phase systems (ATPS) into a microfluidic flow-through process was performed using an AM approach. Thus, standard lab-equipment was complemented with tailor-made and 3D printed devices, in order to create a flexible and cheap process set up. The technology transfer was conducted within the DMAIC (Define, Measure, Analyse, Improve and Control) framework to provide a systematic process development and process performance evaluation. Implementation of the developed microfluidic process set up was successful. Additionally, two main factors influencing cell partitioning in the ATPS case study were identified, namely, cell load and fluid velocities.

Keywords: additive manufacturing (AM), process development, cell separation, technology transfer, microfluidics

7.1 Introduction

The additive manufacturing (AM) technology has evolved constantly over the last decades and is considered to gain even more importance in the near future. The possibility to print in 3 dimensions triggers all kinds of innovations and inspires new ways in designing and material usage. [210–212] Especially, the research and development (R&D) environment and academia values these advantages. AM facilitates a flexible and fast production of self-developed equipment and prototypes, leading to an over-all shortening in development time. [161, 175] Academic research in the field of Biotechnology has, at present, focused mainly on 3D printing of tailor-made lab equipment [167–178, 213, 214] including molding tools for the production of microfluidic devices [168, 169, 171, 213] and tailored multiwell plates [173, 175, 176]. In particular, the implementation of 3D printed devices into high-throughput screening (HTS) platforms poses an increase of value e.g. rapid prototype development [161, 170, 171, 173, 175–178]. HTS technologies are state-of-the-art in biotechnology research and an integral part in process development of the pharmaceutical industry. [59, 140, 141, 143, 149–151, 215] Combining HTS with AM technologies promotes creativity and flexibility among this community and contributes to the concept of knowledge based process development. Process development in research and industry needs to be structured, systematic and must deal with limited resources concerning time, personal, budget and sample volume. [215–217] Thus, it is important to keep focused during process development using AM technologies, since the possibilities and creativity seems almost limitless. One approach to channel the creativity without getting lost in the possibilities, using AM technologies as tool in process development, is to apply the DMAIC (Define, Measure, Analyse, Improve and Control) methodology. DMAIC is the six sigma framework structuring process improvement projects in its five stages. Six sigma is, in general, applied when an already running process needs to be improved. [218–221] Using six sigma is not exclusive for manufacturing process improvement e.g. in pharmaceutical industry [219, 222] it can also be applied when a workflow needs to be improved e.g. in a clinic environment [223–225]. A controversial discussion is ongoing whether six sigma should be used in R&D, since it seems to decrease flexibility. [226] However, using the DMAIC methodology as a roadmap in process development projects, without the rigid six sigma approach, is highly beneficial. [221, 223–225, 227] The first stage define gives a precise and comprehensive view of the project. Subsequently, the initial situation and goals are described. Additionally, a timeline might be specified and project members are selected. In the measure phase the process is defined more specific and a suitable and validated analytical strategy must be implemented. Then, the process is evaluated concerning process performance. In the analytic phase a root-cause investigation is performed, leading to an identification of main factors for process failure or poor process performance. In the improve phase the main factors are verified and corrective actions are planned and implemented. The final control phase is used to evaluate the process optimisation and implementation of an ongoing monitoring system to guarantee high process performance. [219, 224, 225] Thus, using the well-established tools of HTS and the DMAIC methodology in combination with the promising AM technologies is highly beneficial for process development. Such an approach does not only contribute to the concept of knowledge based process development,

it also speeds up project cycle times in addition to the unlimited freedom of creativity in process set up.
Here, we report the usage of AM technologies as tool in early process development. This was done based on a case study comprising a feasibility analysis of the technology transfer of cell partitioning in aqueous two-phase (ATPS) systems batch HTS data into a flow-through microfluidic process. Cell partitioning in ATPS is known as a method for cell separation for regenerative medicine. However, the applicability is limited since the underlying mechanisms are not fully understood. [53, 54, 189–191] In a previous study, a HTS platform was developed to perform a systematic empirical screening for suitable systems. [60] The findings of the HTS study were now transferred in a microfluidic process. Aiming a fast realisation with low investment costs, 3D printing, as a tool for equipment production, was used in combination with the DMAIC approach.

7.2 Materials and Methods

7.2.1 Stock Solutions

Preparation of all stock solutions and buffers, needed for the ATPS production, were done using ultra-pure water (0.55 μS/cm) obtained from an Arium®proUV water system (Sartorius Stedim Biotech, Goettingen, Germany). Stock solutions of 20 (w/w) % Dextran 500,000 (Pharmacosmos A/S, Holbaeck, Denmark) and 30 (w/w) % PEG 8,000 (Sigma Aldrich, St. Louis, USA) were prepared. 500 mM sodium phosphate (NaPi) buffer with pH 6.6 and 7.4 were prepared as described before. [60] Sodium chloride (NaCl) (Merck, Darmstadt, Germany) was prepared as 500 mM stock solution. All stock solutions and buffers were sterile filtered (Ø 0.22 μm) and stored at room temperature, except the polymer stock solutions which were stored at 4 °C. The flow cytometry staining buffer consisting of phosphate-buffered saline (PBS) (Thermo Fisher Scientific, Waltham, USA) was supplemented with 0.5 % bovine serum albumin (BSA) (Miltenyi Biotech, Bergisch Gladbach, Germany) and 2 mM EDTA (Thermo Fisher Scientific) and stored at 4 °C. Stock isotonic percoll (SIP) was prepared by mixing percoll (GE Healthcare, Piscataway, USA) and 10 x PBS in a 9:1 volume ratio.

7.2.2 Software and Data Processing

BD LSR Fortessa Cell Analyzer was controlled by BD FACSDiva 8.0 (BD Biosciences, San Jose, USA). Flow cytometry data were analysed and visualised using FlowJo V10 (Tree Star Inc., Ashland, USA). The Tecan Freedom Evo 200 was controlled using Evoware 2.5 SP2 standard (Tecan, Crailsheim, Germany). Cetoni NeMESYS syringe pumps were controlled using QmixElements Version: 20140708 (cetoni GmbH, KorbuSSen, Germany). For data storage Excel 2013 (Microsoft, Redmond, WA, USA) was used. Matlab R2015a (The MathWorks, Inc., Natick, USA) was used for data evaluation and visualisation. The construction work was done with the 2D/3D CAD software SolidEdge (Siemens PLM Software, Plano, USA). The GoPro Hero4 camera (GoPro, Inc., San Mateo, USA) was controlled via the GoPro App version 2.6.3.312 (GoPro, Inc.) and a Samsung Galaxy Note Pro SM-P900 (Samsung, Seoul, South Korea).

7.2.3 Additive Manufacturing

An additive manufacturing approach (AM) was used for the fabrication of tailor-made laboratory equipment. The construction work was done with the 2D/3D CAD software SolidEdge (Siemens PLM Software). Depending on the requirements of the designed lab-equipment part, different AM technologies were used. Parts with a high resolution tolerance were printed in house with the inexpensive stereolithography desktop 3D printer form 1+ (Formlabs Inc., Somerville, USA) using the MadeSolid Black Resin (Redresin, Barcelona, Spain). In order to keep investment costs low, fabrication of medium and low resolution tolerance were outsourced. Parts with medium resolution tolerance were manufactured by Sculpteo Pro (Issy-les-Moulineaux, France) using a plastic laser sintering approach (material: polished black plastic). Parts with low resolution tolerance were manufactured by Proform AG (Marly, Switzerland) using a stereolithography approach (material: Accura Xtreme).

7.2.4 Microfluidic Device Production

The microfluidic device was produced as previously described [168, 169] using the two component polydimethylsiloxane (PDMS) curing system Elastosil 601 (Wacker Chemie, Burghausen, Germany) with the exception that the chip bonding was performed in a sterile hood to reduce particle load in the surrounding area.

7.2.5 ATPS Preparation

ATPS were prepared under sterile conditions with a total volume of 20 mL prior to use according to **table 7.1** in a 50 mL reaction tube using water for injection (WFI) (Thermo Fisher Scientific). ATPS were mixed and centrifuged for 20 min at 4000 rpm for phase separation. Top and bottom phase were taken and kept under sterile conditions prior to use.

Table 7.1: Characterization of the used ATPS

system	NaCl	NaPi
Dextran MW 500,000 [% (w/w)]	5.0	5.0
PEG MW 8,000 [% (w/w)]	4.0	4.0
salt supplementation	0.14 M NaCl, 0.01 M NaPi (pH 6.6)	0.11 M NaPi (pH 7.4)
density top phase [g/cm^3]	1.0194 ±0.0016	1.0235 ±0.0001
density bottom phase [g/cm^3]	1.0450 ±0.0002	1.0522 ±0.0008
Δ density [g/cm^3]	|0.0256|	|0.0287|
viscosity top phase [Pa*s]	3.66 ±0.04	3.6 ±0.08
viscosity bottom phase [Pa*s]	25.11 ±0.64	26.62 ±0.27
Δ viscosity [Pa*s]	|21.45|	|23.02|

7.2.6 Viscosity and Density Measurements

Viscosity measurements of the ATPS top and bottom phases were done using a RheoScope 1 (Thermo Fisher Scientific, Waltham, USA) equipped with a cone-plate sensor (diameter 50 mm, angle 1 °) at room temperature (shear stress: 0.1 - 10 Pa). Density was measured

at room temperature using the density sensor MicroLDS (Integrated Sensing Systems, Inc., Ypsilanti, USA).

7.2.7 Cell Culture

The promyelocytic cell line HL-60 was purchased from CLS (Cell Lines Service, Eppelheim, Germany). Cell culture reagents were purchased from Thermo Fisher Scientific, unless otherwise stated. Culture media consisted of RPMI 1640 with GlutaMAX supplemented with 15 (v/v) % fetal bovine serum (FBS), 1 (v/v) % sodium pyruvate, 1 (v/v) % non-essential amino acids (NEAA), and 0.5 (v/v) % Penicillin/Streptomycin. Cells were propagated at 37 °C in a 5 % CO_2 incubator and split every 3 - 4 days to a concentration of 1.5 x 10^5 cells/mL. All experiments were done with undifferentiated cells.

7.2.8 Cell Density Characterisation

Density gradient centrifugation using percoll is a well-known cell separation method. [38, 39, 228, 229] In this study, an alternated protocol was used for cell density analysis, where each gradient step was prepared separately. The procedure is depicted in **supplementary data 7.1**. The gradient from 60 (v/v) % - 30 (v/v) % SIP (16 gradient steps) with a total step volume of 650 μL was prepared in 1.5 mL reaction tubes (Eppendorf, Hamburg, Germany) using a Tecan Freedom Evo® 200 liquid-handling station (LHS). Followed by a gentle, manual overlaying of each gradient step with 100 μL cell suspension (8 x 10^6 cells/mL in PBS supplemented with 1 mM EDTA). Reaction tubes were centrifuged for 20 min at 4000 g. Afterwards, a 30 μL sample was taken at the middle of the reaction tube and diluted in 250 μL flow cytometry staining buffer. Cells were stained with the viability dye 7-AAD (Biolegend) according to the manufacturers instructions. Dead cells were gated using heat inactivated controls (70 °C, 10 min). The flow cytometry analysis was performed using an LSR Fortessa by BD Bioscience equipped with a BD™ high-throughput sampler in combination with 96-well U bottom plates (BD Falcon™, Franklin Lakes, USA). A defined sample volume of 100 μL was analysed and the following settings were applied: sample flow rate: 3 μL/s, sample volume: 100 μL, mixing volume: 100 μL, mixing speed: 250 μL/s, four mixing cycles and a wash volume of 800 μL. Density measurements of the SIP gradient steps was performed as described above.

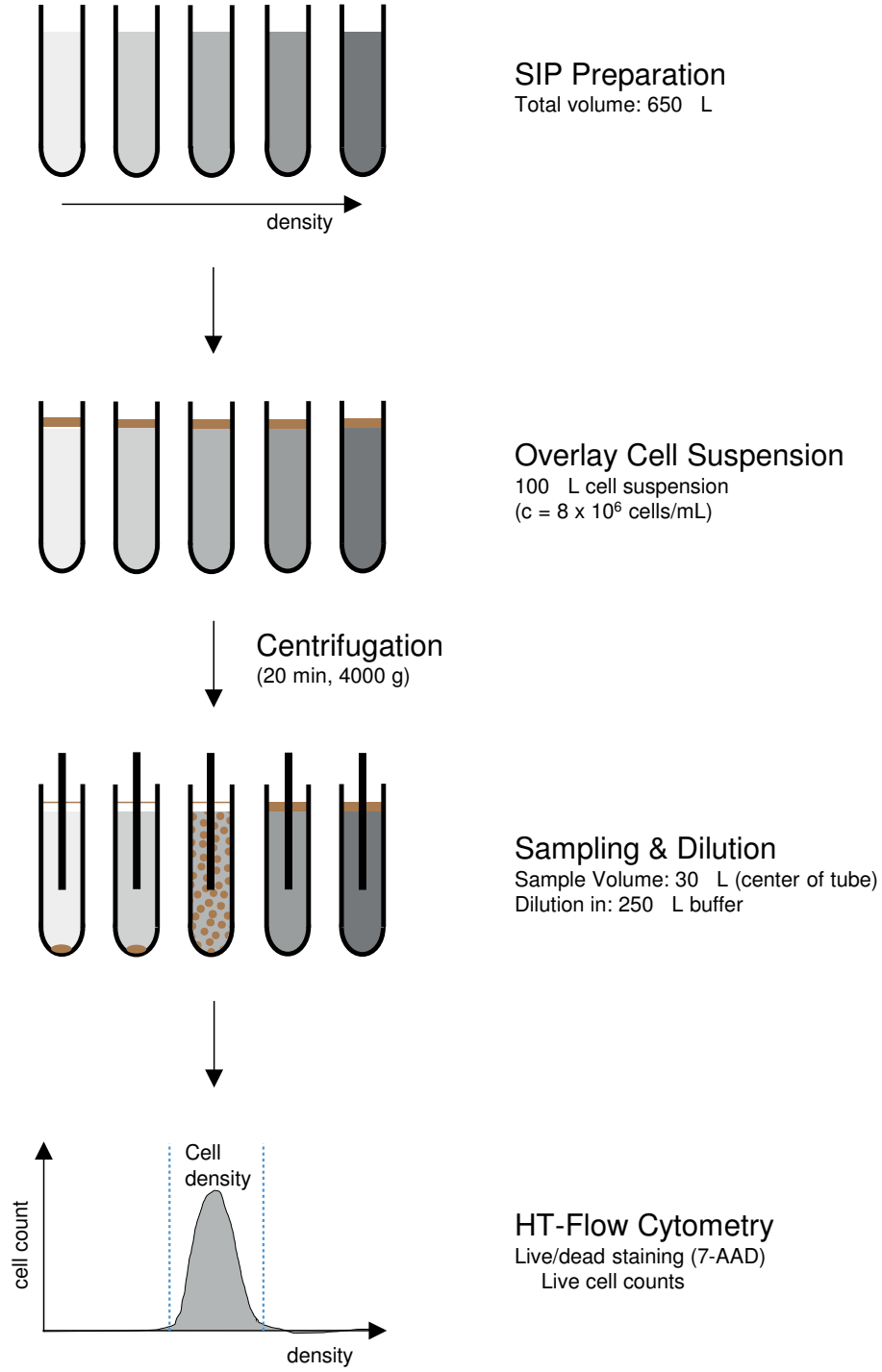

Supplementary Data 7.1: Overview of the cell density characterisation procedure. After SIP step gradient perpetration in individual tubes, the SIP is gently overlaid with cell suspension. By centrifugation the cells are distributed according to their density. Sampling is done in the centre of the tube, diluted and live cell count is analysed by high-throughput flow cytometry (HT-flow cytometry).

7.2.9 Flow Cytometry Analysis

Flow cytometry was performed using a LSR Fortessa from BD Bioscience. Prior to analysis, cells were resuspended in flow cytometry staining buffer and stained with the viability dye 7-AAD (Biolegend, San Diego, USA), according to the manufacturers instructions. Dead cells were gated using heat inactivated controls (70 °C, 10 min).

7.3 Results and Discussion

In the present work, the power of 3D printing as a tool in early process development was demonstrated. This was done based on a case study comprising a feasibility analysis for the technology transfer of batch HTS data into a flow-through microfluidic process. The basis of the project was the findings of a previous batch HT screening of cell partitioning in ATPS. [60] Aiming at fast realization with low investment costs, 3D printing, as a tool for equipment production, was used in combination with the DMAIC approach. Following, the DMAIC stages are presented.

Define

In the define phase, the initial situation for the technology transfer was described. A general concept was conceived, bottlenecks identified and solution approaches developed. Driving force for the initiation of this technology transfer project was the successful identification of ATPS suitable for cell partitioning of the model cell line HL-60 via batch HT screening. [60] Two ATPS were selected for the technology transfer project. Both systems consisted of 5 (w/w) % dextran (MW 500,000) and 4 (w/w) % PEG (MW 8,000), but differed in salt supplementation. One ATPS was supplemented with 0.14 M NaCl and 0.01 M NaPi (pH 6.6). Using this ATPS, HL-60 cells were found in the interphase in the batch experiments. The second ATPS was supplemented with 0.11 M NaPi (pH 7.4), here, cells were detected predominantly in the top phase (65 %) and in the interphase. [60]

First, a general microfluidic process set up was developed. **(fig. 7.2)** The cell suspension, top and bottom phase were pumped individually in the microfluidic device with three in- and outlets. Fluid velocities were chosen so that cells are focused at the interphase. To analyse the cell partitioning between top and bottom phase, a video was recorded near the outlet of the microfluidic device, using a microscope camera. Automatization of the video analysis was realized via a snap shot analytic which enabled the estimation of cells in top and bottom phase. Additionally, live cell rate were determined via flow cytometry by analysing pooled samples as performed in the batch screening.

Aiming at fast implementation of the process set up with low initial investment costs, four equipment bottlenecks were identified, while the key equipment (microscope, flow cytometer, three piston pumps and molding tool for the microfluidic device production) were on hand. Missing parts were a suitable camera integrated in the microscope, a replication master for the production of the microfluidic device, a fractionator for sampling flow cytometry probes and a frame for the microfluidic device. 3D models of the designed equipment are shown in **fig. 7.3**. The Eclipse TS 100 microscope (Nikon GmbH, Düsseldorf, Germany) was used for the process set up. The microscope has an integrated camera shaft, however, a suitable camera was not available in the group. Hence, a low investment solution was

designed, using an inexpensive GoPro Hero4 (GoPro, Inc., San Mateo, USA). The camera was installed over the camera shaft using a designed and 3D printed camera mount. A 10 x magnification objective needed to be installed between the shaft and the camera. The mount was printed using the desktop stereolithograpy 3D printer form 1+ (Formlabs Inc.). **(fig. 7.3 A)** For the production of the microfluidic device the previously developed molding tool was used. [168] However, the design for the replication master needed to be

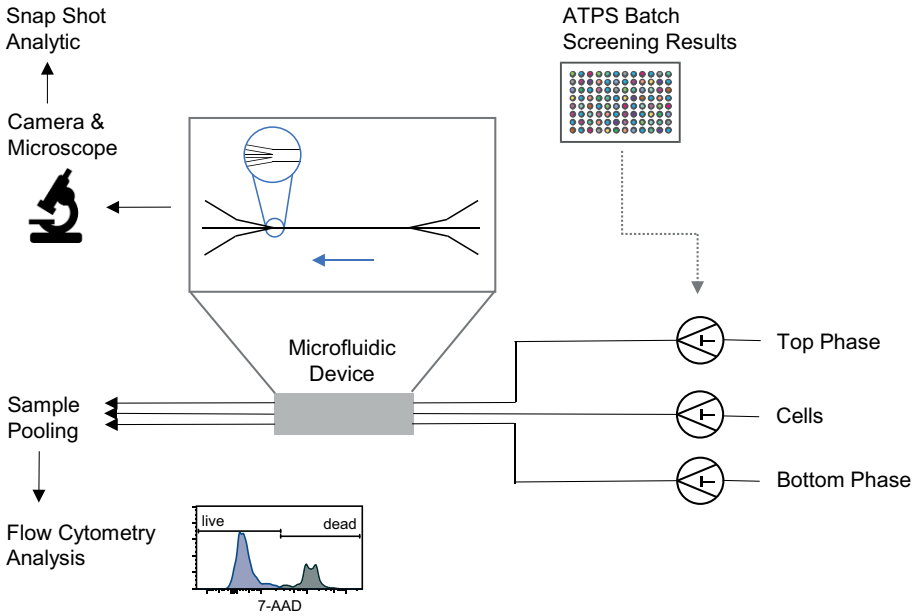

Figure 7.2: Overview of the developed process set up. Previously, cell partitioning in ATPS was screened and optimal systems were chosen for the technology transfer into a microfluidic process. Cell suspension, top and bottom phase is pumped individually in the microfluidic device with three in- and outlets. During the process a video near the outlet is recorded using the microscope camera. The video is then automatically analysed via the developed snap shot analytic. The snap shot analytic enables the automatic estimation of cells in top and bottom phase. Additionally, live cell rate is determined via flow cytometry by analysing pooled samples.

customized. The molding tool is designed to produce microfluidic devices in a microtiter plate format. Thus, the replication master was designed in microtiter plate format with two identical microfluidic channels with 3 in- and outlets. The channels were designed as described by Tsukamoto *et al.* [230] (channel length = 50 mm; channel width = 0.5 mm; channel height = 0.1 mm). Since the replication master has a low resolution tolerance, it was manufactured by Proform AG using a stereolithography approach. **(fig. 7.3 B)** For sampling of probes for the flow cytometry analysis, a manual tailor-made fractionator was designed and 3D printed by Sculpteo Pro. The fractionator was designed with optimal installation space, leading to the opportunity to integrate it on the microscope table. The three microfluidic outlets were connected, thus, samples could be fractionated in 1.5 mL tubes. **(fig. 7.3 C)** To stabilize the flexible PDMS microfluidic device on the microscope

table, a frame was designed and 3D printed by Sculpteo Pro. The frame consisted of three parts, the bottom plate, an inlet- and outlet bridge. The in- and outlet tubing were connected with the microfluidic device and stabilized via the bridges using fittings. **(fig. 7.3 D)**

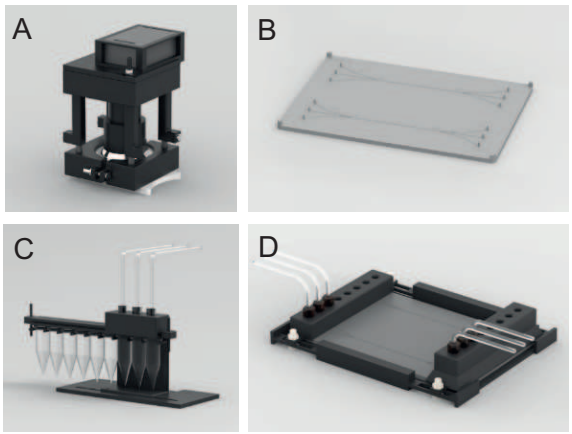

Figure 7.3: 3D models of designed equipment, needed for the process set up. **A** Camera mount: small high performance camera was used and installed via mount using the existing camera shaft. **B** Microfluidic replication master: the replication master was designed in a microtiter plate format with two identical microfluidic channels with 3 in- and outlets. **C** Manual tailor-made fractionator: the fractionator was designed with optimal installation space, leading to the opportunity to integrate it on the microscope table. The three microfluidic outlets were connected, samples can be fractionated in 1.5 mL tubes. **D** Frame for the microfluidic device: the frame consists of three parts, the bottom plate, an outlet- and inlet bridge. The in- and outlet tubing were connected with the microfluidic device and stabilized via the bridges using fittings.

Besides the missing equipment parts, an automated video analysis tool needed to be developed. Automatic counting of the cells in the top and bottom phase was realized using a snapshot analytic in Matlab. The method is divided into two steps: (i) Detection of the phase boundary using Hough-Transformation and (ii) Counting of the cells using regional maximum. Per experiment, 30 snapshots of the video were taken over the duration of the video in the same timely distance. For the detection of the phase boundary (i), the images were first converted into a gray color image and inverted. The images were opened morphologically and converted into a binary image based on a threshold. With the Hough-Transformation the phase boundary could be located. The proceeding for the automatic cell counting in a snap shot (ii) is shown in **fig. 7.4**. First, the image area representing the microfluidic channel was selected. **(fig. 7.4 A)** Then, the image is converted into a gray scale image. For the deblurring of the background a minimum filter is used to find the darkest pixel in an area. **(fig. 7.4 B)** The deblurred image is further converted into a binary image. **(fig. 7.4 C)** On the basis of the binary image the cells are detected. The diameter of a cell of 6 pixels was used as a value for the separation into cells or agglomerates. The distance between the objects were measured. If the distance was

higher than the diameter the objects were declared as a single cell, otherwise the objects were declared as agglomerates. The number of detected cells were then exported in a excel file and detected cells were drawn into the original image. **(fig. 7.4 D)** Cells detected in the bottom phase are indicated as blue, while agglomerates are marked as green. Only one agglomerate (magenta) was detected in the top phase.

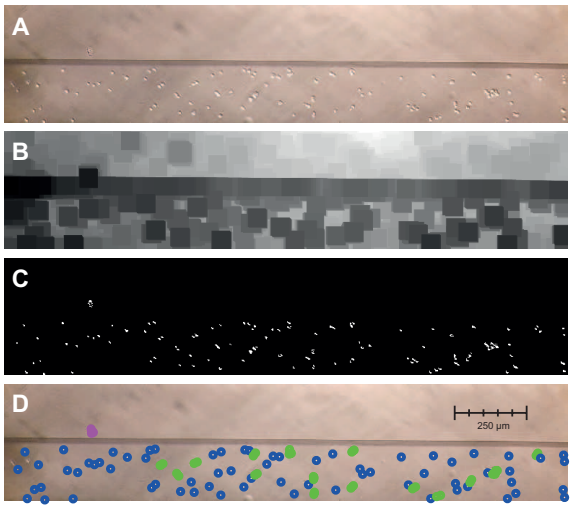

Figure 7.4: Working steps of the snap shot analytic script for the automatic cell counting in the bottom and top phase. **A** Selection of the essential image area, **B** usage of minimum filter to find the darkest pixel in each region, **C** subtraction of the background, conversion into a binary image, **D** original image with indicated detected cells and agglomerates. Cells detected in bottom phase are indicated **blue**, agglomerates are indicated **green**. Agglomerates in top phase are indicated **magenta**.

Measure

In the measure phase, the experimental set up was specified and the snap shot analytic was validated. Subsequently, the conduction and evaluation of the cell partitioning experiments, using the developed flow-through microfluidic set up, were realized.

First, the top and bottom phase was prepared as described earlier. Additionally, the HL-60 cell suspension was prepared with a final concentration of 20 x 10^6 cells/mL in 1 mM EDTA in PBS. Each fluid was pumped individually using 3 Cetoni NeMESYS syringe pumps (cetoni GmbH). For the top and bottom phase, the pumps were equipped with a 500 μL syringe, while the pump for the cell suspension was equipped with a 100 μL syringe. The top phase was introduced into the microfluidic device via the upper inlet and the bottom phase via the bottom inlet. The cell suspension was introduced in the middle inlet. The cells were focused at the interphase by applying suitable velocity patterns for the three fluids. In general, two velocity patterns were evaluated as described in **table 7.2**. The TS 100 microscope (Nikon GmbH) with the integrated GoPro Hero4 camera (GoPro, Inc.) was used for video recording of the microfluidic channel outlet. The following camera settings were applied: 120 fps, field of view = narrow. Three videos were taken after 5 min,

each 30 s (n = 3; sample size = 30 snap shots; total = 3 x 30 = 90 snap shots). The videos were analysed using the described snap shot analytic. Additionally, fractionated samples were pooled and live cell ratio was evaluated using the earlier described flow cytometry method (live/dead staining using 7-AAD).

Table 7.2: Velocity patterns of the experimental procedure

Velocity pattern TP / cell suspension / BP*	**NaCl**	**NaPi**
fast [μL/s]	0.25 / 0.02 / 0.055	0.25 / 0.02 / 0.055
slow [μL/s]	0.1 / 0.01 / 0.02	0.02 / 0.0004 / 0.0015

*TP = top phase; BP = bottom phase

The implementation of the developed experimental set up was confirmed by a proof of concept experiment. **(fig. 7.5)** Microscopic pictures of the microfluidic device inlet, the centre of the channel and the outlet were taken. Cells were focused successfully at the channel inlet branch and partitioned in the bottom phase channel downstream. Just in front of the channel outlet, a video was taken and analysed via the developed snap shot analytic described earlier. Using this video-based tool cells were detected and counted in top and bottom phase individually, additionally, cell agglomerates were excluded. Fractioning of flow cytometry probes could be realized exactly as planned using the 3D printed fractionation device. Accordingly, the implementation of the process set up was successful.

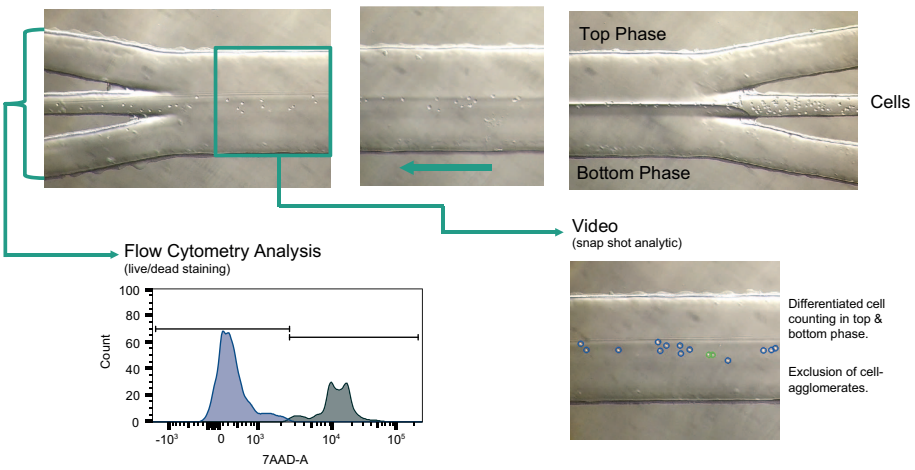

Figure 7.5: Proof of concept. Pictures of the microfluidic device inlet, the centre of the channel and the outlet. Top phase, cell suspension and bottom phase were pumped individually. The velocities are chosen that the cells are focused at the interphase and channel downstream partitioned in the bottom phase (centre picture). Just before the outlet, a video was taken and analysed via the developed snap shot analytic. Using this video-based tool, cells are detected and counted in top and bottom phase individually, additionally, cell agglomerates are excluded. Live/dead analysis using flow cytometry in combination with 7-AAD staining was done with the pooled sample.

Subsequently, the snap shot analytic was evaluated by analysing the cell detection hit

ratio. For this purpose a comparison of manual cell counting and the automatic snap shot analytic was performed. Cell counting of 20 snap shots was done by 3 different individuals in comparison to the developed snap shot analytic. Hit ratio (HR) calculation was done as described in **eq. (7.1)**:

$$HR = \frac{counts}{actual \quad counts} \tag{7.1}$$

The ranges of the hit ratio determination is shown in **fig. 7.6**. Manual counting performed by three individuals showed overestimation (HR > 1) as well as underestimation (HR < 1) of cells and a wide range of the hit ratio. In contrast, the snap shot analytic showed only a slight underestimation of cells with a narrow hit ratio range. Thus, the developed snap shot analytic can be implemented in the process set up. The advantages of this approach (e.g. economy of time, objective cell counting and small range) outweigh the small systematic error of cell underestimation.

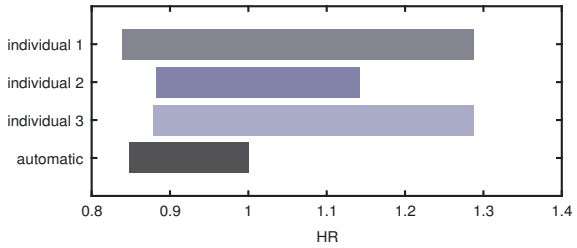

Figure 7.6: Cell detection hit rate (HR) ranges of three individuals (manual counting) and the automatic detection via the developed snap shot analytic. The hit ranges were calculated using 20 video frames.

Following the successful implementation of the developed flow-through microfluidic process set up, cell partitioning experiments were performed. Evaluation was done concerning transferability of batch data. Experiments were performed with two ATPS differing in the salt supplementation **(table 7.1)** and two velocity profiles **(table 7.2)**. Shown is the total count of 3 x 30 = 90 snap shots and the partitioning coefficient (q) in top and bottom phase as time series plot for each experiment **(fig. 7.7)**. Partitioning coefficient (q) is calculated according to **eq. (7.2)**:

$$q_x = \frac{cell\ count\ in\ x}{total\ cell\ count} \tag{7.2}$$

$_x$ = top or bottom phase

In green is shown q_{top} and in blue q_{bottom}, while the orange line represents the overall mean (n = 90). Raw data as well as the mean of each sample with 30 snap shots (n = 30) is plotted for both total cell count and q. The results for the experiment with NaCl supplemented ATPS with the fast velocity profile is shown in **fig. 7.7 A & C**. No trend in total cell counts were observed, however, the total mean (3 x 30 = 90) was

relatively low with 9.9 cells per snap shot **(fig. 7.7 A)**. Cells predominantly partitioned in the bottom phase with a total q_{bottom} of 0.99 **(fig. 7.7 C)**, while in batch experiments cells predominantly were found in the interphase. [60] Thus, results were not in compliance with the batch data. Total cell counts were slightly higher with a total mean (3 x 30 = 90) of 17.13 cells per snap shot for the experiment with NaPi supplemented ATPS with the fast velocity profile. A decrease in total cell number was observed **(fig. 7.7 B)**. Additionally, a fluctuation of the partitioning coefficient could be observed with a total q_{bottom} of 0.66. In contrast, batch data showed a predominantly cell partitioning in the top phase (65 %) **(fig. 7.7 D)**. [60]
The results for the experiment with NaCl supplemented ATPS with the slow velocity profile is shown in **fig. 7.7 E & G**. A slight decrease of total cell counts were observed with a total mean (3 x 30 = 90) of 21.08 cells per snap shot **(fig. 7.7 E)**. Cells also predominantly partitioned in the bottom phase with a total q_{bottom} of 0.88 **(fig. 7.7 G)**. Total q_{bottom} decreased 0.11 in comparison with the fast velocity pattern experiment. Much higher total cell counts were observed for the experiment with NaPi supplemented ATPS with the slow velocity profile with a total mean (3 x 30 = 90) of 58.81 cells per snap shot, in addition, a decrease in total cell count was observed **(fig. 7.7 F)**. A decrease in q_{bottom} and consequently an increase in q_{top} was also observed (q_{bottom} = 0.67) **(fig. 7.7 H)**.

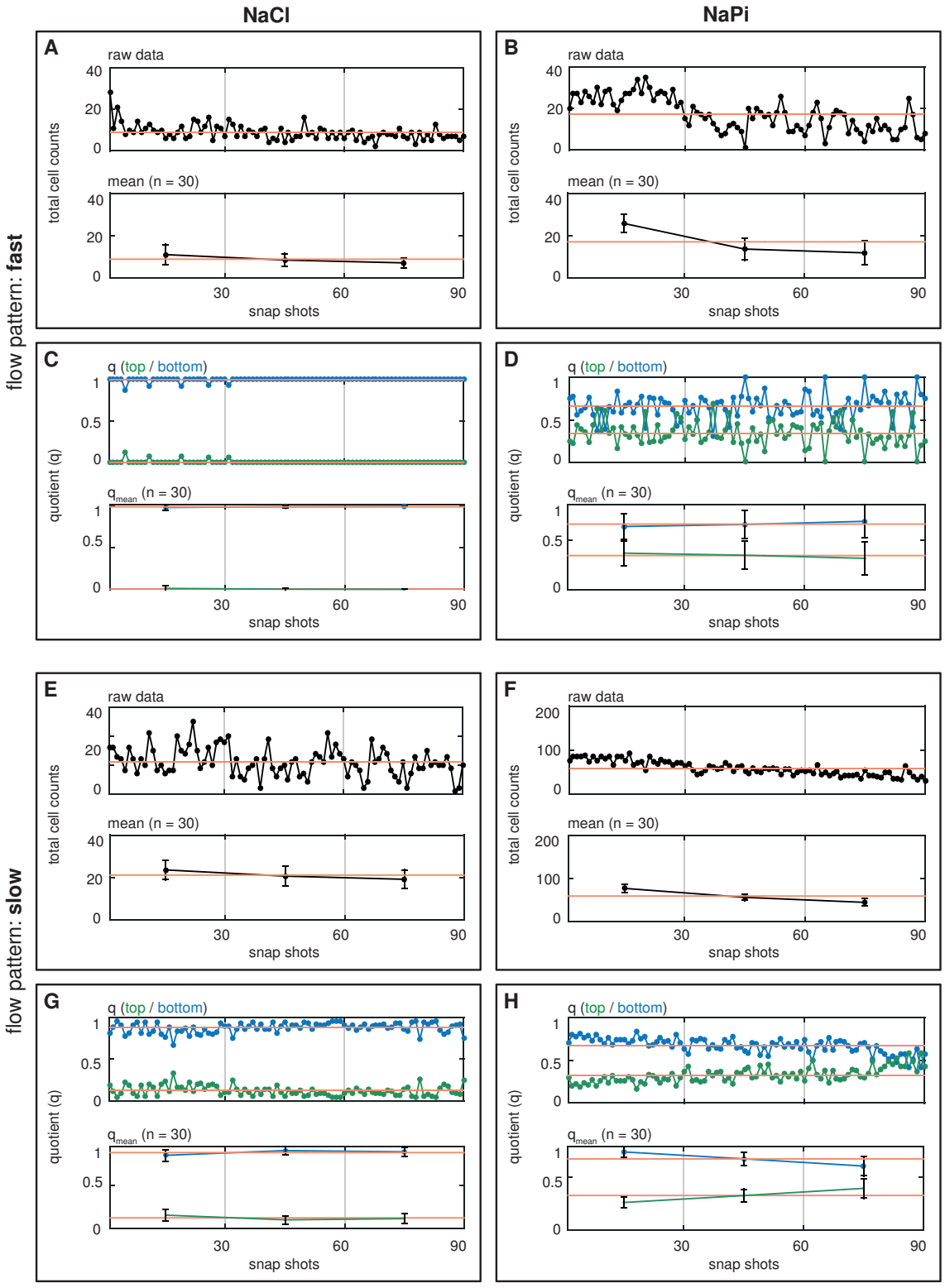
NaCl
NaPi
flow pattern: fast
flow pattern: slow
A
B
C
D
E
F
G
H
raw data
mean (n = 30)
total cell counts
q (top / bottom)
quotient (q)
snap shots

Figure 7.7: Evaluation of the influence of salt supplementation in ATPS on cell partitioning using the developed flow-through microfluidic process set up. Shown is the total count of 3 x 30 = 90 snap shots and the partitioning coefficient (q) in top and bottom phase as time series plot. On the left side is shown the results of the experiments using ATPS supplemented with NaCl and on the right side the results of the NaPi supplemented ATPS. Evaluated were two different velocity profiles: fast (top) and slow (bottom). **A** Time series plot of the total cell count of the cell partitioning experiment with NaCl supplemented ATPS applying the fast velocity pattern. **top:** plotted raw date, **bottom:** mean of sample (sample = 3, n = 30). The orange line represents the overall mean (n = 90). **B** Time series plot of the total cell count of the cell partitioning experiment with NaPi supplemented ATPS applying the fast velocity pattern. **top:** plotted raw date, **bottom:** mean of sample (sample = 3, n = 30). The orange line represents the overall mean (n = 90). **C** Time series plot of the partitioning coefficient (q) in top **(green)** and bottom **(blue)** phase of the cell partitioning experiment with NaCl supplemented ATPS applying the fast velocity pattern. **top:** plotted raw date, **bottom:** mean of sample (sample = 3, n = 30). The orange line represents the overall mean (n = 90). **D** Time series plot of the partitioning coefficient (q) in top **(green)** and bottom **(blue)** phase of the cell partitioning experiment with NaPi supplemented ATPS applying the fast velocity pattern. **top:** plotted raw date, **bottom:** mean of sample (sample = 3, n = 30). The orange line represents the overall mean (n = 90). **E** Time series plot of the total cell count of the cell partitioning experiment with NaCl supplemented ATPS applying the slow velocity pattern. **top:** plotted raw date, **bottom:** mean of sample (sample = 3, n = 30). The orange line represents the overall mean (n = 90). **F** Time series plot of the total cell count of the cell partitioning experiment with NaPi supplemented ATPS applying the slow velocity pattern. **top:** plotted raw date, **bottom:** mean of sample (sample = 3, n = 30). The orange line represents the overall mean (n = 90). **G** Time series plot of the partitioning coefficient (q) in top **(green)** and bottom **(blue)** phase of the cell partitioning experiment with NaCl supplemented ATPS applying the slow velocity pattern. **top:** plotted raw date, **bottom:** mean of sample (sample = 3, n = 30). The orange line represents the overall mean (n = 90). **H** Time series plot of the partitioning coefficient (q) in top **(green)** and bottom **(blue)** phase of the cell partitioning experiment with NaPi supplemented ATPS applying the slow velocity pattern. **top:** plotted raw date, **bottom:** mean of sample (sample = 3, n = 30). The orange line represents the overall mean (n = 90).

In addition to the cell partitioning behaviour, cell viability is a critical process parameter. The evaluation of the process influence on cell viability was done using flow cytometry analysis in combination with a 7-AAD staining. The results are shown in **fig. 7.8**. A cell viability loss could be observed for all experiments. Higher cell viability loss was observed for fast velocity profiles (∼7 %) in comparison to slow velocity profile experiments. However, cell viability loss was higher for ATPS supplemented with NaCl (fast = 29.11; slow = 21.7) than for NaPi (fast = 23.3; slow = 16.33) supplementation.
During the measurement phase a general problem with cell aggregation in tubing between pump and microfluidic device was observed. If visible cell agglomeration was acknowledged, the experiment was prematurely terminated. For this reason, experiments were performed if a variation in cell number per snap shot could be seen in data before the visual observation. Examples of trend in total cell counts per snap shots are shown in **fig. 7.9**. Depicted are the time series plots of two experiments with the same experimental set up. Both experiments were done with NaPi supplemented ATPS and the slow velocity pattern. However, an increase of total cell number was observed **(fig. 7.9 A)** as well as a decrease

in cell number **(fig. 7.9 B)**. Consequently, trends were also observed for the partitioning coefficients. Lower total cell number per snap shot leads to a convergence of q_{bottom} and q_{top} **(fig. 7.9 C & D)**.

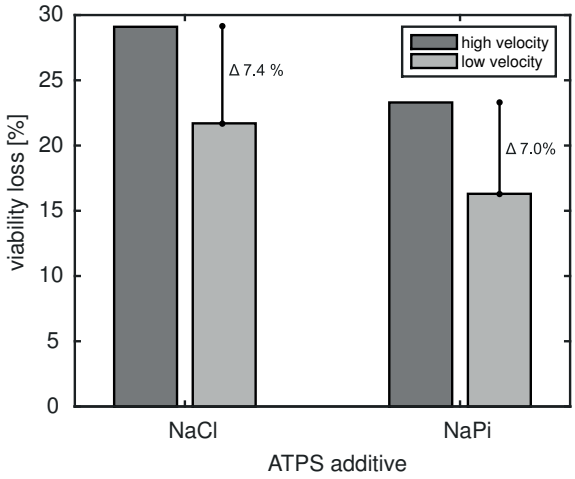

Figure 7.8: Evaluation of cell viability loss caused by microfluidic flow-through cell partitioning experiments. Flow cytometry analysis in combination with 7-AAD staining was performed. Tested were two ATPS differing in their salt supplementation (NaCl/NaPi) and two velocity patterns (fast/slow).

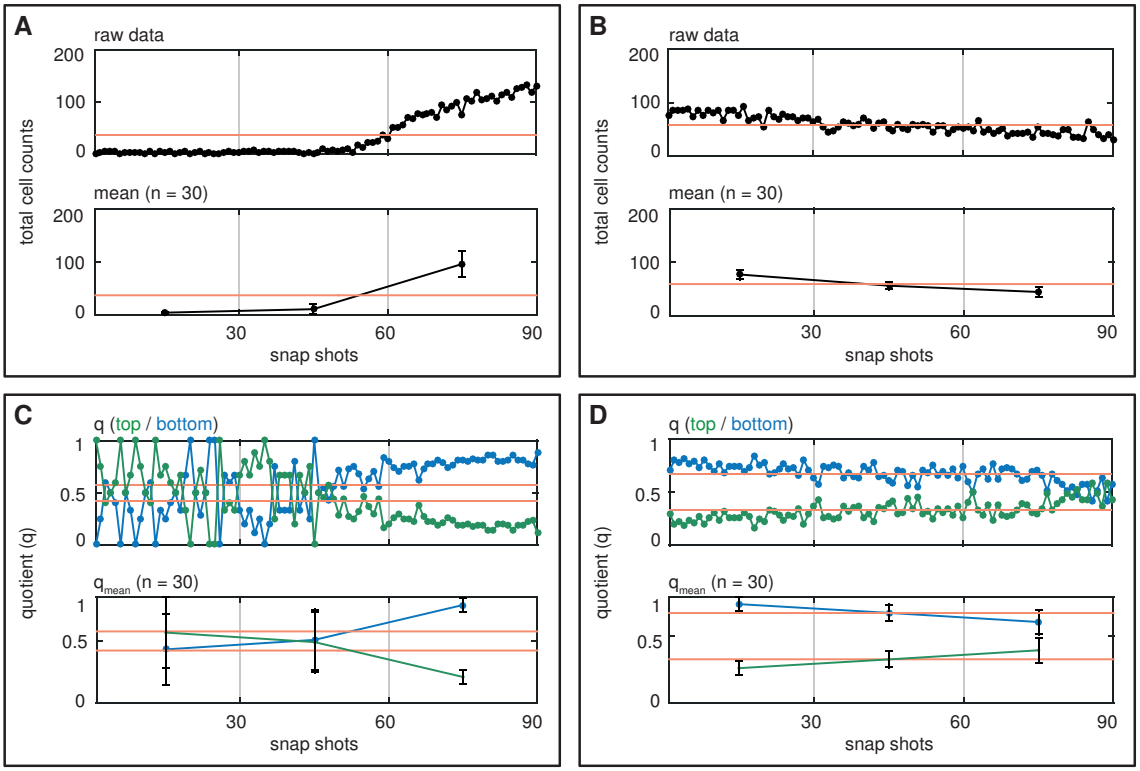

Figure 7.9: Trends in total cell number for experiments with ATPS supplemented with NaPi and a slow velocity pattern. Shown is the total count of 3 x 30 = 90 snap shots and the partitioning coefficient (q) in top and bottom phase as time series plot. **A** Increase in total cell number. **B** Decrease in total cell number. **C** Partitioning coefficient for increasing total cell number. **D** Partitioning coefficient for decreasing total cell number.

Analyse

In the analyse phase an evaluation of the collected data was done regarding poor process performance. The successful implementation of the developed process set up could be confirmed through the proof of concept experiment. Using the rapid prototyping approach, missing equipment was identified, designed, 3D printed and implemented inexpensively and without any delay. Thus, 3D printing is an excellent tool for process development with the opportunity to optimise the set up or adapt it to new applications.

Continuous cell partitioning in ATPS using a microfluidic approach has been described in literature earlier. [230–234] However, in contrast to the literature three mayor issues, namely cell viability loss, batch data incongruity and trends in cell load, were identified in this work. The brainstorming technique was applied to identify underlying mechanisms, leading to the issues. Groundwork for the brainstormed reasons were a systematic process consideration and the process understanding. The knowledge gained is summarized in **fig. 7.10** as fishbone diagram. Cell viability is a critical cell parameter which is known to be compromised by processing cells in a flow system. As indicated by the flow cytometry results, slower velocities might lead to a less pronounced loss of cell viability. [235–239]

Fluid velocities are also considered to be the major cause for the disagreement with the batch data. [231] Both systems show a more pronounced cell partitioning in the bottom phase independent of salt supplementation. Whereas, the batch HTS data shows a

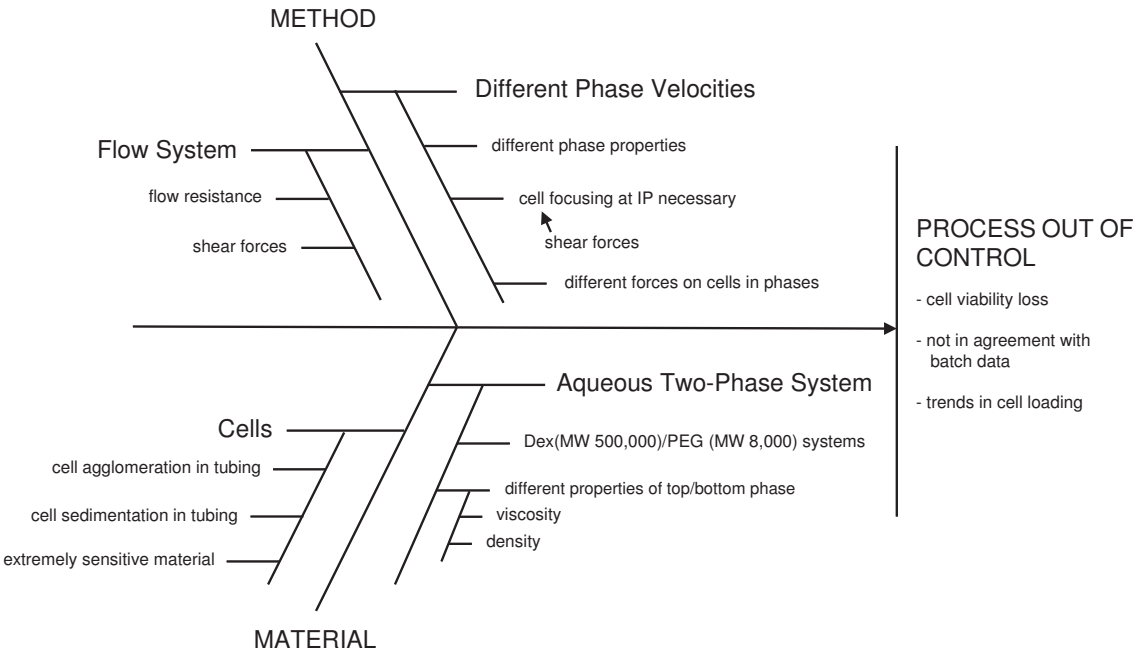

Figure 7.10: Fishbone-diagram: relationships between process parameter and occurring issues.

more pronounced cell partitioning into the top phase when supplemented with NaPi and adsorption to the interphase in NaCl supplemented ATPS. Thus, fluid velocities of the phases are identified as critical process parameter (CPP) influencing multiple aspects of the process and should be investigated in more detail in the improve phase. The variation of cell loading represents a major practical issue. In addition, the results indicate an influence of cell loading on cell partitioning. Both increase and decrease of cells per snap shot (cell load) were observed. The observation of visible cell agglomerates in the tubing supports the theory of sedimentation/agglomeration of cells in the tubing. Cell sedimentation/agglomeration theoretically leads to a decrease in cell load, while introducing accumulated cells into the microfluidic device leads to a drastic increase in cell load.

Outlook Improve & Control

Two critical process parameters were identified in the analyse phase, namely, fluid velocities and cell load. Subsequently, optimisation approaches were developed. As discussed earlier, flow velocity studies should be performed to evaluate optimal process parameters. Additionally, the fluctuating cell load must be addressed. *Yamada et al.* [231] proposed an alternative channel design with only two in- and outlets to do so. Cells are suspended in one phase and focused via a pinched region. Changing the channel design presents no problem, since the replication master was part of the rapid prototyping approach.

Using the proposed two-channel design in combination with density optimized ATPS, cell sedimentation could be prevented. Cell sedimentation becomes obsolete when cells are suspended in fluids with higher or same density than cells. Thus, cell density was evaluated, as described in the **supplementary data 7.1**, in addition to ATPS characterization **(table 7.1)**. The results are summarized in **fig. 7.11** . The main cell peak were found between 1.05 1.07 g/cm^3. Top phase of both systems and the bottom phase of the NaCl supplemented ATPS are not suitable since they display density < 1.03 g/cm^3. Bottom phase of the NaPi supplemented ATPS might be suitable with 1.0522 ± 0.0008 g/cm^3, however, density optimization could be done using the previously described density HTS platform. [177] Changing ATPS composition towards higher fluid density, phases will probably increase the phase viscosity as well. Higher density and viscosity is not favourable concerning cell stress in flow systems. For this reason, the influence of phase properties in combination with phase velocities should be investigated in a further study.

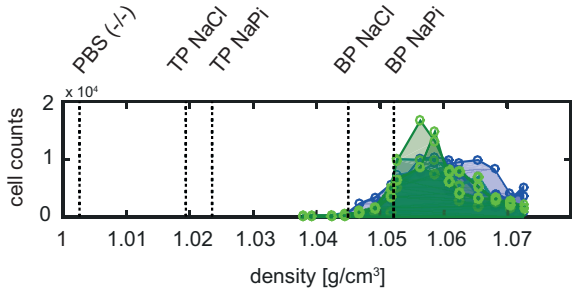

Figure 7.11: Cell density analysis using a percoll step gradient approach (n = 8). Cell counts are shown over density. Additionally, densities of top and bottom phase of the used ATPS supplemented with NaCl or NaPi are shown. PBS density is shown as reference. TP = top phase; BP = bottom phase.

7.4 Conclusions

A process set up for cell partitioning in ATPS using a microfluidic flow-through approach was developed. The project realization was done within the DMAIC framework using AM technologies as tool for manufacturing of missing and tailor-made equipment, needed for the implementation of the process set up. The developed and implemented set up enables cell partitioning in ATPS in a microfluidic flow-through device. Cell suspension, top and bottom phase are individually pumped into a microfluidic device with three in and outlets. Cells are focused at the interphase near the inlet and partition channel downstream. Cell partitioning monitoring is done using a microscopic camera and a developed snap shot analytic for automated cell determination in top and bottom phase. For the evaluation of the critical cell parameter viability, samples are taken at the outlet and analysed via flow cytometry.

In the define phase missing equipment was identified, designed and manufactured using different AM technologies. Aiming low initial investment costs, only an inexpensive desktop 3D printer was used in house. Whenever the printer resolution was not sufficient, the 3D printing process was outsourced to service contractors. The collected data in the measurement phase was used in the analyse phase for the root-cause-investigation since

poor process performance compared to batch experiments was detected, two main factors were identified. Cells seemed to sediment and aggregate in tubing prior to the entry into the microfluidic device, leading to fluctuating cell loading. Additionally, higher fluid velocity has a negative influence on cell partitioning behaviour and cell viability. To improve the process performance a change in microfluidic channel design is suggested in combination with a more detailed fluid velocity study. Reducing the number of in- and outlets enables the suspension of cells in the phase with lower partitioning coefficient. Due to higher phase density, cell sedimentation/agglomeration is inhibited while cells can be focused via a pinched region enabling cell partitioning channel downstream.
Finally, we demonstrated that the AM approach is a powerful tool for process development increasing implementation creativity and reducing project cycle time when combined with a structured approach like the DMAIC framework. We expect that 3D printing will facilitate faster, cheaper, and more creative process development in the biotechnology environment.

Acknowledgements

We thank Prof. A. Hartwig and co-workers from the Institute of Food Chemistry and Toxicology at the Karlsruhe Institute of Technology (KIT) for sharing their labs and equipment with us. We gratefully acknowledge instrumental support by Institute of Mechanical Process Engineering and Mechanics, KIT. We also like to thank C. Radtke for the scientific conversations and technical support concerning MFD production. The authors would like to acknowledge the financial support by the Helmholtz Program BioInterfaces in Technology and Medicine (BIFTM).

7.5 References

38. M. B. Dainiak, A. Kumar, I. Y. Galaev, and B. Mattiasson: 'Methods in Cell Separations'. *Cell Separation. Advances in Biochemical Engineering/Biotechnology.* Ed. by A. Kumar, I. Y. Galaev, and B. Mattiasson. Vol. 106. Springer Berlin Heidelberg, 2007: pp. 1–18.

39. H. Pertoft: 'Fractionation of cells and subcellular particles with Percoll'. *Journal of Biochemical and Biophysical Methods* (2000), vol. 44(1): pp. 1–30.

53. P.Å. Albertsson: 'Partitioning of cell particles and macromolecules: Separation and purification of biomolecules, cell organelles, membranes and cells in aqueous polymer two phase systems and their use in biochemical analysis and biotechnology'. 3rd ed. John Wiley & Sons, New York, 1986.

54. H. Walter, D. E. Brooks, and D. Fisher: 'Partitioning in Aqueous Two-Phase Systems: Theory, Methods, Uses, and Applications to Biotechnology'. Academic Press, Inc., Orlando, USA, 1985.

59. S. A. Oelmeier, F. Dismer, and J. Hubbuch: 'Application of an aqueous twophase systems highthroughput screening method to evaluate mAb HCP separation'. *Biotechnology and Bioengineering* (2010), vol. 108(1): pp. 69–81.

60. S. Zimmermann, S. Gretzinger, M.-L. Schwab, C. Scheeder, P. K. Zimmermann, S. A. Oelmeier, E. Gottwald, A. Bogsnes, M. Hansson, A. Staby, and J. Hubbuch: 'High-throughput downstream process development for cell-based products using aqueous two-phase systems'. *Journal of Chromatography A* (2016), vol. 1464: pp. 1–11.

140. R. Macarron, M. N. Banks, D. Bojanic, D. J. Burns, D. A. Cirovic, T. Garyantes, D. V. S. Green, R. P. Hertzberg, W. P. Janzen, J. W. Paslay, U. Schopfer, and G. Sittampalam: 'Impact of high-throughput screening in biomedical research'. *Nature reviews. Drug discovery* (2011), vol. 10: pp. 188–195.

141. L. M. Mayr and D. Bojanic: 'Novel trends in high-throughput screening'. *Current Opinion in Pharmacology* (2009), vol. 9(5): pp. 580–588.

143. R. P. Hertzberg and A. J. Pope: 'High-throughput screening: new technology for the 21st century'. *Current Opinion in Chemical Biology* (2000), vol. 4(4): pp. 445–451.

149. K.l M. cki: 'High throughput process development in biomanufacturing'. *Current Opinion in Chemical Engineering* (2014), vol. 6: pp. 25–32.

150. R. Bhambure, K. Kumar, and A. S. Rathore: 'High-throughput process development for biopharmaceutical drug substances'. *Trends in Biotechnology* (2011), vol. 29(3): pp. 127–135.

151. C.Heath and R. Kiss: 'Cell Culture Process Development: Advances in Process Engineering'. *Biotechnology Progress* (2007), vol. 23(1): pp. 46–51.

161. B. C. Gross, J. L. Erkal, S. Y. Lockwood, C. Chen, and D. M. Spence: 'Evaluation of 3D Printing and Its Potential Impact on Biotechnology and the Chemical Sciences'. *Analytical Chemistry* (2014), vol. 86(7): pp. 3240–3253.

167. M. Coakley and D. E. Hurt: '3D Printing in the Laboratory: Maximize Time and Funds with Customized and Open-Source Labware'. *Journal of Laboratory Automation* (2016), vol. 21(4): pp. 489–495.

168. A. Waldbaur, J. Kittelmann, C. P. Radtke, J. Hubbuch, and B. E. Rapp: 'Microfluidics on liquid handling stations (µF-on-LHS): an industry compatible chip interface between microfluidics and automated liquid handling stations'. *Lab Chip* (12 2013), vol. 13: pp. 2337–2343.

169. C. P. Radtke, M.-T. Schermeyer, Y. C. Zhai, J. Göpper, and J. Hubbuch: 'Implementation of an analytical microfluidic device for the quantification of protein concentrations in highthroughput format'. *Engineering in Life Sciences* (2016), vol. 16(6): pp. 515–524.

170. C. Chen, Y. Wang, S. Y. Lockwood, and D. M. Spence: '3D-printed fluidic devices enable quantitative evaluation of blood components in modified storage solutions for use in transfusion medicine'. *Analyst* (2014), vol. 139(13): pp. 3219–3226.

171. T. Femmer, A. Jans, R. Eswein, N. Anwar, M. Moeller, M. Wessling, and A. J. C. Kuehne: 'High-Throughput Generation of Emulsions and Microgels in Parallelized Microfluidic Drop-Makers Prepared by Rapid Prototyping'. *ACS Applied Materials & Interfaces* (2015), vol. 7(23): pp. 12635–12638.

172. F. Kazenwadel, E. Biegert, J. Wohlgemuth, H. Wagner, and M. Franzreb: 'A 3Dprinted modular reactor setup including temperature and pH control for the compartmentalized implementation of enzyme cascades'. *Engineering in Life Sciences* (2016), vol. 16(6): pp. 560–567.

173. C.-K. Su and J.-C. Chen: 'Reusable, 3D-printed, peroxidase mimicincorporating multi-well plate for high-throughput glucose determination'. *Sensors and Actuators B: Chemical* (2017), vol. 247: pp. 641–647.

174. T. H. Lücking, F. Sambale, S. Beutel, and T. Scheper: '3Dprinted individual labware in biosciences by rapid prototyping: A proof of principle'. *Engineering in Life Sciences* (2015), vol. 15(1): pp. 51–56.

175. T. H. Lücking, F. Sambale, B. Schnaars, D. BulnesAbundis, S. Beutel, and T. Scheper: '3Dprinted individual labware in biosciences by rapid prototyping: In vitro biocompatibility and applications for eukaryotic cell cultures'. *Engineering in Life Sciences* (2015), vol. 15(1): pp. 57–64.

176. J. N. Wittbrodt, U. Liebel, and J. Gehrig: 'Generation of orientation tools for automated zebrafish screening assays using desktop 3D printing'. *BMC Biotechnology* (2014), vol. 14(1): p. 36.

177. S. Amrhein, M.-L. Schwab, M. Hoffmann, and J. Hubbuch: 'Characterization of aqueous two phase systems by combining lab-on-a-chip technology with robotic liquid handling stations'. *Journal of Chromatography A* (2014), vol. 1367: pp. 68–77.

178. S. Amrhein, K. C. Bauer, L. Galm, and J. Hubbuch: 'Noninvasive high throughput approach for protein hydrophobicity determination based on surface tension'. *Biotechnology and Bioengineering* (2015), vol. 112(12): pp. 2485–2494.

189. J. M. S. Cabral: 'Cell Partitioning in Aqueous Two-Phase Polymer Systems'. *Adv. Biochem. Eng. Biotechnol* (2007), vol. 106: pp. 151–171.

190. R. R. G. Soares, A. M. Azevedo, J. M. Van Alstine, and M. R. Aires-Barros: 'Partitioning in aqueous twophase systems: Analysis of strengths, weaknesses, opportunities and threats'. *Biotechnology Journal* (2015), vol. 10(8): pp. 1158–1169.

191. P. S. Gascoine, D. Fisher: 'The dependence of cell partition in two-polymer aqueous phase systems on the electrostatic potential between the phases'. *Biochemical Society Transactions* (1984), vol. 12(6): pp. 1085–1086.

210. M. Savastano, C. Amendola, F. D'Ascenzo, and E. Massaroni: '3-D Printing in the Spare Parts Supply Chain: An Explorative Study in the Automotive Industry'. *Digitally Supported Innovation*. Ed. by L. Caporarello, F. Cesaroni, R. Giesecke, and M. Missikoff. Springer International Publishing, Cham, 2016: pp. 153–170.

211. B. Panda, M. J. Tan, I. Gibson, and C. K. Chua: 'The Disruptive Evolution Of 3D Printing'. *Proc. of the 2nd Intl. Conf. on Progress in Additive Manufacturing*. Research Publishing, Singapore, 2016: pp. 152–157.

212. T. Rayna and L. Striukova: 'From rapid prototyping to home fabrication: How 3D printing is changing business model innovation'. *Technological Forecasting and Social Change* (2016), vol. 102: pp. 214–224.

213. J. C. McDonald, M. L. Chabinyc., S. J. Metallo., J. R. Anderson., A. D. Stroock, and G. M. Whitesides: 'Prototyping of Microfluidic Devices in Poly(dimethylsiloxane) Using Solid-Object Printing'. *Analytical Chemistry* (2002), vol. 74(7): pp. 1537–1545.

214. T. Baden, A. M. Chagas, G. Gage, T. Marzullo, L. L. Prieto-Godino, and T. Euler: 'Open Labware: 3-D Printing Your Own Lab Equipment'. *PLOS Biology* (2015), vol. 13(3): pp. 1–12.

215. S. Moses, M. Manahan, A. Ambrogelly, and W. Ling: 'Assessment of AMBR^{TM} as a model for high-throughput cell culture process development strategy'. *Advances in Bioscience and Biotechnology* (2012), vol. 3(7): pp. 918–927.

216. T. Davila: 'An empirical study on the drivers of management control systems' design in new product development'. *Accounting, Organizations and Society* (2000), vol. 25(4): pp. 383–409.

217. F. Li, Y. Hashimura, R. Pendleton, J. Harms, E. Collins, and B. Lee: 'A Systematic Approach for Scale-Down Model Development and Characterization of Commercial Cell Culture Processes'. *Biotechnology Progress* (2006), vol. 22(3): pp. 696–703.

218. F. Johannsen, S. Leist, and G. Zellner: 'Six sigma as a business process management method in services: analysis of the key application problems'. *Information Systems and e-Business Management* (2011), vol. 9(3): pp. 307–332.

219. T. Friedli, P. Basu, D. Bellm, and J. Werani: *Leading Pharmaceutical Operational Excellence: Outstanding Practices and Cases*. Springer-Verlag Berlin Heidelberg, 2013.

220. J. Antony, A. S. Bhuller, M. Kumar, K. Mendibil, and D. C. Montgomery: 'Application of Six Sigma DMAIC methodology in a transactional environment'. *International Journal of Quality & Reliability Management* (2012), vol. 29(1): pp. 31–53.

221. D. C. Montgomery and C. M. Borror: 'Systems for modern quality and business improvement'. *Quality Technology & Quantitative Management* (2017), vol. 14(4): pp. 343–352.

222. K. Joshi, A. Asthana, S. Pande, G. S. Asthana, K. Singh, and G. Goomber: 'An Overview on Interrelationship between Quality by Design (QbD) & Six Sigma'. *World Journal of Pharmacy and Pharmaceutical Sciences* (2015), vol. 4(11): pp. 445–457.

223. G. Improta, G. Balato, M. Romano, F. Carpentieri, P. Bifulco, M. A. Russo, D. Rosa, M. Triassi, and M. Cesarelli: 'Lean Six Sigma: a new approach to the management of patients undergoing prosthetic hip replacement surgery'. *Journal of Evaluation in Clinical Practice* (2015), vol. 21(4): pp. 662–672.

224. M. Taner, B. Sezen, and K. M. Atwat: 'Application of Six Sigma methodology to a diagnostic imaging process'. *International journal of health care quality assurance* (2012), vol. 25(4): pp. 274–290.

225. G. Improta, G. Balato, M. Romano, A. M. Ponsiglione, E. Raiola, M. A. Russo, P. Cuccaro, L. C. Santillo, and M. Cesarelli: 'Improving performances of the knee replacement surgery process by applying DMAIC principles'. *Journal of Evaluation in Clinical Practice* (2017), vol. 23(6): pp. 1401–1407.

226. S. W. Carleysmith, A. M. Dufton, and K. D. Altria: 'Implementing Lean Sigma in pharmaceutical research and development: a review by practitioners'. *R&D Management* (2009), vol. 39(1): pp. 95–106.

227. F. Marti: 'Lean Six Sigma method in Phase 1 clinical trials: a practical example'. *The Quality Assurance Journal* (2005), vol. 9(1): pp. 35–39.

228. R. López-Franco, J. Moreno-Cuevas, and M. González-Garza: 'Percoll Gradient Optimization for Blood CD133+ Stem Cell Recovery'. *Stem Cell Discovery* (2014), vol. 4: pp. 61–66.

229. M. González-González, P. Vázquez-Villegas, C. García-Salinas, and M. Rito-Palomares: 'Current strategies and challenges for the purification of stem cells'. *Journal of Chemical Technology & Biotechnology* (2012), vol. 87(1): pp. 2–10.

230. M. Tsukamoto, S. Taira, S. Yamamura, Y. Morita, N. Nagatani, Y. Takamura, and E. Tamiya: 'Cell separation by an aqueous two-phase system in a microfluidic device'. *Analyst* (2009), vol. 134(10): pp. 1994–1998.

231. M. Yamada, V.Kasim, M. Nakashima, J. Edahiro, and M. Seki: 'Continuous cell partitioning using an aqueous two-phase flow system in microfluidic devices'. *Biotechnology and Bioengineering* (2004), vol. 88(4): pp. 489–494.

232. K. Vijayakumar, S. Gulati, A. J. deMello, and J. B. Edel: 'Rapid cell extraction in aqueous two-phase microdroplet systems'. *Chem. Sci.* (2010), vol. 1(4): pp. 447–452.

233. J. R. SooHoo and G. M. Walker: 'Microfluidic aqueous two phase system for leukocyte concentration from whole blood'. *Biomedical Microdevices* (2009), vol. 11(2): pp. 323–329.

234. K.-H. Nam, W.-J. Chang, H. Hong, S.-M. Lim, D.-I. Kim, and Y.-M. Koo: 'Continuous-Flow Fractionation of Animal Cells in Microfluidic Device Using Aqueous Two-Phase Extraction'. *Biomedical Microdevices* (2005), vol. 7(3): pp. 189–195.

235. D. Di Carlo, D. Irimia, R. G. Tompkins, and M. Toner: 'Continuous inertial focusing, ordering, and separation of particles in microchannels'. *Proceedings of the National Academy of Sciences* (2007), vol. 104(48): pp. 18892–18897.

236. S. C. Hur, N. K. Henderson-MacLennan., E. R. B. McCabe., and D. Di Carlo: 'Deformability-based cell classification and enrichment using inertial microfluidics'. *Lab Chip* (2011), vol. 11(5): pp. 912–920.

237. M. M. Wang, E. Tu, D. E. Raymond, J. M. Yang, H. Zhang, N. Hagen, B. Dees, E. M. Mercer, A. H. Forster, I. Kariv, P. J. Marchand, and W. F: Butler: 'Microfluidic sorting of mammalian cells by optical force switching'. *Nature Biotechnology* (2005), vol. 23(1): pp. 83–87.

238. A. Wolff, I. R. Perch-Nielsen, U. D. Larsen, P. Friis, G. Goranovic, C. R. Poulsen, J. P. Kutter, and P. Telleman: 'Integrating advanced functionality in a microfabricated high-throughput fluorescent-activated cell sorter'. *Lab Chip* (2003), vol. 3(1): pp. 22–27.

239. J. Seidl, R. Knuechel, and L. A. Kunz-Schughart: 'Evaluation of membrane physiology following fluorescence activated or magnetic cell separation'. *Cytometry* (1999), vol. 36(2): pp. 102–111.

CHAPTER 8

Automated Image Processing as an Analytical Tool in Cell Cryopreservation for Bioprocess Development

Sarah Gretzinger[1,2], Stefanie Limbrunner[2], Jürgen Hubbuch[1,2,**]

[1] Institute of Functional Interfaces (IFG), Karlsruhe Institute of Technology (KIT), Eggenstein-Leopoldshafen, Germany

[2] Institute of Engineering in Life Sciences, Section IV: Biomolecular Separation Engineering, Karlsruhe Institute of Technology (KIT), Karlsruhe, Germany

[**] Corresponding author. Email: juergen.hubbuch@kit.edu

Bioprocess and Biosystems Engineering Feb 2019; 42, doi:10.1007/s00449-019-02071-3

Abstract

The continuous availability of cells with defined cell characteristics represents a crucial issue in the biopharmaceutical and cell therapy industry. Here, development of cell banks with a long-term stability is essential and ensured by a cryopreservation strategy. The strategy needs to be optimized for each cell application individually and usually comprises controlled freezing, storage at ultra-low temperature, and fast thawing of cells. This approach is implemented by the development of master and working cell banks. Currently, empirical cryopreservation strategy development is standard but a knowledge based approach would be highly advantageous.

In this article, we report the development of a video-based tool for the characterisation of freezing and thawing behaviour in cryopreservation process to enable a more knowledge based cryopreservation process development. A successful tool validation was performed with a model cryopreservation process for the β-cell line INS-1E. Performance was evaluated for two working volumes (1.0 mL and 2.0 mL), based on freezing-thawing rates (20 °C to -80 °C) and cell recovery and increase of biomass, to determine tool flexibility and practicality. Evaluation confirmed flexibility by correctly identifying a delay in freezing and thawing for the larger working volume. Further more, a decrease in cell recovery from 0.94 ($\pm$ 0.14) % using 1.0 mL working volume to 0.61 ($\pm$ 0.05) % using a 2.0 mL working volume displays tool practicality.

The video-based tool proposed in this study presents a powerful tool for cell specific optimisation of cryopreservation protocols. This can facilitate faster and more knowledge based cryopreservation process development.

Keywords: automated image processing, controlled freezing, cryopreservation, process development tool, thawing

8.1 Introduction

In the upcoming era of cell therapy, any bioprocess step dealing with cells needs to be challenged and potentially reengineered to serve large scale operations. One of the unit operations used is the so-called cryopreservation step. Cryopreservation is an essential technology for long-term storage of eukaryotic cells and is applied when continuous access of cells with consistent cell characteristics, concerning genetic and metabolic changes, is crucial. [72] This includes cell line maintenance for routine cell culture applications [72], biopharmaceutical production [74, 75], reproductive medicine [71, 76] and cell therapy in the field of regenerative medicine [1, 73, 84]. Usually, the concept of cell banking is applied to manage the robust and controlled supply of cells with defined characteristics. This includes cell storage at ultra-low temperatures in a controlled and well defined process environment, while monitoring the critical cell characteristics. [1, 72, 74, 75, 77, 78] Ultra-low temperature storage stops cell metabolism completely. However, freezing and thawing induces severe cell stress because of intra- and extracellular ice formation as well as osmotic effects. In turn, this stress leads to cell membrane damages and, ultimate, to cell death. [72, 79] Therefore, cryopreservation process optimisation is necessary for the development of an effective cell bank displaying high post-thaw cell viability.
Process parameters influencing post-thaw cell viability are well described in literature. [71, 72, 74, 75, 78, 80, 81] The list of critical parameter includes cell loading [80], cell characteristics (e.g. suspension cells, monolayer or colony growth) [78, 81, 240], cryoprotectant agents and agent concentration [71, 87], process volume [73, 75, 77, 82, 83], and freezing/thawing rates [73, 74, 77, 84–86]. Additionally, a controlled freezing process is preferable to ensure cell viability and process robustness. [73, 74, 77, 81, 84, 89] It is reported that slow cooling rates in combination with dimethyl sulfoxide (DMSO) as cryoprotectant and fast thawing results in relatively good recovery for a number of mammalian cell lines [72, 74, 75]. However, process optimization is required for each cell line individually, as cell behaviour differs between cell lines. [72, 74, 75, 86]
Complex interplay between process parameters, such as the effect of cryoprotectant agents or sample volume on freezing and cooling rates, and their combined effect on process performance hinders the advancement of cell-specific cryopreservation strategy development. A tool for systematic and empiric screening freezing and thawing behaviour would be beneficial but is currently missing. [71, 72, 74, 75, 241]
Digital image processing is widely used for optical sample analysis. In life science research it has been applied to crystallisation process development and monitoring [242–244], quantification of cell growth [245–247], analysis of neuronal calcium signaling [248], cell migration analysis [249], and blastocyst stage prediction of human embryo development [76]. Digital image processing has also been used in cryopreservation process development to monitor osmotic cell response [250] and to determine nucleation temperature during cryopreservation [79] as a function of different process parameters such as cryoprotectant agent types. This indicates applicability of digital image processing for cryopresentation process development, but expensive cryomicroscopy equipment limits general usability [79, 250].
In this study, we report the development and experimental validation of a video analysis tool for the characterisation of cryopreservation sample freezing and thawing behaviour. To

improve general usability, off-the-shelf imaging equipment and entry-level image processing algorithms were used. This resulted in an automated image-based tool for the detection of the frozen over state and complete thawing of samples. A case study with the β-cell line INS-1E and DMSO as a cryoprotectant was used to validate the performance. This was performed with a working volume of 1.0 mL and 2.0 mL to demonsrate flexibility of the developed tool. Subsequently, intact viable cell monitoring during the cryopreservation process was performed to determine the influence of freeze and thaw behaviour on cell recovery and proliferation as a function of increasing working volume. The results obtained by the proposed digital imaging tool were in good agreement with literature values, which shows its applicability for cryopreservation strategy development.

8.2 Materials and Methods

8.2.1 Stock Solutions

Cell culture reagents were purchased from Thermo Fisher Scientific (Waltham, USA), unless otherwise stated. Culture media consisted of RPMI 1640 with GlutaMAX supplemented with 10 (v/v) % FBS, 1 (v/v) % sodium pyruvate, 1 (v/v) % Penicillin / Streptomycin, 10 mM HEPES, 2 mM L-Glutamine and 50 μM β-mercaptoethanol (Sigma-Aldrich, St. Louis, USA). Cryomedia consisted of RPMI 1640 with GlutaMAX supplemented with 20 (v/v) % FBS, 1 (v/v) % sodium pyruvate, 10 (v/v) % DMSO (Sigma-Aldrich), 1 (v/v) % Penicillin / Streptomycin, 10 mM HEPES, 2 mM L-Glutamine and 50 μM β-mercaptoethanol (Sigma-Aldrich). Both media were stored at 8 °C. Phosphate-buffered saline was purchased from Thermo Fisher Scientific and stored at room temperature. All stock solutions were kept under sterile conditions.

8.2.2 Software and Data Processing

The software iTools Version 9.57.11 (Eurotherm, Worthing, UK) was used to control the EF600M 105 & 106. For data storage Excel 2013 (Microsoft, Redmond, WA, USA) was used. MATLAB R2015a (The MathWorks, Inc., Natick, USA) was used for data evaluation and visualization.

8.2.3 Controlled Freezing and Thawing

Freezing evaluation studies were preformed with cryomedia and a working volume of 1.0 mL and 2.0 mL. An identical freezing profile **(table 8.1)** was applied for all runs. For experiments with 1.0 mL working volume, an EF600M 106 (55 x 1.8 mL cryovials, 1.0 mL max. fill; Grant Instruments, Cambridgeshire, UK) and 1.8 mL cryovials (VWR International GmbH, Bruchsal, Germany; height (h) = 40 mm, diameter (d) = 12 mm, h/d = 3.33, u-bottom) were used. Experiments with 2.0 mL working volume were performed using an EF600M 105 (1 x SBS microplate; Grant Instruments) in combination with a tailored adapter for tissue cryovials (FluidiX Ltd, Cheshire, UK; h = 26 mm, d = 15 mm, h/d = 1.73, flat-bottom). The adapter was designed according to a 24 well SBS microplate **(fig. 8.1)**. Both instruments were controlled via iTools Version 9.57.11 (Eurotherm). Thawing was performed, for both working volumes, in 37 °C pre-warmed water bath.

Table 8.1: Freezing profile applied to a working volume of 1 and 2 mL

Increments	**Temperature**
start temp.	20 °C
cool	from 20 to - 5 °C at 2 °C min^{-1}
cool	from - 5 °to - 7 °C at 1 °C min^{-1}
hold	at - 7 °C for 10 min
cool	from - 7 °to - 80 °C at 1 °C min^{-1}
hold	at - 80 °C

To monitor freezing/thawing behaviour, all runs were preformed with opened cryovials. Video monitoring was done for all freezing and thawing runs using a GoPro Hero4 (GoPro, Inc., San Mateo, USA) controlled via the GoPro App version 2.6.3.312 (GoPro, Inc.) and a Samsung Galaxy Note Pro SM-P900 (Samsung, Seoul, South Korea). Following camera settings were applied: field of view: narrow; resolution: 1080 p; frames per second: 25.

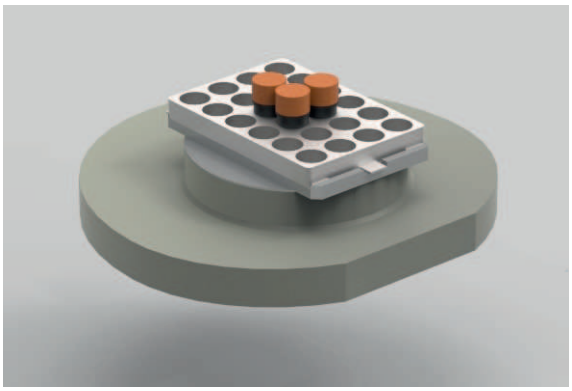

Figure 8.1: Schematic illustration of the tailored tissue vial adapter placed on the EF600M 105 cryo-head. The adapter design is based on a 24 well SBS microplate, three tissue vials are depicted.

8.2.4 Video Analysis

An automated image-based method was developed to detect the time point where the samples were frozen over. It was realised using a snapshot analytic method in MATLAB, which was divided into two steps: (i) pre-processing and (ii) analysis of the pixel intensity values to detect the frozen over state.
Pre-processing (i) was necessary to locate the vials in the image. As a result of design differences of the two cryo devices, two different vial area detection methods were employed.

The adapter for the EF600M 105 (2 mL vials) was designed according to the 24 well format (SBS microplate). Resulting in 6 vials in x-direction and 4 vials in y-direction. A mask with 24 circles with a diameter of 90 pixels was generated and automatically drawn onto the image. Mask generation was done by user-defining the centre of the vial at the top end on the left. The same was done for the centre of the vial at the bottom end on the right. The distance between the two markers was calculated in the x- and y-direction. The distance between the two vials was then divided by the number of vials in the appropriate direction. The design of the EF600M 106 (1 mL vials) is based on a cubic close packing of 55 vials, where each vial was represented by a circle with a diameter of 60 pixels.The centre of each analysed vial was user-defined. Circles, with a diameter of 60 pixels, were subsequently drawn onto the image. For the detection of the frozen over state (ii) one snapshot per second was taken and analysed. For each vial and snapshot, the mean pixel intensity of the defined image area was calculated with the function mean available in MATLAB and plotted over time (mean pixel intensity curve). The mean pixel intensity was chosen because it correlates with cristallization activity during freezing. A floating mean value filter (20 values) was applied to smooth data. With the smoothed data, the inflection point was determined. The inflection point was defined as the slope maximum of the mean pixel intensity curve. The inflection point was used as reference point for determination of start and end point of cryomedium water cristallization. Crystallization activity is low at the beginning and end of sample freezing and was defined as 1 % difference to the inflection point slope. Crystallisation started when the difference value was < 1 % the difference value of the inflection point to the left. The sample is frozen over (end of crystallisation) was reached when the difference value is < 1 % the difference value of the inflection point to the right. In some cases a spline interpolation needed to be done before the slope was calculated. For example when a small rotating ice block was observed in a vial during visual examination of the video. Here, a small artificial peak in mean pixel intensity was observed, which was automatically detected and the peak width was calculated. The spline interpolation was then performed for the peak width with a margin of 20 values before and after the peak gap. The (i) pre-processing and freezing analysis (ii) is shown in figure **fig. 8.2 A & B**.

A similar pre-processing (i) appraoch was used to determine the thawed state time point. For analysis (ii), the mean intensity value of the defined image area for each vial and snap-shot was also calculated and plotted over time (mean pixel intensity curve). The curve was then smoothed with a floating mean value filter (20 values) and slope was calculated. Endpoint of thawing was assumed when the slope of the curve is < 0.02 unit, since the curves did not show an characteristic inflection point. The mean pixel intensity plot for thawing is shown in **fig. 8.2 C**.

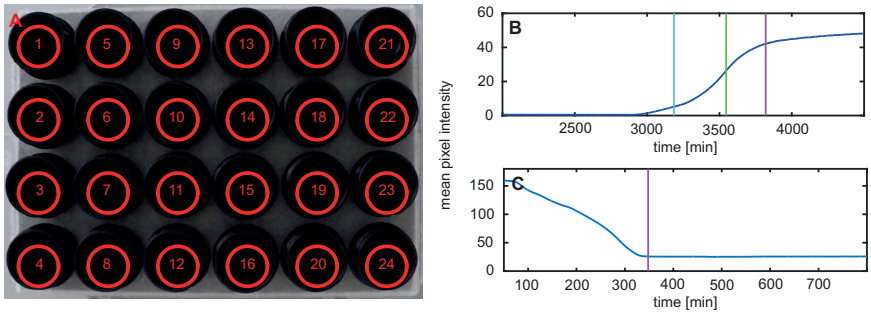

Figure 8.2: Video analysis example of 2 mL vials for freezing and thawing. **A** Pre-processing of snap-shot data. Mask with 24 circles was automatically drawn into the snap-shot, each circle represents the image area of one vial. **B** Freezing pixel intensity curve of one well. Depicted is the calculated mean pixel intensity, smoothed with a floating mean value filter (20 values), over time. **cyan:** freezing start point; **green:** inflection point (slope maximum); **magenta:** freezing end point. The threshold for the start and end point of water crystallisation was defined as a 1 % difference to the inflection point. **C** Thawing pixel intensity curve. Depicted is the calculated mean pixel intensity, smoothed with a floating mean value filter (20 values), over time. **magenta:** thawing end point. Thawing end point was defined for a curve slope < 0.02.

8.2.5 Cell Culture

The study was preformed with the β-model cell line INS-1E [198], kindly provided by Prof. Maechler from the Department of Cell Physiology and Metabolism at the University of Geneva Medical Centre, Switzerland. Cells were cultivated in culture media at 37 °C in a humidified incubator with 5 % CO_2. Cell culture was split every 7 days to a concentration of 6.6 x 10^4 cells/cm^2, media was exchanged after 3 days.

8.2.6 Cell Freezing

Cell freezing was perfomed according to the freezing evaluation study using the EF600M (105 and 106) and applying an identical freezing profile **(table 8.1)**. Cells were suspended in cryomedium to a final concentration of 6 x 10^6 cells/mL and directly transfered to the EF600M (105 or 106). All runs were performed under sterile conditions and cryovials were stored after finishing the freezing profile **(table 8.1)** at - 80 °C for 24 h and transferred to - 196 °C (Arpege 70, Air Liquide Medical GmbH, Düsseldorf, Germany) for 7 days. Transportation was done using a pre-cooled aluminium block (- 80 °C) for both working volumes (1.0 mL and 2.0 mL).

8.2.7 Cell Thawing

After storage of the cryosamples for 7 days at - 196 °C, thawing was performed in a 37 °C pre-warmed water bath. Transportation from the storage tank to the water bath was done using a pre-cooled aluminium block (- 80 °C) for both working volumes (1.0 mL and 2.0 mL). After thawing, cell suspension was quickly transferred in 20 °C pre-warmed culturemedia (1:20) and incubated for 5 min at room temperature (RT), followed by a washing step with PBS (1:10). Finally, cells were resuspended in 7 mL culturmedia and transferred in a culture flask with an area of 25 cm^2. Cells were cultivated for 7 days, with

a media exchange after 3 days. Intact viable cell concentration was estimated by trypan blue exclusion direct after thawing and after 7 days of cultivation by haemocytometer counting.

8.2.8 Statistical Data Analysis

Mean comparison was performed by applying an unequal variances Students t-test, since unequal variances were asserted by an F-test.

8.3 Results

We developed a video analysis-based tool for the characterisation of freezing and thawing behaviour in cell cryopreservation processes. Briefly, video data was acquired during freezing and thawing and offline image processing was used to determine the end point of sample freezing or thawing. The development was done with a model process where cells were suspended in cryo-media, followed by a controlled freezing step to - 80 °C. After a 24 hour incubation at - 80 °C, samples were stored for 7 days at - 196 °C. Subsequently, samples were thawed and the cell were cultivated for 7 days. Additionally, samples were taken before and after freezing and after cultivation to monitor intact viable cells. An overview of the cryopreservation process is shown in **fig. 8.3**. Cryopreservation was preformed with 1.0 mL and 2.0 mL working volume to demonstrate the versatility of the developed tool and sample volume influence on cell recovery and proliferation.

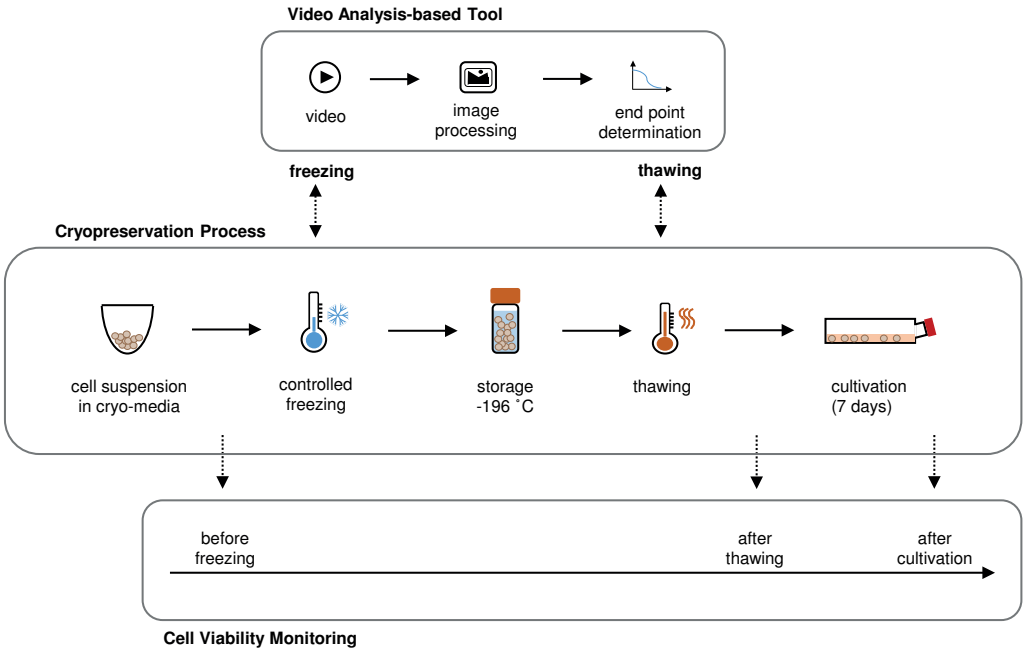

Figure 8.3: Overview of the cell cryopreservation process. Cells were suspended in cryo-media and directly frozen to - 80 °C in a controlled manner. After 24 h at - 80 °C the cryo-samples were transferred in the storage tank (- 196 °C). After 7 days of storage, the samples were thawed and cultivated for 7 days. Samples for intact viable cell monitoring were taken before freezing, after thawing and after cultivation. Additionally, the freezing and thawing process steps were analyzed using the developed video analysis-based tool. Here, a video was taken during freezing and thawing. The video was then analysed via automatic image processing to determine the end point of the freezing and thawing of the samples.

Exemplarily, video analysis is shown in **fig. 8.2** for a 2.0 mL working volume freezing and thawing. Pre-processing shown in **fig. 8.2 A** was performed, for both freezing and thawing videos, to define the image area for each vial. Pre-processing was followed by

mean pixel intensity calculation for the image area of each vial. In **fig. 8.2 B**, smoothed (floating mean value filter, 20 values) mean pixel intensity data is plotted over time during freezing. Depicted is the freezing start point (cyan), the curve inflection point (green) and the freezing end point (magenta). The threshold for the start and end point of water crystallisation was defined as a 1 % difference compared to the inflection point. **fig. 8.2 C** depicts the mean pixel intensity over time during thawing, where the thawing end point (i.e., curve slope of less than 0.02) is highlighted in magenta.
The results of characterisation of the freezing and thawing behaviour are shown in **fig. 8.4**. Freezing was performed in a controlled manner for both working volumes as described in

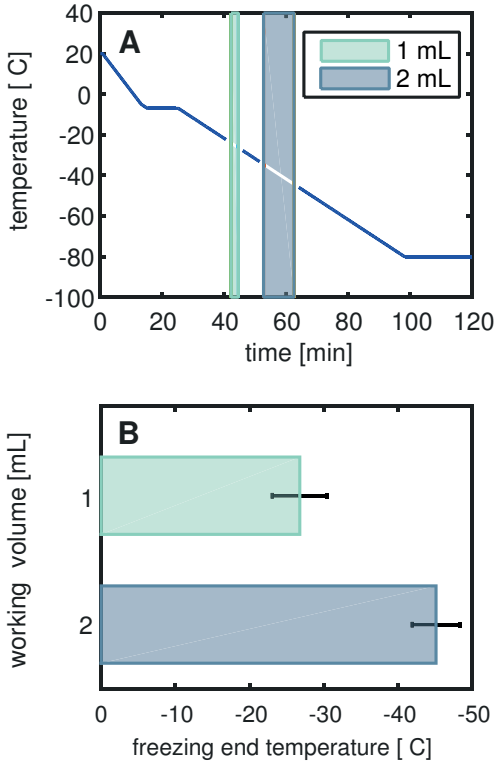

Figure 8.4: Freezing study results with 1 and 2 mL working volume. **A** Freezing profile from 20 °C to -80 °C as described in **table 8.1 (royal blue curve)**. Additionally, the mean freezing start and end point for both working volumes are depicted as bars. **cyan:** 1 mL working volume; **blue:** 2 mL working volume **B** Bar chart of the calculated freezing end temperatures for 1 and 2 mL working volume.

table 8.1. In **fig. 8.4 A**, the employed freezing profile from 20 °C to - 80 °C is shown in royal blue, while the total sample freezing time is shown as vertical bars. The left border of the vertical bar represents the mean start freezing time and the right border of the vertical bar represents the mean end freezing point (n = 9). Freezing data for 1.0 mL working volume and 2.0 mL working volume is shown in cyan and blue, repsectively. Comparing the freezing behaviour of the two working volumes in **fig. 8.4**, freezing starts earlier for 1.0 mL working volume compared to 2.0 mL. Additionally, the total freezing time is also

shorter for 1 mL working volume than 2.0 mL working volume samples. With the video timestamp and freezing profile tracking, mean crystallization end temperature could be determined. **fig. 8.4 B** shows that samples with 1.0 mL working volume are frozen over at - 26.7 °C (± 3.7), while 2.0 mL samples reach the frozen over state later at - 45.1 °C (± 3.2). Thawing behaviour was also evaluated with the digital image processing tool. Thawing was done via incubating the frozen vials in a pre-heated (37 °C) water bath. The results are shown in **fig. 8.5** as bar chart of the mean thawing time (n = 9). Samples with 1.0 mL working volume were completely defrosted after 2.2 min (± 0.2), while defrosting of 2.0 mL samples took 5.9 min (± 0.2). The second part of the study was the intact viable cell

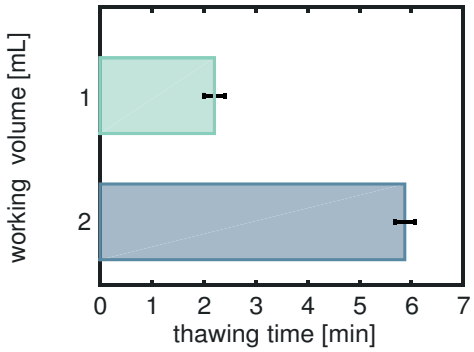

Figure 8.5: Thawing time analysis. Bar chart of the thawing end time for 1 and 2 mL working volume in minutes.

number monitoring during the cryopreservation process as a function of working volume. Samples were analysed before freezing, after thawing and after 7 days of cultivation. Three runs were performed, each with a technical triplicate (n_{total} = 3 x 3 = 9). For comparison of the results of the two working volumes, normalization of the live cell number was done according to **eq. (8.1)**:

$$(live\ cells)_N = \frac{live\ counts}{working\ volume}\ [cells/mL] \tag{8.1}$$

The results of the process robustness evaluation are shown in **fig. 8.6**. Normalized live cell number is shown over the performed runs. The horizontal bar represent the total variance (n = 9). The upper line of the bar represents the mean + SD, while the bottom line represents mean - SD. The robustness evaluation showed no trend and the relative standard deviation was < 11 % for over all time points and both working volumes. Both working volumes showed similar normalized live cell numbers (n = 9) with 5.45 x 10^6 cells/mL (± 0.51 x 10^6) for 1.0 mL working volume and 5.05 x 10^6 cells/mL (± 0.39 x 10^6) for 2.0 mL working volume before freezing. However, the cell number differed after thawing. While the cell number for 1.0 mL working volume only decreased to 5.09 x 10^6 cells/mL (± 0.52 x 10^6), cell number dropped to 3.08 x 10^6 cells/mL (± 0.15 x 10^6) for 2.0 mL working volume. After 7 days of cultivation the cell number increased for 1.0 mL working volume to 10.85 x 10^6 cells/mL (± 1.14 x 10^6) and to 5.35 x 10^6 cells/mL (± 0.53 x 10^6) for 2.0 mL working volume. The summary of these data is shown in **fig. 8.7 A**, where non-cryopreserved control data is represented as horizontal bar. Additionally, two critical

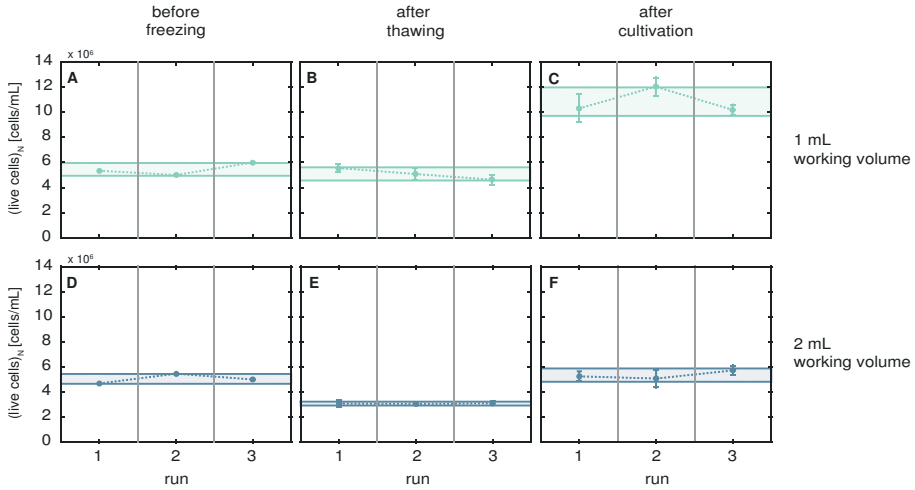

Figure 8.6: Robustness evaluation of cell cryopreservation process. Three runs were performed per experiment, each with a technical triplicate (n_{total} = 3 x 3 = 9). Normalized live cell number is shown over the performed runs. The horizontal bar represent the total variance (n = 9). Upper line = mean + SD; bottom line = mean SD. Evaluation of robustness was done for each process step: **A** before freezing with 1 mL working volume (WV); **B** after thawing with 1 mL WV; **C** after cultivation of 7 days with 1 mL WV **D** before freezing with 2 mL WV **E** after thawing with 2 mL WV **F** after cultivation of 7 days with 2 mL WV.

process numbers, namely cell recovery and biomass increase, were calculated in order to evaluate process performance. Evaluation was done based on the normalized cell number (n = 3 x 3 x 3 = 9). Cell recovery was calculated according to **eq. (8.2)**, the results are shown in **fig. 8.7 B**.

$$R_{\mathrm{N}} = \frac{after\ thawing}{before\ freezing} \tag{8.2}$$

Cell recovery of $R_N = 0.94\ (\pm\ 0.14)$ was observed for 1.0 mL working volume, while 2.0 mL working volume showed $R_N = 0.61\ (\pm\ 0.05)$. Cell biomass increase was calculated according to **eq. (8.3)**, the results are shown in **fig. 8.7 C**.

$$B_{\mathrm{N}} = \frac{after\ cultivation}{before\ freezing} \tag{8.3}$$

The biomass increase of 1.0 mL working volume $B_N = 2.01\ (\pm\ 0.34)$ indicates a cell doubling compared to initial live cell number, while 2.0 mL working volume process showed no increase of initial cell number with a $B_N = 1.06\ (\pm\ 0.13)$.

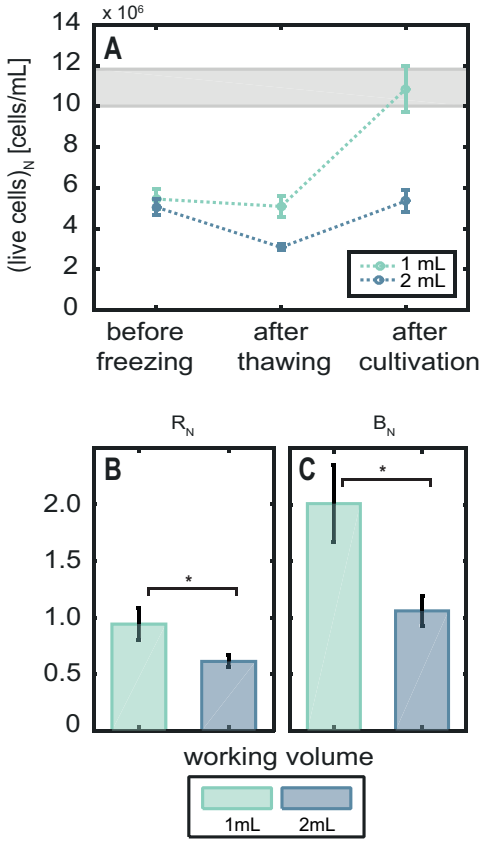

Figure 8.7: Summary of cryopreservation process ($n_{total} = 9$). **A** Normalized live cell number over process steps is shown. The gray horizontal bar represents the control cell number of non-cryopreserved cells (upper line: mean + SD; bottom line: mean - SD). **B** Bar chart of the cell recovery factor (R_N) for 1 and 2 mL working volume (WV). **C** Bar chart of the cell proliferation factor (B_N) for 1 and 2 mL WV. Asterisks indicates statistical significance (unequal variances Students t-test; $p < 0.0001$).

8.4 Discussion

Cooling and heating rates, among other process parameters, have been described as important factors concerning post-thawing cell viability [73, 74, 77, 84–86] and need to be optimized for each cell line individually [72, 74, 75, 86]. The aim of the present study was to develop a tool for the characterisation of freezing and thawing behaviour, applicable for cell cryopreservation process development.

The tool was realised as offline analytic, using a video analysis approach to detect both the frozen over state and the thawing end point. Automatization of the video-based analytic was done in MATLAB by evaluating the mean pixel intensity, as this variable changes with ice formation or thawing. A pre-processing step, where the image area of each vial is defined, allows individual analysis of several samples in parallel, followed by calculation of

the mean pixel intensity of each sample. The formation of ice is represented by an increase of mean pixel intensity, while ice thawing will lead to a decrease. When plotted over time, characteristic curves for freezing and thawing occur, which are used for the calculation of the beginning and ending of ice formation. In the present study, cryopreservation was done with two different working volumes to investigate the flexibility of the tool. Pre-processing of video data was unique for each working volume concerning image area and vial assembly which highlights the flexibility of the tool and indicates fast adaptation to new applications. The performance of the tool was demonstrated with a case study where the influence of scale up (1.0 mL and 2.0 mL working volume) on freezing and thawing behaviour was analysed. The performance was evaluated based on cell recovery and biomass increase. A conventional cryopreservation process was performed using the model cell line INS-1E. Freezing was done in a controlled manner using the EF600M freezing equipment (20 to - 80 °C) and 7 day storage at - 196 °C, followed by a fast thawing step in a 37 °C pre-warmed water bath. DMSO was used as cryoprotectand as it is commonly used for cryopreservation of mammalian cell lines. [72, 74]

In the first part of the study, the developed video-based tool was used to evaluate the freezing and thawing behaviour considering a scale up from 1.0 mL to 2.0 mL working volume. It has been widely reported in literature that controlled freezing is favourable for cell cryopreservation concerning cell viability and for process quality control for cell-based products or cell banks for biopharmaceutical production. [73, 74, 77, 81, 84, 89] For both working volumes the same controlled freezing profile was performed using the EF600M. The EF600M is a nitrogen and ethanol free device for controlled freezing and has already been used for cryopreservation studies. [73, 83] In the present study, the EF600M 106 was used for freezing of 1.0 mL working volume, while the EF600M 105 was used in combination with a customized adapter for freezing 2.0 mL samples. Here, vials for tissue cryopreservation were used, leading to an adapter design based on 24 well microplate format (SBS). The results have shown that ice formation starts earlier with 1.0 mL working volume and the time to reach the frozen over state is also faster. For better comparison the crystallisation end point was calculated, which represents the profile temperature of the process and not the sample temperature. While 1.0 mL working solution samples were frozen at - 26.7 °C (± 3.7), the 2.0 mL working solution samples reach that status at - 45.1 °C (± 3.2). It is assumed that the observed crystallization end point differences occur due heat transfer effects caused by different EF600M approaches and cryovial geometry. The EF600M 106 used for 1.0 mL working volume cryovials is used without an additional adapter. This means that the cooling head is in direct contact with the cryovials. In comparison, the EF600M 105, used for the 2.0 mL working volume cryovials, needs an additional adapter which is not actively cooled. This might lead to delayed heat transfer into the sample. Additionally, the two cryovials differ in geometry. Both are cynlidrical but the 1.0 mL vial has a height to diameter ratio of 3.3 while a ratio of 1.73 is used for the 2.0 mL vial. This ratio difference has been reported in literature as negative effect in scale up. [73, 75, 82] It is also assumed that volume increase and cryovial geometry difference are the major causes for the delayed thawing time of the 2.0 mL samples. The 1.0 mL working samples are completely ice free after 2.2 min (± 0.2), while defrosting of 2.0 mL samples took 5.9 min (± 0.2). This shows that the developed tool is capable of automatically detecting well

described freezing and thawing behaviour.
To investigate the influence of the working volume on cell cryopreservation, a intact viable cell monitoring during the process was performed. Samples were taken before freezing, after thawing and after 7 days of cultivation. Three runs were done per experiment, each with a technical triplicate ($n_{total} = 3$ x $3 = 9$). The robustness evaluation has shown no variations of intact viable cell number between the runs and the relative standard deviation was < 11 % for all time points and both working volumes. Therefore, the process is in control and the observed differences comparing the two working volumes are valid. Two critical process parameter were defined for process evaluation and comparison of the two working volumes: cell recovery and biomass increase. While the cell recovery indicates the direct influence of cryopreservation on intact viable cell number, the second critical process parameter indicates the ability to increase the total biomass. Cryopreservation had a minor influence on cells use a 1.0 mL working volume with a cell recovery of 0.94 ($\pm$ 0.14). The cell number doubled after 7 days of cultivation ($B_N = 2.01$ ($\pm$ 0.34)), which is in compliance with the non-cryopreserved control sample. In contrast, only 61 % ($R_N = 0.61$ ($\pm$ 0.05)) of the cells were recovered when cryopreserved in 2.0 mL working volume. These samples showed no increase in total cell number ($B_N = 1.06$ ($\pm$ 0.13)).
In summary, a successful tool validation was performed by analysing freeze and thawing behaviour for a scale up from a 1.0 mL working volume to a working volume of 2.0 mL. Using the developed tool, a delay in freezing and thawing was observed with the 2.0 mL working volume, which is in agreement with literature [73, 75, 77, 82, 83]. Subsequently, cryopreservation process performance was evaluated via intact viable cell monitoring. Here, a negative effect represented by declining cell recovery and proliferation was observed due to working volume scale up. These findings correspond with literature data and thereby demonstrate the usefulness of the developed video-based tool in cryopreservation process development. Additionally, fast and easy adaptation of the method concerning new applications like scale up and change in devices is another advantage. The development of the tool for evaluation of freezing and thawing behaviour is the groundwork for future studies concerning adapter and freezing profile optimization for 2.0 mL working volume. This tool could also be applied to screen cryoprotectant agents and concentrations, since these process parameters also influence the freezing and thawing behaviour and have a direct influence on cell viability. [71, 74, 87] The developed tool can facilitate a more knowledge-based cryopreservation process development in research and development of the pharmaceutical industry.

8.5 Conclusion

A video analysis-based tool for knowledge-based cell cryopreservation process development was designed. It was realised as offline video analytic, using an inexpensive automated digital image processing approach. The developed tool allows for the characterisation of freezing and thawing behaviour through evaluation of the mean pixel intensity represented by a cryosample in video snapshots. Plotting the mean pixel intensity of a cryosample over time results in characteristic curves for freezing and thawing. Freezing of samples lead to an increase in pixel intensity and subsequent thawing is represented by a decrease. These characteristic curves were used to determine the frozen over state and complete thawing of

samples.
Performance of the tool was demonstrated by a cryopreservation scale up case study with a model process using the mammalian β-cell line INS-1E. Here, cells were slowly frozen in a controlled manner using DMSO as cryoprotectant, stored at ultra-low temperatures for 7 days, followed by rapid thawing in a pre-warmed (37 °C) water bath. The process was performed with two working volumes (1.0 mL and 2.0 mL) in order to evaluate the flexibility of the tool. It was found that an increase of working volume from 1.0 mL to 2.0 mL results in a delay in freezing and thawing behaviour of cryosamples. This is in good agreement with literature [73, 75, 77, 82, 83], thereby confirming the performance of the developed tool. Additionally, the influence of working volume on cell recovery and proliferation was analysed. Intact viable cell monitoring showed an influence on cell post-thaw behaviour, underlining the need for a knowledge based process evaluation.
We believe that the integration of the developed video-based tool, for characterisation of freezing and thawing behaviour, can facilitate a more systematic cryopreservation process development. Furthermore, using the developed tool in combination with a systematic screening approach would lead to a deeper process knowledge, necessary in a good manufacturing practice (GMP) environment for cell-based products. Comprehensive studies should focus on different video material e.g. using a thermal imaging camera would allow for a closed container set up.

Acknowledgements

We thank Prof. Hartwig and co-workers from the Institute of Food Chemistry at the Karlsruhe Institute of Technology (KIT) for sharing their labs and equipment and, additionally, the staff of the workshops form the Institute of Functional Interface and Institute for Inorganic Chemistry at the KIT for their assistance. We would also like to thank Prof. Maechler, from the Department of Cell Physiology and Metabolism at the University of Geneva Medical Centre, Switzerland for providing the rat beta-cell line INS-1E. This work was supported by the Helmholtz Program BioInterfaces in Technology and Medicine (BIFTM).

Conflicts of Interests

The authors have no conflicts to declare.

8.6 References

1. A. A. Vertès, N. Qureshi, A. I. Caplan, and L. E. Babiss, eds.: *Stem Cells in Regenerative Medicine: Science, regulation and business strategies*. Wiley-Blackwell, 2016.

71. A. Z. Higgins, D. K. Cullen, M. C. LaPlaca, and J. O .M. Karlsson: 'Effects of freezing profile parameters on the survival of cryopreserved rat embryonic neural cells'. *Journal of Neuroscience Methods* (2011), vol. 201(1): pp. 9–16.

72. B. Grout, J. Morris, and M. McLellan: 'Cryopreservation and the maintenance of cell lines'. *Trends in Biotechnology* (1990), vol. 8: pp. 293–297.

73. I. Massie, C. Selden, H. Hodgson, B. Fullerand S. Gibbons, and J. G. Morris: 'GMP Cryopreservation of Large Volumes of Cells for Regenerative Medicine: Active Control of the Freezing Process'. *Tissue Engineering Part C: Methods* (2014), vol. 20(9): pp. 693–702.

74. R. Heidemann, S. Lünse, D. Tran, and C. Zhang: 'Characterization of cellbanking parameters for the cryopreservation of mammalian cell lines in 100 mL cryobags'. *Biotechnology Progress* (2010), vol. 26(4): pp. 1154–1163.

75. M. I. Kleman, K. Oellers, and E. Lullau: 'Optimal conditions for freezing CHOS and HEK293EBNA cell lines: Influence of Me2SO, freeze density, and PEImediated transfection on revitalization and growth of cells, and expression of recombinant protein'. *Biotechnology and Bioengineering* (2008), vol. 100(5): pp. 911–922.

76. C. C. Wong, K. E. Loewke, N. L. Bossert, B. Behr, C. J. De Jonge, T. M. Baer, and R. A. Reijo Pera: 'Non-invasive imaging of human embryos before embryonic genome activation predicts development to the blastocyst stage'. *Nature biotechnology* (2010), vol. 28: pp. 1115–21.

77. Y. Li and T. Ma: 'Bioprocessing of Cryopreservation for Large-Scale Banking of Human Pluripotent Stem Cells'. *BioResearch Open Access* (2012), vol. 1(5): pp. 205–214.

78. C. J. Hunt: 'The Banking and Cryopreservation of Human Embryonic Stem Cells'. *Transfusion Medicine and Hemotherapy* (2007), vol. 34: pp. 293–304.

79. D. Freimark, C. Sehl, C. Weber, K. Hudel, P. Czermak, N. Hofmann, R. Spindler, and B. Glasmacher: 'Systematic parameter optimization of a Me_2SO- and serum-free cryopreservation protocol for human mesenchymal stem cells'. *Cryobiology* (2011), vol. 63(2): pp. 67–75.

80. W. De Loecker, V. A. Koptelov, V. I. Grischenko, and P. De Loecker: 'Effects of Cell Concentration on Viability and Metabolic Activity during Cryopreservation'. *Cryobiology* (1998), vol. 37(2): pp. 103–109.

81. C. B Ware, A. M. Nelson, and C. A. Blau: 'Controlled-rate freezing of human ES cells'. *BioTechniques* (2005), vol. 38(6): pp. 879–883.

82. P. Kilbride, S. Lamb, S. Milne, S. Gibbons, E. Erro, J. Bundy, C. Selden, B. Fuller, and J. Morris: 'Spatial considerations during cryopreservation of a large volume sample'. *Cryobiology* (2016), vol. 73(1): pp. 47–54.

83. P. Kilbride, G. J. Morris, S. Milne, B. Fuller, J. Skepper, and C. Selden: 'A scale down process for the development of large volume cryopreservation'. *Cryobiology* (2014), vol. 69(3): pp. 367–375.

84. Y. Zhou, Z. Fowler, A. Cheng, and R. Sever: 'Improve process uniformity and cell viability in cryopreservation'. *BioProcess International* (2012), vol. 10: pp. 70–76.

85. J. O. M .Karlsson, A. Eroglu, T. L.Toth, E. G. Cravalho, and M. Tonerr: 'Fertilization and development of mouse oocytes cryopreserved using a theoretically optimized protocol'. *Human Reproduction* (1996), vol. 11(6): pp. 1296–1305.

86. F. Dumont, P.-A. Marechal, and P. Gervais: 'Cell Size and Water Permeability as Determining Factors for Cell Viability after Freezing at Different Cooling Rates'. *Applied and Environmental Microbiology* (2004), vol. 70(1): pp. 268–272.

87. E. J. Woods, B. C. Perry, J. J. Hockema, L. Larson, D. Zhou, and W. S. Goebel: 'Optimized cryopreservation method for human dental pulp-derived stem cells and their tissues of origin for banking and clinical use'. *Cryobiology* (2009), vol. 59(2): pp. 150–157.

89. T. Buhl, T. J. Legler, A. Rosenberger, A. Schardt, M. P. Schön, and H. A. Haenssle.: 'Controlled-rate freezer cryopreservation of highly concentrated peripheral blood mononuclear cells results in higher cell yields and superior autologous T-cell stimulation for dendritic cell-based immunotherapy'. *Cancer Immunology, Immunotherapy* (2012), vol. 61(11): pp. 2021–2031.

198. A .Merglen, S. Theander, B. Rubi, G. Chaffard, C. B. Wollheim, and P. Maechler: 'Glucose Sensitivity and Metabolism-Secretion Coupling Studied during Two-Year Continuous Culture in INS-1E Insulinoma Cells'. *Endocrinology* (2004), vol. 145(2): pp. 667–678.

240. C. Routledge and W. J. Armitage: 'Cryopreservation of cornea: a low cooling rate improves functional survival of endothelium after freezing and thawing'. *Cryobiology* (2003), vol. 46(3): pp. 277–283.

241. C. Hunt: 'Cryopreservation of Human Stem Cells for Clinical Application: A Review'. *Transfus Medicine Hemotherapy* (2011), vol. 38(2): pp. 107–123.

242. ÁBorsos, B. Szilágyi, P. S. Agachi, and Z. K. Nagy: 'Real-Time Image Processing Based Online Feedback Control System for Cooling Batch Crystallization'. *Organic Process Research & Development* (2017), vol. 21(4): pp. 511–519.

243. W. A. Moeglein, R. Griswold, B. L. Mehd, N. D. Browning, and J. Teuton: 'Applying shot boundary detection for automated crystal growth analysis during in situ transmission electron microscope experiments'. *Advanced Structural and Chemical Imaging* (2017), vol. 3(1): pp. 2–11.

244. K. Kumar, V. Kumarr, J. Lal, H. Kaurt, and J. Singh: 'A simple 2D composite image analysis technique for the crystal growth study of L-ascorbic acid'. *Microscopy Research and Technique* (2017), vol. 80: pp. 615–626.

245. M. A. L. Smith and L. A. Spomer: 'Direct quantification of in vitro cell growth through image analysis'. *In Vitro Cellular & Developmental Biology* (1987), vol. 23(1): pp. 67–70.

246. C. R. Thomas and G. C. Paul: 'Applications of image analysis in cell technology'. *Current Opinion in Biotechnology* (1996), vol. 7(1): pp. 35–45.

247. J. Selinummi, J. Seppälä, O. Yli-Harja, and J. A. Puhakka: 'Software for quantification of labeled bacteria from digital microscope images by automated image analysis'. *BioTechniques* (2005), vol. 39(6): pp. 859–863.

248. Y. Levin-Schwartz, D. R. Sparta, J. F. Cheer, and T. Adali: 'Parameter-free automated extraction of neuronal signals from calcium imaging data'. *2017 IEEE International Conference on Acoustics, Speech and Signal Processing (ICASSP)* (2017), vol.: pp. 1033–1037.

249. C.-C. Liang, A. Y. Park, and J.L. Guan: 'In vitro scratch assay: a convenient and inexpensive method for analysis of cell migration in vitro'. *Nature Protocols* (2007), vol. 2(2): pp. 329–333.

250. R. Spindler, B. Rosenhahn, N. Hofmann, and B. Glasmacher: 'Video analysis of osmotic cell response during cryopreservation'. *Cryobiology* (2012), vol. 64(3): pp. 250–260.

CHAPTER 9

A Tool Box for the Prediction of Media Process Performance for Cell Cryopreservation

Sarah Gretzinger[1,2], Stefanie Limbrunner[2], Jürgen Hubbuch[1,2,**]

[1] Institute of Functional Interfaces (IFG), Karlsruhe Institute of Technology (KIT), Eggenstein-Leopoldshafen, Germany

[2] Institute of Engineering in Life Sciences, Section IV: Biomolecular Separation Engineering, Karlsruhe Institute of Technology (KIT), Karlsruhe, Germany

[**] Corresponding author. Email: juergen.hubbuch@kit.edu

in preperation

Abstract

Cryopreservation is a well described method for cell long-term storage. However, when applied in a good manufacturing practice (GMP) production of e.g. biopharmaceuticals or cell-based products in regenerative medicine, more sophisticated requirements need to be met. A major focus for the GMP production is on the cryomedia composition, since they need to be chemically defined and free of toxic or animal-derived compounds. Hence, the commonly used cryoprotectants dimethyl sulfoxide (DMSO) and fetal bovine serum (FBS) are excluded. In this article, we describe an analytical tool box for the prediction of media cell cryopreservation process performance by characterization of media properties, freeze/thaw behaviour and media toxicity. We demonstrate the usefulness of the tool box in a case study with the β-model cell line INS-1E, where four media were screened including a positive and negative control in addition to two commercially available DMSO and FBS-free cryomedia. The tool box data indicated that the commercial Biofreeze® media shows inferior performance for INS-1E, while the second commercial cryomedia CryoSOfree™ is clearly a possible candidate. These findings were confirmed by a conventional viability monitoring study during the cryopreservation process. We believe that the tool box facilitates a fast pre-selection of possible candidates with a small number of cells, shortening the overall process development time. Hence, the tool box is highly beneficial. However, the predictive power needs to be proven in further extended experiments.

Keywords: cell cryopreservation, long-term storage, predictive tool box, pre-selection, process development, cryomedia formulation

9.1 Introduction

Efficient long-term storage of eukaryotic cell lines is an essential issue in many biotechnological application fields e.g. cell line maintenance for routine cell culture applications [72], biopharmaceutical production [74, 75], reproductive medicine [71, 76] and cell therapy in the field of regenerative medicine [1, 73, 84]. Here, continues supply of cells with constant genetic and metabolic features is crucial and often solved by the concept of cell banking. Meaning cryopreservation of cells with subsequent storage at ultra-low temperatures in highly controlled process environment, while monitoring critical cell characteristics. [1, 72, 74, 75, 77, 78] The concept of cell cryopreservation is well described in literature and general protocols are available. A common approach to avoid severe cell damage during freezing and thawing, due to extra- and intracellular ice formation as well as osmotic effects [72, 79, 90, 94, 251], is the use of dimethyl sulfoxide (DMSO) as cryoprotectant, slow freezing rates and a fast thawing protocol. [72, 74, 75, 88, 91, 92] However, successful post-thaw cell survival needs to be optimized individually for every cell line and is influenced by a number of process parameter. [75, 86, 95] These parameter include cell loading [80], cell characteristics e.g. suspension cells, monolayer or colony growth [78, 81, 240], cryoprotectant agents and concentration [71, 87], process volume (scale up) [73, 75, 77, 82, 83] and freezing/thawing rates [73, 74, 77, 84–86]. Preferable is a process with controlled freezing, especially in a good manufacturing practice (GMP) environment. [73, 74, 77, 81, 84, 88, 89, 252] When developing a process for the cryopreservation of clinical applications e.g. biopharmaceuticals of cell-based products, a major focus is on the optimization of the cryomedia composition. Here, chemically defined media are required by authorities without any toxic or animal-derived components, which exclude the well described cryoprotectants DMSO and the addition of fetal bovine serum (FBS). [90–93, 96–98, 253–256] FBS is commonly added to the media to protect cells from free oxygen radicals associated with freezing and could be replaced by serum from other sources e.g. recombinant produced serum. [79, 92, 257] Additionally, numerous cryoprotectans have already been described in literature. They can be divided in extracellular and intracellular cryoprotectant agents. [91, 93–98] Extracellular cryoprotectant agents are mostly sugars or high molecular weight polymers e.g. polyethylene glycol (PEG) and do not penetrate the cell membrane. Prominent examples of membrane penetrating intracellular cryoprotectant agents are DMSO, glycerol or 1,2-propanediol [91, 93, 98], which differ in up take rates [95]. However, the selection of a cryoprotectant agent and concentration cannot be optimized independently, since other process parameter e.g. freezing rate might be influenced as well. [71] Hence, a systematic empirical screening is necessary for a more directed process development. [71, 72, 74, 75, 241] The screening for alternative cryoprotectant agents with optimal concentrations have already been described for different cell lines. [100–102, 253] However, a rather traditional cryopreservation screening is time and material consuming. A predictive tool for the preliminary exclusion of non-applicable cryoprotectant agents would be highly beneficial. A pre-screening would not only narrow down possible cryoprotectant agent candidates, additionally, process knowledge could be gathered in parallel, necessary in a GMP environment.

In this study, we describe an analytical tool box for the prediction of cryomedia process

performance by characterization of media properties, freeze/thaw behaviour and cell response to cryomedia exposure (toxicity). The predictive power was evaluated in a case study with the β-model cell line INS-1E, where four different media were screened for cryopreservation application. The screening compromised a DMSO containing cryomedia as positive control, the culture media as negative control and two commercially available, DMSO- and serum-free cryomedia. The media process performance was evaluated by a viability monitoring during the cryopreservation process with subsequent calculation of the critical process parameter cell recovery and proliferation. Finally, the applicability of the four screened cryomedia for the use in a cryopreservation process for the cell line INS-1E was evaluated.

9.2 Materials and Methods

9.2.1 Stock Solutions

Cell culture reagents were purchased from Thermo Fisher Scientific (Waltham, USA), unless otherwise stated. Culture media consisted of RPMI 1640 with GlutaMAX supplemented with 10 (v/v) % FBS, 1 (v/v) % sodium pyruvate, 1 (v/v) % Penicillin / Streptomycin, 10 mM HEPES, 2 mM L-Glutamine and 50 μM β-mercaptoethanol (Sigma-Aldrich, St. Louis, USA). The culture media was also used as negative control in the cryopreservation study. Additionally, three cryomedia were used, two commercially available, DMSO-free cryomedia, namely, CryoSOfree^{TM} (Sigma-Aldrich, St. Louis, USA) and Biofreeze$^{®}$ (Biochrom GmbH, Berlin, Germany) and as control a DMSO containing cryomedia. The DMSO containing cryomedia consisted of RPMI 1640 with GlutaMAX supplemented with 20 (v/v) % FBS, 1 (v/v) % sodium pyruvate, 10 (v/v) % DMSO (Sigma-Aldrich), 1 (v/v) % Penicillin / Streptomycin, 10 mM HEPES, 2 mM L-Glutamine and 50 μM β-mercaptoethanol (Sigma-Aldrich). All media were stored at 8 °C. Phosphate-buffered saline (PBS) was purchased from Thermo Fisher Scientific and stored at room temperature. All stock solutions were kept under sterile conditions.

9.2.2 Software and Data Processing

The software iTools Version 9.57.11 (Eurotherm, Worthing, UK), was used to control the EF600M 106. BD LSR Fortessa Cell Analyzer was controlled by BD FACSDiva 8.0 (BD Biosciences, San Jose, USA). Flow cytometry data were analysed and visualised using FlowJo V10 (Tree Star Inc., Ashland, USA). For data storage Excel 2013 (Microsoft, Redmond, WA, USA) was used. MATLAB R2015a (The MathWorks, Inc., Natick, USA) was used for data evaluation and visualization. Radar plots were generated using RStudio Version 1.1.383.

9.2.3 Cell Culture

The β-model cell line INS-1E [198] was kindly provided by Prof. Maechler from the Department of Cell Physiology and Metabolism at the University of Geneva Medical Centre, Switzerland. Cells were seeded with a concentration of 6.6 x 10^4 cells/cm^2 every 7 days, media exchange was performed after 3 days. The cultivation was done in a humidified incubator with 5 % CO_2.

9.2.4 Cell Cryopreservation

Cryopreservation was done with all 4 media, namely, cell culture media (RPMI), DMSO containing (DMSO), CryoSOfree^{TM} (Sigma) and Biofreeze$^{®}$ (Merck) with a 1 mL working volume using 1.8 mL cryovials (VWR International GmbH, Bruchsal, Germany). Cell cryopreservation was performed according to a previous study. [258] Briefly, cells were suspended in cryomedia to a final concentration of 6 x 10^6 cells/mL and frozen to - 80 °C in a controlled manner using the EF600 M 106 (55 x 1.8 mL cryovials, 1.0 mL max. fill; Grant Instruments, Cambridgeshire, UK). The freezing profile is listed in **table 9.1**. After a 24 h incubation at - 80 °C, samples were stored for 7 days at - 196 °C (Arpege 70, Air Liquide Medical GmbH, Düsseldorf, Germany). Followed by a fast thawing step in a 37 °C pre-warmed water bath. Cells were then quickly transferred for 5 min in a 20 °C pre-warmed culture media (1:20) and washed once with PBS (1:10). Then, cells were cultivated for 7 days in 7 mL culture media using a culture flask with an area of 25 cm^2. Media was exchanged after 3 days. Viability monitoring was performed by estimating intact live cell concentration using haemocytometer counting. Trypan blue dye exclusion was used to distinguish between intact live cells and damaged/dead cells. Samples were analysed after cell suspension in cryomedia, direct after thawing and after 7 days of cultivation.

Table 9.1: Freezing profile

Increments	**Temperature**
start temp.	20 °C
cool	from 20 to - 5 °C at 2 °C min^{-1}
cool	from - 5 °to - 7 °C at 1 °C min^{-1}
hold	at - 7 °C for 10 min
cool	from - 7 °to - 80 °C at 1 °C min^{-1}
hold	at - 80 °C

9.2.5 Characterization of Freezing and Thawing Behavior

Freezing and thawing behaviour of the used media for cryopreservation was analysed using a video-based tool previously described. [258] Here, an automated image processing approach is used to determine the state of frozen over or complete defrosting of a sample. Videos were taken with a GoPro Hero4 (GoPro, Inc., San Mateo, USA) controlled via the GoPro App version 2.6.3.312 (GoPro, Inc.) and a Samsung Galaxy Note Pro SM-P900 (Samsung, Seoul, South Korea). Following camera settings were applied: field of view: narrow; resolution: 1080 p; frames per second: 25.

9.2.6 Media Characterization

Viscosity measurements were done using an Anton Paar Physica MCR 301 rheometer (Anton Paar GmbH, Grax, Austria) equipped with a 50 mm diameter parallel plate geometry (PP50). Shear stress was increased from 10 - 20 Pa (300 data points).
Osmolarity was analysed using a vapour pressure osmometer model VAPRO® 5600 (Wescor Inc., Logan, USA). Viscosity and osmolartiy was measured at room temperature.

9.2.7 Cell Response Characterization

For the evaluation if the process time has an effects on cells suspended (c = 6 x 10^6 cells/mL) in cryomedia, a kinetic study was performed. Here, damaged/dead cell ratio was determined using a haemocytometer counting in combination with trypan blue dye exclusion. Samples were analysed at regular intervals for 250 min. Damaged/dead cell ratio was plotted over time and validated. If there was a change in the ratio over time it was rated 1 (yes), otherwise with a 0 (no).
Flow cytometry was used to evaluate cryomedia toxicity. Here, cells were analysed in cryomedia (c = 6 x 10^6 cells/mL) using an LSR Fortessa by BD Bioscience. Additionally, a diluted cell sample (1:8, in PBS) was analysed to evaluate the cell response to osmotic pressure changes. A gating strategy **(fig. 9.1)** was applied for both sample types (undiluted & diluted) were the control population was defined by means of a control sample (undiluted cells in culture media). Then, cell loss was calculated on basis of the control sample.

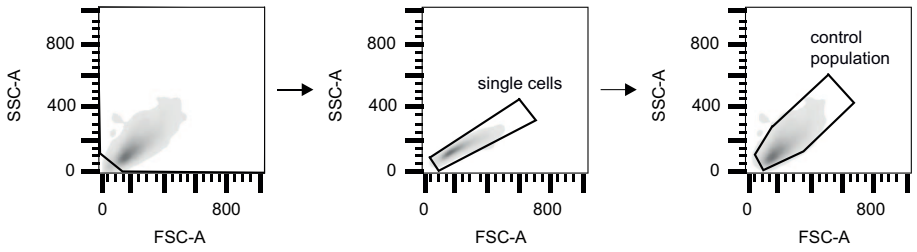

Figure 9.1: Gating strategy for undiluted and diluted cell samples. Only single cells were evaluated, a control population gate was defined by means of a positive control (cells in culture media). FSC-A: forward scatter peak area, SSC-A: side scatter peak area.

9.2.8 Data Normalization

Tool box data was displayed as radar charts. For this reason, data was normalized according to **table 9.2**.

Table 9.2: Summary of tool box parameter and normalization

	Parameter	Unit	Normalization
Media Properties	osmolarity	[mmol/kg]	$x' = (x - x_{min})/(x_{max} - x_{min})$
	viscosity	[mPa*s]	$x' = (x - x_{min})/(x_{max} - x_{min})$
Physical Behaviour	freezing end temp.	[°C]	$x' = a + ((x - x_{min})\ (a+b)/(x_{max} - x_{min}))$
	thawing end time	[min]	$x' = a + ((x - x_{min})\ (a+b)/(x_{max} - x_{min}))$
Cell response	kinetic	1/0 (yes/no)	-
	cell loss (undiluted)	(%)	$x' = x/100$
	cell loss (diluted)	(%)	$x' = x/100$

a = 0.5, b = 0.3

9.3 Results

In the present work, we describe a tool box for the prediction of media process performance in cell cryopreservation. The tool box compromises the characterization of media properties, freezing and thawing behaviour and cell response to media. The applicability of the tool box was evaluated in a case study with the β-model cell line INS-1E, screening four cryopreservation media. Additionally, the cryomedia process performance was evaluated via a cell viability monitoring during the cryopreservation process in order to validate the predicted process performance. The media screening included a DMSO containing media since it showed a good process with the cell line INS-1E performance in a previous study [258], the culture media without any cryoprotectant (as negative control) and two commercially available, DMSO-free cryomedia. The tool box was applied, thus, characterization of media properties, freezing and thawing behaviour and cell response to media was performed. Characterization of media properties included the measurement of osmolarity and viscosity. For the characterization of freezing and thawing behaviour the previously developed video-based tool [258] was used. Cell response was analysed by flow cytometry and a simple kinetic study. An overview of the screening procedure is depicted in **fig. 9.2**. Additionally, the process performance was determined as previously described. [258] Briefly, cryopreservation process was performed and samples were taken for the viability monitoring before freezing, after thawing and after cultivation (7 days).
In the first part of the study, characterization of media properties, freezing and thawing behaviour and cell response to media was done by using the described tool box, in order to evaluate if a prediction of media process performance is possible. Media property characterization included osmolarity and viscosity measurements. The osmolority range for the four tested media was from 293 mmol/kg to 1832 mmol/kg and the viscosity range from 1.07 mPa*s to 5.3 mPa*s. Freezing and thawing behaviour was characterized as previously described. [258] Freezing was performed in a controlled manner using the EF600 M 106

as described in **table 9.1** from 20 °C to - 80 °C. Due to the video timestamp and the

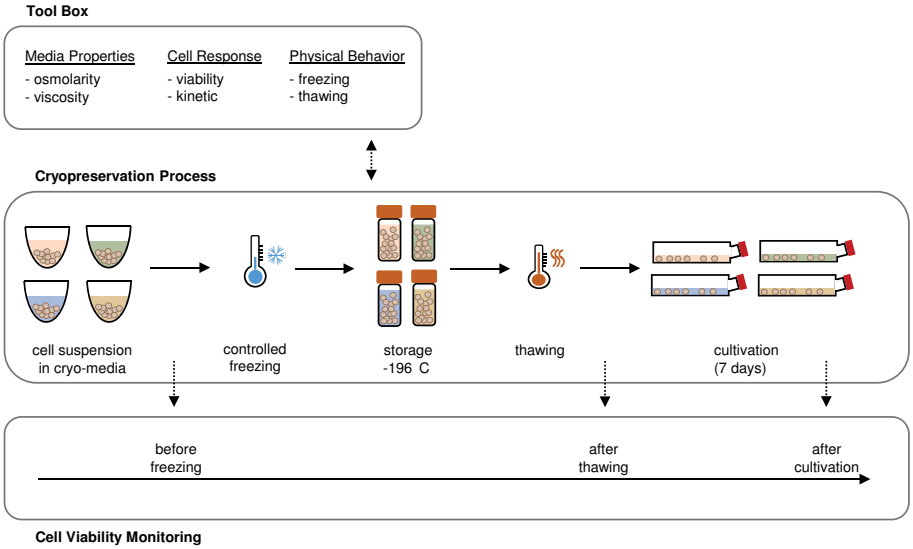

Figure 9.2: Overview of the cryomedia screening. Four media were screened regarding the use for cryopreservation of the β-model cell line INS-1E. The cryopreservation process was performed with the selected media. Cells were suspended in cryo-media and directly frozen to - 80 °C in a controlled manner. After 24 h at - 80 °C the cryo-samples were transferred in the storage tank (- 196 °C). After 7 days of storage, the samples were thawed and cultivated for 7 days. Samples for intact cell viability monitoring were taken before freezing, after thawing and after cultivation. Additionally, a tool box was used for the characterization of the cryomedia. The tool box was applied to characterize media propteries, cell response and physical behaviour. It facilitates the measurement of osmolarity and viscosity, the cell response, namely, viability in the media and a kinetic study and the characterization of freezing and thawing behaviour.

freezing profile tracking, mean crystallization end temperature could be determined. To note, this represents the profile temperature of the process and not the sample temperature. The range of the crystallization end temperature was between - 20.5 °C and - 32.6 °C for the tested media. Additionally, the thawing end time was analysed and the range was from 2.0 min to 4.1 min. For the characterization of cell response caused by the media, two different approaches were performed. First, a simple kinetic study of cell death was done in order to evaluate the influence of process time on intact cell viability. Therefore, damaged/dead cell ratio was determined and plotted over time **(supplementary data 9.3)**. The kinetic results were classified as 0 when a constant cell damaged/death ratio was observed and classified as 1 if there was an increase in cell damaged/death ratio. No increase in cell damaged/death ratio was observed, except for the the Biofreeze® media (Merck), here, an increase could be seen. For the evaluation of media toxicity (undiluted) and cell response to changes in osmotic pressure (diluted), a flow cytometry analysis was performed with undiluted and diluted samples. The results are shown in **fig. 9.4**, here, the dotplot of the FSC-A and SSC-A signal of the single cell population is shown. Cell loss [%] was determined on the basis of the control population of the control sample **(fig. 9.4 C)**. The cell loss for the undiluted samples were between 0.0 % and 10.9 % and for the

diluted samples from 0.0 % to 56.2 %.

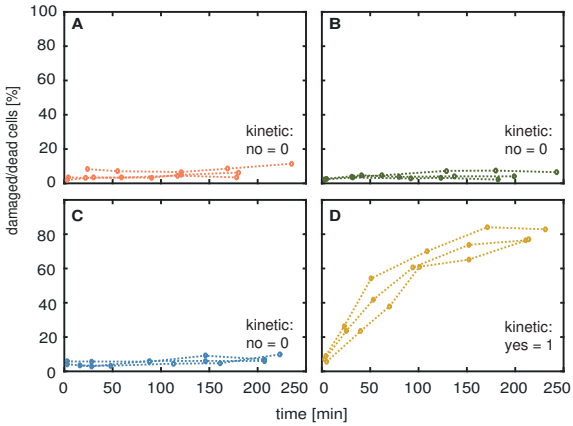

Supplementary Data 9.3: Process time evaluation regarding intact cell viability. Kinetic study of cell death in cryopreservation media (n = 3). The ratio of damaged/dead cells [%] is plotted over time [min] for **A** cryomedia containing DMSO (DMSO), **B** culture media (RPMI), **C** CryoSOfree^{TM} (Sigma) and **D** Biofreeze® (Merck). The data is evaluated if there is an increase in damaged/cell death ratio: no = 1, yes = 1.

The tool box data is summarized as radar charts in **fig. 9.5**. The solid lines represent the mean, while the standard deviation is plotted as black circles and dashed lines. All data were normalized (range [0 1]) according to **table 9.2**. The cryomedia containing DMSO (DMSO) **(fig. 9.5 A)** showed a high value for osmolarity, medium values for freezing and thawing behaviour and low values for viscosity, kinetic, cell loss undiluted and diluted. The negative control culture media (RPMI) **(fig. 9.5 B)** featured extremely low values for all tested parameter, except for the freezing and thawing behaviour, here, medium values were observed. The CryoSOfree^{TM} media (Sigma) **(fig. 9.5 C)** featured high values for osmolarity and viscosity, medium values for freezing and thawing and low values for the kinetic, cell loss undiluted and diluted. The Biofreeze® medium (Merck) **(fig. 9.5 D)** featured high values for osmolarity and kinetic, medium values for freezing, thawing and cell loss (diluted) and low values for viscosity and cell loss (undiluted). Comparing the two commercially available cryomedia, with yet unknown process performance, with the positive and negative controls, the assumption was made that the CryoSOfree^{TM} media (Sigma) are applicable for cryopreservation with the cell line INS1-E, while the Biofreeze® medium (Merck) showed toxic effects and is likely to exhibit a poor process performance.

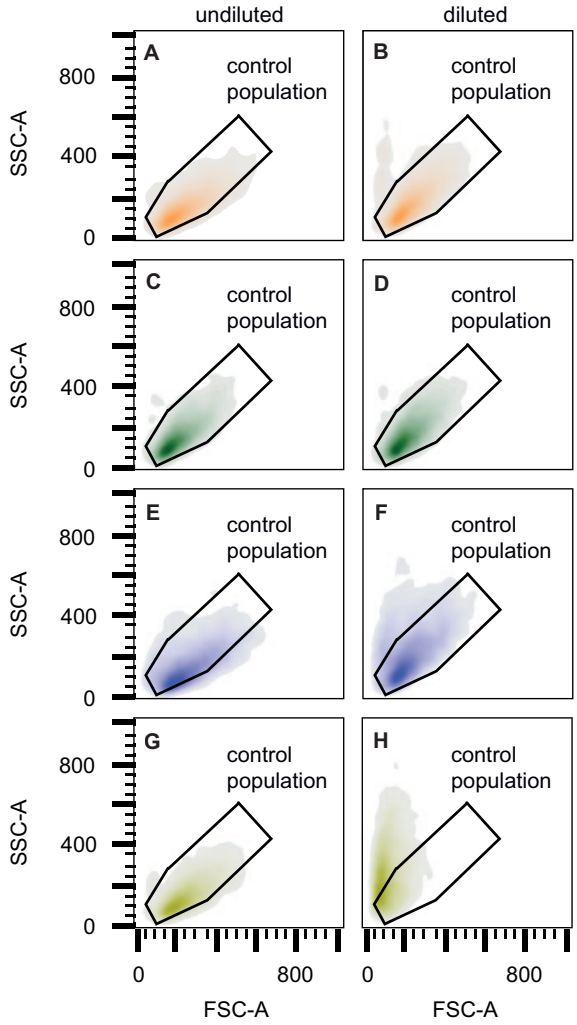

Figure 9.4: Flow cytometry data. Evaluation of media toxicity (undiluted) and cell response to changes in osmotic pressure (diluted). Dotplot of the FSC-A and SSC-A signal of single cell population. The depicted control population was gated according to the control sample (**C**). Dotplots of undiluted samples are depicted on the **left**, while dotplots of the diluted samples are depicted on the **right**. **A & B** cryomedia containing DMSO (DMSO), **C & D** culture media (RPMI), **E & F** CryoSOfree^{TM} (Sigma) and **G & H** Biofreeze$^{®}$ (Merck). FSC-A: forward scatter peak area, SSC-A: side scatter peak area.

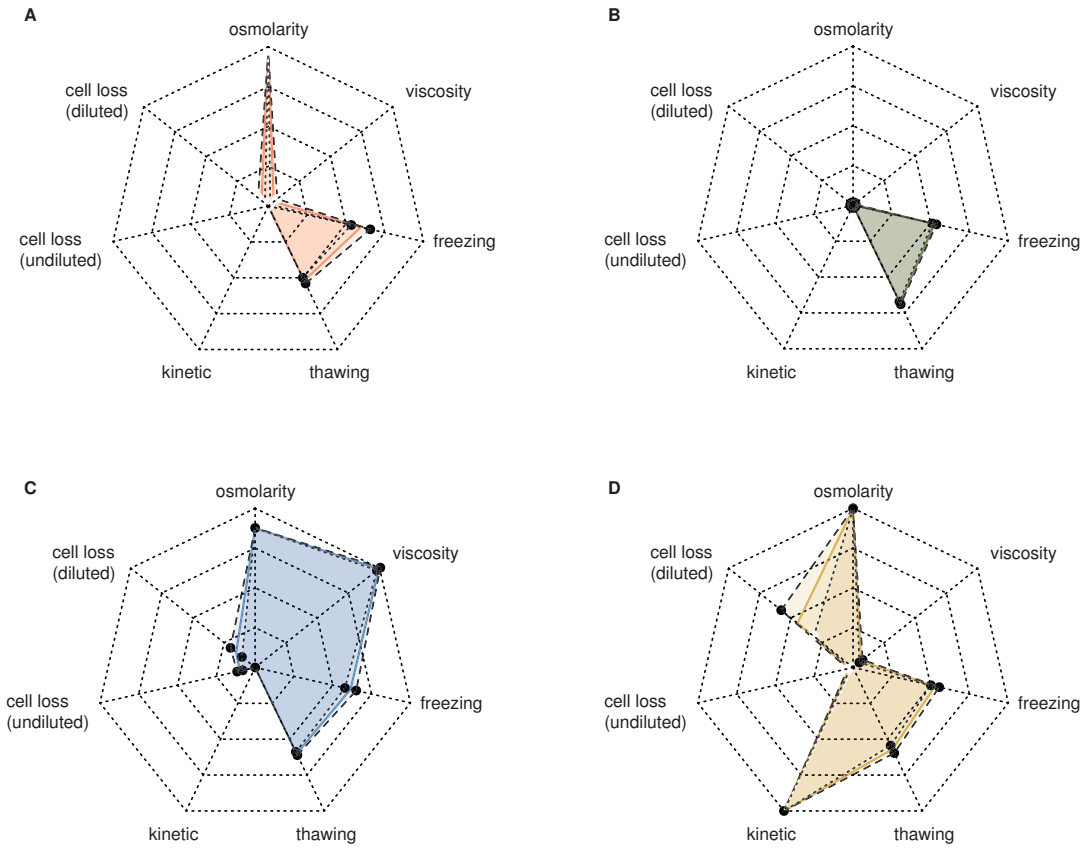

Figure 9.5: Summary of the characterization of the selected cryomedia using the described tool box. Analyzed were the media properties osmolarity and viscosity, the freezing and thawing bahaviour and the cell response, namely, kinetic study and cell loss (of undiluted and diluted cell samples). All data were normalized (range [0 1]) according to **table 9.2**. The data is shown as radar charts for **A** cryomedia containing DMSO (DMSO), **B** culture media (RPMI), **C** CryoSOfree^{TM} (Sigma) and **D** Biofreeze® (Merck). The solid lines represent the mean, while the standard deviation is plotted as black circles and dashed lines.

In the second part of the study, cell viability monitoring during the cryopreservation process was performed with subsequent evaluation of the process performance of each tested media. For comparison of the results, normalization of the live cell number was done according to **eq. (9.1)** [258]:

$$(live\ cells)_{\mathrm{N}} = \frac{live\ counts}{working\ volume}\ [cells/mL] \tag{9.1}$$

Intact cell viability was determined before freezing, after thawing and after 7 days of cultivation. The summary of the viability monitoring is displayed in **fig. 9.6 A**. The normalized intact live cell number is plotted over process steps (n = 9). The gray horizontal bar represents the control cell number of non-cryopreserved cells (upper line: mean + SD; bottom line: mean - SD). All four media showed similar live cell numbers before freezing [(4.15 - 5.45) x 10^6 cells/mL]. While the cell number stays approximately the same for the DMSO containing media (DMSO) and CryoSOfree$^{\mathrm{TM}}$ (Sigma) after thawing, there is a decrease in intact live cell number to 1.2 x 10^6 cells/mL for the Biofreeze® media (Merck). No intact live cells were detected after freezing for the culture media (RPMI). After 7 days of cultivation the intact live cell number increased to 10.85 x 10^6 cells/mL (± 1.14 x 10^6) for the DMSO containing media (DMSO), for the CryoSOfree$^{\mathrm{TM}}$ media (Sigma) to 8.34 x 10 cells/mL (± 1.05 x 10^6) and for the Biofreeze® media (Merck) to 3.85 x 10^6 cells/mL (± 1.00 x 10^6). No intact live cells were detected after cultivation for the culture media (RPMI).
Subsequently, two critical process parameter, namely cell recovery and cell biomass increase, were determined for evaluation of media process performance. Evaluation was done based on the normalized cell number. Cell recovery was calculated according to **eq. (9.2)** [258].

$$R_{\mathrm{N}} = \frac{after\ thawing}{before\ freezing} \tag{9.2}$$

Cell biomass increase was calculated according to **eq. (9.3)** [258].

$$B_{\mathrm{N}} = \frac{after\ cultivation}{before\ freezing} \tag{9.3}$$

The results are summarized as dotplot in **fig. 9.6 B**. Cell biomass increase is plotted over cell recovery for the evaluation of process performance. High cell recovery with R_N = 0.94 (± 0.14) and cell biomass increase B_N = 2.01 (± 0.34) was observed for the DMSO containing media (DMSO). Followed by the CryoSOfree$^{\mathrm{TM}}$ media (Sigma) with R_N = 0.84 (± 0.11) and B_N = 1.75 (± 0.38). In comparison, Biofreeze® media (Merck) showed a relatively low cell recovery with R_N = 0.22 (± 0.03) and B_N = 0.95 (± 0.25). No live cells were recovered for the culture media (RPMI), subsequently no cell biomass increase was shown.

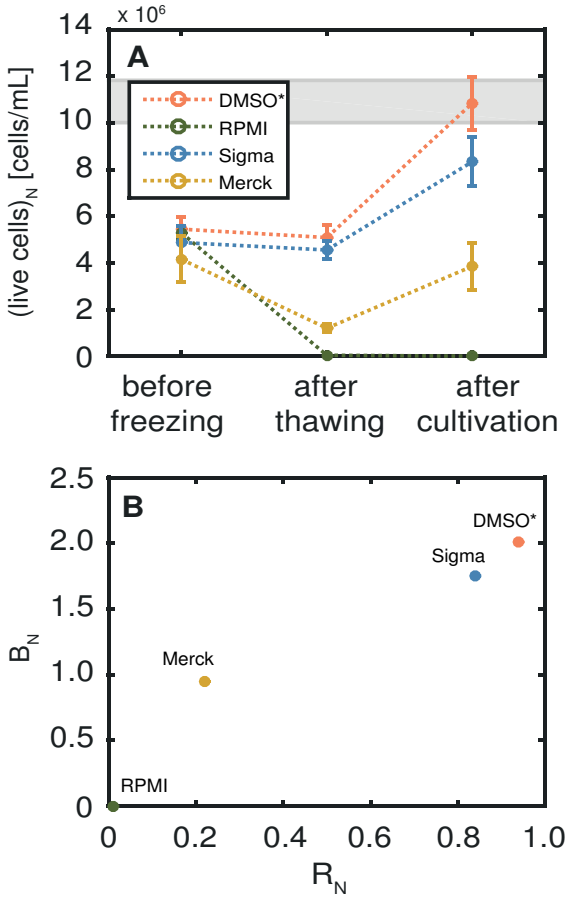

Figure 9.6: Cell viability monitoring of the cryopreservation process with the cell line INS-1E. **A** Normalized live cell number over process steps is shown (n = 9). The gray horizontal bar represents the control cell number of non-cryopreserved cells (upper line: mean + SD; bottom line: mean - SD). **B** Dotplot of the cell recovery factor (R_N) and the cell biomass increase factor (B_N) for the evaluation of media process performance.
* data from [258]

9.4 Discussion

We investigated if a prediction of media process performance in cell cryopreservation can be accessed through the characterization of media properties, freezing/thawing behavior and the media toxicity. The characterization methods are summarized as tool box which comprises an osmolarity and viscosity measurement for media characterization, the previously developed video-based tool [258] for the characterization of the freezing and thawing behaviour, a simple kinetic study and flow cytometry for the analysis of media toxicity. A case study with the β-model cell line INS-1E was performed, screening four cryopreservation media. A process performance prediction using the described tool box, was done. Additionally, the prediction was validated via a conventional viability monitoring during cell cryopreservation, with a subsequent calculation of the critical process performance

parameter cell recovery and cell biomass increase.
In the first part of the study, the predictive power of the described tool box, concerning media cryopreservation process performance for the β-model cell line INS-1E, was investigated. In literature, various factors influencing post-thawing intact cell viability are described. [71, 72, 74, 75, 78, 80, 81] Hence, the tool box needs to cover several aspects of the cryopreservation process, namely, media properties, freezing/thawing behaviour and media toxicity. Osmolarity is a media property closely related with supplementation of cryoprotectants, resulting in an increase in osmolarity. [259–263] Additionally, the media viscosity was measured. To our knowledge, the influence of viscosity on post-thawing cell viability was not reported so far. However, the use of polymers or other high molecular weight molecules as cryoprotectant agents may increase the media viscosity, leading to a more complex process for big scale production. In our experience, the automatic handling of viscous fluids needs to be additionally optimized, especially the cell resuspension in such a media. [200] Thus, media viscosity might have not a direct influence on cell post-thaw survival, but can cause issues concerning automatization and up scaling, which is a valuable insight in early process development stage. The cryomedia composition can also have an influence on freezing behavior. [260] Since the optimal freezing and thawing profile is crucial for a successful cell cryopreservation [73, 74, 77, 84–86, 90, 94, 95, 98], the characterization of freezing and thawing behaviour was implemented in the tool box by using the previously developed video-based tool [258]. Another crucial issue in cell cryopreservation is the cryoprotectant toxicity. [88, 100, 101, 255] This was addressed by a flow cytometry analysis and a simple kinetic study. Flow cytometry analysis was performed with undiluted samples and in PBS diluted samples. While the analysis of undiluted samples provides conclusion of instant media composition toxicity, the analysis of diluted samples indicates if the cells can cope fast changes in osmolarity, which simulates the washing step after thawing. Briefly, cryomedia are associated with higher osmolarity [259–263], when diluted in PBS the osmolarity is decreased to an almost physiological value (PBS osmolarity according to manufacturer: 270 - 300 mOsm/kg). It is also reported in literature, that cryoprotectant exposure time may influence intact cell viability. [98] Consequently, a simple kinetic study was implemented in the tool box, where intact cell viability was measured over 250 min by haemocytometer counting in combination with trypan blue dye exclusion. The described tool box was applied for the characterization of all four media.
The DMSO containing media (DMSO), which is considered as an example for good process performance [258], displayed the following features: high osmolarity, low viscosity, medium freezing and thawing behavior, additionally no toxic effects were observed. These data are in good agreement with the CryoSOfree^{TM} media (Sigma) results, except the high viscosity value. Thus, a high process performance was predicted. As previously described, we think that the viscosity is a soft parameter, meaning that viscosity is not influencing process performance directly, but might increase process complexity. The culture media without any cryoprotection supplemented (RPMI; negative control) displayed, in contrast to all the other media, a low osmolarity. All other features were similar to the results of the DMSO containing media. This was in good agreement with the expectation, since the only difference between those two media is the addition of DMSO and additional serum as cryoprotectants, which causes an increase in osmolarity. [259–263] The lack of

cryoprotectant, however, results in severe cell damage during freezing/thawing resulting in extremely poor process performance, which is also in good agreement with literature [93]. The Biofreeze® media (Merck) displayed the same characteristics for media properties and freezing/thawing behaviour than the DMSO containing media. In contrast, some toxic effects were observed. The kinetic study showed an increase of damaged/death cell ratio over time and the diluted flow cytometry sample showed a cell loss of 44.63 % (± 13.11). These finding might indicate that this commercial media contains intracellular cryoprotectants which are slowly taken up and the release during the washing might not be fast enough. Thus, a poor process performance was predicted.
In the second part of the study, the tool box predictions were validated through a conventional intact cell viability monitoring during the cryopreservation process. In a previously study [258], a DMSO and fetal bovine serum containing culture media (DMSO) showed a $R_N = 0.94$ (± 0.14) and $B_N = 2.01$ (± 0.34) for the β-cell line INS-1E. For this reason, the media was included in the screening as an example for good process performance. Culture media without any cryoprotectant agent (RPMI) was used as example for extremely poor process performance ($R_N = 0.0$; $B_N = 0.0$). [93] Further, the study comprised two commercially available, DMSO-free and serum-free cryomedia, since cryopreservation for clinical applications requires non-toxic cryoprotectant agents and the use of non-animal-derived substances. [90–93, 96–98, 254–256] Both commercial cryomedia are, according to manufacturer, chemically defined, serum- and DMSO-free and has been successfully applied for mammalian cell lines, which makes them good candidates for clinically relevant applications. [79, 264–266] The media are, however, not described in detail by the manufacturer. While the CryoSOfree™ media (Sigma) showed a good process performance with INS-1E ($R_N = 0.84$ (± 0.11); $B_N = 1.75$ (± 0.38)), Biofreeze® media (Merck) showed a relatively poor process performance ($R_N = 0.22$ (± 0.03); $B_N = 0.95$ (± 0.25)). The evaluation of the process performance showed the following ranking: DMSO > Sigma > Merck > RPMI. These findings are in compliance with the tool box predictions.
In summary, the four screened cryomedia showed different process performance which were correctly predicted via the tool box characterization. Thus, the tool box offers a great opportunity for prediction of process performance if a positive and negative example is available and fully described. In this case study, the positive example was the DMSO containing culture media and the negative example culture media without any cryoprotectant. Two commercially available, DMSO- and serum-free cryomedia were tested displaying different process performance. The CryoSOfree™ media showed a good process performance which was successfully predicted via the tool box, since it displayed similar characterized features than the positive control, except the viscosity. However, viscosity is considered as a soft parameter, only important for process development considerations. The Biofreeze® media (Merck), on the other hand, showed poor process performance and displayed some toxic effects on the β-model cell line INS-1E, which makes it not applicable for that specific cell line and would be excluded from further cryopreservation optimization process by the tool box characterization.

9.5 Conclusion

A tool box for the prediction of media process performance for cell cryopreservation was described. The toolbox comprises the characterization of media properties, freezing/thawing behavior and cell response to cryomedia exposure (toxicity). The predictive power is based on the characterization of positive and negative controls. By comparison of the data of media formulations with unknown process performance with the controls, the process performance may be estimated. In this study, four media were screened for the applicability in a cryopreservation process for the β-model cell line INS-1E. The screening comprised a DMSO containing cryomedia as positive control, the culture media as negative control and two commercially available DMSO and serumfree cryomedia with unknown process performance. Using the described tool box, the commercial available cryomedia Biofreeze® media was identified as non-applicable due to cell toxicity effects, while the second commercial available cryomedia CryoSOfree™ was identified as possible candidate. However, the tool box reliability, sensitivity and robustness needs to be further proven in a study comprising more data. We believe that the described tool box could contribute to faster and more directed process development for cell cryopreservation. Using the tool box a pre-selection of possible candidates could be done with a small amount of cells in short time, shortening the time to market for clinical applications. Additionally, the tool box in combination with multivariate data analysis (MVDA) could contribute to a deeper process knowledge, which is also important for a GMP production of clinical applications. Another advantage of the tool box is the easy adaptation to new projects by implementing the measurement of e.g. critical cell criteria. The usage of flow cytometry analysis allows an additional measurement of e.g. specific cell markers important for cell therapeutic safety and effect especially in stem cell applications.

Funding sources

This work was supported by the Helmholtz Program BioInterfaces in Technology and Medicine (BIFTM).

Conflicts of Interests

The authors have no conflicts to declare.

Acknowledgements

We thank Prof. Hartwig and co-workers from the Institute of Food Chemistry at the Karlsruhe Institute of Technology (KIT) for sharing their labs and Marieke Klijn for the scientific conversation. We would also like to thank Prof. Maechler, from the Department of Cell Physiology and Metabolism at the University of Geneva Medical Centre, Switzerland for providing the rat beta-cell line INS-1E.

9.6 References

1. A. A. Vertès, N. Qureshi, A. I. Caplan, and L. E. Babiss, eds.: *Stem Cells in Regenerative Medicine: Science, regulation and business strategies*. Wiley-Blackwell, 2016.

71. A. Z. Higgins, D. K. Cullen, M. C. LaPlaca, and J. O .M. Karlsson: 'Effects of freezing profile parameters on the survival of cryopreserved rat embryonic neural cells'. *Journal of Neuroscience Methods* (2011), vol. 201(1): pp. 9–16.

72. B. Grout, J. Morris, and M. McLellan: 'Cryopreservation and the maintenance of cell lines'. *Trends in Biotechnology* (1990), vol. 8: pp. 293–297.

73. I. Massie, C. Selden, H. Hodgson, B. Fullerand S. Gibbons, and J. G. Morris: 'GMP Cryopreservation of Large Volumes of Cells for Regenerative Medicine: Active Control of the Freezing Process'. *Tissue Engineering Part C: Methods* (2014), vol. 20(9): pp. 693–702.

74. R. Heidemann, S. Lünse, D. Tran, and C. Zhang: 'Characterization of cellbanking parameters for the cryopreservation of mammalian cell lines in 100 mL cryobags'. *Biotechnology Progress* (2010), vol. 26(4): pp. 1154–1163.

75. M. I. Kleman, K. Oellers, and E. Lullau: 'Optimal conditions for freezing CHOS and HEK293EBNA cell lines: Influence of Me2SO, freeze density, and PEImediated transfection on revitalization and growth of cells, and expression of recombinant protein'. *Biotechnology and Bioengineering* (2008), vol. 100(5): pp. 911–922.

76. C. C. Wong, K. E. Loewke, N. L. Bossert, B. Behr, C. J. De Jonge, T. M. Baer, and R. A. Reijo Pera: 'Non-invasive imaging of human embryos before embryonic genome activation predicts development to the blastocyst stage'. *Nature biotechnology* (2010), vol. 28: pp. 1115–21.

77. Y. Li and T. Ma: 'Bioprocessing of Cryopreservation for Large-Scale Banking of Human Pluripotent Stem Cells'. *BioResearch Open Access* (2012), vol. 1(5): pp. 205–214.

78. C. J. Hunt: 'The Banking and Cryopreservation of Human Embryonic Stem Cells'. *Transfusion Medicine and Hemotherapy* (2007), vol. 34: pp. 293–304.

79. D. Freimark, C. Sehl, C. Weber, K. Hudel, P. Czermak, N. Hofmann, R. Spindler, and B. Glasmacher: 'Systematic parameter optimization of a Me_2SO- and serum-free cryopreservation protocol for human mesenchymal stem cells'. *Cryobiology* (2011), vol. 63(2): pp. 67–75.

80. W. De Loecker, V. A. Koptelov, V. I. Grischenko, and P. De Loecker: 'Effects of Cell Concentration on Viability and Metabolic Activity during Cryopreservation'. *Cryobiology* (1998), vol. 37(2): pp. 103–109.

81. C. B Ware, A. M. Nelson, and C. A. Blau: 'Controlled-rate freezing of human ES cells'. *BioTechniques* (2005), vol. 38(6): pp. 879–883.

82. P. Kilbride, S. Lamb, S. Milne, S. Gibbons, E. Erro, J. Bundy, C. Selden, B. Fuller, and J. Morris: 'Spatial considerations during cryopreservation of a large volume sample'. *Cryobiology* (2016), vol. 73(1): pp. 47–54.

83. P. Kilbride, G. J. Morris, S. Milne, B. Fuller, J. Skepper, and C. Selden: 'A scale down process for the development of large volume cryopreservation'. *Cryobiology* (2014), vol. 69(3): pp. 367–375.

84. Y. Zhou, Z. Fowler, A. Cheng, and R. Sever: 'Improve process uniformity and cell viability in cryopreservation'. *BioProcess International* (2012), vol. 10: pp. 70–76.

85. J. O. M .Karlsson, A. Eroglu, T. L.Toth, E. G. Cravalho, and M. Tonerr: 'Fertilization and development of mouse oocytes cryopreserved using a theoretically optimized protocol'. *Human Reproduction* (1996), vol. 11(6): pp. 1296–1305.

86. F. Dumont, P.-A. Marechal, and P. Gervais: 'Cell Size and Water Permeability as Determining Factors for Cell Viability after Freezing at Different Cooling Rates'. *Applied and Environmental Microbiology* (2004), vol. 70(1): pp. 268–272.

87. E. J. Woods, B. C. Perry, J. J. Hockema, L. Larson, D. Zhou, and W. S. Goebel: 'Optimized cryopreservation method for human dental pulp-derived stem cells and their tissues of origin for banking and clinical use'. *Cryobiology* (2009), vol. 59(2): pp. 150–157.

88. M. L. Thompson, E. J. Kunkel, and R. O. Ehrhardt: 'Standardized Cryopreservation of Stem Cells'. *Stem Cell Technologies in Neuroscience*. Ed. by A. K. Srivastava, E. Y. Snyder, and Y. D. Teng. New York, NY: Springer New York, 2017. Chap. 13: pp. 193–203.

89. T. Buhl, T. J. Legler, A. Rosenberger, A. Schardt, M. P. Schön, and H. A. Haenssle.: 'Controlled-rate freezer cryopreservation of highly concentrated peripheral blood mononuclear cells results in higher cell yields and superior autologous T-cell stimulation for dendritic cell-based immunotherapy'. *Cancer Immunology, Immunotherapy* (2012), vol. 61(11): pp. 2021–2031.

90. J. G. Baust, D. Gao, and J. M. Baust: 'Cryopreservation: An emerging paradigm change'. *Organogenesis* (2009), vol. 5(3): pp. 90–96.

91. W. Asghar, R. El Assal, H. Shafiee, R. M. Anchan, and U. Demirci: 'Preserving human cells for regenerative, reproductive, and transfusion medicine'. *Biotechnology Journal* (2014), vol. 9(7): pp. 895–903.

92. J. R. Moldenhauer: 'Cell Culture Preservation and Storage for Industrial Bioprocesses'. *Handbook of Industrial Cell Culture: Mammalian, Microbial, and Plant Cells*. Ed. by V. A. Vinc and S. R. Parekh. Totowa, NJ: Humana Press, 2003. Chap. 18: pp. 483–514.

93. S. S. Buchanan, S. A. Gross, J. P. Acker, M. Toner, J. F. Carpenter, and D. W. Pyatt: 'Cryopreservation of Stem Cells Using Trehalose: Evaluation of the Method Using a Human Hematopoietic Cell Line'. *Stem Cells and Development* (2004), vol. 13(3): pp. 295–305.

94. W. J. Armitage and B.K. Juss: 'The influence of cooling rate on survival of frozen cells differs in monolayers and suspensions'. *Cryo-Letters* (1996), vol. 17: pp. 213–218.

95. H. T. Meryman: 'Cryopreservation of living cells: principles and practice'. *Transfusion* (2007), vol. 47(5): pp. 935–945.

96. T. Du, L. Chao, S. Zhao, L. Chi, D. Li, Y. Shen, Q. Shi, and X. Deng: 'Successful cryopreservation of whole sheep ovary by using DMSO-free cryoprotectant'. *Journal of Assisted Reproduction and Genetics* (2015), vol. 32(8): pp. 1267–1275.

97. S. Thirumala, X. Wu, J. M. Gimble, and R. V. Devireddy: 'Evaluation of Polyvinylpyrrolidone as a Cryoprotectant for Adipose Tissue-Derived Adult Stem Cells'. *Tissue Engineering Part C: Methods* (2010), vol. 16(4): pp. 783–792.

98. B. Fuller, J. Gonzalez-Molina, E. Erro, J. De Mendonca, S. Chalmers, M. Awan, A. Poirier, and C. Selden: 'Applications and optimization of cryopreservation technologies to cellular therapeutics'. *Cell Gene Therapy Insights* (2017), vol. 3(5): pp. 359–378.

100. A. Hennes, L. Gucciardo, S. Zia, F. Lesage, N. Lefèvre, L. Lewi, A. Vorsselmans, T. Cos, R. Lories, J. Deprest, and J. Toelen: 'Safe and effective cryopreservation methods for longterm storage of humanamnioticfluidderived stem cells'. *Prenatal Diagnosis* (2015), vol. 35(5): pp. 456–462.

101. I. I. Katkov, N. G. Kan, F. Cimadamore, B. Nelson, E. Y. Snyder, and A. V. Terskikh: 'DMSO-Free Programmed Cryopreservation of Fully Dissociated and Adherent Human Induced Pluripotent Stem Cells'. *Stem Cells International* (2011), vol. 2011.

102. V. Keros, B. Rosenlund, K. Hultenby, L. Aghajanova, L. Levkov, and O. Hovatta: 'Optimizing cryopreservation of human testicular tissue: comparison of protocols with glycerol, propanediol and dimethylsulphoxide as cryoprotectants'. *Human Reproduction* (2005), vol. 20(6): pp. 1676–1687.

198. A .Merglen, S. Theander, B. Rubi, G. Chaffard, C. B. Wollheim, and P. Maechler: 'Glucose Sensitivity and Metabolism-Secretion Coupling Studied during Two-Year Continuous Culture in INS-1E Insulinoma Cells'. *Endocrinology* (2004), vol. 145(2): pp. 667–678.

200. S. Zimmermann, C. Scheeder, P. K. Zimmermann, A. Bogsnes, M. Hansson, A. Staby, and J. Hubbuch: 'Highthroughput downstream process development for cellbased products using aqueous twophase systems (ATPS) A case study'. *Biotechnology Journal* (2017), vol. 12(2): p. 1600587.

240. C. Routledge and W. J. Armitage: 'Cryopreservation of cornea: a low cooling rate improves functional survival of endothelium after freezing and thawing'. *Cryobiology* (2003), vol. 46(3): pp. 277–283.

241. C. Hunt: 'Cryopreservation of Human Stem Cells for Clinical Application: A Review'. *Transfus Medicine Hemotherapy* (2011), vol. 38(2): pp. 107–123.

251. P. Mazur, S. P. Leibo, and E. H. Y. Chu: 'A two-factor hypothesis of freezing injury: Evidence from Chinese hamster tissue-culture cells'. *Experimental Cell Research* (1972), vol. 71(2): pp. 345–355.

252. G. J. Morris, E. Acton, D. Collins, A. Bos-Mikich, and P. de Sousa: '143. Optimisation of current Good Manufacturing Practice (cGMP) compliant controlled rate freezing for human embryonic stem cells'. *Cryobiology* (2010), vol. 61(3): p. 406.

253. J. Hendriks, J. Riesle, and C. A. van Blitterswijk: 'Co-culture in cartilage tissue engineering'. *Journal of Tissue Engineering and Regenerative Medicine* (2007), vol. 1(3): pp. 170–178.

254. T. R. J. Heathman, V. A. M. Glyn, A. Picken, Q. A. Rafiq, K. Coopman, A. W. Nienow, B. Kara, and C. J. Hewitt: 'Expansion, harvest and cryopreservation of human mesenchymal stem cells in a serum-free microcarrier process'. *Biotechnology and Bioengineering* (2015), vol. 112(8): pp. 1696–1707.

255. O. Rogulska, Y. Petrenko, and A. Petrenko: 'DMSO-free cryopreservation of adipose-derived mesenchymal stromal cells: expansion medium affects post-thaw survival'. *Cytotechnology* (2017), vol. 69(2): pp. 265–276.

256. S. M. Zeisberger, J. C. Schulz, M. Mairhofer, P. Ponsaerts, G. Wouters, D. Doerr, A. Katsen-Globa, M. Ehrbar, J. Hescheler, S. P. Hoerstrup, A. H. Zisch, A. Kolbus, and H. Zimmermann: 'Biological and Physicochemical Characterization of a Serum-and Xeno-Free Chemically Defined Cryopreservation Procedure for Adult Human Progenitor Cells'. *Cell Transplantation* (2011), vol. 20(8): pp. 1241–1257.

257. A. Mitchell, K. A. Rivas, R. Smith, and A. E. Watts: 'Cryopreservation of equine mesenchymal stem cells in 95 % autologous serum and 5 % DMSO does not alter post-thaw growth or morphology in vitro compared to fetal bovine serum or allogeneic serum at 20 or 95 % and DMSO at 10 or 5 %'. *Stem Cell Research & Therapy* (2015), vol. 6: pp. 1–12.

258. S. Gretzinger, S. Limbrunner, and J. Hubbuch: 'Automated Image Processing as an Analytical Tool in Cell Cryopreservation for Bioprocess Development'. *Bioprocess and Biosystems Engineering* (2019), vol. 42: pp. 665–675.

259. S. M. Rahman, S. K. Majhi, T. Suzuki, S. Matsukawa, C. A. Strüssmann, and R. Takai: 'Suitability of cryoprotectants and impregnation protocols for embryos of Japanese whiting Sillago japonica'. *Cryobiology* (2008), vol. 57(2): pp. 170–174.

260. H. Woelders, A. Matthijs, and B. Engel: 'Effects of Trehalose and Sucrose, Osmolality of the Freezing Medium, and Cooling Rate on Viability and Intactness of Bull Sperm after Freezing and Thawing'. *Cryobiology* (1997), vol. 35(2): pp. 93–105.

261. M. K. Soylu, Z. Nur, B. Ustuner, I. Dogan, H. Sairkaya, U. Gunay, and K. Ak: 'Effects of Various Cryoprotective Agents and Extender Osmolality on Post-thawed Ram Semen'. *Bull Vet Inst Pulawy* (2007), vol. 51: pp. 241–246.

262. C. Koshimoto and P. Mazur: 'The effect of the osmolality of sugar-containing media, the type of sugar, and the mass and molar concentration of sugar on the survival of frozen-thawed mouse sperm'. *Cryobiology* (2002), vol. 45(1): pp. 80–90.

263. M. R. Polovina: *Cryopreservation solution*. US Patent 5,759,764. June 1998.

264. R. Chinnadurai, I. B. Copland, M. A. Garcia, C. T. Petersen, C. N. Lewis, E. K. Waller, A. D. Kirk, and J. Galipeau: 'Cryopreserved Mesenchymal Stromal Cells Are Susceptible to T-Cell Mediated Apoptosis Which Is Partly Rescued by IFNγ Licensing'. *STEM CELLS* (2016), vol. 34(9): pp. 2429–2442.

265. K. Matsumura and S.-H. Hyon: 'Polyampholytes as low toxic efficient cryoprotective agents with antifreeze protein properties'. *Biomaterials* (2009), vol. 30(27): pp. 4842–4849.

266. K. Matsumura, J. Y. Bae, and S. H. Hyon: 'Polyampholytes as Cryoprotective Agents for Mammalian Cell Cryopreservation'. *Cell Transplantation* (2010), vol. 19(6 - 7): pp. 691–699.

CHAPTER 10

3D Bioprinting - Flow Cytometry as Analytical Strategy for 3D Cell Structures

Sarah Gretzinger[1,2], Nicole Beckert[2], Andrew Gleadall[3], Cornelia Lee-Thedieck[1], Jürgen Hubbuch[1,2,*]

[1] Institute of Functional Interfaces (IFG), Karlsruhe Institute of Technology (KIT), Eggenstein-Leopoldshafen, Germany

[2] Institute of Engineering in Life Sciences, Section IV: Biomolecular Separation Engineering, Karlsruhe Institute of Technology (KIT), Karlsruhe, Germany

[3] Manufacturing and Process Technologies, Faculty of Engineering, University of Nottingham, University Park, Nottingham NG7 2RD, UK

[*] Corresponding author. Email: juergen.hubbuch@kit.edu

Bioprinting 2018 Sep; 11, e00023. https://doi.org/10.1016/j.BPRINT.2018.e00023

Abstract

The importance of 3D printing technologies increased significantly over the recent years. They are considered to have a huge impact in regenerative medicine and tissue engineering, since 3D bioprinting enables the production of cell-laden 3D scaffolds. Transition from academic research to pharmaceutical industry or clinical applications, however, is highly dependent on developing a robust and well-known process, while maintaining critical cell characteristics. Hence, a directed and systematic approach to 3D bioprinting process development is required, which also allows for the monitoring of these cell characteristics. This work presents the development of a flow cytometry-based analytical strategy as a tool for 3D bioprinting research.

The development was based on a model process using a commercially available alginate-based bioink, the β-cell line INS-1E, and direct dispensing as 3D bioprinting method. We demonstrated that this set-up enabled viability and proliferation analysis. Additionally, use of an automated sampler facilitated high-throughput screenings. Finally, we showed that each process step, e.g. suspension of cells in bioink or 3D printing, cross-linking of the alginate scaffold after printing, has a crucial impact on INS-1E viability. This reflects the importance of process optimisation in 3D bioprinting and the usefulness of the flow cytometry-based analytical strategy described here. The presented strategy has a great potential as a cell characterisation tool for 3D bioprinting and may contribute to a more directed process development.

Keywords: 3D bioprinting; process development; flow cytometry; cell viability, cell proliferation

10.1 Introduction

The possibility to build three-dimensional (3D), cell-laden constructs by three-dimensional bioprinting had a major impact in life science research and is expected to be a key technology in the field of tissue engineering and regenerative medicine [103–105]. Currently, academic research is focusing on developing human diseases 3D tissue models or models for drug discovery screenings [267, 268] and, in the long term, for transplantation of e.g. artificial pancreatic tissue [114] or structural cartilage repair [269]. Although 3D bioprinting is a relatively young research field, various 3D bioprinting technologies are available and have been used already, including robotic dispensing, inkjet printing, and stereolithography. [106, 109] A common feature of these technologies is the use of so-called "bioinks" as scaffold materials. Cells are resuspended in the bioink and 3D-printed in a layer-by-layer manner. Hydrogels are prevalently used as bioinks, since these are known to provide a cell-friendly environment and have often been applied in the field of tissue engineering. Additionally, they need to be printable when used as bioinks. Each technology has different requirements regarding e.g. rheology, shape fidelity, and the ability of cross-linking the bioink. [106, 109, 112, 113] Moreover, the post-printing behaviour of the scaffold needs to be considered. Depending on the tissue, different mechanical strengths and stiffnesses must be guaranteed to generate a functional, artificial 3D tissue model. Bone tissue, for example, differs extremely from cartilage tissue. Hence, 3D bioprinting is a highly multidisciplinary field, where biologists, materials scientists, and mechanical engineers need to cooperate closely together in order to develop a strategy for each 3D tissue model as regards the post-printing biological function, 3D printing technology, and bioink compatibility, the objective being to meet biological needs and ensure printability. [104, 109, 113, 270] *Malda et al.* [109] proposed the concept of the biofabrication window, which summarises the relations between bioink properties, keeping shape fidelity, polymer concentration of the hydrogel components, and post-printing cell viability. In general, higher polymer concentrations in the bioink translate into good shape fidelity, but might produce hydrogels too stiff for post-printing cell survival, and proliferation. [109] Therefore, a systematic approach to bioink development has been pursued. [271–274] Many publications cover the relationship between bioink properties, printing parameters, and cell survival. [275–279]

For a successful transition from academic research to pharmaceutical industry or clinical applications, a general and deeper process knowledge and directed process development are essential. Hence, using a systematic high-throughput process development (HTPD) approach would be highly beneficial. [114–116] High-throughput screening (HTS) technology has already been state-of-the-art in process development of pharmaceutical industry for many years and has already proven that it is a powerful tool to reduce development time and gain a deeper process knowledge, especially in combination with sophisticated statistical analysis. [140, 141, 143, 144, 149] HTS platforms are also available for stem cell research [136, 137] and downstream process development for cell-based products [200]. A major part in the development of these platforms is the integration of an appropriate and HTS-capable analytical method. When developing a 3D bioprinting process, it is extremely important to analyse the influence of this process on cell behaviour. Two general concepts can be applied: non-destructive testing, e.g. metabolic cell assays, where a supernatant

sample is analysed or destructive testing, e.g. qPCR or flow cytometry. While simple metabolic assays or DNA quantification methods, which provide only cumulative signals, are suited for screenings with only one non-differentiable cell line, flow cytometry or qPCR can be applied, if a more complex cell characterisation is needed. In both cases, the capability of the assay must be validated and optimised for a 3D printing approach. For example, metabolic assays might be insufficient for 3D tissues, since diffusion might be limited [106, 276, 280, 281]. When using flow cytometry, it must be possible to dissolve the 3D structure and obtain a single cell suspension. Flow cytometry has already proven that it is a powerful tool in cell-therapy process development [27, 128], which indicates that it might also be an essential tool in 3D bioprinting process development, since it is HTS-capable and variable in terms of measurable cell characteristics, although it is a destructive method.
Here, development of a flow cytometry-based analytical strategy for 3D cell printing applications is reported. The strategy encompasses a proliferation and live/dead ratio analysis. The method developed was evaluated based on a case study using the β-model cell line INS-1E and a commercially available alginate-based bioink. For 3D printing, the direct dispensing method was applied. The process consisted of the following steps: suspending cells in bioink, 3D bioprinting, post-printing cross-linking of the bioink by ionic gelation, dissolution of 3D structures by the means of de-gelation, and analysis. First, we evaluated the CellTrace^{TM} Violet-based proliferation analysis for bioprinted INS-1E cells. Subsequently, we evaluated the analytical strategy developed using 3D-printed fluorescence beads and fixed cells. Using the two artificial samples, effects of the printing process on living cells were excluded. The evaluation covered the applicability of 3D-printed samples and HTS capability, with the goal to verify suitability of the method for 3D bioprinting. Finally, the influence of each process step on the β-model cell line INS-1E was evaluated using the developed flow cytometry method.

10.2 Materials & Methods

10.2.1 Stock solutions

The fixation buffer consisted of phosphate-buffered saline (Thermo Fisher Scientific, Waltham, USA) supplemented with 3.6 (v/v)% formaldehyde (Sigma-Aldrich, St. Louis, USA). Storage buffer consisted of phosphate-buffered saline (Thermo Fisher Scientific) supplemented with 1 (v/v)% bovine serum albumin (Miltenyi, Bergisch Gladbach, Germany). Both buffers were kept under sterile conditions and stored at 8 $°C$. The de-gelating solution was prepared with ultra-pure water (0.55 μS/cm) obtained from an Arium®proUV water system (Sartorius Stedim Biotech, Goettingen, Germany). The solution consisted of 50 mM trisodium citrate (Sigma-Aldrich) and 104 mM NaCl (Merck KGaA, Darmstadt, Germany) and was sterile filtered (Ø 0.22 μm, VWR International GmbH, Bruchsal, Germany) after preparation (storage temperature: room temperature). In this study, the commercially available bioink CellINK (CellINK AB, Gothenburg, Sweden) was used. The bioink was previously optimized towards printability and shape fidelity by adding nano-cellulose. [272–274] CellINK was stored at 8 $°C$. The cross-linking solution ($CaCl_2$) was purchased as part of the bioink kit from CellINK AB (CellINK AB) and stored at room temperature.

10.2.2 Software and data processing

The 3D Discovery^{TM} was controlled by the HMI (Human Machine Interface) Software (regenHU 3D Discovery 8.23.9.38, regenHU, Villaz-St-Pierre, Switzerland). G-code generation was done using a revised version of the 'Scaffold Designer' developed by *Ruiz-Cantu et al.* [282]. It was customized for the use of the regenHU print-head CF-300N in order to generate round scaffolds. The 'Scaffold Designer' was complemented by the use of a Matlab-based script to increase labware flexibility. The script enables use of 6-well plates by calculating the centre of the wells used and amplifying the scaffold g code. Excel 2013 (Microsoft, Redmond, USA) was used for data storage. Data evaluation and visualisation were performed with Matlab R2015a (The MathWorks, Inc., Natick, USA). BD LSR Fortessa Cell Analyzer was controlled by BD FACSDiva 8.0 (BD Biosciences, San Jose, USA). Flow cytometry data were analysed and visualised using Flow Jo V10 (Tree Star Inc., Ashland, USA).

10.2.3 Cell culture

The β-cell line INS-1E [198] was kindly provided by Prof. Maechler from the Department of Cell Physiology and Metabolism at the University of Geneva Medical Centre, Switzerland. Cell culture reagents were purchased from Thermo Fisher Scientific, unless stated otherwise. Cells were cultivated in RPMI 1640 with GlutaMAX supplemented with 10 % FBS, 1 % sodium pyruvate, 1 % Penicillin/Streptomycin, 10 mM HEPES, 2 mM L-Glutamine and 50 μM beta mercaptoethanol (Sigma-Aldrich) at 37 $°C$ in a humidified 5 % CO_2 incubator. The cell culture was split every 7 days to a concentration of 6.6 x 10^4 cells/cm^2, the medium was exchanged after 3 days.

10.2.4 Cell staining & fixation

Prior to cell staining with CellTrace^{TM} Violet (Thermo Fisher Scientific), cells were trypsinized. Staining was performed with a working concentration of 5 μM dye according to the manufacturer's instructions. The dye belongs to the group of carboxyfluorescein succinimidyl ester (CFSE)-like dyes which enables proliferation by dye dilution. [283, 284] For viability studies, cells were stained with 7-Aminoactinomycin D (7-AAD) (Biolegend, San Diego, USA) according to the manufacturer's instructions. It bedlongs to the group of DNA binding dyes which is excluded by live cells. The dead cell control sample was generated by heat treatment (70 $°C$, 10 min). Cell fixation was done for evaluating experiments by incubation of stained cells in fixation buffer (c = 1 x 10^6 cells/mL, 15 min, at room temperature). Fixed cells were stored at 8 $°C$ in storage buffer (c = 1 x 10^6 cells/mL) in the dark prior to use.

10.2.5 Flow cytometric analysis

Flow cytometry is a single cell analytic method that facilitates multivariate analysis depending on cell morphology and fluorescence staining. Briefly, cell samples are hydrodynamically focuse. Thus, single cells pass by laser beams, placed orthogonal to the sample stream. The light emitted from the sample is detected via optical filters and array of photo-detectors. Detected singe cell fluorescence signals are visualized as histogram or dot-plots when looking at two signals. [134] The analysis was performed using an LSR Fortessa by BD Bioscience

equipped with a BD^{TM} high-throughput sampler. Unless stated otherwise, flow cytometry analysis was performed using the high-throughput sampler in combination with 96-well U bottom plates (BD Falcon^{TM}, Franklin Lakes, USA). When using the high-throughput sampler, a defined sample volume of 100 μL was analysed and the following settings were applied: sample flow rate: 3 μL/s, sample volume: 100 μL, mixing volume: 100 μL, mixing speed: 250 μL/s, four mixing cycles and a wash volume of 800 μL.

10.2.6 Proliferation analysis

Cell proliferation was analysed in triplicates (biological triplicates; n = 3) with 5 μM CellTrace^{TM} Violet stained, and for control with unstained, cells in culture flasks with an area of 25 cm^2 for a period of 5 days. The cultivation was done according to the cell culture protocol. Both unstained and stained cells were trypsinized prior to analysis. Cell concentration was estimated by haemocytometer counting. Trypan blue dye exclusion was used to distinguish live/dead cells. Flow cytometry analysis was performed with CellTrace^{TM} Violet-stained cell samples (non-fixed), without the use of the high-throughput sampler. A validation culture (5 μM CellTraceTM Violet-stained cells, flask area = 175 cm^2, n = 1) was analysed after 3 days of cultivation.

10.2.7 3D Bioprinting

First, CellTrace^{TM} Violet-stained cells or beads were suspended in the CellInk bioink (CELLINK AB) using the CELLMIXER (CELLINK AB) until a final concentration of 5.7 x 10^6 cells/mL or 1.48 x 10^6 beads/mL (Count Bright^{TM} absolute counting beads, Thermo Fisher Scientific) was reached. When using fixed cells, 38 % of the cells were dead-stained using 7-AAD, while cell-free culture media was used as negative control.
3D printing was performed using a 3D Discovery system (regenHU Ltd.) enclosed in a sterile hood and equipped with a micro valve-based inkjet print-head (CF-300N), a pneumatically driven print-head for direct, time-pressure-dependent printing (DD-135N), a screw-driven extrusion deposition-based print-head (HM-300H), and a UV cross-linking unit (UV-365NM). Printing experiments were exclusively performed with the valve-based CF-300N print-head with a 300 μm diameter nozzle (inner diameter = 300 μm, external diameter = 500 μm, length = 2.4 mm) and a matching valve for direct dispensing (inner diameter = 300 μm, stroke = 100 μm). All removable parts of the CF-300N (inlet adapter with o-ring, luer-lock adapter, valve, and nozzle) were autoclaved (LSVA 40/60, ZIRBUS technology GmbH, Bad Grund, Germany) before utilisation. Round scaffolds of 9 mm in diameter and 4 horizontal and vertical lines (line spacing 2.25 mm) were printed up to a height of 3 mm directly into 6 well glass bottom plates (Cellvis, Mountain View, USA). Printing was performed with the following parameters: dosing distance: 0.05 mm, valve opening time: 1200 μs, valve closing time: 2000 μs, dispensing pressure: 0.029 - 0.034 MPa, printing speed: 11 mm/s. After printing, the scaffolds were incubated separately in 1 mL cross-linking solution (CELLINK AB) for 20 min at room temperature. Scaffolds were stored in 3 mL phosphate-buffered saline (Thermo Fisher Scientific) at 8 $^\circ C$ in the dark prior to use.
For flow cytometry analysis, scaffolds were cut into small pieces using a scalpel (VWR) and incubated in 4 mL de-gelating solution for 30 min at 37 $^\circ C$. After incubation, samples were

resuspended until no solid particles were visible. Samples containing non-fixed cells were, additionally, stained with 7-AAD for live/dead discrimination according to manufacturers instructions.

10.3 Results

We developed a flow cytometry-based analytical strategy as a tool for cell characterization in 3D bioprinting process development. This was done based on a model process using a commercially available, alginate-based bioink, the β-cell line INS-1E, and the direct dispensing method for 3D bioprinting **(fig. 10.1)**. Briefly, the cells were stained with CellTrace™ Violet dye and resuspended in bioink prior to printing. Due to the use of an alginate-based bioink, cross-linking of the alginate scaffolds was accomplished after printing by ionic gelation. Cell analysis was performed using a flow cytometry approach. Hence, de-gelation of the cell-laden scaffold was required prior to analysis. Use of the CellTrace™ Violet dye and 7-AAD staining facilitated cell proliferation and viability determination. Additionally, data deconvolution was done based on cell staining to eliminate bias caused by the bioink component. The selected commercially available and ready-to-use bioink had been optimised previously in terms of printability. In order to obtain a higher shape fidelity, nano-cellulose was added to the bioink as thickener. [272–274]

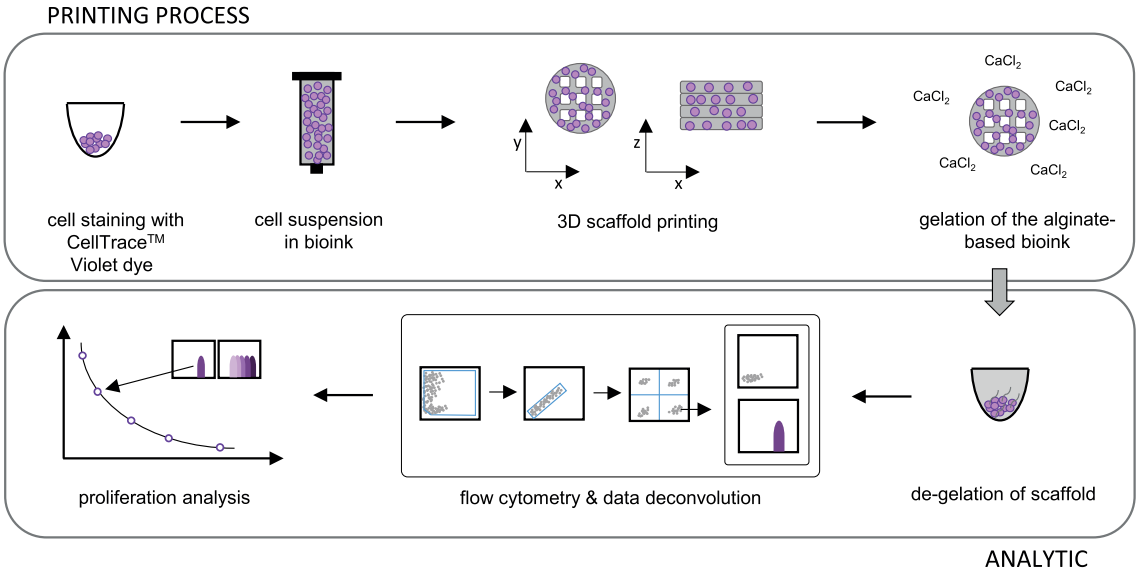

Figure 10.1: Overview of the process strategy used for the case study. INS-1E cells were stained with CellTrace™ Violet and suspended in an alginate-based bioink before 3D cell-laden scaffolds were printed. After printing, the alginate-based bioink was gelated using divalent cations in order to obtain scaffold stability. Cell analysis was performed using flow cytometry. First, scaffolds were de-gelated in order to obtain a cell suspension. After data deconvolution, cell proliferation and the live/dead ratio could be determined.

The nano-cellulose fibres are non-soluble by de-gelation and are, hence, present in de-gelated scaffolds samples **(fig. 10.2 A)**. A picture of a 3D-printed scaffold is shown in **fig. 10.2**

B. As can be seen in the light microscopy of a de-gelated scaffold **(fig. 10.2 A)** and the light microscopy image of trypsinized INS-1E cells **(fig. 10.2 C)**, the sizes of the fibres vary over a wide range and sometimes even correspond to the sizes of cells. For this reason, a gating strategy **(fig. 10.4)** was developed to eliminate the flow cytometry signals of the fibres.

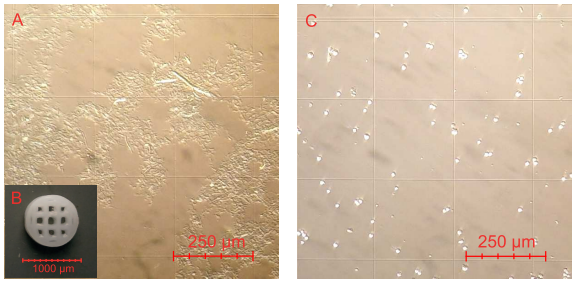

Figure 10.2: **A** Light microscopy image of a de-gelated cell-free scaffold. The 3D structure is completely dissolved except for the nano-cellulose fibres used as thickeners in the bioink. **B** Image of the 3D-printed scaffold with a diameter of 9 mm. **C** Light microscopy image of trypsinized INS-1E cells for size comparison.

The first part of the study was aimed at evaluating the CellTrace^{TM} Violet-based proliferation analysis for the cell line INS-1E. Unstained and stained cells were cultivated over a duration of 5 days. Every day, the cell density and the mode of the CellTrace^{TM} Violet-A signal were determined. As can be seen in **fig. 10.3 A**, the intensity of the CellTrace^{TM} Violet-A signal decreased over cultivation time. The mode of each intensity peak was determined using the software Flow Jo V10 (Tree Star) and plotted against cultivation days. The signal decreased exponentially over the cultivation time **(fig. 10.3 B)**. Data could be fitted to **eq. (10.1)** with $r^2 = 0.9874$.

$$y = a \times exp(b \times x) \tag{10.1}$$

Using the empirically determined equation, the duration of cultivation of a validation sample was determined correctly (day 3). In contrast to the decreasing signal intensity, cell density in both cultures increased over time **(fig. 10.3 C)**. The growth curve of the stained cells was lower than that of the unstained culture over the observed cultivation time. This was expected since cell staining represents cell stress. Still, the validation sample cell density matched the growth curve of the unstained culture.
Applying this CellTrace^{TM} Violet-based proliferation analysis to 3D bioprinted samples, however, requires data deconvolution to eliminate the flow cytometry signal of the fibres added to the bioink as thickener. The gating strategy for data deconvolution is shown in **fig. 10.4**. Single cells are gated for CellTrace^{TM} Violet staining and, based on a 7-AAD staining, into live/dead populations. The bioink component signal is located in the unstained-live gate, whereas the signal of the stained cells is located in either the stained-dead or stained-live gate. For the proliferation analysis, the 'stained -live' population is additionally displayed as histogram of the CellTrace^{TM} Violet signal.
The second part of the study was aimed at evaluating the developed flow cytometry strategy

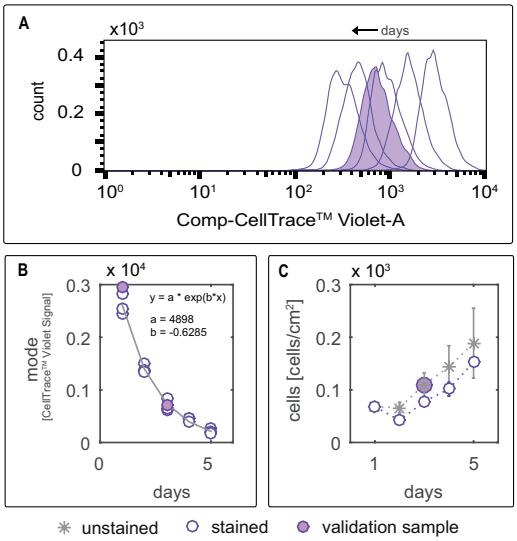

Figure 10.3: Proliferation analysis of CellTrace^{TM} Violet-stained cells using flow cytometry. **A** Histogram of the CellTrace^{TM} Violet signal of growth curve samples (day 1-5). Histograms without filling represent calibration samples and the histogram with filling the validation sample. Evaluation of the proliferation analysis: **B** mode of the CellTrace^{TM} Violet signal plotted over the cultivation time with exponential regression ($y = a \times \exp(b \times x)$). Fit parameters of the regression with 95 % prediction bounds (shown in parentheses) and r^2: a = 4898 (4444, 5352), b = -0.6285 (-0.6879, -0.5691), and $r^2 = 0.9874$ (n = 3, biological triplicate). Purple circles represent stained cell data and filled purple circles show data of stained validation samples. **C** Growth curve of unstained and CellTrace^{TM} Violet-stained cells over the cultivation of 5 days (n = 3, biological triplicate). Grey stars represent data points of unstained control cells. Purple circles represent stained cell data and filled purple circles show data of stained validation samples.

using two artificial test samples (fluorescence beads and fixed cells), since the influence of the process on the cells was unknown. Meaning, the analysed cell characterisitcs e.g viability or cell size could be altered by the printing process. For this reason, the artificial on-living test samples were used.
First, the strategy was evaluated with respect to HTS compatibility. Both validation test sets showed a linear correlation between total counts and stained (live & dead) counts over the calibration range of 5,000 - 150,000 total counts (n = 3; biological triplicate) with $r^2 = 0.9952$ for the bead test data set and $r^2 = 0.9757$ for the fixed cells data set. **(fig. 10.5)** The spillover of the bioink signal into the stained gates (populations: stained-live + tained-dead) was determined to be below 0.06 % over the calibration range from 5,000 - 150,000 counts (n = (3x3) 9 per calibration point (8-point calibration)). The spillover was determined by analyzing cell- and bead-free samples. Secondly, the influence of the printing process on beads and fixed cells was evaluated. In **fig. 10.6** the results after each process step are shown for both beads and fixed cells. On the **left** the results of the beads and on the **right** the results of the fixed cells test set. The control samples being **A** & **B**, **C** & **D** samples after suspension of beads or fixed cells, **E** & **F** after

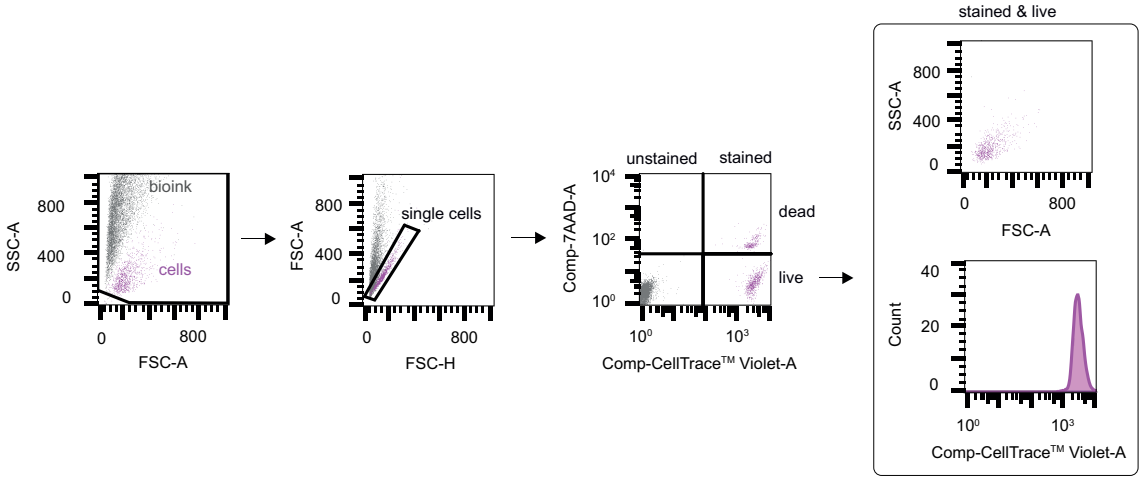

Figure 10.4: Deconvolution method for de-gelated cell-laden 3D printed scaffolds. Single cells are gated for CellTrace^{TM} Violet staining (stained) and divided into live/dead populations by 7-AAD staining. The bioink component signal is located in the unstained-live gate, whereas the signal of the stained cells is located in either the stained-dead or stained-live gate. For the proliferation analysis, the stained-live population is additionally displayed as histogram of the CellTrace^{TM} Violet signal and dot plot of the forward and sideward scatter. FSC-A: forward scatter peak area, SSC-A: side scatter peak area, FSC-H: forward scatter peak height.

printing, and **G** & **H** after gelation and de-gelation. The dot plot of single cells and the respective dot plot of the FSC-A and SSC-A signal for each sample are depicted (bead samples: stained-dead gate, fixed cell samples: stained-live gate). The location of the bead population (stained-dead) does not change in terms of the 7-AAD signal and CellTrace^{TM} Violet signal over all process steps. However, there is a tail of the bead population that extends towards the bioink population (unstained-live) after suspension of the beads in bioink **(fig. 10.6 C)** and after gelation and de-gelation **(fig. 10.6 G)**. The dot plot of the FSC-A and SSC-A signals of the bead population (stained-dead) indicates higher light scattering of the beads after all process steps. These findings correlate with the results of the fixed cell test data set, except for the change in the 7-AAD signal. The bioink population is located in the unstained-live gate after all process steps and the intensity of the CellTrace^{TM} Violet signal is not changed as a result of the process. Nevertheless, the live and dead populations merge more and more after each step, which is reflected by a change in the 7-AAD signal. When looking at the dot plot of the FSC-A and SSC-A signals of the stained and live cells, a higher increase of light scattering can be observed.

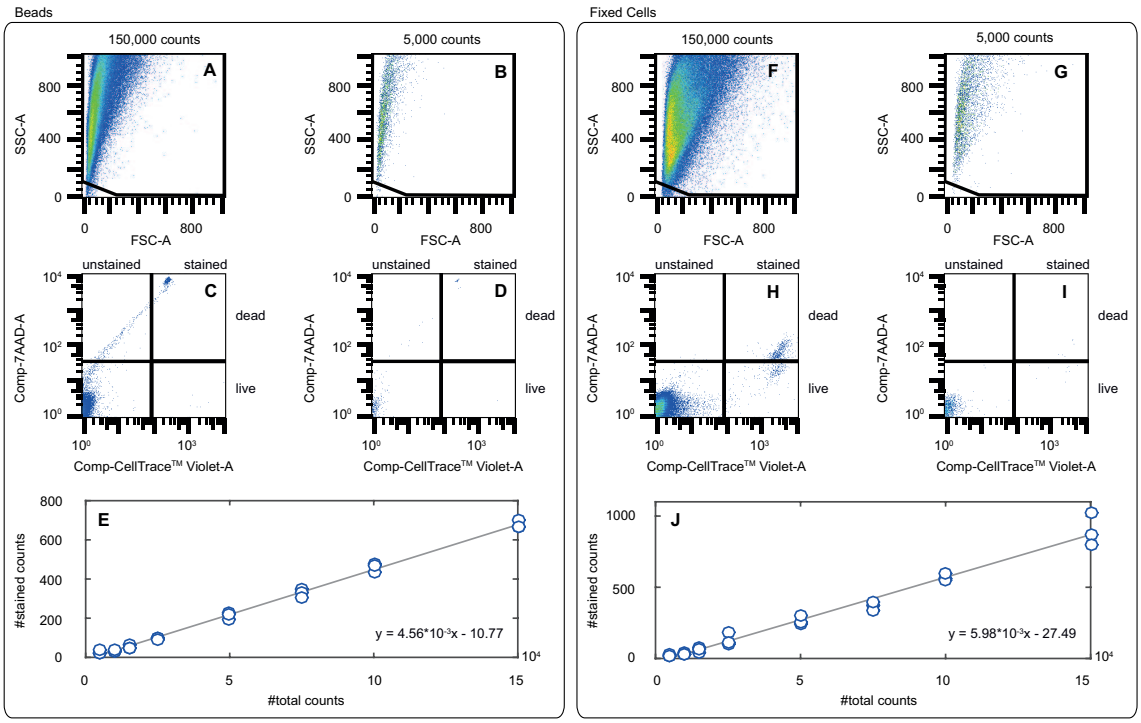

Figure 10.5: Evaluation of HTS flow cytometry for de-gelated 3D printed samples with beads and fixed cells over a range of 5,000 - 150,000 counts (8-point calibration with n = 3 per point). As an example of printed bead samples, the dot plots of the FSC-A and SSC-A, **A** for 150,000 and **B** for 5,000 counts, are shown. Additionally, the dot plots of the 7-AAD and CellTrace^{TM} Violet signals of the single bead population are shown for **C** 150,000 and **D** 5,000 counts. **E** Linear regression (y = ax+b) of stained counts (populations: stained-live + stained-dead) with bead-containing samples. Fit parameters of the regression with 95 % prediction bounds (shown in parentheses) and r^2: a = 0.004589 (0.004451, 0.004727), b = -10.77 (-20.71, -0.8225), and r^2 = 0.9952 (n = 3, biological triplicate). As an example of printed fixed cell samples, the dot plots of FSC-A and SSC-A are shown **F** for 150,000 and **G** for 5,000 counts. Additionally, the dot plots of the 7-AAD and CellTrace^{TM} Violet signals of the single cell population are shown for **H** 150,000 and **I** 5,000 counts. **J** Linear regression (y = ax+b) of stained counts (populations: stained-live + stained-dead) with fixed cell-containing samples. Fit parameters of the regression with 95 % prediction bounds (shown in parentheses) and r^2: a = 0.005979 (0.005562, 0.006396), b = -27.49 (-57.58, 2.598), and r^2 = 0.9757 (n = 3, biological triplicate). Additionally, the spillover of the bioink signal into the stained gates (populations: stained-live + stained-dead) was determined to be smaller than 0.06 % over the calibration space 5,000 - 150,000 counts (n = 9 per calibration point (8-point calibration)). FSC-A: forward scatter peak area, SSC-A: side scatter peak area.

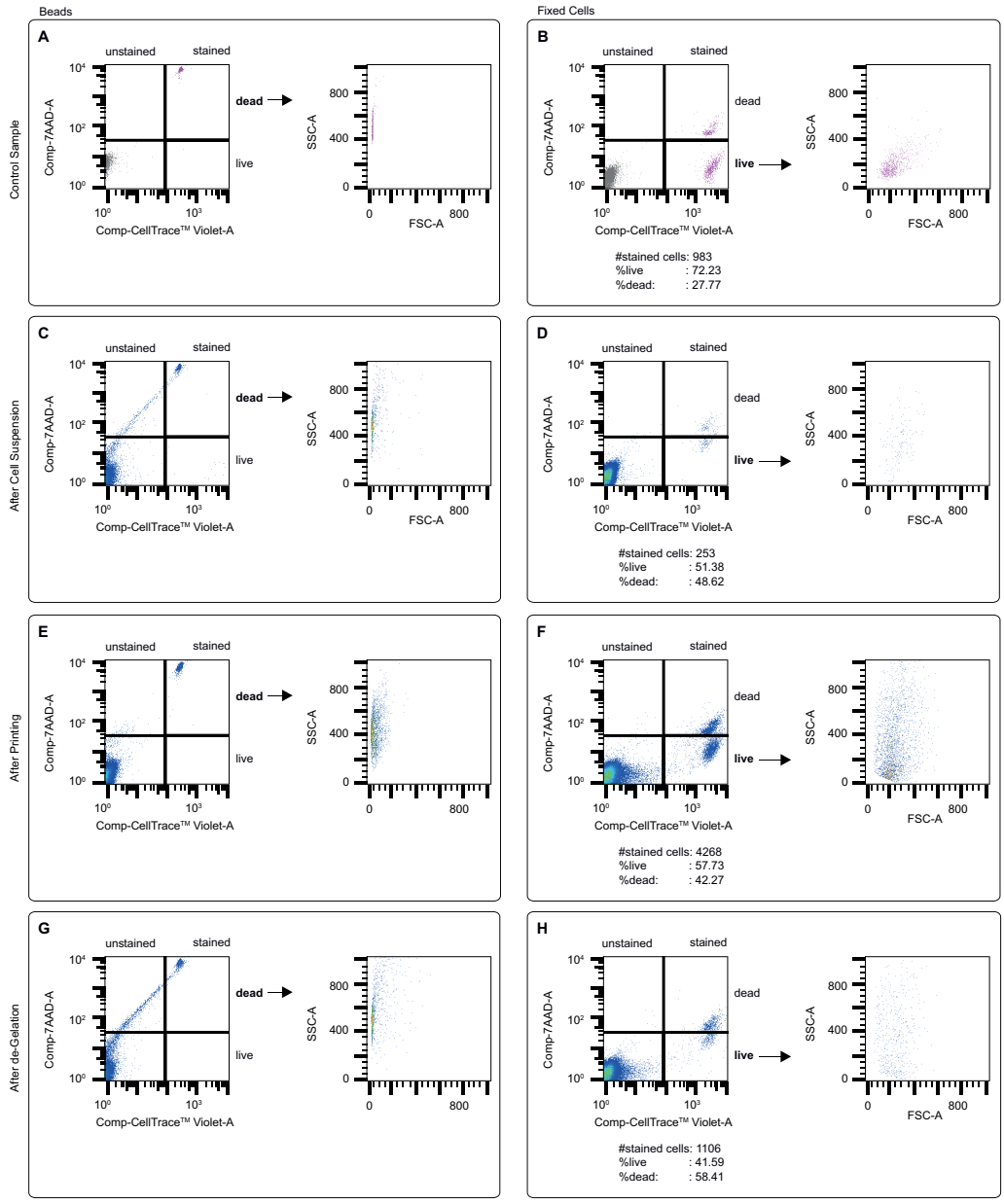

Figure 10.6: Evaluation of the influence of process steps on flow cytometry for de-gelated printed samples with beads and fixed cells. Shown is the dot plot of the 7-AAD signal and CellTrace^{TM} Violet signal of the single cell population with the corresponding dot plot of the FSC-A and SSC-A signal (bead samples: stained-dead population, fixed cell samples: stained-live population). **A** bead control sample, **B** fixed cell control sample, **C** bead sample after suspension in bioink, **D** fixed cell sample after suspension in bioink, **E** bead sample after printing, **F** fixed cell sample after printing, **G** bead sample after gelation and de-gelation, **H** fixed cell sample after gelation and de-gelation. FSC-A: forward scatter peak area, SSC-A: side scatter peak area.

In the third part of the study, the developed flow cytometry analysis strategy was used to evaluate the model printing process **(fig. 10.1)** for the β-cell line INS-1E (CellTrace^{TM} Violet stained). When using alginate-based bioink, cross-linking is achieved by ionic gelation with divalent cations after printing, which is reversible and can also be de-gelated via e.g. a citric acid buffer. First, the influence of the two process buffers, namely, cross-linking solution ($CaCl_2$) and de-gelating solution (50 mM trisodium citrate), on cell viability was evaluated. Cells were incubated in the solutions according to the process procedure. In **fig. 10.7** the dot plot of the 7-AAD signal and CellTrace^{TM} Violet signal of the single cell population is shown. Incubating cells in cross-linking solution for 20 min (RT) caused a viability loss of 34 % **(fig. 10.7 A)**. No viability loss was observed when cells were incubated for 30 min in de-gelating solution (37 $°C$) **(fig. 10.7 B)**. Viability loss was calculated in comparison to the PBS control. Additionally, the influence of each process

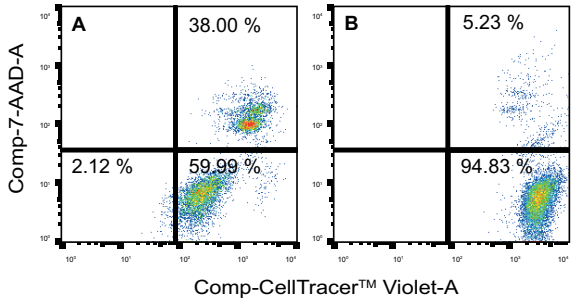

Figure 10.7: Evaluation of cross-linking for the alginate-based bioink using the INS-1E cell line. The dot plot of the 7-AAD signal and CellTrace^{TM} Violet signal of the single cell population is shown. The ratio of live and dead cells is indicated. A after 20 min incubation in cross-linking solution (RT) (live: 59.99 %, dead: 38.00 %), B after 30 min incubation in de-gelating solution (37 $°C$) (live: 94.83 %, dead: 5.23 %). Control sample in PBS (live: 94.22 %, dead: 5.84 %). RT: room temperature.

step (suspension in bioink, printing, gelation & de-gelation) on the INS-1E cells was screened. The screening results are shown in **fig. 10.8**. The dot plots of the single cell gate of the 7-AAD and CellTrace^{TM} Violet signals **(left)** and the dot plot of the SSC-A and CellTrace^{TM} Violet signals of the same gate **(right)** are depicted to obtain information about changes in light scattering. The data of the control sample **(fig. 10.8 A & B)** reveal three clearly separated populations for bioink (unstained-live gate), live-stained cells, and dead-stained cells. A time control sample was also measured to exclude any influence of process time on cell behavior, meaning a cell suspension aliquot was taken after cell harvest and kept under process conditions (room temperature) without any further processing until analysis. **(fig. 10.8 C & D)** The data show a minor loss of viability of 5.74 % due to process time, no changes in the CellTrace^{TM} Violet signal or light scattering were observed. However, no live cell population was detected after suspension of the cells in bioink, a shift of the dead cell population in the CellTrace^{TM} Violet signal was observed. The populations of the dead cells and the bioink signal are located closely to each other and not completely separated, as the CellTrace^{TM} Violet signal has decreased and the 7-AAD signal of the bioink component has shifted towards higher signal intensities. **(fig. 10.8 E)** This is also true for light scattering. Here **(fig. 10.8 F)**, two closely located populations are visible

with an increased light scattering tendency. These observations are also made for the samples after printing **(fig. 10.8 G & H)** and after gelation and de-gelation **(fig. 10.8 I & J)**. However, the shifting of the signal increase with every process step. In comparison, the bioink and cell signals are not shifted when analyzing fixed cell samples after gelation and de-gelation. **(fig. 10.8 K & L)** There is only a shift of the 7-AAD signal which leads to a merged live/dead population, as already mentioned **(fig. 10.6)**. Two completely separated populations for bioink and fixed cells can be seen, which also have a higher light scattering signal.

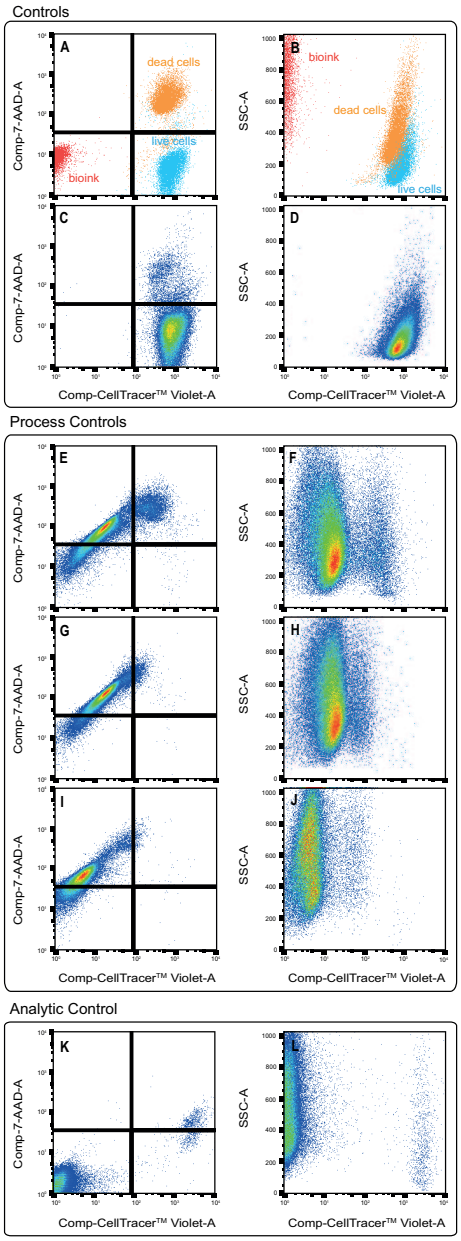

Figure 10.8: Influence of the printing process on the INS-1E cell line (CellTrace^{TM} Violet-stained). Dot plot of the 7-AAD signal and CellTrace^{TM} Violet signal of the single cell population **(left)** and the respective dot plot of the FSC-A and SSC-A signals of the same single cell population **(right)**. **A & B** control samples, **C & D** time control samples (meaning: a cell suspension aliquot was taken after cell harvest and kept under process conditions (temp.: room temperature) without any further processing until analysis) **E & F** after suspension in bioink, **G & H** after printing, **I & J** after gelation and de-gelation, **K & L** analytical control of fixed cells after gelation and de-gelation. FSC-A: forward scatter peak area, SSC-A: side scatter peak area.

10.4 Discussion

The aim of the present work was to develop a flow cytometry-based analytical strategy for use in high-throughput processes development for 3D cell printing applications. For this purpose, a case study was performed using the β-cell line INS-1E and a commercially available, alginate-based bioink. In addition, cell proliferation and the live/dead ratio of the printed cells were to be analysed in a high-throughput manner.
In the first part of the study, we evaluated the applicability of the proliferation analysis using the cell staining dye CellTrace^{TM} Violet. The dye belongs to the group of carboxyfluorescein succinimidyl ester (CFSE)-like dyes and enables proliferation analysis by fluorescence dye dilution and flow cytometry. [283, 284] It has been widely used for proliferation analysis [285–287] and performed great concerning tolerance, brightness of cell labelling, and uniformity. Performance, however, can differ for each cell line [288]. The data obtained for the model cell line INS-1E demonstrated suitability of this proliferation analysis method as part of a flow cytometry-based analytical strategy. The model cell line INS-1E showed an exponential decrease in the mode of the CellTrace^{TM} Violet signal over 5 days of cultivation. Stained cells showed lower cell densities over time, although a validation test sample was determined correctly. Additionally, CellTrace^{TM} Violet staining was found to allow for the elimination of the solid bioink component signal by applying a gating strategy **(fig. 10.4)**. This signal elimination is crucial when de-gelated, cell-laden 3D printing samples are analysed, since the fraction of solid bioink components is much higher than that of the cells in the de-gelated sample.
For 3D cell printing process development, a systematic approach is highly recommended to obtain reproducible and robust results with high cell viability rates. Hence, a high-throughput approach is favourable. It was demonstrated earlier that high-throughput flow cytometry is an excellent tool in downstream process development, even if the instrument is not equipped with precision pumps [60].
In the second part of this study, we evaluated if this is also true for 3D cell printing process development. For this purpose, we used test samples to exclude the process influence on living cells. Fluorescence beads with a diameter of approximately 7 μm, showing a bright fluorescence signal in both channels (CellTrace^{TM} Violet & 7-AAD), were used as test sample with only one population. To increase the test samples' complexity, fixed cells with 38 % dead cell population were used. The results of both test samples demonstrated the suitability of the method for high-throughput applications, since a low spillover of the bioink signal in the cell gates was observed and a linear correlation between stained counts and total counts was shown. The linear correlation enables the opportunity to implement cell quantification using flow cytometry in future studies, as previously demonstrated. [128]
Additionally, we evaluated the process influence using both test samples. The beads showed no signal shift in both channels and only a slight increase in light scattering, which indicated no influence of the process steps on the beads. The results of the fixed cell samples, however, reflected an influence of the process on the fixed cells. The FSC/SSC pattern of the process samples deviated from that of the control sample **(fig. 10.6)**. Furthermore, a shift of the 7-AAD signal for the live, fixed cell population was observed. Signal intensity increased with every process step until the printing sample exhibited a completely merged live and

dead population **(fig. 10.6 H)**. We assume that this signal shift is related to the process, since the control sample shows two separate populations for live and dead cells. Briefly, 7-AAD staining is normally not suitable for cell fixation since the procedure compromises the cell membrane leading to dye uptake by "living" cells. However, the short timescales in the present study meant that no dye uptake by "living" cells was displayed by our control samples. This indicates that the suspension and printing process were responsible for enhanced 7-AAD uptake, potentially due to mechanical stress. In further experiments, actinomycin D should be added to the samples to prevent 7-AAD leaking in fixed cell samples. [289]

In the third part of this study, we used the developed flow cytometry-based strategy to investigate the influence of each process step (suspension of cells in bioink, 3D printing, and cross-linking) on the model β-cell line INS-1E. Our data revealed a drastic decrease of cell viability, whereas the time control showed no viability loss. Additionally, a decrease in the CellTrace^{TM} Violet signal of the cell population and a change in the FSC/SSC pattern were observed. These features were not found in the dead cell control sample **(fig. 10.8 A & B)**, where only a slight change of the FSC/SSC pattern and no shift in the CellTrace^{TM} Violet signal were observed. We assume that a leakage of CellTrace^{TM} Violet-labelled proteins and an additional adsorption of these proteins by the soluble bioink components occurred. The same signal shifts were seen for the samples after printing **(fig. 10.8 G & H)** and after gelation and de-gelation **(fig. 10.8 I & J)**. Additionally, buffer evaluation showed that the used de-gelating solution has no influence on cell viability, while incubating cells in cross-linking solution causes a 34 % loss in cell viability **(fig. 10.7)**.

In summary, the data of the case study reflect a strong need for process optimization when using the model β-cell line INS-1E and a commercially available bioink. Using the knowledge, gatheres during the present work, will assist future work immensely. In order to make it assecible, the findings of the current research are summarized in **table 10.1**. Thus, it can be used as a guidance for future cell printing studies. Here, different options for process optimization are listed with their potential relationships and the potential influence on critical parameter. The critical parameters are further divided into critical process related parameters and critical cell parameters, which can be measured via the developed flow cytometry-based tool. Although the influence between parameters will vary for different applications, this table gives an indication of where the most important dependencies exist. In the present proof of concept study, the process strategy **(fig. 10.1)** was meant to be simple and easy to implement. For this reason, a commercially available bioink, optimized for printing without the need of a sacrificial material, was chosen. What became apparent, however, is that the overriding critical process parameter (CPP) is cell viability in respect to the different additives and bioink, as well as mechanical stress during printing. When looking at the data for the suspension of the cells in bioink, it is unclear whether the viability loss and change in the CellTrace^{TM} Violet signal are caused by the mechanical stress of the mixing process or by the contact with the bioink itself. This needs to be addressed by further investigations that are to include a toxicity study of the bioink, followed by an evaluation of the mixing process. Several static mixer designs are to be evaluated with respect to mechanical stress. Moreover, the cross-linking strategy should be optimized. In this study we used the cross-linking solution delivered with the commercial

bioink. The alginate-based bioink is cross-linked by ionic gelation using calcium chloride. The incubation with the cross-linking solution causes a viability loss and also calcium is involved in the insulin secretion of β-cells [198]. Hence, it should be replaced by other divalent cations. Alginate can be gelated using other divalent cations which, however, might change the hydrogel properties that can influence cell proliferation within the 3D printed scaffolds. [290–293] This highlights the need of a systematical screening for crosslinking divalent cations. The developed analytical strategy can be used to optimize hydrogel crosslinking by performing a simple toxicity test with different cations, in combination with post-printing cell proliferation analysis. Using the same analytical method for early studies e.g. the toxicity test and post-printing studies e.g. proliferation analysis is also an advantage and might lead to a deeper process knowledge.

Table 10.1: Matrix of influencing Critical Process Parameters (CPP)*

			Critical Process Related Parameters		Critical Cell Parameters	
	Options	**Interrelations**	**Print Integrity**	**Process Complexity**	**Cell Viability**	**Cell Proliferation**
3D printing strategy	3D printing techology	bioink	+++	±	+++ cell stress	±
	sacrificial material	printing method, object geometry	+++	+++ additional process step for removal	± cell toxicity	± cell toxicity
	object geometry	printing method, bioink & sacrificial material	± printer resolution etc.	±	±	± oxygen/nutrient supply
Material	bioink	printing method & cell line	+++	±	+++ cell toxicity	+++ bioink post-processing behaviour
	crosslinking	printing method & bioink	+++	additional process step	± cell toxicity	+++ bioink post-processing behaviour
Cell Culture	cell line	dependent on tissue which should be mimicked & bioink	+++ acceptable mech. stress	±	+++	+++
	cell load	cell culture & cell mixing	± bioink viscosity/density	±	±	+++
	cell mixing	cells in bioink or cell growth on object surface	± bioink viscosity/density	addittional process step	+++ shear stress	+++ growth behaviour
	cell staining	as part of analytical strategy	-	additional process step	± cell-specific optimization	± cell growth rate

* based on experience gained from current work

+++ huge impact; ± might have an influence; - little influence

10.5 Conclusion

A flow cytometry-based analytical strategy for 3D bioprinting process development was developed. The strategy was validated using a model process with the β-cell line INS-1E, an alginate-based, commercially available bioink, and a direct dispensing 3D bioprinter. Flow cytometry represents a destructive analysis method in the field of 3D bioprinting. For this reason, de-gelation using citric acid was performed to dissolve the cell-laden 3D alginate scaffolds. The de-gelating solution was found to have no effect on cell viability.
The developed strategy enables a CellTrace^{TM} Violet-based cell proliferation analysis and a 7-AAD-based live/dead recognition. Data deconvolution was done to eliminate the bias caused by fibers added to the commercially available bioink as thickener. Use of an automated sampler was found to enable high-throughput analysis. The strategy was validated using two artificial test samples, namely, fluorescence beads and fixed cells. No process influence on bead signals was observed, whereas a 7-AAD und SSC-A signal shift was detected for fixed cells. Additionally, process influence on the β-model cell line INS-1E was evaluated using the flow cytometry-based strategy developed. The data indicated a major process influence on cell viability. Further optimisation of the 3D bioprinting process is necessary.
A systematic approach to 3D printing process development is highly recommended to obtain reproducible and robust results with high cell viability rates. It would also be favourable to apply the same analytical method in all process development stages, from early phase of bioink cross-linking evaluation to the late stage, where the cells post-printing behaviour in culture needs to be analysed. We consider flow cytometry to be a powerful tool to study global process influence on cell characteristics. For detailed structural analyzis of the 3D printed objects, an microscopic approach as orthogonal method must be implemented in addition. However, flow cytometry allows for the specific development of a 3D bioprinting process, in particular when complex cell characterisation of e.g. in case of printed stem cells or simultaneous printed multiple cell lines is needed in a high-throughput manner.

Acknowledgements

We thank Professor Hartwig and co-workers from the Food Chemistry and Toxicology Group and Professor Franzreb and co-workers from the Institute of Functional Interfaces of the Karlsruhe Institute of Technology (KIT) for sharing their labs and equipment. We would also like to thank Professor Maechler from the Department of Cell Physiology and Metabolism of the University of Geneva Medical Centre, Switzerland, for providing the rat beta-cell line INS-1E. Finally, we acknowledge Stefanie Limbrunner (KIT) and Saskia Kraus (KIT) for excellent technical assistance.

Funding sources

This work was supported by the Helmholtz Program "BioInterfaces in Technology and Medicine (BIFTM)."

Conflicts of interests

The authors have no conflicts to declare.

10.6 References

16. N. M. Mount, S. J. Ward, P. Kefalas, and J. Hyllner: 'Cell-based therapy technology classifications and translational challenges'. *Philos Trans R Soc Lond B Biol Sci.* (2015), vol. 370: p. 20150017.

27. J. Carmen, S. R. Burger, M. McCaman, and J. A. Rowley: 'Developing assays to address identity, potency, purity and safety: cell characterization in cell therapy process development'. *Regenerative Medicine* (2012), vol. 7(1): pp. 85–100.

60. S. Zimmermann, S. Gretzinger, M.-L. Schwab, C. Scheeder, P. K. Zimmermann, S. A. Oelmeier, E. Gottwald, A. Bogsnes, M. Hansson, A. Staby, and J. Hubbuch: 'High-throughput downstream process development for cell-based products using aqueous two-phase systems'. *Journal of Chromatography A* (2016), vol. 1464: pp. 1–11.

103. J. Groll et al.: 'Biofabrication: reappraising the definition of an evolving field'. *Biofabrication* (2016), vol. 8(1): p. 013001.

104. V. Mironov, T. Trusk, V. Kasyanov, S. Little, R. Swaja, and R. Markwald: 'Biofabrication: a 21st century manufacturing paradigm'. *Biofabrication* (2009), vol. 1(2): p. 022001.

105. S. H. Huang, P. Liu, A. Mokasdar, and L. Hou: 'Additive manufacturing and its societal impact: a literature review'. *The International Journal of Advanced Manufacturing Technology* (2013), vol. 67(5): pp. 1191–1203.

106. A. Atala and J. J. Yoo: 'Essentials of 3D Biofabrication and Translation'. Boston: Academic Press, Inc., 2015.

107. L. A. L. Fliervoet and E. Mastrobattista: 'Drug delivery with living cells'. *Advanced Drug Delivery Reviews* (2016), vol. 106: pp. 63–72.

109. J. Malda, J. Visser, F. P. Melchels, T. Jüngst, W. E. Hennink, W. J. A. Dhert, J. Groll, and D. W. Hutmacher: '25th Anniversary Article: Engineering Hydrogels for Biofabrication'. *Advanced Materials* (2013), vol. 25(36): pp. 5011–5028.

110. T. J. Hinton, Q. Jalleratn, R. N. Palchesko, J. H. Park, M. S. Grodzicki, H.-J. Shuen, M. H. Ramadan, A. R. Hudson, and A. W. Feinberg: 'Three-dimensional printing of complex biological structures by freeform reversible embedding of suspended hydrogels'. *Science Advances* (2015), vol. 1(9).

111. K. Arcaute, B. K. Mann, and R. B. Wicke: 'Stereolithography of Three-Dimensional Bioactive Poly(Ethylene Glycol) Constructs with Encapsulated Cells'. *Annals of Biomedical Engineering* (2006), vol. 34(9): pp. 1429–1441.

112. R. R.Jose, M. J. Rodriguez, T. A. Dixon, F. Omenetto, and D. L. Kaplan: 'Evolution of Bioinks and Additive Manufacturing Technologies for 3D Bioprinting'. *ACS Biomaterials Science & Engineering* (2016), vol. 2(10): pp. 1662–1678.

113. T. Billiet, M. Vandenhaute, J. Schelfhout, S. Van Vlierberghe, and P. Dubruel: 'A review of trends and limitations in hydrogel-rapid prototyping for tissue engineering'. *Biomaterials* (2012), vol. 33(26): pp. 6020–6041.

114. J. Song and J. R. Millman: 'Economic 3D-printing approach for transplantation of human stem cell-derived β-like cells'. *Biofabrication* (2016), vol. 9(1): p. 015002.

115. R. M. Costa, S. Rauf, and C. A. E. Hauser: 'Towards biologically relevant synthetic designer matrices in 3D bioprinting for tissue engineering and regenerative medicine'. *Current Opinion in Biomedical Engineering* (2017), vol. 2: pp. 90–98.

116. J. G. Hunsberger, S. Goel, J. Allickson, and A. Atala: 'Five Critical Areas that Combat High Costs and Prolonged Development Times for Regenerative Medicine Manufacturing'. *Current Stem Cell Reports* (2017), vol. 3(2): pp. 77–82.

117. J. Visser, B. Peters, T. J. Burger, J. Boomstra, W. J. A. Dhert, F. P. W. Melchels, and J. Malda: 'Biofabrication of multi-material anatomically shaped tissue constructs'. *Biofabrication* (2013), vol. 5(3): p. 035007.

118. J. G. Torres-Rendon, M. Köpf, D. Gehlen, A. Blaeser, H. Fischer, L. De Laporte, and A. Walther: 'Cellulose Nanofibril Hydrogel Tubes as Sacrificial Templates for Freestanding Tubular Cell Constructs'. *Biomacromolecules* (2016), vol. 17(3): pp. 905–913.

128. S. Zimmermann, S. Gretzinger, C. Scheeder, M.L. Schwab, S. A. Oelmeier, A. Osberghaus, E. Gottwald, and J. Hubbuch: 'Highthroughput cell quantification assays for use in cell purification development enabling technologies for cell production'. *Biotechnology Journal* (2016), vol. 11(5): pp. 676–686.

134. S. F. Ibrahim and G. van den Engh: 'Flow Cytometry and Cell Sorting'. *Cell Separation: Fundamentals, Analytical and Preparative Methods*. Ed. by A. Kumar, I. Y. Galaev, and B. Mattiasson. Berlin, Heidelberg: Springer Berlin Heidelberg, 2007: pp. 19–39.

136. S. Desbordes, D. Placantonakis, A. Ciro, N. D. Socc, Gabsang Lee, H.Djaballah, and L. Studer: 'High-Throughput Screening Assay for the Identification of Compounds Regulating Self-Renewal and Differentiation in Human Embryonic Stem Cells'. *Cell stem cell* (2008), vol. 2: pp. 602–12.

137. Y. Mei, M. Goldberg, and D. Anderson: 'The development of high-throughput screening approaches for stem cell engineering'. *Current Opinion in Chemical Biology* (2007), vol. 11(4): pp. 388–393.

140. R. Macarron, M. N. Banks, D. Bojanic, D. J. Burns, D. A. Cirovic, T. Garyantes, D. V. S. Green, R. P. Hertzberg, W. P. Janzen, J. W. Paslay, U. Schopfer, and G. Sittampalam: 'Impact of high-throughput screening in biomedical research'. *Nature reviews. Drug discovery* (2011), vol. 10: pp. 188–195.

141. L. M. Mayr and D. Bojanic: 'Novel trends in high-throughput screening'. *Current Opinion in Pharmacology* (2009), vol. 9(5): pp. 580–588.

143. R. P. Hertzberg and A. J. Pope: 'High-throughput screening: new technology for the 21st century'. *Current Opinion in Chemical Biology* (2000), vol. 4(4): pp. 445–451.

144. P. Jones, S. McElroy, A. Morrison, and A. Pannifer: 'The importance of triaging in determining the quality of output from high-throughput screening'. *Future Medicinal Chemistry* (2015), vol. 7(14): pp. 1847–1852.

149. K.ł M. cki: 'High throughput process development in biomanufacturing'. *Current Opinion in Chemical Engineering* (2014), vol. 6: pp. 25–32.

198. A .Merglen, S. Theander, B. Rubi, G. Chaffard, C. B. Wollheim, and P. Maechler: 'Glucose Sensitivity and Metabolism-Secretion Coupling Studied during Two-Year Continuous Culture in INS-1E Insulinoma Cells'. *Endocrinology* (2004), vol. 145(2): pp. 667–678.

200. S. Zimmermann, C. Scheeder, P. K. Zimmermann, A. Bogsnes, M. Hansson, A. Staby, and J. Hubbuch: 'Highthroughput downstream process development for cellbased products using aqueous twophase systems (ATPS) A case study'. *Biotechnology Journal* (2017), vol. 12(2): p. 1600587.

267. X. Ma, X. Qu, W. Zhu, Y.-S. Li, S. Yuan, H. Zhang, J. Liu, P. Wang, C. S. E. Lai, F. Zanella, G.-S. Feng, F. Sheikh, S. Chien, and S. Chen: 'Deterministically patterned biomimetic human iPSC-derived hepatic model via rapid 3D bioprinting'. *PNAS* (2016), vol. 113(8): pp. 2206–2211.

268. Y. Zhao, R. Yao, L. Ouyang, H. Ding, T. Zhang, K. Zhang, S. Cheng, and W. Sun: 'Three-dimensional printing of Hela cells for cervical tumor model in vitro'. *Biofabrication* (2014), vol. 6(3): p. 035001.

269. X. Cui, K. Breitenkamp, M. G. Finn, and D. D. DLima M. Lot and: 'Direct Human Cartilage Repair Using Three-Dimensional Bioprinting Technology'. *Tissue Eng. Part A* (2012), vol. 18: pp. 1304–1312.

270. J. M. Lee and W. Y. Yeong: 'Design and Printing Strategies in 3D Bioprinting of CellHydrogels: A Review'. *Advanced Healthcare Materials* (2016), vol. 5(22): pp. 2856–2865.

271. J. Jia, D. J. Richards, S. Pollard, Y. Tan, J. Rodriguez, R. P. Visconti, T. C. Trusk, M. J. Yost, H. Yao, R. R. Markwald, and Y. Mei: 'Engineering alginate as bioink for bioprinting'. *Acta Biomaterialia* (2014), vol. 10(10): pp. 4323–4331.

272. H. Martínez Ávila, S. Schwarz, N. Rotter, and P. Gatenholm: '3D bioprinting of human chondrocyte-laden nanocellulose hydrogels for patient-specific auricular cartilage regeneration'. *Bioprinting* (2016), vol. 1-2: pp. 22–35.

273. K. Markstedt, A. Mantas, I. Tournier, H. Martínez Ávila, D. Hägg, and P. Gatenholm: '3D Bioprinting Human Chondrocytes with Nanocellulose-Alginate Bioink for Cartilage Tissue Engineering Applications'. *Biomacromolecules* (2015), vol. 16(5): pp. 1489–1496.

274. M. Müller, E. Öztürk, Ø. Arlov, P. Gatenholm, and M. Zenobi-Wong: 'Alginate Sulfate–Nanocellulose Bioinks for Cartilage Bioprinting Applications'. *Annals of Biomedical Engineering* (2017), vol. 45(1): pp. 210–223.

275. J. H. Y. Chung, S. Naficy, Z. Yue, R. Kapsa, A. Quigley, S. E. Moulton, and G. G. Wallace: 'Bio-ink properties and printability for extrusion printing living cells'. *Biomater. Sci.* (7 2013), vol. 1: pp. 763–773.

276. S. V. Murphy, A. Skardal, and A. Atala: 'Evaluation of hydrogels for bioprinting applications'. *Journal of Biomedical Materials Research Part A* (2013), vol. 101 A(1): pp. 272–284.

277. K. Nair, M. Gandhi, S. Khalil, K. Chang Yan, M. Marcolongo, K. Barbee, and W. Sun: 'Characterization of cell viability during bioprinting processes'. *Biotechnology Journal* (2009), vol. 4(8): pp. 1168–1177.

278. M. Neufurth, X. Wang, H. C. Schröder, Q. Feng, B. Diehl-Seifert, T. Ziebart, R. Steffen, S. Wang, and W. E.G. Müller: 'Engineering a morphogenetically active hydrogel for bioprinting of bioartificial tissue derived from human osteoblast-like SaOS-2 cells'. *Biomaterials* (2014), vol. 35(31): pp. 8810–8819.

279. Y. Yu, Y. Zhang, and J. A. Martin amd I. T. Ozbolat: 'Evaluation of Cell Viability and Functionality in Vessel-like Bioprintable Cell-Laden Tubular Channels'. *ASME. J Biomech Eng.* (2013), vol. 153(9): pp. 091011-091011-9.

280. K. W. Ng, D. T.W. Leong, and D. W. Hutmacher: 'The Challenge to Measure Cell Proliferation in Two and Three Dimensions'. *Tissue Engineering* (2005), vol. 11(1-2): pp. 182–191.

281. G. Marchioli, L. van Gurp, P. P. van Krieken, D. Stamatialis, M. Engelse, C. A. van Blitterswijk, M. B. J. Karperien, E. de Koning, J. Alblas, L. Moroni, and A. A. van Apeldoorn: 'Fabrication of three-dimensional bioplotted hydrogel scaffolds for islets of Langerhans transplantation'. *Biofabrication* (2015), vol. 7(2): p. 025009.

282. L. Ruiz-Cantu, A. Gleadall, C. Faris, J. Segal, K. Shakesheff, and J. Yang: 'Characterisation of the surface structure of 3D printed scaffolds for cell infiltration and surgical suturing'. *Biofabrication* (2016), vol. 8(1): p. 015016.

283. *User Guide: CellTrace^{TM} Cell Proliferation Kits.* https://www.thermofisher.com/order/catalog/product/C34557. accessed September 25, 2017.

284. J. Begum, W. Day, C. Henderson, S. Purewal, J. Cerveira, H. Summers, P. Rees, D. Davies, and A. Filby: 'A method for evaluating the use of fluorescent dyes to track proliferation in cell lines by dye dilution'. *Cytometry Part A* (2013), vol. 83(12): pp. 1085–1095.

285. B. J. C. Quah and C. R. Parish: 'New and improved methods for measuring lymphocyte proliferation in vitro and in vivo using CFSE-like fluorescent dyes'. *Journal of Immunological Methods* (2012), vol. 379(1): pp. 1–14.

286. A. Filby, E. Perucha, H. Summers, P. Rees, P. Chana, S. Heck, G. M. Lord, and D. Davies: 'An imaging flow cytometric method for measuring cell division history and molecular symmetry during mitosis'. *Cytometry Part A* (2011), vol. 79(7): pp. 496–506.

287. O. Thaunat, A. G. Granja, P. Barral, A. Filby, B. Montaner, L. Collinson, N. Martinez-Martin, N. E. Harwood, A. Bruckbauer, and F. D. Batista: 'Asymmetric Segregation of Polarized Antigen on B Cell Division Shapes Presentation Capacity'. *Science* (2012), vol. 335(6067): pp. 475–479.

288. A. Filby, J. Begum, M. Jalal, and W. Day: 'Appraising the suitability of succinimidyl and lipophilic fluorescent dyes to track proliferation in non-quiescent cells by dye dilution'. *Methods* (2015), vol. 82. Flow Cytometry Methods and Approaches: pp. 29–37.

289. I. Schmid, C. H. Uittenbogaart, B. Keld, and J. V. Giorgi: 'A rapid method for measuring apoptosis and dual-color immunofluorescence by single laser flow cytometry'. *Journal of Immunological Methods* (1994), vol. 170(2): pp. 145–157.

290. S.K. Bajpai and S. Sharma: 'Investigation of swelling/degradation behaviour of alginate beads crosslinked with Ca^{2+} and Ba^{2+} ions'. *Reactive and Functional Polymers* (2004), vol. 59(2): pp. 129–140.

291. Y. Mørch, I. Donati, B. Strand, and G. Skjåk-Bræk: 'Effect of Ca^{2+}, Ba^{2+}, and Sr^{2+} on Alginate Microbeads'. *Biomacromolecules* (2006), vol. 7: pp. 1471–80.

292. P. Agulhon, V. Markova, M. Robitzer, F. Quignard, and T. Mineva: 'Structure of Alginate Gels: Interaction of Diuronate Units with Divalent Cations from Density Functional Calculations'. *Biomacromolecules* (2012), vol. 13: pp. 1899–907.

293. B. A. Harper, S. Barbut, L.T. Lim, and M. F. Marcone: 'Effect of Various Gelling Cations on the Physical Properties of "Wet" Alginate Films'. *Journal of Food Science* (2014), vol. 79(4): E562–E567.

CHAPTER 11

Conclusion & Outlook

Translating cell-based therapeutics from academia towards a commercial/clinical application still represents a challenging and interdisciplinary task. The focus of this doctoral thesis was the development and implementation of process development tools, contributing to a more directed and systematic process development approach. Using such tools would be highly beneficial in order to tackle a major obstacle of this therapeutic class: the inherent complexity of living cells in combination with the limited experience/process knowledge. In order to demonstrate the power, applicability and variety of process development tools for cell-based therapeutics, this thesis covered several unit operations. The first part of the thesis focused on the unit operation cell separation, while the second part focused on cell formulation unit operations, namely, cell cryopreservation and bioprinting.

The first part of this thesis covered the unit operation cell separation. Here, a previously developed HTS platform was used to investigate the influence of the critical parameter TLL and molecular weight on cell partitioning in PEG-dextran ATPS buffered with NaPi. First, a cell barcoding strategy was implemented enabling a fast and multiplex cell analysis. Subsequently, a case study was performed with five model cell lines showing that ATPS containing low PEG molecular weights and high dextran molecular weights facilitate high cell line resolution. Hence, the presented case study demonstrated the applicability of the HTS platform in combination with CCD-modeling for the investigation of cell partitioning in ATPS, which strongly indicates the usefulness of this approach as cell downstream processing development tool allowing for a systematic and directed screening. However, clinically relevant cell populations might be more complex which highlights the need for comprehensive screenings.

Furthermore, a technology transfer was performed based on a case study using the model cell line HL-60. A process set up, allowing for the investigation of cell partitioning in ATPS in a microfluidic flow-through mode, was successfully developed. The development was done within the DMAIC framework using additive manufacturing technologies as tool for the fast, cheap and easy realization of tailored equipment complementing standard laboratory equipment. Using only inexpensive bench top 3D printer and service contractors, the development of the microfluidic process set up with integrated video-based analysis could be realized with low investment. Additionally, a root-cause investigation was performed to evaluate parameter, causing poor microfluidic process performance in comparison to the batch HTS data. On that basis, two main factors were identified: (1) fluctuating cell number due to cell sedimentation and aggregation in tubing; (2) decreased cell viability in dependence to fluid velocity which also had a negative influence on cell

partitioning behavior. In general, the presented case study approved the usage of 3D printing technologies as effective process development tools, shortening development time line while simultaneously increasing creativity in process setup when combined with a structuring approach like the DMAIC framework.
The second part of this thesis was centered around cell formulation unit operations. First, a video-based tool was developed allowing for the characterization of the critical cryopreservation process parameter freezing and thawing behavior. The tool performance was successfully confirmed by a cryopreservation scale up study from 1 to 2 mL working volume. Using the tool, a delay in freezing and thawing behavior due to working volume increase was detected which is in good agreement with literature. Additionally, a conventional cryopreservation, monitoring cell viability and proliferation, was performed highlighting the need for optimization since the 2 mL samples with a delayed freezing behavior showed poor survival and proliferation rates. Thus, the integration of the developed tool would be highly beneficial for cryopreservation process development for cell-based therapeutics allowing for a systematic screening. It would also contribute to the intended QbD approach since it also generate deeper process knowledge.
Subsequently, the developed video-based tool was implemented in a predictive tool box enabling the prediction of media process performance for cell cryopreservation by characterization of media properties, freezing/thawing behavior and cell response to cryomedia exposure (toxicity). Screening for alternative cryomedia formulations (without any toxic or animal-derived components) is essential for cell-based therapeutics since it needs to be in accordance with GMP requirements. A case study was conducted aiming at the evaluation of the applicability of two commercial DMSO-free cryomedia for the β-model cell line INS-1E. Additionally, the cryomedia screening included a positive control (DMSO containing cryomedia) and a negative control (without any cryoprotectant). Applying the tool box in combination with process knowledge of the positive and negative control, the commercial available cryomedia Biofreeze® media was classified as media with inferior performance. The second commercial available cryomedia CryoSOfree™ was, at the same time, identified as possible candidate for the β-model cell line INS-1E. These findings highlight the need for a systematic screening for effective cryomedia formulation for each cell application. While the tool box needs to be evaluated more closely in a comprehensive study in order to prove its performance (reliability, sensitivity and robustness), it could contribute to faster and more directed process development for cell cryopreservation. In future, the described tool box could be used for pre-selection of possible candidates since it would streamline sample volume, as well as, development time. An additional advantage of the described tool box is the usage of flow cytometry analysis for toxicity evaluation. Hence, it could easily be adapted to new projects by implementing the measurement of e.g. critical cell criteria which is highly beneficial for clinical applications.
Monitoring critical cell characteristics (CCC) during process development or manufacturing is essential for cell-based therapeutics since changes are directly linked to therapeutic efficiency and patient safety. This is especially important for the process development of enabling technologies like bioprinting. Hence, a flow cytometry-based analytical strategy was developed for bioprinting applications. The development was done based on a model process using the β-model cell line INS-1E, an alginate-based, commercially available

bioink, and a direct dispensing 3D bioprinter. The strategy includes cell staining, 3D object deconstruction, flow cytometry analysis using an autosampler, as well as, data deconvolution. Two cell dyes were used allowing for the analysis of the CCC cell viability (7-AAD staining) and proliferation (CellTrace^{TM} Violet-based). The 3D object deconstruction is necessary since flow cytometry is a single cell analysis method. In the presented case study, de-gelating of the alginate-based bioink could be successfully performed using citric acid without a decrease in cell viability. However, the used commercial bioink contained fibers as thickener to improve the printability which could not be dissolved. For this reason, a data deconvolution strategy was implemented in order to eliminate the bias caused by the fiber signal. A successful strategy validation was performed using two artificial test samples. Subsequently, bioprinting process monitoring was performed. The monitoring indicated a major process influence on the β-model cell line INS-1E viability, highlighting the need for process optimization. Using the developed flow cytometry-based analytical strategy for bioprinting process development applications would contribute to a more directed and systematic approach. Additionally, the developed analytical strategy allows for high-throughput analysis due to the use of an automated sampler. Another advantage of the developed strategy is the simple implementation of additional CCC measurements allowing for complex cell characterization e.g. when printed multiple cell lines simultaneously or stem cells.

In conclusion, the doctoral thesis has shown that general process development tools and strategies from the pharmaceutical industry are applicable for cell-based products. Several process development tools and strategies have been developed within this doctoral thesis facilitating an advance in cell-based therapeutic process development. Using the presented approaches would be highly beneficial since they follow the general principle of miniaturization and automation enabling a simplified, accelerated, systematic and more directed process development. The presented work has demonstrated the applicability of those principles for inherent complex products like living cell material and might routinely be implemented in cell therapeutic industry process development campaigns. Hence, future projects will involve comprehensive studies with clinically relevant material.

CHAPTER 12

Comprehensive Reference List

1. A. A. Vertès, N. Qureshi, A. I. Caplan, and L. E. Babiss, eds.: *Stem Cells in Regenerative Medicine: Science, regulation and business strategies*. Wiley-Blackwell, 2016.
2. M. A. Fischbach, J. A. Bluestone, and W. A. Lim: 'Cell-based therapeutics: the next pillar of medicine'. *Science translational medicine* (2013), vol. 5(179): 179ps7.
3. S. Petit-Zeman: 'Regenerative Medicine'. *Nature biotechnology* (2001), vol. 19: pp. 201–206.
4. C. Mason, D. A. Brindley, E. J. Culme-Seymour, and N. L. Davie: 'Cell therapy industry: billion dollar global business with unlimited potential'. *Regenerative Medicine* (2011), vol. 6(3): pp. 265–272.
5. A. French, J. Y. Suh, C. Y. Suh, L. Rubin, R. Barker, K. Bure, B. Reeve, and D. A. Brindley: 'Global strategic partnerships in regenerative medicine'. *Trends in Biotechnology* (2014), vol. 32(9): pp. 436–440.
6. E. J. Culme-Seymour, N. L. Davie, D. A. Brindley, S. Edwards-Parton, and C. Mason: 'A decade of cell therapy clinical trials (20002010)'. *Regenerative Medicine* (2012), vol. 7(4): pp. 455–462.
7. E. Ratcliffe, K. E. Glen, M. W. Naing, and D. J. Williams: 'Current status and perspectives on stem cell-based therapies undergoing clinical trials for regenerative medicine: case studies'. *British Medical Bulletin* (2013), vol. 108(1): pp. 73–94.
8. E. Gluckman, H. E. Broxmeyer, A. D. Auerbach, H. S. Friedman, G. W. Douglas, A. Devergie, H. Esperou, D. Thierry, G. Socie, P. Lehn, S. Cooper, D. English, J. Kurtzberg, J. Bard, and E. A. Boyse: 'Hematopoietic Reconstitution in a Patient with Fanconi's Anemia by Means of Umbilical-Cord Blood from an HLA-Identical Sibling'. *New England Journal of Medicine* (1989), vol. 321(17): pp. 1174–1178.
9. F. Aversa et al.: 'Treatment of High-Risk Acute Leukemia with T-CellDepleted Stem Cells from Related Donors with One Fully Mismatched HLA Haplotype'. *New England Journal of Medicine* (1998), vol. 339(17): pp. 1186–1193.
10. E. A. Copelan: 'Hematopoietic Stem-Cell Transplantation'. *New England Journal of Medicine* (2006), vol. 354(17): pp. 1813–1826.

11. B. M. Davies et al.: 'A quantitative, multi-national and multi-stakeholder assessment of barriers to the adoption of cell therapies'. *Journal of Tissue Engineering* (2017), vol. 8: p. 2041731417724413.
12. A. Nagpal, C. Juttner, M. A. Hamilton-Bruce, P. Rolan, and S. A. Koblar: 'Stem cell therapy clinical research: A regulatory conundrum for academia'. *Advanced Drug Delivery Reviews* (2017), vol. 122: pp. 105–114.
13. S. de Wilde, H.-J. Guchelaar, C. Herberts, M. Lowdell, M. Hildebrandt, M. Zandvliet, and P. Meij: 'Development of cell therapy medicinal products by academic institutes'. *Drug Discovery Today* (2016), vol. 21(8): pp. 1206–1212.
14. D. G. M. Coppens, M. L. Bruin, H. G. M. Leufkens, and J. Hoekman: 'Global Regulatory Differences for Gene and CellBased Therapies: Consequences and Implications for Patient Access and Therapeutic Innovation'. *Clinical Pharmacology & Therapeutics* (2018), vol. 103(1): pp. 120–127.
15. B. P. Dodson and A. D. Levine: 'Challenges in the translation and commercialization of cell therapies'. *BMC Biotechnology* (2015), vol. 15(1): p. 70.
16. N. M. Mount, S. J. Ward, P. Kefalas, and J. Hyllner: 'Cell-based therapy technology classifications and translational challenges'. *Philos Trans R Soc Lond B Biol Sci.* (2015), vol. 370: p. 20150017.
17. Cynober, Timothé: *Why Are There Only 10 Cell and Gene Therapies in Europe?* https://labiotech.eu/atmp-cell-gene-therapy-ema/. April 4, 2018; accessed April 30, 2018.
18. E. Hanna, C. Rémuzat, P. Auquier, and M. Toumi: 'Advanced therapy medicinal products: Current and future perspectives'. (2016), vol. 4.
19. D. M. Smith, E. J. Culme-Seymour, and C. Mason: 'Evolving Industry Partnerships and Investments in Cell and Gene Therapies'. *Cell Stem Cell* (2018), vol.
20. C. Schneider et al.: 'Challenges with advanced therapy medicinal products and how to meet them'. *Nature reviews. Drug discovery* (2010), vol. 9: pp. 195–201.
21. S. de Wilde, L. Veltrop-Duits, M. Hoozemans-Strik, T. Ras, J. Blom-Veenman, H.-J. Guchelaar, M. Zandvliet, and P. Meij: 'Hurdles in clinical implementation of academic advanced therapy medicinal products: A national evaluation'. *Cytotherapy* (2016), vol. 18(6): pp. 797–805.
22. D. A. Brindley, A. L. French, R. Baptista, N.Timmins, T. Adams, and I. Wall andK. Bure: 'Cell therapy bioprocessing technologies and indicators of technological convergence'. *BioProcess International* (Mar. 2014), vol. 12: pp. 14–21.
23. N. Trainor, A. Pietak, and T. Smith: 'Rethinking clinical delivery of adult stem cell therapies'. *Nature biotechnology* (8 2014), vol. 32: pp. 729–735.
24. R. L. Bartel: 'Chapter 8 - Stem Cells and Cell Therapy: Autologous Cell Manufacturing'. *Translational Regenerative Medicine*. Ed. by A. Atala and J. G. Allickson. Boston: Academic Press, 2015. Chap. 8: pp. 107–112.

25. B. M. Davies et al.: 'Quantitative assessment of barriers to the clinical development and adoption of cellular therapies: A pilot study'. *Journal of Tissue Engineering* (2014), vol. 5: p. 2041731414551764.

26. N. Davie, D. A. Brindley, E. J. Culme-Seymour, and C. Mason: 'Streamlining cell therapy manufacture: From clinical to commercial scale'. *BioProcess International* (2012), vol. 10: pp. 24–49.

27. J. Carmen, S. R. Burger, M. McCaman, and J. A. Rowley: 'Developing assays to address identity, potency, purity and safety: cell characterization in cell therapy process development'. *Regenerative Medicine* (2012), vol. 7(1): pp. 85–100.

28. A. I. Caplan, C. Mason, and B. Reeve: 'The 3Rs of Cell Therapy'. *STEM CELLS Translational Medicine* (2017), vol. 6(1): pp. 17–21.

29. Novartis Global Communications: *Media Release: Novartis reaches another regulatory milestone for CTL019 (tisagenlecleucel) with submission of its MAA* to EMA for children, young adults with r/r B-cell ALL and adult patients with r/r DLBCL*. https://www.novartis.com/news/media-releases/novartis-reaches-another-regulatory-milestone-ctl019-tisagenlecleucel-submission. November 6, 2017; accessed Mai 6, 2018.

30. A. Mullard: 'PRIME time at the EMA'. *Nature reviews. Drug discovery* (2017), vol. 16(4): pp. 226–228.

31. *The First CAR-T Therapy Is Not Living Up to Expectations*. https://labiotech.eu/kymriah-car-t-therapy-novartis-sales/. April 24, 2018; accessed Mai 5, 2018.

32. R. S. Weinberg: 'Chapter 81 - Overview of Cellular Therapy'. *Transfusion Medicine and Hemostasis*. Ed. by B. H. Shaz, C. D. Hillyer, M. Roshal, and C. S. Abrams. Second Edition. San Diego: Elsevier, 2013. Chap. 81: pp. 533–540.

33. S. Eaker, E. Abraham, J. Allickson, T. A. Brieva, D. Baksh, T. R. J. Heathman, B. Mistry, and N. Zhang: 'Bioreactors for cell therapies: Current status and future advances'. *Cytotherapy* (2017), vol. 19(1): pp. 9–18.

34. Q. A. Rafiq and F. Masrin: 'Downstream Processing for Cell-Based Therapies'. *BioPharm International* (2017), vol. 30(4).

35. Y. Levinson, Y. Eylon, A. Heymann, A. Zaretsky-Rits, and O Karnieli: 'Foundation Elements for Cell Therapy Smart Scaling'. *BioProcess International* (2015), vol. 13(4): pp. 10–19.

36. K. Schriebl, S. Lim, A. Choo, A. Tscheliessnig, and A. Jungbauer: 'Stem cell separation: A bottleneck in stem cell therapy'. *Biotechnology Journal* (2010), vol. 5(1): pp. 50–61.

37. J. Pattasseril, H. Varadaraju, L. Lock, and J. A. Rowley: 'Downstream Technology Landscape for Large-Scale Therapeutic Cell Processing'. *BioProcess International* (2013), vol. 11(3): pp. 38–47.

38. M. B. Dainiak, A. Kumar, I. Y. Galaev, and B. Mattiasson: 'Methods in Cell Separations'. *Cell Separation. Advances in Biochemical Engineering/Biotechnology.* Ed. by A. Kumar, I. Y. Galaev, and B. Mattiasson. Vol. 106. Springer Berlin Heidelberg, 2007: pp. 1–18.

39. H. Pertoft: 'Fractionation of cells and subcellular particles with Percoll'. *Journal of Biochemical and Biophysical Methods* (2000), vol. 44(1): pp. 1–30.

40. S. Eaker, M. Armant, H. Brandwein, S. Burger, A. Campbell, C. Carpenito, D. Clarke, T. Fong, O. Karnieli, K. Niss, W. Van't Hof, and R. Wagey: 'Concise Review: Guidance in Developing Commercializable Autologous/PatientSpecific Cell Therapy Manufacturing'. *STEM CELLS Translational Medicine* (2013), vol. 2(11): pp. 871–883.

41. D. R. Gossett, W. M. Weaver, A. J. Mach, S. C. Hur, H. T. K. Tse, W. Lee, H. Amini, and D. Di Carlo: 'Label-free cell separation and sorting in microfluidic systems'. *Analytical and Bioanalytical Chemistry* (2010), vol. 397(8): pp. 3249–3267.

42. D. F. Stroncek, V. Fellowes, C. Pham, D. H. Fowler, L. V. Wood, and M. Sabatino: 'Counter-flow elutriation of clinical peripheral blood mononuclear cell concentrates for the production of dendritic and T cell therapies'. *Journal of Translational Medicine* (2014), vol. 12(1): p. 241.

43. A. Fesnak, C. Lin, D. L. Siegel, and M. V. Maus: 'CAR-T Cell Therapies From the Transfusion Medicine Perspective'. *Transfusion Medicine Reviews* (2016), vol. 30(3): pp. 139–145.

44. X. Wang and I. Rivière: 'Clinical manufacturing of CAR T cells: foundation of a promising therapy'. *Molecular therapy oncolytics* (2016), vol. 3: p. 16015.

45. B. Cunha, M. Serra, C. Peixoto, M. Silva, M. Carrondo, and P. Alves: 'Designing clinical-grade integrated strategies for the downstream processing of human mesenchymal stem cells'. *BMC Proceedings* (2013), vol. 7: P103.

46. D. F. Stroncek, D. W. Lee, J. Ren, M. Sabatino, S. Highfill, H. Khuu, N. N. Shah, R. N. Kaplan, T. J. Fry, and C. L. Mackall: 'Elutriated lymphocytes for manufacturing chimeric antigen receptor T cells'. *Journal of Translational Medicine* (2017), vol. 15(1): p. 59.

47. M. Eyrich, S. C. Schreiber, J. Rachor, J. Krauss, F. Pauwels, J. Hain, M. Wölfl, M. B. Lutz, S. de Vleeschouwer, P. G. Schlegel, and S. W. Van Gool: 'Development and validation of a fully GMP-compliant production process of autologous, tumor-lysate-pulsed dendritic cells'. *Cytotherapy* (2014), vol. 16(7): pp. 946–964.

48. S. Hassan, A. S. Simaria, H. Varadaraju, S. Gupta, K. Warren, and S. S. Farid: 'Allogeneic cell therapy bioprocess economics and optimization: downstream processing decisions'. *Regenerative Medicine* (2015), vol. 10(5): pp. 591–609.

49. P. A. MarichalGallardo and M. M. Álvarez.: 'Stateoftheart in downstream processing of monoclonal antibodies: Process trends in design and validation'. *Biotechnology Progress* (2012), vol. 28(4): pp. 899–916.

50. A. A. Shukla, B. Hubbard, T. Tressel, S. Guhan, and D. Low: 'Downstream processing of monoclonal antibodiesApplication of platform approaches'. *Journal of Chromatography B* (2007), vol. 848(1): pp. 28–39.

51. U. Gottschalk: 'Bioseparation in Antibody Manufacturing: The Good, The Bad and The Ugly'. *Biotechnology Progress* (2008), vol. 24(3): pp. 496–503.

52. A. Higuchi, C.-W. Chuang, Q.-D. Ling, S.-C. Huang, L.-M. Wang, H. Chen, Y. Chang, H.-C. Wang, J.-T. Bing, Y. Chang, and S.-T. Hsu: 'Differentiation ability of adipose-derived stem cells separated from adipose tissue by a membrane filtration method'. *Journal of Membrane Science* (2011), vol. 366(1): pp. 286–294.

53. P.Å. Albertsson: 'Partitioning of cell particles and macromolecules: Separation and purification of biomolecules, cell organelles, membranes and cells in aqueous polymer two phase systems and their use in biochemical analysis and biotechnology'. 3rd ed. John Wiley & Sons, New York, 1986.

54. H. Walter, D. E. Brooks, and D. Fisher: 'Partitioning in Aqueous Two-Phase Systems: Theory, Methods, Uses, and Applications to Biotechnology'. Academic Press, Inc., Orlando, USA, 1985.

55. M. W. Beijerinck: 'Ueber eine Eigentümlichkeit der löslichen Stärke'. *Centralblatt für Bakteriologie und Parasitenkunde und Infektionskrankheiten* (1896), vol. 2: pp. 697–699.

56. R. Hatti-Kaul: *Aqueous Two-Phase Systems: Methods and Protocols: Methods and Protocols*. Totowa, NJ: Humana Press, 2000.

57. M. Rito-Palomares and J. Benavides: *Aqueous Two-Phase Systems for Bioprocess Development for the Recovery of Biological Products*. Food Engineering Series. Springer International Publishing, 2017.

58. M. Bensch, B. Selbach, and J. Hubbuch: 'High throughput screening techniques in downstream processing: Preparation, characterization and optimization of aqueous two-phase systems'. *Chemical Engineering Science* (2007), vol. 62(7): pp. 2011–2021.

59. S. A. Oelmeier, F. Dismer, and J. Hubbuch: 'Application of an aqueous twophase systems highthroughput screening method to evaluate mAb HCP separation'. *Biotechnology and Bioengineering* (2010), vol. 108(1): pp. 69–81.

60. S. Zimmermann, S. Gretzinger, M.-L. Schwab, C. Scheeder, P. K. Zimmermann, S. A. Oelmeier, E. Gottwald, A. Bogsnes, M. Hansson, A. Staby, and J. Hubbuch: 'High-throughput downstream process development for cell-based products using aqueous two-phase systems'. *Journal of Chromatography A* (2016), vol. 1464: pp. 1–11.

61. P. A. Albertsson: 'Particle fractionation in liquid two-phase systems The composition of some phase systems and the behaviour of some model particles in them application to the isolation of cell walls from microorganisms'. *Biochimica et Biophysica Acta* (1958), vol. 27: pp. 378–395.

62. H. Walter, F. D. Raymond, and D. Fisher: 'Erythrocyte partitioning in dextranpoly(ethylene glycol) aqueous phase systems: Events in phase and cell separation'. *Journal of Chromatography A* (1992), vol. 609(1): pp. 219–227.

63. H. Walter, E. J. Krob, R. Garza, and G .S. Ascher: 'Partition and countercurrent distribution of erythrocytes and leukocytes from different species'. *Experimental Cell Research* (1969), vol. 55(1): pp. 57–64.

64. L. C. Craig and O. Post: 'Apparatus for Countercurrent Distribution'. *Analytical Chemistry* (1949), vol. 21(4): pp. 500–504.

65. G. Johansson: 'EXTRACTION | Multistage Countercurrent Distribution'. *Encyclopedia of Separation Science*. Ed. by I. D.Wilson. Oxford: Academic Press, 2000: pp. 1398–1405.

66. P. Å. Albertsson and G. D. Baird: 'Counter-current distribution of cells'. *Experimental Cell Research* (1962), vol. 28(2): pp. 296–322.

67. C. J. Connon, ed.: *Bioprocessing for Cell Based Therapies*. Wiley-Blackwell, 2016.

68. F. Atouf: 'Cell-Based Therapies Formulations: Unintended components'. *The AAPS Journal* (2016), vol. 18(4): pp. 844–848.

69. R. Brandenberger, S. Burger, A. Campbell, T. Fong, E. Lapinskas, and J. A. Rowley: 'Cell Therapy Bioprocessing - Integrating Process and Product Development for the Next Generation of Biotherapeutics'. *BioProcess International* (2011), vol.: pp. 30–37.

70. A. Campbell, T. Brieva, L. Raviv, J. Rowley, K. Niss, H. Brandwein, S. Oh, and O. Karnieli: 'Concise Review: Process Development Considerations for Cell Therapy'. *STEM CELLS Translational Medicine* (2015), vol. 4(10): pp. 1155–1163.

71. A. Z. Higgins, D. K. Cullen, M. C. LaPlaca, and J. O .M. Karlsson: 'Effects of freezing profile parameters on the survival of cryopreserved rat embryonic neural cells'. *Journal of Neuroscience Methods* (2011), vol. 201(1): pp. 9–16.

72. B. Grout, J. Morris, and M. McLellan: 'Cryopreservation and the maintenance of cell lines'. *Trends in Biotechnology* (1990), vol. 8: pp. 293–297.

73. I. Massie, C. Selden, H. Hodgson, B. Fullerand S. Gibbons, and J. G. Morris: 'GMP Cryopreservation of Large Volumes of Cells for Regenerative Medicine: Active Control of the Freezing Process'. *Tissue Engineering Part C: Methods* (2014), vol. 20(9): pp. 693–702.

74. R. Heidemann, S. Lünse, D. Tran, and C. Zhang: 'Characterization of cellbanking parameters for the cryopreservation of mammalian cell lines in 100 mL cryobags'. *Biotechnology Progress* (2010), vol. 26(4): pp. 1154–1163.

75. M. I. Kleman, K. Oellers, and E. Lullau: 'Optimal conditions for freezing CHOS and HEK293EBNA cell lines: Influence of Me2SO, freeze density, and PEImediated transfection on revitalization and growth of cells, and expression of recombinant protein'. *Biotechnology and Bioengineering* (2008), vol. 100(5): pp. 911–922.

76. C. C. Wong, K. E. Loewke, N. L. Bossert, B. Behr, C. J. De Jonge, T. M. Baer, and R. A. Reijo Pera: 'Non-invasive imaging of human embryos before embryonic genome activation predicts development to the blastocyst stage'. *Nature biotechnology* (2010), vol. 28: pp. 1115–21.

77. Y. Li and T. Ma: 'Bioprocessing of Cryopreservation for Large-Scale Banking of Human Pluripotent Stem Cells'. *BioResearch Open Access* (2012), vol. 1(5): pp. 205–214.

78. C. J. Hunt: 'The Banking and Cryopreservation of Human Embryonic Stem Cells'. *Transfusion Medicine and Hemotherapy* (2007), vol. 34: pp. 293–304.

79. D. Freimark, C. Sehl, C. Weber, K. Hudel, P. Czermak, N. Hofmann, R. Spindler, and B. Glasmacher: 'Systematic parameter optimization of a Me_2SO- and serum-free cryopreservation protocol for human mesenchymal stem cells'. *Cryobiology* (2011), vol. 63(2): pp. 67–75.

80. W. De Loecker, V. A. Koptelov, V. I. Grischenko, and P. De Loecker: 'Effects of Cell Concentration on Viability and Metabolic Activity during Cryopreservation'. *Cryobiology* (1998), vol. 37(2): pp. 103–109.

81. C. B Ware, A. M. Nelson, and C. A. Blau: 'Controlled-rate freezing of human ES cells'. *BioTechniques* (2005), vol. 38(6): pp. 879–883.

82. P. Kilbride, S. Lamb, S. Milne, S. Gibbons, E. Erro, J. Bundy, C. Selden, B. Fuller, and J. Morris: 'Spatial considerations during cryopreservation of a large volume sample'. *Cryobiology* (2016), vol. 73(1): pp. 47–54.

83. P. Kilbride, G. J. Morris, S. Milne, B. Fuller, J. Skepper, and C. Selden: 'A scale down process for the development of large volume cryopreservation'. *Cryobiology* (2014), vol. 69(3): pp. 367–375.

84. Y. Zhou, Z. Fowler, A. Cheng, and R. Sever: 'Improve process uniformity and cell viability in cryopreservation'. *BioProcess International* (2012), vol. 10: pp. 70–76.

85. J. O. M .Karlsson, A. Eroglu, T. L.Toth, E. G. Cravalho, and M. Tonerr: 'Fertilization and development of mouse oocytes cryopreserved using a theoretically optimized protocol'. *Human Reproduction* (1996), vol. 11(6): pp. 1296–1305.

86. F. Dumont, P.-A. Marechal, and P. Gervais: 'Cell Size and Water Permeability as Determining Factors for Cell Viability after Freezing at Different Cooling Rates'. *Applied and Environmental Microbiology* (2004), vol. 70(1): pp. 268–272.

87. E. J. Woods, B. C. Perry, J. J. Hockema, L. Larson, D. Zhou, and W. S. Goebel: 'Optimized cryopreservation method for human dental pulp-derived stem cells and their tissues of origin for banking and clinical use'. *Cryobiology* (2009), vol. 59(2): pp. 150–157.

88. M. L. Thompson, E. J. Kunkel, and R. O. Ehrhardt: 'Standardized Cryopreservation of Stem Cells'. *Stem Cell Technologies in Neuroscience*. Ed. by A. K. Srivastava, E. Y. Snyder, and Y. D. Teng. New York, NY: Springer New York, 2017. Chap. 13: pp. 193–203.

89. T. Buhl, T. J. Legler, A. Rosenberger, A. Schardt, M. P. Schön, and H. A. Haenssle.: 'Controlled-rate freezer cryopreservation of highly concentrated peripheral blood mononuclear cells results in higher cell yields and superior autologous T-cell stimulation for dendritic cell-based immunotherapy'. *Cancer Immunology, Immunotherapy* (2012), vol. 61(11): pp. 2021–2031.

90. J. G. Baust, D. Gao, and J. M. Baust: 'Cryopreservation: An emerging paradigm change'. *Organogenesis* (2009), vol. 5(3): pp. 90–96.

91. W. Asghar, R. El Assal, H. Shafiee, R. M. Anchan, and U. Demirci: 'Preserving human cells for regenerative, reproductive, and transfusion medicine'. *Biotechnology Journal* (2014), vol. 9(7): pp. 895–903.

92. J. R. Moldenhauer: 'Cell Culture Preservation and Storage for Industrial Bioprocesses'. *Handbook of Industrial Cell Culture: Mammalian, Microbial, and Plant Cells*. Ed. by V. A. Vinc and S. R. Parekh. Totowa, NJ: Humana Press, 2003. Chap. 18: pp. 483–514.

93. S. S. Buchanan, S. A. Gross, J. P. Acker, M. Toner, J. F. Carpenter, and D. W. Pyatt: 'Cryopreservation of Stem Cells Using Trehalose: Evaluation of the Method Using a Human Hematopoietic Cell Line'. *Stem Cells and Development* (2004), vol. 13(3): pp. 295–305.

94. W. J. Armitage and B.K. Juss: 'The influence of cooling rate on survival of frozen cells differs in monolayers and suspensions'. *Cryo-Letters* (1996), vol. 17: pp. 213–218.

95. H. T. Meryman: 'Cryopreservation of living cells: principles and practice'. *Transfusion* (2007), vol. 47(5): pp. 935–945.

96. T. Du, L. Chao, S. Zhao, L. Chi, D. Li, Y. Shen, Q. Shi, and X. Deng: 'Successful cryopreservation of whole sheep ovary by using DMSO-free cryoprotectant'. *Journal of Assisted Reproduction and Genetics* (2015), vol. 32(8): pp. 1267–1275.

97. S. Thirumala, X. Wu, J. M. Gimble, and R. V. Devireddy: 'Evaluation of Polyvinylpyrrolidone as a Cryoprotectant for Adipose Tissue-Derived Adult Stem Cells'. *Tissue Engineering Part C: Methods* (2010), vol. 16(4): pp. 783–792.

98. B. Fuller, J. Gonzalez-Molina, E. Erro, J. De Mendonca, S. Chalmers, M. Awan, A. Poirier, and C. Selden: 'Applications and optimization of cryopreservation technologies to cellular therapeutics'. *Cell Gene Therapy Insights* (2017), vol. 3(5): pp. 359–378.

99. S. Thirumala, J. M. Gimble, and R. V. Devireddy: 'Cryopreservation of stromal vascular fraction of adipose tissue in a serumfree freezing medium'. *Journal of Tissue Engineering and Regenerative Medicine* (2010), vol. 4(3): pp. 224–232.

100. A. Hennes, L. Gucciardo, S. Zia, F. Lesage, N. Lefèvre, L. Lewi, A. Vorsselmans, T. Cos, R. Lories, J. Deprest, and J. Toelen: 'Safe and effective cryopreservation methods for longterm storage of humanamnioticfluidderived stem cells'. *Prenatal Diagnosis* (2015), vol. 35(5): pp. 456–462.

101. I. I. Katkov, N. G. Kan, F. Cimadamore, B. Nelson, E. Y. Snyder, and A. V. Terskikh: 'DMSO-Free Programmed Cryopreservation of Fully Dissociated and Adherent Human Induced Pluripotent Stem Cells'. *Stem Cells International* (2011), vol. 2011.

102. V. Keros, B. Rosenlund, K. Hultenby, L. Aghajanova, L. Levkov, and O. Hovatta: 'Optimizing cryopreservation of human testicular tissue: comparison of protocols with glycerol, propanediol and dimethylsulphoxide as cryoprotectants'. *Human Reproduction* (2005), vol. 20(6): pp. 1676–1687.

103. J. Groll et al.: 'Biofabrication: reappraising the definition of an evolving field'. *Biofabrication* (2016), vol. 8(1): p. 013001.

104. V. Mironov, T. Trusk, V. Kasyanov, S. Little, R. Swaja, and R. Markwald: 'Biofabrication: a 21st century manufacturing paradigm'. *Biofabrication* (2009), vol. 1(2): p. 022001.

105. S. H. Huang, P. Liu, A. Mokasdar, and L. Hou: 'Additive manufacturing and its societal impact: a literature review'. *The International Journal of Advanced Manufacturing Technology* (2013), vol. 67(5): pp. 1191–1203.

106. A. Atala and J. J. Yoo: 'Essentials of 3D Biofabrication and Translation'. Boston: Academic Press, Inc., 2015.

107. L. A. L. Fliervoet and E. Mastrobattista: 'Drug delivery with living cells'. *Advanced Drug Delivery Reviews* (2016), vol. 106: pp. 63–72.

108. S. A. Langhans: 'Three-Dimensional in Vitro Cell Culture Models in Drug Discovery and Drug Repositioning'. *Frontiers in Pharmacology* (2018), vol. 9: p. 6.

109. J. Malda, J. Visser, F. P. Melchels, T. Jüngst, W. E. Hennink, W. J. A. Dhert, J. Groll, and D. W. Hutmacher: '25th Anniversary Article: Engineering Hydrogels for Biofabrication'. *Advanced Materials* (2013), vol. 25(36): pp. 5011–5028.

110. T. J. Hinton, Q. Jalleratn, R. N. Palchesko, J. H. Park, M. S. Grodzicki, H.-J. Shuen, M. H. Ramadan, A. R. Hudson, and A. W. Feinberg: 'Three-dimensional printing of complex biological structures by freeform reversible embedding of suspended hydrogels'. *Science Advances* (2015), vol. 1(9).

111. K. Arcaute, B. K. Mann, and R. B. Wicke: 'Stereolithography of Three-Dimensional Bioactive Poly(Ethylene Glycol) Constructs with Encapsulated Cells'. *Annals of Biomedical Engineering* (2006), vol. 34(9): pp. 1429–1441.

112. R. R.Jose, M. J. Rodriguez, T. A. Dixon, F. Omenetto, and D. L. Kaplan: 'Evolution of Bioinks and Additive Manufacturing Technologies for 3D Bioprinting'. *ACS Biomaterials Science & Engineering* (2016), vol. 2(10): pp. 1662–1678.

113. T. Billiet, M. Vandenhaute, J. Schelfhout, S. Van Vlierberghe, and P. Dubruel: 'A review of trends and limitations in hydrogel-rapid prototyping for tissue engineering'. *Biomaterials* (2012), vol. 33(26): pp. 6020–6041.

114. J. Song and J. R. Millman: 'Economic 3D-printing approach for transplantation of human stem cell-derived β-like cells'. *Biofabrication* (2016), vol. 9(1): p. 015002.

115. R. M. Costa, S. Rauf, and C. A. E. Hauser: 'Towards biologically relevant synthetic designer matrices in 3D bioprinting for tissue engineering and regenerative medicine'. *Current Opinion in Biomedical Engineering* (2017), vol. 2: pp. 90–98.

116. J. G. Hunsberger, S. Goel, J. Allickson, and A. Atala: 'Five Critical Areas that Combat High Costs and Prolonged Development Times for Regenerative Medicine Manufacturing'. *Current Stem Cell Reports* (2017), vol. 3(2): pp. 77–82.

117. J. Visser, B. Peters, T. J. Burger, J. Boomstra, W. J. A. Dhert, F. P. W. Melchels, and J. Malda: 'Biofabrication of multi-material anatomically shaped tissue constructs'. *Biofabrication* (2013), vol. 5(3): p. 035007.

118. J. G. Torres-Rendon, M. Köpf, D. Gehlen, A. Blaeser, H. Fischer, L. De Laporte, and A. Walther: 'Cellulose Nanofibril Hydrogel Tubes as Sacrificial Templates for Freestanding Tubular Cell Constructs'. *Biomacromolecules* (2016), vol. 17(3): pp. 905–913.

119. I. R. Harris, F. Meacle, and D. Powers: 'Automation in cell therapy manufacturing'. *BioProcess International* (2016), vol. 14: pp. 18–21.

120. International Council for Harmonisation of Technical Requirements for Pharmaceuticals for Human Use: *ICH Harmonised tripartite guideline: Pharmaceutical Development Q8(R2)*. http://www.ich.org/fileadmin/Public_Web_Site/ICH_Products/Guidelines/Quality/Q8_R1/Step4/Q8_R2_Guideline.pdf. August , 2009; accessed Mai 20, 2018.

121. B. Preti, A. M. Daus, B. Hampson, and C. Sumens: 'Mapping Success for Commercial Cell Therapy Manufacturing'. *BioProcess International* (2015), vol.

122. Y. Y. Lipsitz, N. E. Timmins, and P. Zandstra: 'Quality cell therapy manufacturing by design'. *Nature biotechnology* (4 2016), vol. 34: pp. 393–400.

123. V. M. C. Quent, D. Loessner, T. Friis, J. C. Reichert, and D. W. Hutmacher: 'Discrepancies between metabolic activity and DNA content as tool to assess cell proliferation in cancer research'. *Journal of Cellular and Molecular Medicine* (2010), vol. 14(4): pp. 1003–1013.

124. H. Mueller, M. U. Kassack, and M. Wiese: 'Comparison of the Usefulness of the MTT, ATP, and Calcein Assays to Predict the Potency of Cytotoxic Agents in Various Human Cancer Cell Lines'. *Journal of Biomolecular Screening* (2004), vol. 9(6): pp. 506–515.

125. O. Kepp, L. Galluzzi, M. Lipinski, J. Yuan, and G. Kroemer: 'Cell death assays for drug discovery'. *Nature reviews. Drug discovery* (2011), vol. 10: pp. 221–237.

126. B. Méry, J.-B. Guy, A. Vallard, S. Espenel, D. Ardail, C. Rodriguez-Lafrasse, C. Rancoule, and N. Magné: 'In Vitro Cell Death Determination for Drug Discovery: A Landscape Review of Real Issues'. *Journal of Cell Death* (2017), vol. 10.

127. M. Butler and M. Spearman: 'Cell Counting and Viability Measurements'. *Animal Cell Biotechnology: Methods and Protocols*. Ed. by Pörtner, Ralf. Totowa, NJ: Humana Press, 2007: pp. 205–222.

128. S. Zimmermann, S. Gretzinger, C. Scheeder, M.L. Schwab, S. A. Oelmeier, A. Osberghaus, E. Gottwald, and J. Hubbuch: 'Highthroughput cell quantification assays for use in cell purification development enabling technologies for cell production'. *Biotechnology Journal* (2016), vol. 11(5): pp. 676–686.

129. Molecular Probes: *CyQUANT® Direct Cell Proliferation Assay Kit*. http://www.thermofisher.com/order/catalog/product/C35011. revised Juli, 2009; accessed Mai 26, 2018.

130. F. Bonnier, M. E. Keating, T. P. Wróbel, K. Majzner, M. Baranska, A. Garcia-Munoz, A. Blanco, and H. J. Byrne: 'Cell viability assessment using the Alamar blue assay: A comparison of 2D and 3D cell culture models'. *Toxicology in Vitro* (2015), vol. 29(1): pp. 124–131.

131. G. K. Y. Chan, T. L. Kleinheinz, D. Peterson, and J. G. Moffat: 'A Simple High-Content Cell Cycle Assay Reveals Frequent Discrepancies between Cell Number and ATP and MTS Proliferation Assays'. *PLOS ONE* (2013), vol. 8(5): pp. 1–15.

132. L. J. Jones, M. Gray, S. T. Yue, R. P. Haugland, and V. L. Singer: 'Sensitive determination of cell number using the CyQUANT cell proliferation assay'. *Journal of Immunological Methods* (2001), vol. 254(1): pp. 85–98.

133. D. Barnett, V. Granger, L. Whitby, I. Storie, and J. T. Reilly: 'Absolute $CD4^+$ Tlymphocyte and $CD34^+$ stem cell counts by singleplatform flow cytometry: the way forward'. *British Journal of Haematology* (1999), vol. 106(4): pp. 1059–1062.

134. S. F. Ibrahim and G. van den Engh: 'Flow Cytometry and Cell Sorting'. *Cell Separation: Fundamentals, Analytical and Preparative Methods*. Ed. by A. Kumar, I. Y. Galaev, and B. Mattiasson. Berlin, Heidelberg: Springer Berlin Heidelberg, 2007: pp. 19–39.

135. P. O. Krutzik and G. P. Nolan: 'Fluorescent cell barcoding in flow cytometry allows high-throughput drug screening and signaling profiling'. *Nature methods* (2006), vol. 3: pp. 361–368.

136. S. Desbordes, D. Placantonakis, A. Ciro, N. D. Socc, Gabsang Lee, H.Djaballah, and L. Studer: 'High-Throughput Screening Assay for the Identification of Compounds Regulating Self-Renewal and Differentiation in Human Embryonic Stem Cells'. *Cell stem cell* (2008), vol. 2: pp. 602–12.

137. Y. Mei, M. Goldberg, and D. Anderson: 'The development of high-throughput screening approaches for stem cell engineering'. *Current Opinion in Chemical Biology* (2007), vol. 11(4): pp. 388–393.

138. International Council for Harmonisation of Technical Requirements for Pharmaceuticals for Human Use: *Harmonised tripartite guideline: Validation of Analytical Procedures: Text and Methodology Q2(R1)*. https://www.ich.org/fileadmin/Public_Web_Site/ICH_Products/Guidelines/Quality/Q2_R1/Step4/Q2_R1__Guideline.pdf. incooperated November 2005; accessed Mai 20, 2018.

139. J. F. Loring, T. C. McDevitt, S. P. Palecek, D. V. Schaffer, P. W. Zandstra, and R. M. Nerem: 'A Global Assessment of Stem Cell Engineering'. *Tissue Engineering Part A* (2014), vol. 20(19-20): pp. 2575–2589.

140. R. Macarron, M. N. Banks, D. Bojanic, D. J. Burns, D. A. Cirovic, T. Garyantes, D. V. S. Green, R. P. Hertzberg, W. P. Janzen, J. W. Paslay, U. Schopfer, and G. Sittampalam: 'Impact of high-throughput screening in biomedical research'. *Nature reviews. Drug discovery* (2011), vol. 10: pp. 188–195.

141. L. M. Mayr and D. Bojanic: 'Novel trends in high-throughput screening'. *Current Opinion in Pharmacology* (2009), vol. 9(5): pp. 580–588.

142. I. Coma, L. Clark, E. Diez, G. Harper, J. Herranz, G. Hofmann, M. Lennon, N. Richmond, M. Valmaseda, and R. Macarron: 'Process Validation and Screen Reproducibility in High-Throughput Screening'. *Journal of Biomolecular Screening* (2009), vol. 14(1): pp. 66–76.

143. R. P. Hertzberg and A. J. Pope: 'High-throughput screening: new technology for the 21st century'. *Current Opinion in Chemical Biology* (2000), vol. 4(4): pp. 445–451.

144. P. Jones, S. McElroy, A. Morrison, and A. Pannifer: 'The importance of triaging in determining the quality of output from high-throughput screening'. *Future Medicinal Chemistry* (2015), vol. 7(14): pp. 1847–1852.

145. C. B. Black, T. D. Duensing, L. S. Trinkle, and T. R. Dunlay: 'Cell-Based Screening Using High-Throughput Flow Cytometry'. *ASSAY and Drug Development Technologies* (2011), vol. 9(1): pp. 13–20.

146. J. Simm et al.: 'Repurposing High-Throughput Image Assays Enables Biological Activity Prediction for Drug Discovery'. *Cell CHemical Biologys* (2018), vol. 25(5): p611–618.e3.

147. M. V. Ferreira, W. Jahnen-Dechent, and S. Neuss: 'Standardization of Automated Cell-Based Protocols for Toxicity Testing of Biomaterials'. *Journal of Biomolecular Screening* (2011), vol. 16(6): pp. 647–654.

148. J. Hubbuch: 'Editorial: Highthroughput process development'. *Biotechnology Journal* (2012), vol. 7(10): p. 1185.

149. K.ł M. cki: 'High throughput process development in biomanufacturing'. *Current Opinion in Chemical Engineering* (2014), vol. 6: pp. 25–32.

150. R. Bhambure, K. Kumar, and A. S. Rathore: 'High-throughput process development for biopharmaceutical drug substances'. *Trends in Biotechnology* (2011), vol. 29(3): pp. 127–135.

151. C.Heath and R. Kiss: 'Cell Culture Process Development: Advances in Process Engineering'. *Biotechnology Progress* (2007), vol. 23(1): pp. 46–51.

152. M. Wiendahl, P. S. Wierling, J. Nielsen, D. F. Christensen, J. Krarup, A. Staby, and J. Hubbuch: 'High Throughput Screening for the Design and Optimization of Chromatographic Processes Miniaturization, Automation and Parallelization of Breakthrough and Elution Studies'. *Chemical Engineering & Technology* (2008), vol. 31(6): pp. 893–903.

153. K. Rege, M. Pepsin, B. Falcon, L. Steele, and M. Heng: 'Highthroughput process development for recombinant protein purification'. *Biotechnology and Bioengineering* (2006), vol. 93(4): pp. 618–630.

154. R. Bareither, N. Bargh, R. Oakeshott, K. Watts, and D. Pollard: 'Automated disposable small scale reactor for high throughput bioprocess development: A proof of concept study'. *Biotechnology and Bioengineering* (2013), vol. 110(12): pp. 3126–3138.

155. S. Rameez, S. S. Mostafa, C. Miller, and A. A. Shukla: 'Highthroughput miniaturized bioreactors for cell culture process development: Reproducibility, scalability, and control'. *Biotechnology Progress* (2014), vol. 30(3): pp. 718–727.

156. S. Konstantinidis, S. Kong, S. Chhatre, A. Velayudhan, E. Heldin, and N. TitchenerHooker: 'Strategic Assay Selection for analytics in highthroughput process development: Case studies for downstream processing of monoclonal antibodies'. *Biotechnology Journal* (2012), vol. 7(10): pp. 1256–1268.

157. T. Rayna and L. Striukova: 'The Impact of 3D Printing Technologies on Business Model Innovation'. *Digital Enterprise Design & Management: Proceedings of the Second International Conference on Digital Enterprise Design and Management DED&M 2014*. Ed. by P.-J. Benghozi, D. Krob, A. Lonjon, and H. Panetto. Springer Publishing Company, Incorporated, 2014: pp. 119–132.

158. I. J. Petrick and T. W. Simpson: '3D Printing Disrupts Manufacturing: How Economies of One Create New Rules of Competition'. *Research-Technology Management* (2013), vol. 56(6): pp. 12–16.

159. R. S. Kalva: '3d Printing -the Future of Manufacturing (the next Industrial Revolution)'. *International Journal of Innovations in Engineering and Technology* (2015), vol. 5(1): pp. 184–190.

160. C. W. Hull: 'Apparatus for production of three-dimensional objects by stereolithography'. US 4575330 A. https://patents.google.com/patent/US4575330. 1986.

161. B. C. Gross, J. L. Erkal, S. Y. Lockwood, C. Chen, and D. M. Spence: 'Evaluation of 3D Printing and Its Potential Impact on Biotechnology and the Chemical Sciences'. *Analytical Chemistry* (2014), vol. 86(7): pp. 3240–3253.

162. F. Krujatz, A. Lode, J. Seidel, T. Bley, M. Gelinsky, and J. Steingroewer: 'Additive BiotechChances, challenges, and recent applications of additive manufacturing technologies in biotechnology'. *New Biotechnology* (2017), vol. 39: pp. 222–231.

163. K. V. Wong and A. Hernandez: 'Review of Additive Manufacturing'. *ISRN Mechanical Engineering* (2012), vol. 2012(Article ID 208760): 10 pages.

164. H. Bikas, P. Stavropoulos, and G. Chryssolouris: 'Additive manufacturing methods and modelling approaches: a critical review'. *The International Journal of Advanced Manufacturing Technology* (2016), vol. 83(1): pp. 389–405.

165. N. Guo and M. C. Leu: 'Additive manufacturing: technology, applications and research needs'. *Frontiers of Mechanical Engineering* (2013), vol. 8(3): pp. 215–243.

166. T. J. Snyder et al.: '3D Systems Technology Overview and New Applications in Manufacturing, Engineering, Science, and Education'. *3D Printing and Additive Manufacturing* (2014), vol. 1(3): pp. 169–176.

167. M. Coakley and D. E. Hurt: '3D Printing in the Laboratory: Maximize Time and Funds with Customized and Open-Source Labware'. *Journal of Laboratory Automation* (2016), vol. 21(4): pp. 489–495.

168. A. Waldbaur, J. Kittelmann, C. P. Radtke, J. Hubbuch, and B. E. Rapp: 'Microfluidics on liquid handling stations (µF-on-LHS): an industry compatible chip interface between microfluidics and automated liquid handling stations'. *Lab Chip* (12 2013), vol. 13: pp. 2337–2343.

169. C. P. Radtke, M.-T. Schermeyer, Y. C. Zhai, J. Göpper, and J. Hubbuch: 'Implementation of an analytical microfluidic device for the quantification of protein concentrations in highthroughput format'. *Engineering in Life Sciences* (2016), vol. 16(6): pp. 515–524.

170. C. Chen, Y. Wang, S. Y. Lockwood, and D. M. Spence: '3D-printed fluidic devices enable quantitative evaluation of blood components in modified storage solutions for use in transfusion medicine'. *Analyst* (2014), vol. 139(13): pp. 3219–3226.

171. T. Femmer, A. Jans, R. Eswein, N. Anwar, M. Moeller, M. Wessling, and A. J. C. Kuehne: 'High-Throughput Generation of Emulsions and Microgels in Parallelized Microfluidic Drop-Makers Prepared by Rapid Prototyping'. *ACS Applied Materials & Interfaces* (2015), vol. 7(23): pp. 12635–12638.

172. F. Kazenwadel, E. Biegert, J. Wohlgemuth, H. Wagner, and M. Franzreb: 'A 3Dprinted modular reactor setup including temperature and pH control for the compartmentalized implementation of enzyme cascades'. *Engineering in Life Sciences* (2016), vol. 16(6): pp. 560–567.

173. C.-K. Su and J.-C. Chen: 'Reusable, 3D-printed, peroxidase mimicincorporating multi-well plate for high-throughput glucose determination'. *Sensors and Actuators B: Chemical* (2017), vol. 247: pp. 641–647.

174. T. H. Lücking, F. Sambale, S. Beutel, and T. Scheper: '3Dprinted individual labware in biosciences by rapid prototyping: A proof of principle'. *Engineering in Life Sciences* (2015), vol. 15(1): pp. 51–56.

175. T. H. Lücking, F. Sambale, B. Schnaars, D. BulnesAbundis, S. Beutel, and T. Scheper: '3Dprinted individual labware in biosciences by rapid prototyping: In vitro biocompatibility and applications for eukaryotic cell cultures'. *Engineering in Life Sciences* (2015), vol. 15(1): pp. 57–64.

176. J. N. Wittbrodt, U. Liebel, and J. Gehrig: 'Generation of orientation tools for automated zebrafish screening assays using desktop 3D printing'. *BMC Biotechnology* (2014), vol. 14(1): p. 36.

177. S. Amrhein, M.-L. Schwab, M. Hoffmann, and J. Hubbuch: 'Characterization of aqueous two phase systems by combining lab-on-a-chip technology with robotic liquid handling stations'. *Journal of Chromatography A* (2014), vol. 1367: pp. 68–77.

178. S. Amrhein, K. C. Bauer, L. Galm, and J. Hubbuch: 'Noninvasive high throughput approach for protein hydrophobicity determination based on surface tension'. *Biotechnology and Bioengineering* (2015), vol. 112(12): pp. 2485–2494.

179. X. P. Tan, Y.J. Tan, C.S.L. Chow, S.B. Tor, and W.Y. Yeong: 'Metallic powder-bed based 3D printing of cellular scaffolds for orthopaedic implants: A state-of-the-art review on manufacturing, topological design, mechanical properties and biocompatibility'. *Materials Science and Engineering: C* (2017), vol. 76: pp. 1328–1343.

180. W. Lei and L. Jing: 'Compatible hybrid 3D printing of metal and nonmetal inks for direct manufacture of end functional devices'. *Science China Technological Sciences* (2014), vol. 57(11): pp. 2089–2095.

181. A. Padmanabhan and J. Zhang: 'Cybersecurity risks and mitigation strategies in additive manufacturing'. *Progress in Additive Manufacturing* (2018), vol. 3(1): pp. 87–93.

182. M. Al-Rubeai, M. Naciri: *Stem Cells and Cell Therapy.* Springer, Netherlands, 2014.

183. A. Trounson and C. McDonald: 'Stem Cell Therapies in Clinical Trials: Progress and Challenges'. *Cell Stem Cell* (2015), vol. 17(1): pp. 11–22.

184. P. J. Amos, E. Cagavi Bozkulak, and Y. Qyang: 'Methods of Cell Purification: A Critical Juncture for Laboratory Research and Translational Science'. *Cells Tissues Organs* (2012), vol. 195: pp. 26–40.

185. G. M. C. Rodrigues, C. A. V. Rodrigues, T. G. Fernandes, M. M. Diogo, and J. M. S. Cabral: 'Clinical-scale purification of pluripotent stem cell derivatives for cell-based therapies'. *Biotechnology journal* (2015), vol. 10: pp. 1103–1114.

186. C. Stemberger et al.: 'Novel Serial Positive Enrichment Technology Enables Clinical Multiparameter Cell Sorting'. *PLOS ONE* (2012), vol. 7(4): e35798.

187. T. G. Fernandes, C. A.V. Rodrigues, M. M. Diogo, and J. M. S. Cabral: 'Stem cell bioprocessing for regenerative medicine'. *Journal of Chemical Technology & Biotechnology* (2014), vol. 89(1): pp. 34–47.

188. A. Chen, S. Ting, J. Seow, S. Reuveny, and S. Oh: 'Considerations in designing systems for large scale production of human cardiomyocytes from pluripotent stem cells'. *Stem Cell Research & Therapy* (2014), vol. 5(1): p. 12.

189. J. M. S. Cabral: 'Cell Partitioning in Aqueous Two-Phase Polymer Systems'. *Adv. Biochem. Eng. Biotechnol* (2007), vol. 106: pp. 151–171.

190. R. R. G. Soares, A. M. Azevedo, J. M. Van Alstine, and M. R. Aires-Barros: 'Partitioning in aqueous twophase systems: Analysis of strengths, weaknesses, opportunities and threats'. *Biotechnology Journal* (2015), vol. 10(8): pp. 1158–1169.

191. P. S. Gascoine, D. Fisher: 'The dependence of cell partition in two-polymer aqueous phase systems on the electrostatic potential between the phases'. *Biochemical Society Transactions* (1984), vol. 12(6): pp. 1085–1086.

192. H. Walter: 'Cell partitioning in two-polymer aqueous phase systems'. *Trends in Biochemical Sciences* (1978), vol. 3(2): pp. 97–100.

193. G. Johansson: 'Partition of salts and their effects on partition of proteins in a dextran-poly(ethylene glycol)-water two-phase system'. *Biochimica et Biophysica Acta (BBA) - Protein Structure* (1970), vol. 221(2): pp. 387–390.

194. R. Reitherman, S. D. Flanagan, and S. H. Barondes: 'Electromotive phenomena in partition of erythrocytes in aqueous polymer two phase systems'. *Biochimica et Biophysica Acta (BBA) - General Subjects* (1973), vol. 297(2): pp. 193–202.

195. W. Fan, U. Bakir, and C. E. Glatz: 'Contribution of protein charge to partitioning in aqueous twophase systems'. *Biotechnology and Bioengineering* (1998), vol. 59(4): pp. 461–470.

196. H. Walter, E. J. Krob, and A. Pedram: 'Subfractionation of cell populations by partitioning in dextran-poly (ethylene glycol) aqueous phases. Discriminating and Nondiscriminating systems'. *Cell Biophysics* (1982), vol. 4(4): pp. 273–284.

197. D. Forciniti, C. K. Hall, and M .R. Kula: 'Interfacial tension of polyethyleneglycol-dextran-water systems: influence of temperature and polymer molecular weight'. *Journal of Biotechnology* (1990), vol. 16(3): pp. 279–296.

198. A .Merglen, S. Theander, B. Rubi, G. Chaffard, C. B. Wollheim, and P. Maechler: 'Glucose Sensitivity and Metabolism-Secretion Coupling Studied during Two-Year Continuous Culture in INS-1E Insulinoma Cells'. *Endocrinology* (2004), vol. 145(2): pp. 667–678.

199. P. R. Bevington and D. K. Robinson: 'Data Reduction and Error Analysis for the Physical Sciences'. 3rd ed. McGraw Hill, New York, USA, 2003.

200. S. Zimmermann, C. Scheeder, P. K. Zimmermann, A. Bogsnes, M. Hansson, A. Staby, and J. Hubbuch: 'Highthroughput downstream process development for cellbased products using aqueous twophase systems (ATPS) A case study'. *Biotechnology Journal* (2017), vol. 12(2): p. 1600587.

201. G. Johansson: 'Effects of salts on the partition of proteins in aqueous polymeric biphasic systems.' *Acta chemica Scandinavica. Series B: Organic chemistry and biochemistry* (1974), vol. 28: pp. 873–82.

202. M. Vis, V. F. D. Peters, R. H. Tromp, and B. H. Erné: 'Donnan Potentials in Aqueous Phase-Separated Polymer Mixtures'. *Langmuir* (2014), vol. 30(20): pp. 5755–5762.

203. Y. Liu, R. Lipowsky, and R. Dimova: 'Concentration Dependence of the Interfacial Tension for Aqueous Two-Phase Polymer Solutions of Dextran and Polyethylene Glycol'. *Langmuir* (2012), vol. 28(8): pp. 3831–3839.

204. R. S. King, H. W. Blanch, and J. M. Prausnitz: 'Molecular thermodynamics of aqueous twophase systems for bioseparations'. *AIChE Journal* (1988), vol. 34(10): pp. 1585–1594.

205. J. R. Luther and C. E. Glatz: 'Genetically engineered charge modifications to enhance protein separation in aqueous twophase systems: Charge directed partitioning'. *Biotechnology and Bioengineering* (1995), vol. 46(1): pp. 62–68.

206. J. M. Van Alstine: 'Eukaryotic cell partitioning: experimental considerations'. *Aqueous Two-Phase Systems: Methods and Protocols*. Ed. by R. Hatti-Kaul. Totowa, New Jersey: Humana Press, 2000: pp. 119–142.

207. H. Walter, F. A. Al-Romaihi, E. J. Krob, and G. V. Seaman.: 'Fractionation of K-562 cells on the basis of their surface properties by partitioning in two-polymer aqueous-phase systems'. *Cell Biophysics* (1987), vol. 10(3): pp. 217–232.

208. H. Walter and K. E. Widen: 'Cell partitioning in two-polymer aqueous phase systems and cell electrophoresis in aqueous polymer solutions. Human and rat young and old red blood cells'. *Biochimica et Biophysica Acta (BBA) - Biomembranes* (1994), vol. 1194(1): pp. 131–137.

209. H. Walter and R. P. Coyle: 'Effect of membrane modification of human erythrocytes by enzyme treatment on their partition in aqueous dextran-polyethylene glycol two-phase systems'. *Biochimica et Biophysica Acta (BBA) - General Subjects* (1968), vol. 165(3): pp. 540–543.

210. M. Savastano, C. Amendola, F. D'Ascenzo, and E. Massaroni: '3-D Printing in the Spare Parts Supply Chain: An Explorative Study in the Automotive Industry'. *Digitally Supported Innovation*. Ed. by L. Caporarello, F. Cesaroni, R. Giesecke, and M. Missikoff. Springer International Publishing, Cham, 2016: pp. 153–170.

211. B. Panda, M. J. Tan, I. Gibson, and C. K. Chua: 'The Disruptive Evolution Of 3D Printing'. *Proc. of the 2nd Intl. Conf. on Progress in Additive Manufacturing*. Research Publishing, Singapore, 2016: pp. 152–157.

212. T. Rayna and L. Striukova: 'From rapid prototyping to home fabrication: How 3D printing is changing business model innovation'. *Technological Forecasting and Social Change* (2016), vol. 102: pp. 214–224.

213. J. C. McDonald, M. L. Chabinyc., S. J. Metallo., J. R. Anderson., A. D. Stroock, and G. M. Whitesides: 'Prototyping of Microfluidic Devices in Poly(dimethylsiloxane) Using Solid-Object Printing'. *Analytical Chemistry* (2002), vol. 74(7): pp. 1537–1545.

214. T. Baden, A. M. Chagas, G. Gage, T. Marzullo, L. L. Prieto-Godino, and T. Euler: 'Open Labware: 3-D Printing Your Own Lab Equipment'. *PLOS Biology* (2015), vol. 13(3): pp. 1–12.

215. S. Moses, M. Manahan, A. Ambrogelly, and W. Ling: 'Assessment of AMBR^{TM} as a model for high-throughput cell culture process development strategy'. *Advances in Bioscience and Biotechnology* (2012), vol. 3(7): pp. 918–927.

216. T. Davila: 'An empirical study on the drivers of management control systems' design in new product development'. *Accounting, Organizations and Society* (2000), vol. 25(4): pp. 383–409.

217. F. Li, Y. Hashimura, R. Pendleton, J. Harms, E. Collins, and B. Lee: 'A Systematic Approach for Scale-Down Model Development and Characterization of Commercial Cell Culture Processes'. *Biotechnology Progress* (2006), vol. 22(3): pp. 696–703.

218. F. Johannsen, S. Leist, and G. Zellner: 'Six sigma as a business process management method in services: analysis of the key application problems'. *Information Systems and e-Business Management* (2011), vol. 9(3): pp. 307–332.

219. T. Friedli, P. Basu, D. Bellm, and J. Werani: *Leading Pharmaceutical Operational Excellence: Outstanding Practices and Cases*. Springer-Verlag Berlin Heidelberg, 2013.

220. J. Antony, A. S. Bhuller, M. Kumar, K. Mendibil, and D. C. Montgomery: 'Application of Six Sigma DMAIC methodology in a transactional environment'. *International Journal of Quality & Reliability Management* (2012), vol. 29(1): pp. 31–53.

221. D. C. Montgomery and C. M. Borror: 'Systems for modern quality and business improvement'. *Quality Technology & Quantitative Management* (2017), vol. 14(4): pp. 343–352.

222. K. Joshi, A. Asthana, S. Pande, G. S. Asthana, K. Singh, and G. Goomber: 'An Overview on Interrelationship between Quality by Design (QbD) & Six Sigma'. *World Journal of Pharmacy and Pharmaceutical Sciences* (2015), vol. 4(11): pp. 445–457.

223. G. Improta, G. Balato, M. Romano, F. Carpentieri, P. Bifulco, M. A. Russo, D. Rosa, M. Triassi, and M. Cesarelli: 'Lean Six Sigma: a new approach to the management of patients undergoing prosthetic hip replacement surgery'. *Journal of Evaluation in Clinical Practice* (2015), vol. 21(4): pp. 662–672.

224. M. Taner, B. Sezen, and K. M. Atwat: 'Application of Six Sigma methodology to a diagnostic imaging process'. *International journal of health care quality assurance* (2012), vol. 25(4): pp. 274–290.

225. G. Improta, G. Balato, M. Romano, A. M. Ponsiglione, E. Raiola, M. A. Russo, P. Cuccaro, L. C. Santillo, and M. Cesarelli: 'Improving performances of the knee replacement surgery process by applying DMAIC principles'. *Journal of Evaluation in Clinical Practice* (2017), vol. 23(6): pp. 1401–1407.

226. S. W. Carleysmith, A. M. Dufton, and K. D. Altria: 'Implementing Lean Sigma in pharmaceutical research and development: a review by practitioners'. *R&D Management* (2009), vol. 39(1): pp. 95–106.

227. F. Marti: 'Lean Six Sigma method in Phase 1 clinical trials: a practical example'. *The Quality Assurance Journal* (2005), vol. 9(1): pp. 35–39.

228. R. López-Franco, J. Moreno-Cuevas, and M. González-Garza: 'Percoll Gradient Optimization for Blood CD133+ Stem Cell Recovery'. *Stem Cell Discovery* (2014), vol. 4: pp. 61–66.

229. M. González-González, P. Vázquez-Villegas, C. García-Salinas, and M. Rito-Palomares: 'Current strategies and challenges for the purification of stem cells'. *Journal of Chemical Technology & Biotechnology* (2012), vol. 87(1): pp. 2–10.

230. M. Tsukamoto, S. Taira, S. Yamamura, Y. Morita, N. Nagatani, Y. Takamura, and E. Tamiya: 'Cell separation by an aqueous two-phase system in a microfluidic device'. *Analyst* (2009), vol. 134(10): pp. 1994–1998.

231. M. Yamada, V.Kasim, M. Nakashima, J. Edahiro, and M. Seki: 'Continuous cell partitioning using an aqueous two-phase flow system in microfluidic devices'. *Biotechnology and Bioengineering* (2004), vol. 88(4): pp. 489–494.

232. K. Vijayakumar, S. Gulati, A. J. deMello, and J. B. Edel: 'Rapid cell extraction in aqueous two-phase microdroplet systems'. *Chem. Sci.* (2010), vol. 1(4): pp. 447–452.

233. J. R. SooHoo and G. M. Walker: 'Microfluidic aqueous two phase system for leukocyte concentration from whole blood'. *Biomedical Microdevices* (2009), vol. 11(2): pp. 323–329.

234. K.-H. Nam, W.-J. Chang, H. Hong, S.-M. Lim, D.-I. Kim, and Y.-M. Koo: 'Continuous-Flow Fractionation of Animal Cells in Microfluidic Device Using Aqueous Two-Phase Extraction'. *Biomedical Microdevices* (2005), vol. 7(3): pp. 189–195.

235. D. Di Carlo, D. Irimia, R. G. Tompkins, and M. Toner: 'Continuous inertial focusing, ordering, and separation of particles in microchannels'. *Proceedings of the National Academy of Sciences* (2007), vol. 104(48): pp. 18892–18897.

236. S. C. Hur, N. K. Henderson-MacLennan., E. R. B. McCabe., and D. Di Carlo: 'Deformability-based cell classification and enrichment using inertial microfluidics'. *Lab Chip* (2011), vol. 11(5): pp. 912–920.

237. M. M. Wang, E. Tu, D. E. Raymond, J. M. Yang, H. Zhang, N. Hagen, B. Dees, E. M. Mercer, A. H. Forster, I. Kariv, P. J. Marchand, and W. F: Butler: 'Microfluidic sorting of mammalian cells by optical force switching'. *Nature Biotechnology* (2005), vol. 23(1): pp. 83–87.

238. A. Wolff, I. R. Perch-Nielsen, U. D. Larsen, P. Friis, G. Goranovic, C. R. Poulsen, J. P. Kutter, and P. Telleman: 'Integrating advanced functionality in a microfabricated high-throughput fluorescent-activated cell sorter'. *Lab Chip* (2003), vol. 3(1): pp. 22–27.

239. J. Seidl, R. Knuechel, and L. A. Kunz-Schughart: 'Evaluation of membrane physiology following fluorescence activated or magnetic cell separation'. *Cytometry* (1999), vol. 36(2): pp. 102–111.

240. C. Routledge and W. J. Armitage: 'Cryopreservation of cornea: a low cooling rate improves functional survival of endothelium after freezing and thawing'. *Cryobiology* (2003), vol. 46(3): pp. 277–283.

241. C. Hunt: 'Cryopreservation of Human Stem Cells for Clinical Application: A Review'. *Transfus Medicine Hemotherapy* (2011), vol. 38(2): pp. 107–123.

242. ÁBorsos, B. Szilágyi, P. S. Agachi, and Z. K. Nagy: 'Real-Time Image Processing Based Online Feedback Control System for Cooling Batch Crystallization'. *Organic Process Research & Development* (2017), vol. 21(4): pp. 511–519.

243. W. A. Moeglein, R. Griswold, B. L. Mehd, N. D. Browning, and J. Teuton: 'Applying shot boundary detection for automated crystal growth analysis during in situ transmission electron microscope experiments'. *Advanced Structural and Chemical Imaging* (2017), vol. 3(1): pp. 2–11.

244. K. Kumar, V. Kumarr, J. Lal, H. Kaurt, and J. Singh: 'A simple 2D composite image analysis technique for the crystal growth study of L-ascorbic acid'. *Microscopy Research and Technique* (2017), vol. 80: pp. 615–626.

245. M. A. L. Smith and L. A. Spomer: 'Direct quantification of in vitro cell growth through image analysis'. *In Vitro Cellular & Developmental Biology* (1987), vol. 23(1): pp. 67–70.

246. C. R. Thomas and G. C. Paul: 'Applications of image analysis in cell technology'. *Current Opinion in Biotechnology* (1996), vol. 7(1): pp. 35–45.

247. J. Selinummi, J. Seppälä, O. Yli-Harja, and J. A. Puhakka: 'Software for quantification of labeled bacteria from digital microscope images by automated image analysis'. *BioTechniques* (2005), vol. 39(6): pp. 859–863.

248. Y. Levin-Schwartz, D. R. Sparta, J. F. Cheer, and T. Adali: 'Parameter-free automated extraction of neuronal signals from calcium imaging data'. *2017 IEEE International Conference on Acoustics, Speech and Signal Processing (ICASSP)* (2017), vol.: pp. 1033–1037.

249. C.-C. Liang, A. Y. Park, and J.L. Guan: 'In vitro scratch assay: a convenient and inexpensive method for analysis of cell migration in vitro'. *Nature Protocols* (2007), vol. 2(2): pp. 329–333.

250. R. Spindler, B. Rosenhahn, N. Hofmann, and B. Glasmacher: 'Video analysis of osmotic cell response during cryopreservation'. *Cryobiology* (2012), vol. 64(3): pp. 250–260.

251. P. Mazur, S. P. Leibo, and E. H. Y. Chu: 'A two-factor hypothesis of freezing injury: Evidence from Chinese hamster tissue-culture cells'. *Experimental Cell Research* (1972), vol. 71(2): pp. 345–355.

252. G. J. Morris, E. Acton, D. Collins, A. Bos-Mikich, and P. de Sousa: '143. Optimisation of current Good Manufacturing Practice (cGMP) compliant controlled rate freezing for human embryonic stem cells'. *Cryobiology* (2010), vol. 61(3): p. 406.

253. J. Hendriks, J. Riesle, and C. A. van Blitterswijk: 'Co-culture in cartilage tissue engineering'. *Journal of Tissue Engineering and Regenerative Medicine* (2007), vol. 1(3): pp. 170–178.

254. T. R. J. Heathman, V. A. M. Glyn, A. Picken, Q. A. Rafiq, K. Coopman, A. W. Nienow, B. Kara, and C. J. Hewitt: 'Expansion, harvest and cryopreservation of human mesenchymal stem cells in a serum-free microcarrier process'. *Biotechnology and Bioengineering* (2015), vol. 112(8): pp. 1696–1707.

255. O. Rogulska, Y. Petrenko, and A. Petrenko: 'DMSO-free cryopreservation of adipose-derived mesenchymal stromal cells: expansion medium affects post-thaw survival'. *Cytotechnology* (2017), vol. 69(2): pp. 265–276.

256. S. M. Zeisberger, J. C. Schulz, M. Mairhofer, P. Ponsaerts, G. Wouters, D. Doerr, A. Katsen-Globa, M. Ehrbar, J. Hescheler, S. P. Hoerstrup, A. H. Zisch, A. Kolbus, and H. Zimmermann: 'Biological and Physicochemical Characterization of a Serum-and Xeno-Free Chemically Defined Cryopreservation Procedure for Adult Human Progenitor Cells'. *Cell Transplantation* (2011), vol. 20(8): pp. 1241–1257.

257. A. Mitchell, K. A. Rivas, R. Smith, and A. E. Watts: 'Cryopreservation of equine mesenchymal stem cells in 95 % autologous serum and 5 % DMSO does not alter post-thaw growth or morphology in vitro compared to fetal bovine serum or allogeneic serum at 20 or 95 % and DMSO at 10 or 5 %'. *Stem Cell Research & Therapy* (2015), vol. 6: pp. 1–12.

258. S. Gretzinger, S. Limbrunner, and J. Hubbuch: 'Automated Image Processing as an Analytical Tool in Cell Cryopreservation for Bioprocess Development'. *Bioprocess and Biosystems Engineering* (2019), vol. 42: pp. 665–675.

259. S. M. Rahman, S. K. Majhi, T. Suzuki, S. Matsukawa, C. A. Strüssmann, and R. Takai: 'Suitability of cryoprotectants and impregnation protocols for embryos of Japanese whiting Sillago japonica'. *Cryobiology* (2008), vol. 57(2): pp. 170–174.

260. H. Woelders, A. Matthijs, and B. Engel: 'Effects of Trehalose and Sucrose, Osmolality of the Freezing Medium, and Cooling Rate on Viability and Intactness of Bull Sperm after Freezing and Thawing'. *Cryobiology* (1997), vol. 35(2): pp. 93–105.

261. M. K. Soylu, Z. Nur, B. Ustuner, I. Dogan, H. Sairkaya, U. Gunay, and K. Ak: 'Effects of Various Cryoprotective Agents and Extender Osmolality on Post-thawed Ram Semen'. *Bull Vet Inst Pulawy* (2007), vol. 51: pp. 241–246.

262. C. Koshimoto and P. Mazur: 'The effect of the osmolality of sugar-containing media, the type of sugar, and the mass and molar concentration of sugar on the survival of frozen-thawed mouse sperm'. *Cryobiology* (2002), vol. 45(1): pp. 80–90.

263. M. R. Polovina: *Cryopreservation solution*. US Patent 5,759,764. June 1998.

264. R. Chinnadurai, I. B. Copland, M. A. Garcia, C. T. Petersen, C. N. Lewis, E. K. Waller, A. D. Kirk, and J. Galipeau: 'Cryopreserved Mesenchymal Stromal Cells Are Susceptible to T-Cell Mediated Apoptosis Which Is Partly Rescued by IFNγ Licensing'. *STEM CELLS* (2016), vol. 34(9): pp. 2429–2442.

265. K. Matsumura and S.-H. Hyon: 'Polyampholytes as low toxic efficient cryoprotective agents with antifreeze protein properties'. *Biomaterials* (2009), vol. 30(27): pp. 4842–4849.

266. K. Matsumura, J. Y. Bae, and S. H. Hyon: 'Polyampholytes as Cryoprotective Agents for Mammalian Cell Cryopreservation'. *Cell Transplantation* (2010), vol. 19(6 - 7): pp. 691–699.

267. X. Ma, X. Qu, W. Zhu, Y.-S. Li, S. Yuan, H. Zhang, J. Liu, P. Wang, C. S. E. Lai, F. Zanella, G.-S. Feng, F. Sheikh, S. Chien, and S. Chen: 'Deterministically patterned biomimetic human iPSC-derived hepatic model via rapid 3D bioprinting'. *PNAS* (2016), vol. 113(8): pp. 2206–2211.

268. Y. Zhao, R. Yao, L. Ouyang, H. Ding, T. Zhang, K. Zhang, S. Cheng, and W. Sun: 'Three-dimensional printing of Hela cells for cervical tumor model in vitro'. *Biofabrication* (2014), vol. 6(3): p. 035001.

269. X. Cui, K. Breitenkamp, M. G. Finn, and D. D. DLima M. Lot and: 'Direct Human Cartilage Repair Using Three-Dimensional Bioprinting Technology'. *Tissue Eng. Part A* (2012), vol. 18: pp. 1304–1312.

270. J. M. Lee and W. Y. Yeong: 'Design and Printing Strategies in 3D Bioprinting of CellHydrogels: A Review'. *Advanced Healthcare Materials* (2016), vol. 5(22): pp. 2856–2865.

271. J. Jia, D. J. Richards, S. Pollard, Y. Tan, J. Rodriguez, R. P. Visconti, T. C. Trusk, M. J. Yost, H. Yao, R. R. Markwald, and Y. Mei: 'Engineering alginate as bioink for bioprinting'. *Acta Biomaterialia* (2014), vol. 10(10): pp. 4323–4331.

272. H. Martínez Ávila, S. Schwarz, N. Rotter, and P. Gatenholm: '3D bioprinting of human chondrocyte-laden nanocellulose hydrogels for patient-specific auricular cartilage regeneration'. *Bioprinting* (2016), vol. 1-2: pp. 22–35.

273. K. Markstedt, A. Mantas, I. Tournier, H. Martínez Ávila, D. Hägg, and P. Gatenholm: '3D Bioprinting Human Chondrocytes with Nanocellulose-Alginate Bioink for Cartilage Tissue Engineering Applications'. *Biomacromolecules* (2015), vol. 16(5): pp. 1489–1496.

274. M. Müller, E. Öztürk, Ø. Arlov, P. Gatenholm, and M. Zenobi-Wong: 'Alginate Sulfate–Nanocellulose Bioinks for Cartilage Bioprinting Applications'. *Annals of Biomedical Engineering* (2017), vol. 45(1): pp. 210–223.

275. J. H. Y. Chung, S. Naficy, Z. Yue, R. Kapsa, A. Quigley, S. E. Moulton, and G. G. Wallace: 'Bio-ink properties and printability for extrusion printing living cells'. *Biomater. Sci.* (7 2013), vol. 1: pp. 763–773.

276. S. V. Murphy, A. Skardal, and A. Atala: 'Evaluation of hydrogels for bioprinting applications'. *Journal of Biomedical Materials Research Part A* (2013), vol. 101 A(1): pp. 272–284.

277. K. Nair, M. Gandhi, S. Khalil, K. Chang Yan, M. Marcolongo, K. Barbee, and W. Sun: 'Characterization of cell viability during bioprinting processes'. *Biotechnology Journal* (2009), vol. 4(8): pp. 1168–1177.

278. M. Neufurth, X. Wang, H. C. Schröder, Q. Feng, B. Diehl-Seifert, T. Ziebart, R. Steffen, S. Wang, and W. E.G. Müller: 'Engineering a morphogenetically active hydrogel for bioprinting of bioartificial tissue derived from human osteoblast-like SaOS-2 cells'. *Biomaterials* (2014), vol. 35(31): pp. 8810–8819.

279. Y. Yu, Y. Zhang, and J. A. Martin amd I. T. Ozbolat: 'Evaluation of Cell Viability and Functionality in Vessel-like Bioprintable Cell-Laden Tubular Channels'. *ASME. J Biomech Eng.* (2013), vol. 153(9): pp. 091011-091011-9.

280. K. W. Ng, D. T.W. Leong, and D. W. Hutmacher: 'The Challenge to Measure Cell Proliferation in Two and Three Dimensions'. *Tissue Engineering* (2005), vol. 11(1-2): pp. 182–191.

281. G. Marchioli, L. van Gurp, P. P. van Krieken, D. Stamatialis, M. Engelse, C. A. van Blitterswijk, M. B. J. Karperien, E. de Koning, J. Alblas, L. Moroni, and A. A. van Apeldoorn: 'Fabrication of three-dimensional bioplotted hydrogel scaffolds for islets of Langerhans transplantation'. *Biofabrication* (2015), vol. 7(2): p. 025009.

282. L. Ruiz-Cantu, A. Gleadall, C. Faris, J. Segal, K. Shakesheff, and J. Yang: 'Characterisation of the surface structure of 3D printed scaffolds for cell infiltration and surgical suturing'. *Biofabrication* (2016), vol. 8(1): p. 015016.

283. *User Guide: CellTrace^{TM} Cell Proliferation Kits*. https://www.thermofisher.com/order/catalog/product/C34557. accessed September 25, 2017.

284. J. Begum, W. Day, C. Henderson, S. Purewal, J. Cerveira, H. Summers, P. Rees, D. Davies, and A. Filby: 'A method for evaluating the use of fluorescent dyes to track proliferation in cell lines by dye dilution'. *Cytometry Part A* (2013), vol. 83(12): pp. 1085–1095.

285. B. J. C. Quah and C. R. Parish: 'New and improved methods for measuring lymphocyte proliferation in vitro and in vivo using CFSE-like fluorescent dyes'. *Journal of Immunological Methods* (2012), vol. 379(1): pp. 1–14.

286. A. Filby, E. Perucha, H. Summers, P. Rees, P. Chana, S. Heck, G. M. Lord, and D. Davies: 'An imaging flow cytometric method for measuring cell division history and molecular symmetry during mitosis'. *Cytometry Part A* (2011), vol. 79(7): pp. 496–506.

287. O. Thaunat, A. G. Granja, P. Barral, A. Filby, B. Montaner, L. Collinson, N. Martinez-Martin, N. E. Harwood, A. Bruckbauer, and F. D. Batista: 'Asymmetric Segregation of Polarized Antigen on B Cell Division Shapes Presentation Capacity'. *Science* (2012), vol. 335(6067): pp. 475–479.

288. A. Filby, J. Begum, M. Jalal, and W. Day: 'Appraising the suitability of succinimidyl and lipophilic fluorescent dyes to track proliferation in non-quiescent cells by dye dilution'. *Methods* (2015), vol. 82. Flow Cytometry Methods and Approaches: pp. 29–37.

289. I. Schmid, C. H. Uittenbogaart, B. Keld, and J. V. Giorgi: 'A rapid method for measuring apoptosis and dual-color immunofluorescence by single laser flow cytometry'. *Journal of Immunological Methods* (1994), vol. 170(2): pp. 145–157.

290. S.K. Bajpai and S. Sharma: 'Investigation of swelling/degradation behaviour of alginate beads crosslinked with Ca^{2+} and Ba^{2+} ions'. *Reactive and Functional Polymers* (2004), vol. 59(2): pp. 129–140.

291. Y. Mørch, I. Donati, B. Strand, and G. Skjåk-Bræk: 'Effect of Ca^{2+}, Ba^{2+}, and Sr^{2+} on Alginate Microbeads'. *Biomacromolecules* (2006), vol. 7: pp. 1471–80.

292. P. Agulhon, V. Markova, M. Robitzer, F. Quignard, and T. Mineva: 'Structure of Alginate Gels: Interaction of Diuronate Units with Divalent Cations from Density Functional Calculations'. *Biomacromolecules* (2012), vol. 13: pp. 1899–907.

293. B. A. Harper, S. Barbut, L.T. Lim, and M. F. Marcone: 'Effect of Various Gelling Cations on the Physical Properties of "Wet" Alginate Films'. *Journal of Food Science* (2014), vol. 79(4): E562–E567.

CHAPTER 13

Abbreviations

ADA-SCID	adenosin-desaminase severe combined immunodeficiency
ATMP	Advanced Therapy Medicinal Product
ATP	adenosine triphosphate
ATPS	aqueous two-phase systems
BSA	bovine servum albumin
CAD	computer-aided design
CAR-T cells	chimeric antigen receptor T cell
CCC	critical cell characteristic
CCD	countercurrent distribution
CFSE	carboxyfluorescein succinimidyl ester
cGMP	current Good Manufacturing Practice
CoGs	cost of goods
CPP	critical process parameter
CQAs	critical quality attributes
CT	computed tomography
DMSO	dimethyl sulfoxide
DSP	downstream processing
EMA	European Medicines Agency
EU	European Union
FACS	fluorescence activated cell sorting
FBS	fetal bovine serum
FDA	Food and Drug Administration

FDM	fused deposition modelling
FSC-A	Forward scatter peak area
FSC-H	Forward scatter peak height
GMP	Good Manufacturing Practice
GvHD	graft-versus-host-disease
HMI	Human-Machine Interface
HTPD	high-throughput process development
HTS	high-throughput screening
ICH	international council for harmonisation of technical requirements for pharmaceuticals for human use
IPPD	integrated product and process development
LPLD	Lipoprotein lipase deficiency
MAA	marketing authorization application
mAb	monoclonal antibody
mAbs	monoclonal antibodies
MACS	magnet activated cell sorting
MCB	master cell bank
MRI	magnetic resonance imaging
MTT	3-(4&5-dimethylthiazole-2-yl)-2&5-diphenyl- tetrazoliumbromide
NaCl	sodium chloride
NaPi	sodium phosphate
PBS	phosphate-buffered saline
PEG	polyethylene glycol
QbD	Quality by Design
QCA	critical quality attribute
QTPP	Quality Target Product Profile
R&D	research and development
SSC-A	side scatter peak area
TLL	tie-line length

US	United States
USP	upstream processing
UV	ultraviolet
WCB	working cell bank
WV	working volume
3D	three-dimensional
7-AAD	7-Aminoactinomycin D